

**Protection from Experimental Cerebral
Malaria through the Attenuation of
CXCR3-mediated T Cell Chemotaxis**

Kristin Van Den Ham

Department of Microbiology and Immunology
McGill University, Montréal
April 2017

A thesis submitted to McGill University in partial fulfillment of the
requirements of the degree of Doctor of Philosophy

© Kristin Van Den Ham, 2017

To my parents

Table of Contents

Abstract	6
Résumé	8
Acknowledgements	10
Contribution of Authors	12
Contribution to Original Scientific Knowledge	14
List of Figures	15
List of Tables	18
List of Abbreviations	19
Chapter One: Literature Review	24
1. Epidemiology of Malaria	25
1.1 Malaria Life Cycle	29
1.2 Vector Control	32
1.3 Chemoprophylaxis	35
1.4 Rapid Diagnostic Tests	39
1.5 Treatment of Uncomplicated Malaria	42
1.6 Diagnosis and Treatment of Severe Malaria	47
2. Pathogenesis of Cerebral Malaria	50
2.1 Cellular Adhesion of Parasitized Erythrocytes	50
2.2 Microvascular Endothelial Dysfunction	53
2.3 Proinflammatory Immune Response	56
2.4 Pathophysiological Features of Cerebral Malaria	58
3. Adjunctive Therapies for Cerebral Malaria	64
3.1 Cytoadherence and Microvascular Obstruction	65
3.2 Immunomodulation	67

3.3	Augmentation of Nitric Oxide	69
3.4	Amelioration of Metabolic Acidosis	71
3.5	Reduction of Brain Swelling	74
3.6	Neuroprotective Agents	75
4.	Experimental Cerebral Malaria	77
4.1	The Role of T Cells	80
4.2	Induction of the T Cell Response	81
4.3	Chemotaxis of T Cells to the Brain	86
4.4	Effector Phase of the T Cell Response	92
4.5	Upregulation of CXCR3 Expression on T Cells	104
4.6	Regulatory CD4 ⁺ T Cells	106
5.	Malaria and Iron	110
5.1	Systemic Iron Homeostasis	110
5.2	Malaria and Iron Supplementation	115
5.3	Iron and IFN γ Signalling	119
6.	Protein Tyrosine Phosphatases and the Immune Response	121
6.1	Regulation of Protein Tyrosine Phosphatase Activity	121
6.2	Role of Lck and CD45 in Proximal TCR Signal Transduction	124
	Rationale and Objectives	126
Chapter Two: Iron Prevents the Development of Experimental Cerebral Malaria by		
	Attenuating CXCR3-mediated T Cell Chemotaxis	128
	Preface	129
	Abstract	131
	Introduction	131
	Results	133

Discussion	141
Materials and Methods	145
Acknowledgments	150
Figures and Tables	151
Chapter Three: Protein Tyrosine Phosphatase Inhibition Prevents Experimental Cerebral	
Malaria by Precluding CXCR3 Expression on T Cells	
	179
Preface	180
Abstract	182
Introduction	182
Results	184
Discussion	192
Materials and Methods	197
Acknowledgements	202
Figures	203
Chapter Four: Final Discussion and Conclusions	
	220
Introduction	221
CXCR3-mediated Chemotaxis of T Cells.....	223
NK Cells and CD4 ⁺ Regulatory Cells	226
Hepatic Injury	227
Conclusions	228
References	230

Abstract

More than ninety countries have ongoing malaria transmission, putting nearly half of the population of the world at risk of this disease. Malaria can rapidly progress from a non-specific febrile illness to severe complications that often result in death. Multiple mouse models have been employed to recapitulate and better characterize the pathology induced by malaria. Murine cerebral malaria is caused by infection with *Plasmodium berghei* ANKA, and is dependent on the CXCR3-mediated chemotaxis of T cells and their subsequent sequestration within the brain, which ultimately leads to BBB disruption and neuropathology.

Iron status has been shown to affect the pathogenicity of many infections, including malaria, with some studies suggesting that iron deficiency is protective against clinical malaria and that iron supplementation may increase the risk of severe adverse events. Despite potentially offering protection from malaria, iron deficiency anemia has been associated with impaired cognitive development, necessitating an improved understanding of the interaction between iron and malaria. Additionally, numerous signalling pathways involved in the generation of an immune response rely on tyrosine phosphorylation, and PTP inhibition has been shown to mitigate pathology in various diseases, including parasitic infection. Notably, previous studies have demonstrated that systemic iron levels are capable of regulating PTP activity.

Here we determined that both iron administration and PTP inhibition significantly reduce the incidence of cerebral malaria, concomitant with a marked decrease in the sequestration of CD4⁺ and CD8⁺ T cells within the brain. While both treatments prevented BBB disruption by attenuating the CXCR3-mediated chemotaxis of T cells, iron and PTP inhibition afforded protection by modulating different underlying mechanisms. Iron prevented the upregulation of

CXCR3 on CD4⁺ T cells alone by mitigating the IFN γ -responsiveness of these cells, as indicated by the decreased expression of IFN γ R2 and T-bet and the reduced phosphorylation of STAT1. However, PTP inhibition precluded the expression of CXCR3 on both CD4⁺ and CD8⁺ T cells by preventing the dephosphorylation of the inhibitory tyrosine of Lck, thereby impairing TCR signal transduction.

Additionally, iron supplementation decreased the percentage of NK cells, which have been implicated in augmenting CXCR3 expression on T cells, and increased the percentage of Tregs, which may play a role in attenuating the inflammatory response during ECM. Alternatively, PTP inhibition increased the percentage of IL-10⁺ CD4⁺ T cells by enhancing the frequency of Tr1 cells and both IL-10 and reduced PTP activity were shown to correlate with reduced hepatic pathology. Overall, our results support the crucial role of CXCR3 in mediating the brain sequestration of T cells and the development of neuropathology. Importantly, this work provides insight into the mechanisms that control the upregulation of CXCR3 on T cells, which has previously been poorly characterized.

Résumé

Plus de quatre-vingt-dix pays sont connus comme étant des foyers de transmission active de la malaria, ou paludisme, exposant ainsi près de la moitié de la population mondiale à cette maladie. La malaria peut rapidement progresser d'une infection légère à une forme beaucoup plus grave, causant des complications sévères pouvant souvent entraîner la mort. Jusqu'à maintenant, plusieurs modèles murins ont été utilisés afin de comprendre et mieux caractériser la pathologie induite par la malaria. Le neuropaludisme, ou malaria cérébrale, est causé chez la souris à la suite de l'infection par le parasite *Plasmodium berghei* ANKA. Celle-ci est dépendante de la chimiotaxie des cellules T médiée par CXCR3, de même que par la séquestration subséquente de ces cellules à l'intérieur du cerveau. Ceci menant à la rupture de la barrière hémato-encéphalique et à la neuropathologie.

Il a été démontré que le statut en fer affectait le pouvoir pathogène de plusieurs infections, dont la malaria. Plusieurs études suggérant d'ailleurs qu'une carence en fer confère une protection contre celle-ci, alors qu'un apport supplémentaire en fer augmente le risque de complications sévères liées à la maladie. Malgré la protection potentielle qu'une carence en fer pourrait offrir, l'anémie causée par une telle carence a été associée à des problèmes de développement cognitif. Il est donc nécessaire d'approfondir notre compréhension des interactions entre le fer et la malaria. En outre, de nombreuses voies de signalisation impliquées dans la génération de la réponse immunitaire sont basées sur la phosphorylation des tyrosines. De plus, il a été prouvé qu'une inhibition des PTPs atténuait la pathologie de diverses maladies, incluant les infections parasitaires. Il est à noter que des études précédentes ont établi que des niveaux systémiques de fer peuvent réguler l'activité des PTPs.

Lors de cette étude, nous avons déterminé que l'administration de fer, de même que l'inhibition des PTPs, réduisait de manière significative l'incidence du neuropaludisme, ceci conjointement à une réduction marquée de la séquestration des cellules T CD4⁺ et CD8⁺ à l'intérieur du cerveau. Alors que les deux traitements utilisés ont permis de prévenir la rupture de la barrière hémato-encéphalique en atténuant la chimiotaxie des cellules T médiée par CXCR3, ils ont toutefois conféré leur protection en affectant différents mécanismes fondamentaux. Le fer a empêché l'activation de CXCR3 uniquement sur les cellules T CD4⁺ en atténuant leur capacité de réponse à l'IFN γ , tel qu'indiqué par la réduction de l'expression de l'IFN γ R2 et de T-bet, de même que par la réduction de la phosphorylation de STAT1. Quant à l'inhibition des PTPs, elle a empêché l'expression de CXCR3 sur les cellules T CD4⁺ et les cellules T CD8⁺ en prévenant la déphosphorylation de la tyrosine inhibitrice de Lck, compromettant donc ainsi la transduction du signal TCR (T Cell Receptor).

De plus, un apport complémentaire en fer a entraîné la diminution du pourcentage des cellules tueuses naturelles (NK), cellules qui sont impliquées dans l'augmentation de l'expression de CXCR3 sur les cellules T, et a également causé l'augmentation du pourcentage des cellules Tregs, ces dernières pouvant possiblement jouer un rôle dans l'atténuation de la réponse inflammatoire dans un contexte expérimental de neuropaludisme. Parallèlement, l'inhibition des PTPs a engendré un accroissement du pourcentage des cellules T IL10⁺ CD4⁺ en augmentant la fréquence des cellules Tr1. De même, il a été démontré que l'IL-10 et la réduction de l'activité des PTPs entraînaient une pathologie hépatique réduite. Globalement, nos résultats appuient le rôle crucial de CXCR3 dans la séquestration des cellules T au cerveau, de même que son implication dans le développement de la pathologie. Plus important encore, ce travail donne un aperçu des mécanismes qui contrôlent la régulation à la hausse de CXCR3 des cellules T, mécanismes jusqu'à maintenant très peu caractérisés.

Acknowledgments

First of all, I would like to thank my supervisor Dr. Martin Olivier for giving me the opportunity to do my Ph.D. in his lab. I want to thank you for your advice and encouragement, and for the freedom to pursue my hunches. I would also like to thank the members of my advisory committee, Drs. Kostas Pantopoulos and Martin Richer, for their guidance and insightful comments during our meetings. I further want to thank Dr. Martin Richer and Logan Smith for their advice and contribution to the PTP project, and Dr. Connie Krawczyk and the members of her lab, particularly Alborz Borjian and Giselle Boukhaled, for their help with all things FACS-related. Additionally, I would like to thank Anthony Rainone for his assistance with the analysis of brain-sequestered T cells.

Furthermore, I would like to thank the members of the Olivier lab, both past and present; my time at the Duff and RI-MUHC would not have been the same without you. While I cannot thank everyone individually due to a lack of space, there are a number of people I would be remiss not to mention personally. Special thanks to Dr. Marina Tiemi Shio, who helped me with all of my first forays into mouse work and always made time to give me advice on lab work and presentations, and without whom my first year of grad school would have been substantially more difficult. I would also like to thank Caroline Martel, who was there through all of the highs and lows of grad school and who was a lifeline throughout, including, but definitely not limited to, watching Monty and translating my thesis abstract (gros bisous, B. Spice).

Additionally, I would like to thank all of the sixth floor (and sixth floor-adjacent) people who made my time in Montréal infinitely better: Dr. Anupam Adhikari, Dr. Vanessa Diniz Atyade, Alborz Borjian, Dr. Jan Christian, Dr. Sophie Fougeray, Dr. Amandine Isnard, Ben Li, Emily

Maclean, Lauren Narcross, Adam Peres, Brendan Snarr, Camille Stegen, Alec Sweet and Cynthia Tang. Thanks for the scientific guidance, career advice, camping adventures, fantasy football, innumerable cinq à sept, pétanque and intramural softball. And last, but not least, I would like to thank my parents, Yvonne and Allen Van Den Ham, and my brother Logan Van Den Ham, for their continued love and support.

Contribution of Authors

This thesis was written in a “Manuscript-based thesis” format in accordance with McGill University’s “Guidelines for Thesis Preparation”. All experiments were performed in the laboratories of Dr. Martin Olivier and Dr. Martin Richer. The detailed contributions of all authors are listed below.

Chapter Two: Iron Prevents the Development of Experimental Cerebral Malaria by Attenuating CXCR3-mediated T Cell Chemotaxis

KM Van Den Ham, MT Shio, A Rainone, S Fournier, CM Krawczyk, M Olivier (2015) Iron prevents the development of experimental cerebral malaria by attenuating CXCR3-mediated T cell chemotaxis, *PLOS ONE*, 10 (3):e0118451

KM Van Den Ham: experimental design, contributed to all experimental work, data analysis, manuscript writing and revision, and figure preparation

MT Shio: contributed to experimental work analyzing survival and BBB integrity

A Rainone: contributed to experimental work analyzing brain sequestration of T cells

S Fournier: supervision (A Rainone)

CM Krawczyk: experimental design, contributed to experimental work analyzing splenic cell populations, and manuscript revision

M Olivier: experimental design, manuscript revision, supervision (KM Van Den Ham), and acquisition of financial support

Chapter Three: Protein Tyrosine Phosphatase Inhibition Prevents Experimental Cerebral Malaria by Precluding CXCR3 Expression on T Cells

KM Van Den Ham, LK Smith, MJ Richer, M Olivier (2017) Protein Tyrosine Phosphatase Inhibition Prevents Experimental Cerebral Malaria by Precluding CXCR3 Expression on T Cells. Accepted for publication. (*Scientific Reports*)

KM Van Den Ham: experimental design, all experimental work except for CD3 cross-linking of CD8⁺ T cells, data analysis, manuscript writing and revision, and figure preparation

LK Smith: performed CD3 cross-linking of CD8⁺ T cells, data analysis, and manuscript revision

MJ Richer: experimental design, manuscript revision, supervision (LK Smith), and acquisition of funding

M Olivier: experimental design, manuscript revision, supervision (KM Van Den Ham), and acquisition of funding

Below are the publications to which the candidate had a significant contribution, but are not presented in the thesis.

M Olivier, **K Van Den Ham**, MT Shio, FA Kassa, S Fougeray (2014) Malarial pigment hemozoin and the innate inflammatory response. *Frontiers in Immunology*, **5** (25)

FA Kassa, **K Van Den Ham**, A Rainone, S Fournier, E Boilard, M Olivier (2016) Absence of apolipoprotein E protects mice from cerebral malaria, *Scientific Reports*, 6 (33615)

Contribution to Original Scientific Knowledge

1. Iron dextran prevents the brain sequestration of pathogenic T cells by impairing the CXCR3-mediated chemotaxis of T cells, thereby decreasing the incidence of ECM.
2. Iron dextran attenuates the IFN γ -responsiveness of CD4⁺ T cells by downregulating the surface expression of IFN γ R2, resulting in mitigated expression of CXCR3 on CD4⁺ T cells *in vivo*.
3. Iron dextran decreases the expression of CXCL10 within the brain, impairing the chemotaxis of CXCR3-expressing T cells.
4. Iron dextran increases the percentage of NK cells and decreases the percentage of Tregs in the spleen, and reduces the tissue parasite burden, processes which are thought to contribute to pathology in ECM.
5. PTP inhibition prevents the brain sequestration of pathogenic T cells by impairing the CXCR3-mediated chemotaxis of T cells, thereby decreasing the incidence of ECM.
6. PTP inhibition precludes the upregulation of CXCR3 on both CD4⁺ and CD8⁺ T cells by impairing the dephosphorylation of the inhibitory tyrosine of Lck, resulting in impaired TCR signal transduction. Moreover, CXCR3 expression on CD4⁺ and CD8⁺ T cells is differentially modulated by tyrosine phosphorylation.
7. PTP inhibition increases the production of IL-10 by splenic CD4⁺ T cells by enhancing the percentage of Tr1 cells.
8. IL-10 is required to prevent the development of hepatic pathology during *P. berghei* ANKA infection, and PTP inhibition further attenuates liver damage during ECM.
9. Liver parasite burden is not directly responsible for hepatic pathology in ECM, and IL-10 expression does not limit liver parasite burden.

List of Figures

Chapter One

Figure 1. WHO Regions	28
Figure 2. Malaria Life Cycle	31
Figure 3. Overview of Cerebral Malaria Etiology	63
Figure 4. The Role of CD8 ⁺ T Cells in ECM	109
Figure 5. Systemic Iron Homeostasis	120

Chapter Two

Figure 1. Iron Dextran Prevents the Development of ECM	151
Figure 2. Tissue Parasite Sequestration is Inhibited by Parenteral Iron Supplementation	152
Figure 3. Systemic Inflammation is Augmented in FeD Mice	153
Figure 4. The Expression of Genes Involved in T Cell Chemotaxis are Attenuated by Parenteral Iron Supplementation	154
Figure 5. Sequestration of CD4 ⁺ and CD8 ⁺ T Cells in the Brain is Reduced in FeD Mice	155
Figure 6. The Expression of CXCR3 on Splenic CD4 ⁺ T Cells is Decreased by Parenteral Iron Supplementation	156
Figure 7. Iron Dextran Mitigates the Upregulation of IFN γ R2 and T-bet on CD4 ⁺ T Cells in the Spleen	157
Figure 8. FeD Mice have Modulated Frequencies of Splenic NK Cells and Tregs Early During the Infection	159
Supplementary Figure 1. Mice Fed an Iron-enriched Diet and HJV ^{-/-} Mice are not Protected from ECM	161

Supplementary Figure 2. Iron Dextran Administered after Infection can Prevent the Development of ECM	162
Supplementary Figure 3. RLU Measured in the Blood, Brain, Spleen and Liver	163
Supplementary Figure 4. Systemic Inflammation in FeD Mice is Increased Only Late during the Infection	164
Supplementary Figure 5. Iron Dextran Causes a Minor Delay in the Proliferation of Splenic CD4 ⁺ T Cells	165
Supplementary Figure 6. Percentage of Activated CD4 ⁺ and CD8 ⁺ T Cells in the Spleen is Slightly Decreased in the FeD Mice	166
Supplementary Figure 7. Iron Supplementation Results in a Slight Increase in the Priming Capacity of Splenic cDCs	168
Supplementary Figure 8. A Greater Percentage of Splenic CD4 ⁺ T Cells in FeD Mice Show an Activated Phenotype and Express CXCR3 on Day 3	169
Supplementary Figure 9. Attenuated Expression of IFN γ R2 and T-bet does not Result in Decreased Expression of CXCR3 on Splenic CD8 ⁺ T Cells	170
Supplementary Figure 10. Iron Supplementation Decreases STAT1 Phosphorylation in Splenic CD4 ⁺ T cells in FeD Mice	172

Chapter Three

Figure 1. PTP Inhibition Prevents the Development of ECM	203
Figure 2. bpV(phen) Treatment Increases the Frequency of Regulatory CD4 ⁺ T Cells in the Spleen	204
Figure 3. PTP Inhibition Partially Protects IL-10 Knock-out Mice from <i>P. berghei</i> ANKA Infection	206

Figure 4. bpV(phen) Treatment and IL-10 Mitigate ECM-induced Liver Damage	207
Figure 5. PTP Inhibition Prevents the Brain Sequestration of CD4 ⁺ and CD8 ⁺ T Cells	208
Figure 6. bpV(phen) Treatment Attenuates the Expression of CXCR3 on Splenic CD4 ⁺ and CD8 ⁺ T Cells	210
Figure 7. PTP Inhibition Prevents the Upregulation of CXCR3 and Attenuates TCR-mediated Signalling in Splenic T Cells	211
Supplementary Figure 1. PTP Inhibition Prevents the Development of Neurological Symptoms	213
Supplementary Figure 2. IL-10 Production by CD4 ⁺ T Cells and B Cells	214
Supplementary Figure 3. PTP Inhibition Prevents the Development of Neuropathology in IL-10 Knock-out Mice	215
Supplementary Figure 4. Liver Parasite Load is Dependent on the Onset of Cerebral or Hepatic Symptoms	216
Supplementary Figure 5. PTP Inhibition Decreases the Activation of Splenic CD8 ⁺ T Cells	217
Supplementary Figure 6. bpV(phen)-mediated Reduction of CXCR3 Expression is Not Caused by the Attenuation of T Cell Activation	218
Supplementary Figure 7. PTP Inhibition Attenuates CXCR3 Expression to a Greater Extent during Stimulation Compared to Recovery	219

Chapter Four

Figure 1. Modulation of CXCR3 Expression on T Cells by Iron and bpV(phen)	225
--	-----

List of Tables

Chapter Two

Supplementary Table 1. Immune Response-related Gene Expression in the Brain is Mostly Reduced or Unchanged in FeD Mice	173
Supplementary Table 2. Immune Response-related Gene Expression in the Spleen is Mostly Reduced or Unchanged in FeD Mice	175
Supplementary Table 3. Immune Response-related Gene Expression in the Liver is Mostly Reduced or Unchanged in FeD Mice	177

List of Abbreviations

ADAMTS13: a disintegrin and metalloproteinase with thrombospondin type-1 repeats

ADMA: asymmetrical dimethylarginine

ALT: alanine transaminase

AP-2: activator protein 2

ASC: apoptosis-associated speck-like protein containing a carboxy-terminal CARD

AST: aspartate transaminase

BBB: blood-brain barrier

BMP: bone morphogenetic protein

BMP6: bone morphogenetic protein 6

bpV(phen): potassium bisperoxo (1,10-phenanthroline) oxovanadate (V) trihydrate

CCL5: chemokine (C-C motif) ligand 5

CCR5: chemokine (C-C motif) receptor 5

cDC: conventional dendritic cell

cDNA: complementary deoxyribonucleic acid

CLR: C-type lectin receptor

CR1: complement receptor 1

CSA: chondroitin sulphate A

Csk: C-terminal src kinase

CXCL9: chemokine (C-X-C motif) ligand 9

CXCL10: chemokine (C-X-C motif) ligand 10

CXCL11: chemokine (C-X-C motif) ligand 11

CXCR3: chemokine (C-X-C motif) receptor 3

DC: dendritic cell

DC8: domain cassette 8

DC13: domain cassette 13

DCIR: DC immunoreceptor

DDT: dichlorodiphenyltrichloroethane
DEREG: depletion of Treg
DMT1: divalent metal transporter 1
DNA: deoxyribonucleic acid
DTR: diphtheria toxin receptor
EB: Evans blue
ECM: experimental cerebral malaria
eGFP: enhanced green fluorescent protein
Eomes: eomesodermin
EPCR: endothelial protein C receptor
FasL: Fas ligand
FeD: iron dextran-treated
GAP50: glideosome-associated protein 50
gC1qR: globular C1q receptor
GDF15: growth differentiation factor 15
GFP: green fluorescent protein
GPI: glycosylphosphatidylinositol
GzmB: granzyme B
HCP1: heme carrier protein 1
HFE: hemochromatosis gene
HO-1: heme oxygenase 1
HRG1: heme responsive gene 1
HRP2: *Plasmodium* histidine-rich protein 2
ICAM1: intracellular adhesion molecule 1
Id1: inhibitor of DNA binding 1
IgM: immunoglobulin M
IFN: interferon

IFN γ : interferon γ
IFN γ R2: interferon γ receptor 2
IL-1 β : interleukin-1 β
IL-1R: interleukin-1 receptor
IL-6: interleukin 6
IL-8: interleukin 8
IL-15: interleukin 15
IL-12p70: interleukin 12 (active heterodimer)
IL-10: interleukin 10
i.p.: intraperitoneal
KC: keratinocyte chemoattractant
LAG-3: lymphocyte activation gene 3
LAT: linker for activation of T cells
LDH: *Plasmodium* lactate dehydrogenase
LFA-1: lymphocyte function-associated antigen 1
MAFIA: macrophage Fas-induced apoptosis
MAVS: mitochondrial antiviral signalling protein
MBEC: murine brain endothelial cell
MCP-1: monocyte chemoattractant protein-1
MDA5: melanoma differentiation-associated protein 5
MFI: mean fluorescence intensity
MHC I: major histocompatibility complex I
MHC II: major histocompatibility complex II
mRNA: messenger ribonucleic acid
MyD88: myeloid differentiation factor 88
NFAT: nuclear factor of activated T cells
NK: natural killer

NLR: Nod-like receptor

NLRP3: NLR containing pyrin domain 3

PAR-1: protease-activated receptor 1

PBMC: peripheral blood mononuclear cell

PBS: phosphate-buffered saline

PCR: polymerase chain reaction

pDC: plasmacytoid dendritic cell

PECAM1: platelet endothelial cell adhesion molecule 1

pfcr1: *P. falciparum* chloroquine resistance transporter

PfEMP1: *P. falciparum* erythrocyte membrane protein 1

pfmdr1: *P. falciparum* multidrug resistance 1

PMA: phorbol 12-myristate 13-acetate

PPAR γ : peroxisome proliferator-activated receptor γ

PTK: protein tyrosine kinase

PTP: protein tyrosine phosphatase

PTP-PEST: PTP-proline-, glutamic acid-, serine-, and threonine-rich

RAG: recombination-activating gene

RIFIN: repetitive interspersed family of polypeptides

RLU: relative luminescence units

RLR: RIG-I-like receptor

RNA: ribonucleic acid

SCID: severe combined immunodeficient

SHP-1: SH2 domain-containing phosphatase 1

SLP-76: Src homology 2 domain-containing leukocyte protein of 76 kDa

SMAD: homolog of mothers against decapentaplegic

STAT1: signal transducer and activator of transcription 1/4

STAT4: signal transducer and activator of transcription 4

STEAP: six-transmembrane epithelial antigen of the prostate

STEVOR: subtelomeric variant open reading frame

TAP: transporter associated with antigen processing

T-bet: T-box expressed in T cells

TCR: T cell receptor

TfR2: transferrin receptor 2

TLR: Toll-like receptor

TNF: tumour necrosis factor

Tr1: type 1 regulatory cell

Treg: regulatory T cell

TWSG1: twisted-gastrulation 1

VCAM1: vascular cell adhesion molecule 1

VLA-4: very late antigen 4

WHO: World Health Organization

YETI: YFP-enhanced transcript for IFN γ

YFP: yellow fluorescent protein

ZO-1: zonula occludens-1

Chapter One

Literature Review

1. Epidemiology of Malaria

Malaria has caused pathology in humans for thousands of years (1-3) and is the strongest known selective pressure in the recent history of the human genome (4). Malaria-like diseases have been described in numerous historical texts ranging from Europe to China, and have documented the severe and pervasive effects that malaria has had on the cognitive, physical and socioeconomic capacity of the infected individuals and communities (5). Moreover, the genetic variants in the genome that confer resistance to malaria are responsible for the most common Mendelian diseases in humans (6), such as sickle-cell anemia (7), thalassemia (8), and glucose-6-phosphatase deficiency (9). Thus, malaria has not only had a profound impact on society and culture, but on human evolution itself.

Currently 91 countries have ongoing malaria transmission, putting nearly half of the world's population at risk of this disease (10). According to the latest estimates from the WHO, there were 212 million cases (range 148 – 304 million) and 429, 000 deaths (range 235, 000 – 639,000) due to malaria in 2015 (10). The African Region accounted for 90% of the total malaria cases and 92% of the deaths, followed by the South-East Asia Region, which had 7% of the total malaria cases and 6% of the deaths (10) (Figure 1). Furthermore, children under five are particularly vulnerable to malaria infection, with over two-thirds of all malaria deaths occurring in this age group (10).

Malaria is an infectious, mosquito-borne disease caused by parasites of the *Plasmodium* genus. Humans are the natural host for four different species: *P. falciparum*, *P. vivax*, *P. malariae* and *P. ovale*, and two zoonotic species, *P. knowlesi* and *P. cynomolgi*, have recently been shown to be capable of causing pathology in humans (11,12). Most cases of malaria are caused by either

P. falciparum or *P. vivax*. *P. falciparum* is the most prevalent species in sub-Saharan Africa and is responsible for the majority of severe complications and deaths (~99%) due to malaria (10), while *P. vivax* is the dominant species outside of Africa, and is capable of causing a relapse after the resolution of the primary infection due to a dormant liver stage (13).

The initial symptoms of malaria are non-specific and flu-like, and include fever, headache, malaise, fatigue and muscle ache, with nausea and vomiting occurring frequently (14). The periodic febrile response that characterizes malaria is caused by the synchronous rupture of mature erythrocytic schizonts. The frequency of this event differs between the species of *Plasmodium*, which resulted in malaria historically being defined by the frequency of the induced fever (5). *P. vivax* and *P. malariae* infection were described as benign tertian and quartan fevers, respectively, due to the febrile episodes recurring in two or three day intervals, and *P. falciparum* infection was referred to as subtertian malignant fever, owing to its irregular fever pattern and its association with severe and often fatal complications (5,15).

Although severe pathology is typically the result of infection with *P. falciparum*, *P. vivax* (16) and *P. knowlesi* (17) have also been observed to cause severe malaria. The manifestation of severe symptoms depends on the degree of antimalarial immunity possessed by an individual (18,19). Immunity is dependent upon both the number of malaria infections experienced and the intervals of time between them. Protection against severe malaria is typically achieved after one or two infections, while immunity to the clinical development of malaria requires many frequent infections (18,19). Moreover, immunity is quickly lost after a short period of time (6 to 12 months) without reinfection (5). Thus, due to the time required to attain effective immunity to malaria, severe malaria typically occurs in young children in regions of stable endemicity,

whereas people remain vulnerable to malaria morbidity and mortality throughout their lifetime in regions of unstable endemicity.

Fortunately, increased malaria prevention and control programmes are effectively decreasing the burden of malaria. Between 2000 and 2015, the global cases of malaria were reduced by 41% and the rate of mortality due to malaria decreased by 62% (10). Moreover, of the 106 countries that had ongoing malaria transmission in 2000, 57 reduced their number of new malaria cases by greater than 75% by 2015 (20). Vector control using insecticide-treated mosquito nets and indoor residual spraying; the introduction of rapid diagnostic tests that allow timely and appropriate treatment; and the increased use of highly effective artemisinin-based combination therapies have greatly aided the progress of malaria elimination. However, growing insecticide and drug resistance, and an inadequate understanding of the pathology of severe malaria are threatening the progress achieved so far and are preventing the effective treatment of severe complications.

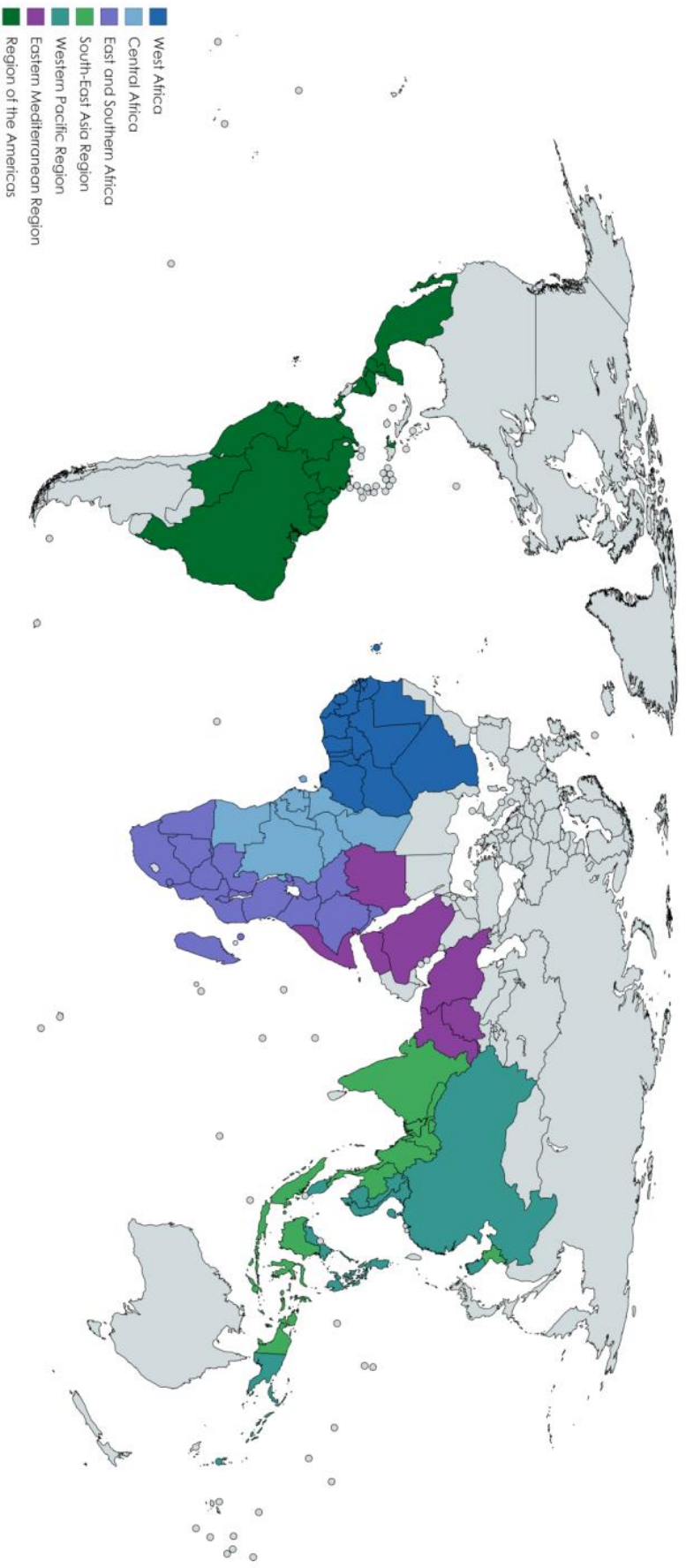


Figure 1. WHO Regions. African Region, West Africa: Algeria, Benin, Burkina Faso, Cabo Verde, Cote d'Ivoire, Gambia, Ghana, Guinea, Guinea-Bissau, Liberia, Mali, Mauritania, Niger, Nigeria, Senegal, Sierra Leone and Togo. **African Region, Central Africa:** Angola, Burundi, Cameroon, Central African Republic, Chad, Congo, Democratic Republic of Congo, Equatorial Guinea, Gabon and Sao Tome and Principe. **African Region, East and Southern Africa:** Botswana, Comoros, Ethiopia, Eritrea, Kenya, Madagascar, Malawi, Mozambique, Namibia, Rwanda, South Africa, South Sudan, Swaziland, Uganda, United Republic of Tanzania, Zambia and Zimbabwe. **South-East Asia Region:** Bangladesh, Bhutan, Democratic People's Republic of Korea, India, Indonesia, Myanmar, Nepal, Thailand and Timor-Leste. **Western Pacific Region:** Cambodia, China, Lao People's Democratic Republic, Malaysia, Papua New Guinea, Philippines, Republic of Korea, Solomon Islands, Vanuatu and Vietnam. **Eastern Mediterranean Region:** Afghanistan, Djibouti, Iran, Pakistan, Saudi Arabia, Somalia, Sudan and Yemen. **Region of the Americas:** Belize, Bolivia, Brazil, Colombia, Ecuador, El Salvador, French Guiana, Guatemala, Guyana, Haiti, Honduras, Mexico, Nicaragua, Panama, Peru, Suriname and Venezuela. **Greater Mekong Sub-region:** Cambodia, Thailand, Lao People's Democratic Republic, Myanmar, Vietnam and Yunnan Province of China. Figure generated by KV using mapchart.net.

1.1 Malaria Life Cycle

Malaria is typically transmitted by the bite of an infected female anopheline mosquito, although blood-borne transmission (resulting from blood transfusion (21) or needle-sharing among intravenous drug users (22)) and congenital transmission (23) can also occur. *Plasmodium* sporozoites, which are present in the salivary glands of the infected mosquito, are injected into the dermis while the mosquito probes for blood (24) (Figure 2). The size of the sporozoite inoculum is highly inconsistent (25) and it has been shown that four to seven bites from *P. falciparum*-infected mosquitoes are required to ensure that 100% of volunteers are infected (26). The sporozoites leave the injection site slowly over several hours following the mosquito bite, with half of the sporozoite inoculum remaining in the skin one hour post-infection (27,28). Approximately 70% of the sporozoites that exit the skin within the first hour enter the bloodstream and traffic to the liver, while the remaining 30% invade the lymphatic vessels and become trapped within the proximal lymph nodes (28).

Upon reaching the liver, the sporozoites cross the liver sinusoidal barrier by passing through Kupffer cells (29,30) and then traverse through several hepatocytes before invading a final hepatocyte and forming a parasitophorous vacuole (30-32). Within the vacuole, the sporozoite undergoes a cycle of asexual amplification known as schizogony, forming an exoerythrocytic schizont that contains tens of thousands of merozoites (15,18). At the end of this clinically silent hepatic stage, merozoite-containing merozoites are released into the bloodstream (33). During *P. vivax* (and *P. ovale*) infection, sporozoites can remain within the liver in a dormant stage called hypnozoites, which are unaffected by the most commonly used anti-malarial drugs and are capable of causing clinical relapse (13).

Once released from the merozoites, the merozoites quickly invade erythrocytes, where they go through another cycle of asexual replication. The merozoites develop into immature or ring stage trophozoites, before progressing to mature trophozoites that undergo schizogony to form an erythrocytic schizont that contains six to thirty-six merozoites (18). Rupture of the schizonts releases the merozoites, allowing another cycle of erythrocyte invasion and parasite replication. The blood-stage of the parasite is responsible for the clinical symptoms of malaria. The synchronous rupture of the erythrocytes occurs at regular time intervals, dependent on the species of *Plasmodium*, and is responsible for the periodic febrile response that characterizes malaria (15,34). Parasitization of the erythrocytes by *P. falciparum*, but not by *P. vivax*, increases the rigidity and adhesiveness of the erythrocytes, augmenting their sequestration within the microvasculature, and contributing to the severe complications of malaria (35-38).

A subset of the merozoites will differentiate into female or male gametocytes upon infection of the erythrocytes (18,39). When ingested by a feeding anopheline mosquito, these forms mature into macrogametes and microgametes, respectively, which are capable of combining to form a zygote (18,39). The zygote transforms into an ookinete and penetrates the gut wall of the mosquito, where it matures into an oocyst, which then undergoes schizogony to produce thousands of sporozoites (18,39). Upon rupture of the oocyst, the sporozoites migrate to the salivary glands and wait for the mosquito to bite another human, thereby completing the infectious cycle (39). Maturation of the infectious sporozoites within the vector typically requires ten to fourteen days following the blood meal, thus female mosquitos need to survive for at least that long to be capable of transmitting the malaria infection (15,40).

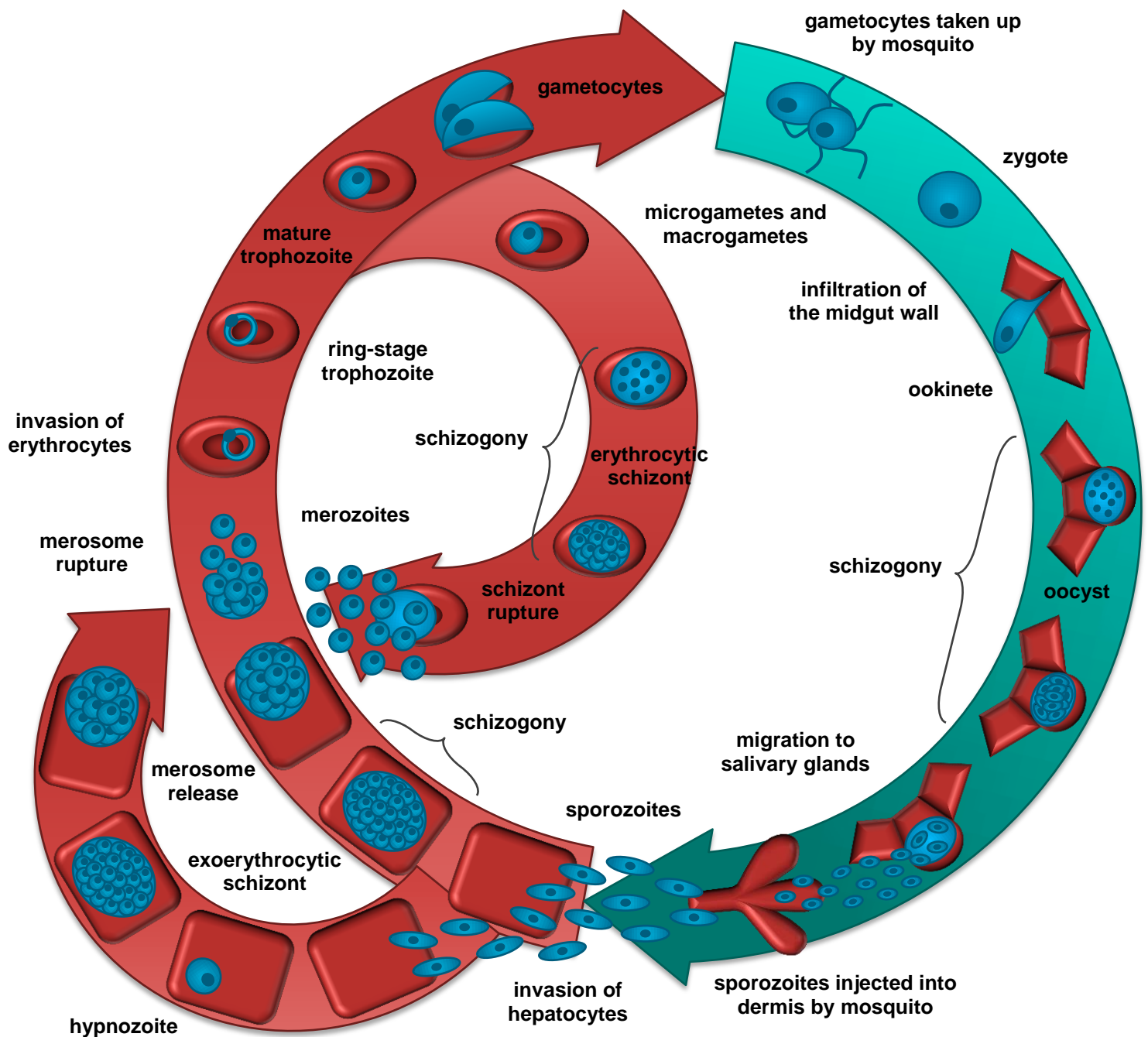


Figure 2. Malaria Life Cycle. Sporozoites are injected into the dermis while the mosquito probes for blood, and slowly leave the injection site by entering the bloodstream. The sporozoites traffic to the liver, invade a hepatocyte and undergo schizogony, forming an exoerythrocytic schizont containing tens of thousands of merozoites. The schizont ruptures and releases the merozoites into the bloodstream. Hypnozoites, a dormant form of the parasite, can form during *P. vivax* (and *P. ovale*) infection. The merozoites invade erythrocytes, develop into ring-stage and mature trophozoites, and undergo another cycle of schizogony to form an erythrocytic schizont containing six to thirty-six merozoites. Rupture of the schizonts releases the merozoites, allowing another cycle of erythrocyte invasion. A subset of merozoites differentiates into female or male gametocytes and is ingested by feeding anopheline mosquitoes. The gametes mature into macrogametes and microgametes, which combine to form a zygote. The zygote transforms into an ookinete and penetrates the gut wall of the mosquito, where it matures into an oocyst, and undergoes schizogony to produce thousands of sporozoites. Upon rupture of the oocyst, the sporozoites migrate to the salivary glands and wait for the mosquito to bite another human. Figure generated by KV.

1.2 Vector Control

Between 2000 and 2015, there was a renewed global interest in vector control for malaria, and the resulting campaigns to deliver insecticide-treated nets achieved significant coverage in endemic countries, resulting in a massive reduction in the burden of malaria (20). Insecticide-treated nets and indoor residual spraying are the two most important measures in the prevention of mosquito bites. It is estimated that during the last fifteen years, insecticide-treated nets were responsible for over two-thirds of the cases prevented by the increased malaria control interventions, while indoor residual spraying accounted for approximately one-tenth (20). Nevertheless, further progress toward the reduction of malaria transmission through vector control is threatened by the lack of adequate coverage and growing insecticide resistance (20).

There are two types of insecticide-treated nets: conventionally-treated nets, which have been treated with an insecticide and need to be re-treated at least once per year; and long-lasting insecticidal nets, which are made with netting material that has insecticide incorporated within the fibres and retain their activity for approximately three years (41). The treated nets provide both a mechanical barrier, that prevents access of the mosquito vectors, and a chemical barrier, that kills mosquitos that come into contact with the insecticide (41). Insecticide-mediated reduction of the vector population also provides protection to those who do not sleep underneath the nets, even at a relatively modest coverage (~60%) of the total population (41,42).

The proportion of the population sleeping under a bed net increased from less than 2% in 2000 to 53% in 2015, with over 178 million nets delivered in 2015 (10,20). Despite increased access to insecticide-treated nets, the number of available nets is still insufficient to achieve universal access. An estimated minimum of 200 million nets, and likely as many as 300

million, would need to be delivered each year to ensure that all individuals at risk of malaria have access to a net (20). The WHO has proposed to correct this inadequacy by providing only long-lasting insecticidal nets and by distributing the nets through existing public health services, such as routine immunizations and antenatal visits (10,41).

Indoor residual spraying involves spraying a long-lasting insecticide on the internal walls and ceilings of dwellings where mosquito vectors are likely to rest after feeding (43). Many of the important malaria vectors are indoor feeding and resting species, resulting in a high probability that an infected mosquito will come into contact with a treated wall, resulting in a progressive decline in both vector longevity and density (43). Unlike insecticide treated nets that interrupt transmission before the mosquito can infect a human with sporozoites, indoor residual spraying mainly inhibits transmission after feeding, preventing the mosquito from transmitting malaria to others in the vicinity (43). Therefore, indoor residual spraying requires high coverage (>85%) to provide effective protection (43).

The Global Malaria Eradication Program, conducted from 1955 to 1969, was largely based on indoor residual spraying and caused a significant reduction in the global malaria burden (43,44). Malaria was eradicated from Europe and several countries in Asia and the Caribbean, and the incidence reduced by at least 90% in many areas of Asia and Southern America (43,44). However, most of the African continent was not involved in this program, and subsequent implementation of indoor residual spraying has been ineffective in large parts of sub-Saharan Africa due to inadequate coverage (43,44). The percentage of the population at risk of malaria that is protected by indoor residual spraying decreased from a maximum of 5.7% in 2010 to 3.1% in 2015 (10). The declining implementation of this strategy may be attributable to a switch from pyrethroids to more expensive insecticides (10).

Currently, pyrethroids are the only class of insecticide available for use in long-lasting insecticidal nets and are used in over 80% of indoor residual spraying (45). Pyrethroids act by disrupting the voltage-gated sodium channels found in insect nerves (46) are relatively safe for use in close proximity to humans (45). However, the extensive use of a single class of insecticide is a major selection pressure for pyrethroid resistance, which is now widespread in *Anopheles gambiae* and *A. funestus* mosquitoes, two major malaria vectors (47,48). A low level of pyrethroid resistance was initially selected through the reactivation of an old DDT resistance mechanism (45). More recently, an increase in resistance was associated with the upregulation of a pyrethroid-metabolizing cytochrome p450 (48,49). This mutation caused resistance several orders of magnitude higher than the DDT mutation, and has prompted a shift to the use of the insecticides DDT and bendiocarb for residual indoor spraying in several African countries (50). New insecticides with different modes of action and reduced use of a single class of insecticide are needed for vector control to remain effective.

In addition to insecticide-treated nets and indoor residual spraying, vector control can also involve larval source management. The WHO issued a position statement in 2012 that recommended larvicide as a supplement to existing vector control in regions where mosquito breeding sites are fixed, readily identifiable and accessible, and where the density of the protected population is sufficiently high to justify the necessary resources (51). Larval source management can include habitat modification or manipulation (*e.g.*, surface water drainage), biological control (*e.g.*, the introduction of predatory fish) or larviciding (*e.g.*, the use of insecticides) (20). Unlike the previously mentioned vector control strategies, larval source management targets the immature, aquatic forms of the vector, thereby decreasing the abundance of the adult vectors and subsequently the incidence of infectious bites (52). In

2014, thirty-two countries reported using habitat modification or manipulation, and forty-five countries reported using biological control or larviciding (20). Nevertheless, the scale of larval source management was not reported, therefore the efficacy of this intervention is difficult to quantify (20).

1.3 Chemoprophylaxis

Beyond inhibiting the transmission of malaria by controlling the vector population, chemoprevention in pregnant women and children has also decreased the incidence of malaria in the most clinically susceptible groups. Chemoprevention is the administration of curative doses of antimalarial medicine to vulnerable populations, regardless of whether the recipient is infected (20). The WHO recommends intermittent preventive treatment for both pregnant women and infants in areas of moderate to high transmission, and seasonal malaria chemoprevention in children under the age of five in areas that have highly seasonal malaria transmission (53).

Sulfadoxine-pyrimethamine is prescribed for intermittent preventive treatment both during pregnancy and in infants, and sulfadoxine-pyrimethamine plus amodiaquine is recommended for seasonal malaria chemoprevention (54-56). Sulfadoxine and pyrimethamine competitively inhibit dihydropteroate synthase (*pfdhps*) and dihydrofolate reductase (*pfdhfr*), respectively, two sequential enzymes involved in tetrahydrofolate synthesis (57). The activities of sulfadoxine and pyrimethamine are synergistic, but they act on the same biosynthesis pathway, therefore they are essentially a single antimalarial agent and not a combination therapy (57). Since folic acid is required for proper fetal development, sulfadoxine-pyrimethamine is only recommended after the first trimester (58-60). Additionally, the

standard doses of folic acid given during pregnancy were not shown to interfere with the efficacy of this treatment (58,61,62).

Sulfadoxine-pyrimethamine plus amodiaquine is recommended for seasonal malaria chemoprevention, as this treatment was shown to confer greater protection than other drug combinations in clinical trials (54,63), and because these drugs retain their efficacy in the regions of Africa with seasonal transmission (54,64). Amodiaquine is rapidly metabolized to desethylamodiaquine, which exerts an antimalarial effect by inhibiting heme detoxification (65). Amodiaquine or amodiaquine plus sulfadoxine-pyrimethamine were also shown to provide protection from malaria-induced pathology during pregnancy comparable to that of sulfadoxine-pyrimethamine; however, the addition of amodiaquine increased the frequency of minor adverse effects (66,67). Similarly, intermittent treatment in infants with amodiaquine offered protection comparable to sulfadoxine-pyrimethamine (68), but minor adverse effects, which appeared to be associated with inaccurate age-based dosing, were reported in the children receiving amodiaquine (69). Therefore the addition of amodiaquine is currently only recommended for seasonal malaria chemoprevention (54).

Administration of sulfadoxine-pyrimethamine during routine antenatal visits was found to decrease the risk of severe maternal anemia, low birth weight and perinatal mortality (70-72). Following a recommendation made by the WHO in 2012, the proportion of pregnant women receiving preventive treatment dramatically increased (20). In 2015, 31% of pregnant women received three or more doses of sulfadoxine-pyrimethamine, compared to 18% in 2014 and just 6% in 2010 (10). The effectiveness of sulfadoxine-pyrimethamine is threatened by the increasing prevalence of multiple resistance-conferring mutations in dihydropteroate synthase and dihydrofolate reductase. In regions with resistant quintuple mutant parasites (*pfdhps-*

K540E), sulfadoxine-pyrimethamine treatment has been shown to remain effective, possibly due to the acquired partial immunity of the pregnant women (72-74). However, the recent emergence of highly resistant sextuple mutant parasites (*pfdhps*-A581G) in Tanzania has been associated with increased treatment failure (75). Therefore, the development of alternative drugs or prevention strategies in pregnant women (and in infants, as discussed below) will be necessary to maintain the efficacy of this intervention.

Due to the increased resistance of the quintuple mutant parasites, intermittent preventive treatment in infants using sulfadoxine-pyrimethamine is only recommended in regions where the prevalence of resistant parasites is less than 50% (76). Given the pervasiveness of quintuple mutants in East Africa (77,78), this recommendation has essentially resulted in the restriction of this protective measure to West Africa, with only one country, Chad, having reported the adoption of an intermittent preventive treatment for infants policy in 2014 (20). Clinical trials have shown that preventive treatment with sulfadoxine-pyrimethamine given at the same time as routine vaccinations decreases the incidence of clinical malaria, anemia and hospital admissions associated with malaria (79,80). Furthermore, administration sulfadoxine-pyrimethamine was not found to have a negative effect on the protective efficacy of the standard immunizations (56). Thus, large-scale implementation of intermittent preventive treatment in infants would likely substantially reduce malaria-related morbidity in regions where drug resistance to sulfadoxine-pyrimethamine is low to moderate.

In addition to chemoprevention aimed at young infants, the WHO also recommends preventive treatment in children under the age of five in regions that have acute seasonal transmission of malaria and where resistance to sulfadoxine-pyrimethamine and amodiaquine is low (20). Across the Sahel subregion of Africa (between the Sahara desert and the

Sudanian savanna), most childhood malaria morbidity and mortality (>60%) occurs during the rainy season (81). Administration of preventive malaria treatment at monthly intervals during this period of time was found to decrease malaria morbidity by 75%, and this reduction was still observed in areas where insecticide-treated net usage was high (82). Approximately 25 million children in the Sahel subregion could benefit from seasonal malaria chemoprevention, although less than 20% of eligible children received this treatment in 2015 (83). Moreover, a recent trial determined that seasonal malaria chemoprevention in children up to the age of ten resulted in a 60% decrease in the incidence of malaria (84), indicating that this intervention has the potential to protect an even larger range of children. Furthermore, an additional 10 million children in Southern Africa could be aided by seasonal preventive treatment if alternative antimalarials with lower levels of drug resistance were found (83).

Beyond the prevention of malaria using prophylactic antimalarial drugs, a malaria vaccine against *P. falciparum* has been developed. The RTS,S/AS01 vaccine is based on a large segment of the circumsporozoite protein of *P. falciparum*, which is expressed during the pre-erythrocytic stage of the parasite's life cycle (85). The carboxy-terminal segment of the circumsporozoite protein is fused to the surface protein of the hepatitis B virus, and is formulated with the novel adjuvant AS01 (85). The vaccine was shown to decrease clinical malaria by 39% and severe malaria by 31.5% in children that received the vaccine when they were between five to seventeen months of age (86). Infants that were given the vaccine between six to fourteen weeks of age, corresponding with the schedule of routine childhood vaccines, only had a 27% decrease in clinical malaria and no significant effect on the prevalence of severe malaria was observed (86).

Recently, the results of a long-term phase II trial of the vaccine demonstrated that its efficacy declined substantially over time; the risk of vaccinated children developing malaria was 35.9% less than the control group after one year, but only 4.4% after seven years (87). The necessity of a fourth booster dose to maintain protection was illustrated by a phase III trial; children receiving a fourth dose of the vaccine had a significantly reduced risk of malaria four years post-vaccination compared to children that only received three doses (88). Based on concerns surrounding the preventive efficacy of the vaccine that were raised by the above studies, and the programmatic feasibility of providing all four doses, the WHO has recommended further evaluation of the four-dose schedule in pilot implementation studies before considering the roll-out of country level vaccine programmes (89).

1.4 Rapid Diagnostic Tests

Historically fever was equated with malaria in endemic countries. Increased implementation of preventive measures, including vector control and chemoprevention, resulted in a massive decrease in the transmission and incidence of malaria over the past decade. Due to this substantial reduction in cases, the proportion of fevers caused by malaria has decreased substantially. Yet efforts to improve access to diagnostic testing and effective antimalarial medicine have lagged behind the implementation of prevention measures, leading to the overdiagnosis of malaria and the underdiagnosis of other febrile illnesses.

Malaria control requires an integrated approach that includes prevention, early and accurate diagnosis, and prompt treatment with effective antimalarial agents. The initial clinical manifestation of malaria typically includes fatigue, headache, vomiting and fever. This non-specific febrile presentation makes it impossible to distinguish malaria from other diseases solely

on the basis of clinical symptoms (90). Presumptive treatment of all fever episodes as malaria without parasitological confirmation not only results in inappropriate treatment, but precludes the proper treatment of fever caused by non-malaria sources, increases the selection pressure for drug resistance, and reduces public trust in the efficacy of antimalarial drugs (90).

Malaria is suspected in any patient that presents with a fever or a recent history of fever, in the absence of symptoms associated with other severe diseases (53). Parasitological confirmation can be accomplished through either microscopy or by a rapid diagnostic test. Microscopy requires well-maintained equipment, highly trained staff, a regular supply of reliable reagents, and electricity, making this diagnostic method unfeasible at all levels of the healthcare system in many countries (90). Alternatively, rapid diagnostic tests need limited training and can be performed in remote areas, affording universal access to accurate parasitological confirmation (90). Diagnostic testing at public health facilities in sub-Saharan Africa increased from 36% of all suspected cases of malaria in 2005, to 76% of all cases in 2015 (10,20). The increased frequency of parasitological confirmation was predominately due to the increased use of rapid diagnostic tests, which accounted for 74% of the diagnostic tests performed in 2015 (10).

Rapid diagnostic tests typically detect one or two different *Plasmodium* antigens in the finger-prick blood of people infected with malaria (53,91). The antigens used as diagnostic targets can be species-specific or conserved across the anthroponotic species of *Plasmodium* (91). *P. falciparum* infection can be identified by species-specific variants of HRP2 and LDH, while *P. vivax* infection can be identified by a species-specific variant of LDH (91). Additionally, panspecific LDH and aldolase are capable of non-specifically detecting *Plasmodium* infection (91).

The accuracy of the rapid diagnostic tests varies between brands and local epidemiological conditions, but overall the tests were shown to have a high panel detection score (sensitivity) and low false-positive rates (92). Moreover, it was demonstrated that withholding antimalarial treatment in febrile patients who had a negative test result was safe and did not increase the risk of complications or death (93). However, *P. falciparum* parasites lacking the HRP2 gene were recently detected in certain areas of South American and sub-Saharan African countries, and in Myanmar, India and Indonesia, potentially compromising the effectiveness of the *P. falciparum*-specific rapid diagnostic tests (10).

Finally, despite the recommendation by the WHO to confirm the presence of parasitemia in all suspected cases of malaria before treatment, the ratio of diagnostic tests performed to treatments administered suggests that many patients are being treated with antimalarial medicine without receiving a positive test result for malaria (10). Interviews with healthcare workers in Uganda indicated that while 92% believed that a positive result confirmed malaria, only 49% believed that a negative result excluded malaria (94). Studies in other settings have also demonstrated this trend, in which healthcare workers were reluctant to not administer antimalarial treatment after a negative result (95,96). Additional concerns with the rapid diagnostic tests included the proper collection of blood, incorrect interpretation of a faint test result, and healthcare workers being unhappy with negative results (95). Thus adherence would likely increase if the healthcare workers were provided with improved training and the ability to appropriately diagnose and treat febrile patients with a negative test result for malaria.

1.5 Treatment of Uncomplicated Malaria

Prompt and effective treatment of malaria after parasitological confirmation is essential to preclude progression to severe malaria and to reduce transmission by decreasing the anthroponotic parasite reservoir (53). If appropriate treatment is given quickly after the initial onset of symptoms, a rapid and full recovery is expected (53). However, if treatment is delayed or ineffective, *P. falciparum* infection can quickly progress to severe malaria, which is typically fatal without treatment (53). Artemisinin-based combination therapies are recommended by the WHO as the first-line treatment of uncomplicated malaria caused by *P. falciparum*, and currently all countries with endemic *P. falciparum* malaria have updated their treatment policy from the use of monotherapies to artemisinin-based combination therapies (53).

Artemisinin-based combination therapies pair a rapidly-acting, but short-lived artemisinin derivative with a long-lasting partner drug (53). The artemisinin component quickly reduces the parasite burden, and the partner drug ensures the elimination of the remaining parasites, thereby preventing the development of resistance to the artemisinin derivative (53). There are five artemisinin-based combination therapies that are currently approved for use: artemether and lumefantrine, artesunate and amodiaquine, artesunate and mefloquine, artesunate and sulfadoxine-pyrimethamine, and dihydroartemisinin and piperaquine (53).

Artemisinin is a sesquiterpene lactone with an endoperoxide bridge, and artemether, artesunate and dihydroartemisinin are semisynthetic lactol derivatives that were developed to manage the low bioavailability of artemisinin (97). Upon ingestion, artemisinin, artemether and artesunate are metabolized to the active metabolite, dihydroartemisinin (98). The antimalarial activity of artemisinins requires the generation of highly reactive carbon-centered radicals through the

cleavage of their endoperoxide bridge (99-101). Despite several decades of research, the iron source required for cleavage and the exact target of the activated artemisinins remain relatively uncertain (102-105). A study published recently validated heme as the predominant source of iron responsible for endoperoxide cleavage and indicated that activated artemisinins likely kill malaria parasites through a promiscuous targeting system (102). Artemisinins exhibit antimalarial activity throughout the asexual erythrocytic stage of the parasite (106), and also against the infectious gametocytes, interrupting malaria transmission (107). They act rapidly, reducing parasite numbers by approximately ten thousand-fold per asexual cycle, resulting in a one hundred million-fold decrease in the parasite load over a typical three-day course (108). Nevertheless, because they have a very short half-life (~1 hour), even five-day courses of artemisinin monotherapy are insufficient to fully clear parasites from the blood (109).

The drugs paired with the artemisinins exert their antimalarial activity through one of two main mechanisms. Sulfadoxine-pyrimethamine competitively inhibits two enzymes involved in folate metabolism (57), while amodiaquine (65,110), mefloquine (110,111), piperazine (112,113), and lumefantrine (114,115) are thought to bind to hemozoin, a heme dimer produced by hemoglobin degradation, preventing the detoxification of free heme to β -hematin. The elimination half-lives of the partner drugs range from the order of three to five days for sulfadoxine-pyrimethamine and lumefantrine, to two weeks for mefloquine and amodiaquine, and four weeks for piperazine (116-119). Extended half-lives offer a period of prophylaxis, but may contribute to increased drug resistance to the partner drugs due to sub-therapeutic concentrations of the drug remaining in the blood for months after treatment (65,120). Moreover, with the exception of lumefantrine, all of the drugs currently used in artemisinin-based combination therapies have been and still are

currently used as monotherapies, resulting in increased selection of resistance-conferring mutations (53).

Artemisinin resistance has been detected in five countries in the Greater Mekong subregion, but there is currently no evidence for resistance to artemisinins outside of this region (10,121). Reduced parasite sensitivity to artemisinins has manifested as delayed parasite clearance (partial resistance), and artemisinin-based combination therapies were shown to retain high cure rates so long as the partner drug remained effective (10,121). However, the failure to rapidly clear parasites has the potential to increase the risk of resistance developing against the partner drugs and could compromise the use of artemisinins in the treatment of severe malaria (20,53). Mutations in the Klech 13 propeller domain were identified as a marker for artemisinin resistance (20,121). More than 200 non-synonymous mutations in the Klech 13 gene have been reported, which were shown to have varying effects on the parasite clearance phenotype (121). Therapeutic efficacy studies conducted in 2015 in three countries in the Greater Mekong subregion identified C580Y as the dominant resistance mutation (121). In response to the increasing resistance of *P. falciparum* to artemisinins (and other antimalarial drugs) and a recommendation made by the WHO in 2014, all of the countries in this region have endorsed a goal to eliminate *P. falciparum* from the Greater Mekong subregion by 2030 (121).

Outside of the Greater Mekong subregion, treatment failure is associated with resistance-conferring mutations to the partner drug (20). Resistance to sulfadoxine-pyrimethamine is resultant of mutations in dihydropteroate synthase (*pfdhps*) and dihydrofolate reductase (*pfdhfr*), two enzymes involved in folate metabolism (57). Sulfadoxine-pyrimethamine has been shown to remain effective in areas with quintuple mutant parasites (*pfdhps*-K540E), but the presence of sextuple mutant parasites (*pfdhps*-A581G) is associated with increased treatment failure (72-75).

The other partner drugs are thought to exert their antimalarial effect by accumulating within the digestive vacuole and inhibiting heme detoxification; accordingly, mutations in the genes *pfcr1* and *pfmdr1*, which encode transport proteins located on the membrane of the digestive vacuole, are molecular markers of resistance to amodiaquine, mefloquine and lumefantrine. Although cross-resistance between the partner drugs can occur, different mutations have been shown to have varying effects on the susceptibility of *P. falciparum* to the different antimalarial drugs. For example, the N86Y mutation in *pfmdr1* confers resistance to amodiaquine, but increases parasite susceptibility to lumefantrine and mefloquine (122). Moreover, the K76T mutation in *pfcr1* is a molecular marker of resistance against amodiaquine (65,123), while resistance to mefloquine and lumefantrine is predominately mediated by an increased copy number of *pfmdr1* (123-126). Recently, amplification of *plasmepsin 2-3* (which encode hemoglobin-digesting proteases) and an E415G substitution within an exonuclease were shown to be markers of piperazine resistance (127,128).

In the absence of resistance to the partner drug, the currently recommended artemisinin-based combination therapies have been shown to have treatment failure rates of less than 5% (129), thus the choice of treatment for a region is determined by the efficacy of the partner drug on the local strains of *P. falciparum* (53). Artesunate and amodiaquine and/or artemether and lumefantrine have been adopted as the first-line treatment in most African countries, and the therapeutic efficacy of both treatments remains high (treatment failure rate of less than 10%) (10,20). Artesunate and sulfadoxine-pyrimethamine is the recommended first-line treatment for India, Somalia, Sudan and five countries in the Middle East (10,20). Overall, the treatment failure rate has been observed to be low, except for in certain areas of India, Somalia and Sudan (20). Artemether and lumefantrine or artesunate and mefloquine are the current first-line

treatments for most of the countries in South America, and have a treatment failure rate of less than 5% or 0%, respectively (10,20). And artesunate and mefloquine and/or dihydroartemisinin and piperazine are the first- or second-line treatments in Cambodia, Malaysia, Myanmar, China, Indonesia, Thailand and Vietnam (10,20).

Outside of Africa, *P. vivax* infection is the most prevalent cause of malaria. *P. vivax* parasites can remain within the liver as hypnozoites, which are unaffected by the most commonly used antimalarial drugs and are capable of causing a clinical relapse (53). Thus, treatment of *P. vivax* infection needs to target both the blood-stage and the liver-stage parasites. A three-day course of either chloroquine or artemisinin-based combination therapy is recommended for the treatment of blood-stage *P. vivax* parasites, dependent upon the regional resistance to chloroquine (53), accompanied by a fourteen-day course of primaquine to treat the hypnozoites and prevent clinical relapse (53,130).

Chloroquine exerts an antimalarial effect by inhibiting heme detoxification (131), and the K76T mutation in the *pfcr* gene is the main molecular marker of resistance against this drug (132). Moreover, artemisinin-based combination therapies generally demonstrate a high level of efficacy against *P. vivax*, with the exception of artesunate and sulfadoxine-pyrimethamine, due to prevalent sulfadoxine-pyrimethamine resistance (53,133). The asexual stages of *P. vivax* are susceptible to primaquine, so chloroquine and primaquine can be considered a combination treatment against the blood-stage infection (53). Primaquine increases the risk of haemolytic anemia in people with glucose-6-phosphate-dehydrogenase enzyme deficiency, consequently primaquine should only be given to these individuals using a modified schedule and under close medical supervision (53).

Surveillance of the therapeutic efficacy of antimalarial drugs is necessary to ensure that the recommended treatment remains effective against the local *Plasmodium* variants. Recurrence of malaria can be the result of reinfection, recrudescence (treatment failure), or relapse (53). Treatment failure can be caused either drug resistance or inadequate exposure to the drug through sub-optimal dosing, poor adherence or substandard medicine (53). Recurrence of *P. falciparum* infection within four weeks is typically thought to be caused by treatment failure and recurrence after four weeks is usually presumed to be a new infection, but PCR genotyping is required to be certain of the distinction (53). Surveillance of the therapeutic efficacy of *P. vivax* malaria is complicated by the possibility of relapse due to hypnozoites (53). However, relapses occurring in less than a month are usually suppressed by the slowly eliminated antimalarial drugs that are used in regions of *P. vivax* endemicity, such as chloroquine, mefloquine and piperazine (53). Thus, reappearance of parasitemia within this time period can still be used as an indication of treatment failure (53). If the total treatment failure proportion is greater than 10%, the WHO recommends that the national malaria treatment policy should be changed (53,121).

1.6 Diagnosis and Treatment of Severe Malaria

If suspected cases of malaria are not quickly confirmed and appropriately treated, uncomplicated malaria can rapidly progress to severe symptoms. Severe malaria typically manifests as coma (cerebral malaria), metabolic acidosis, severe anemia, hypoglycaemia, hyperparasitemia, acute renal failure or acute pulmonary edema, and is almost always fatal if left untreated (53). Even with effective antimalarial treatment and supportive care, the case-fatality rate for severe malaria is still 10-20% overall (53). Moreover, children that recover from cerebral malaria often sustain severe brain injuries and approximately one-quarter develop long-term neurological sequelae, including deficits in gross motor function, loss of speech, blindness, hearing impairments,

behavioural problems and epilepsy (134,135). Thus, there is a need for adjunctive therapies to limit the pathological processes that contribute to both death and disability.

Severe malaria is defined by the WHO as the presentation of one or more of the above symptoms, occurring in the absence of an alternative source, and in the presence of asexual parasitemia (53). Death from severe malaria can occur within hours of admission to a health centre, therefore it is important to achieve therapeutic plasma concentrations of effective antimalarial drugs as quickly as possible (53). The WHO currently recommends treatment with intravenous or intramuscular artesunate for a minimum of 24 hours, followed by a three-day course of artemisinin-based combination therapy (53); however, quinine is still used for the treatment of severe malaria in the majority of countries (10). Parenteral artesunate was shown to decrease mortality from severe malaria by 22.5% - 34.7% compared to parenteral quinine (136-138). A small increase in neurological sequelae at the time of discharge was associated with artesunate treatment of severe malaria in children, but this was hypothesized to be attributable to the severely ill patients that would have died had they received the parenteral quinine, and there was no evidence of a difference in sequelae at 28 days post-discharge (136,137). If artesunate is unavailable, the WHO recommends intramuscular artemether in preference to quinine for the treatment of severe malaria, due to improved clinical outcome (53,139).

Patients with severe malaria also require supportive care to manage the associated complications. The specific syndrome(s) need to be characterized upon admission to the healthcare center through either a blood test (*e.g.*, blood glucose to diagnose hypoglycaemia) or clinical examination (*e.g.*, Glasgow or Blantyre coma score to identify cerebral malaria), and then treated appropriately (53). For example, hypoglycaemia is corrected with a glucose-containing infusion and convulsions are treated with intravenous benzodiazepines or intramuscular paraldehyde (53).

Since the clinical presentation of severe malaria overlaps considerably with septicaemia and pneumonia, broad-spectrum antibiotic treatment is typically given concomitantly with antimalarial drugs until the presence of a bacterial infection can be excluded (53). Notably, coma can also be caused by meningoencephalitis; cerebral malaria generally does not involve meningeal irritation, but bacterial meningitis is almost always fatal, thus a diagnostic lumbar puncture would need to be performed to exclude this condition (53).

The clinical diagnosis of cerebral malaria was found to be incorrect in a substantial proportion of patients with incidental parasitemia following autopsy (140,141). Septicaemia, pneumonia and bacterial meningitis were found to be responsible for coma and death in the majority of the misdiagnosed individuals (140,141). Incorrect diagnosis precludes proper treatment of severe symptoms caused by non-malaria sources, thereby increasing the case-fatality rate (141), and it also undermines studies aimed at identifying the etiology of cerebral malaria. The severity of hemorrhages, axonal damage and BBB disruption in the brain were found to correlate with changes in the retina (142,143). Malaria retinopathy (hemorrhages, retinal whitening and vessel changes) is a set of ocular fundus findings that are collectively unique to malaria (144-147). The severity of retinopathy in Malawian children was shown to correlate with an increased risk of mortality and a prolonged recovery time in survivors (144-146), and the presence of malaria retinopathy was determined to have a sensitivity of 95% and a specificity of 100% when used for the identification of cerebral malaria in parasitemic patients (147). Retinopathy has also been observed in non-cerebral severe malaria, but is generally less severe (145). Fewer studies have been conducted in adults; but malaria retinopathy does not appear to be as prevalent as it is in children with cerebral malaria (147-150). The addition of malaria retinopathy to the diagnosis of pediatric cerebral malaria would likely decrease misdiagnosis in these patients.

The mortality rate and the severity of the sequelae resulting from severe malaria is highly dependent on the clinical manifestation; severe malarial anemia has a relatively low mortality rate, while cerebral malaria has a higher mortality rate and a large risk of long-term neurocognitive impairments (53). In an attempt to reduce the high mortality and complications associated with cerebral malaria, many adjunctive therapies have been evaluated, but none are currently recommended for use and many have been shown to be detrimental (53). An improved understanding of the mechanisms contributing to neuropathology would likely inform the design of effective adjunctive therapies and minimize the pathology associated with cerebral malaria.

2. Pathogenesis of Cerebral Malaria

Cerebral malaria is characterized by the sequestration of parasitized erythrocytes within the microvasculature of the brain (140,151,152). Parasitization of erythrocytes by *P. falciparum* induces the expression of parasite proteins involved in cytoadherence on the surface of the infected erythrocytes, resulting in their accumulation within various organs (153). While the exact etiology of cerebral malaria remains uncertain, obstruction of cerebral microvascular flow (154), widespread endothelial activation (155) and an aberrant inflammatory response (156) are commonly proposed to be responsible for the pathogenesis of cerebral malaria. The relative contributions of each are still a matter of contention, but recent findings suggest that all three likely contribute to the induction of pathophysiology (157).

2.1 Cellular Adhesion of Parasitized Erythrocytes

Erythrocytes infected with immature ring-stage parasites circulate freely in the periphery of patients infected with *P. falciparum*, while erythrocytes infected with mature trophozoites accumulate within various organs (153). During the maturation of the parasite, the adhesive

phenotype of the erythrocyte is changed to enhance the survival of the parasite by reducing splenic clearance. The membrane of the erythrocyte is remodelled to form knobs that serve as platforms for the presentation of PfEMP1, a membrane-embedded cytoadherence protein (158-161). PfEMP1 undergoes extensive antigenic variation to evade host defense mechanisms, and the resulting variants of PfEMP1 exhibit differential affinity for host receptors (162). Moreover, endothelial cells from different vascular beds have distinct transcriptional profiles and express a unique assortment of cell surface receptors (163). Since specific PfEMP1 variants have been shown to correlate with severe disease (164-169), it has been hypothesized that the preferential binding of these variants to different receptors may be responsible for the organ-specific syndromes induced by *P. falciparum* infection (170,171).

Parasitized erythrocytes have been shown to bind to a diverse array of endothelial cell receptors through their repertoire of PfEMP1 variants, including: CD36, E-selectin, ICAM1, P-selectin, PECAM1, VCAM1, EPCR, CSA, thrombospondin and heparan sulphate (172,173). A parasitized erythrocyte can only express one variant at a time, but gene expression can switch at the start of each new asexual cycle, changing the adhesion phenotype of the parasite (174). The pathophysiological significance of the binding of parasitized erythrocytes to the above receptors is unclear; the majority of field isolate studies do not show an association between disease severity and binding to the receptors listed above (172,175). However, the receptors may act synergistically *in vivo* to promote cytoadherence, and the individual receptors may not have a dominant role in promoting adhesion (172,176,177).

PfEMP1 has a high degree of domain compositional order, including twenty-three conserved domain cassettes (178). Most domain cassettes encode two to four domains that are not connected to each other and are located in the N- or C-terminal of the protein (178). Severe

malaria syndromes in children, including cerebral malaria, were observed to be associated with PfEMP1 variants containing the domain cassettes DC8 and DC13 (168). Recently, EPCR was identified as a receptor for both of these domain cassettes (179), and EPCR variants have been shown to correlate with disease severity (180) (Figure 3). Additionally, the expression of ICAM1 has been shown to be upregulated by cytoadherence (181), and both DC13 and DC4 possess dual EPCR- and ICAM1-binding activities (182-184); the initial sequestration of parasites through EPCR may result in further accumulation of parasitized erythrocytes through ICAM1.

Parasitized erythrocytes can also bind to uninfected erythrocytes to form rosettes (185) and to platelets to form clumps (186) (Figure 3). Severe malaria has been associated with rosetting and clumping, but the strength of the correlation varies with the different field isolates (172,187). Uninfected erythrocytes were shown to form rosettes around cytoadherent parasitized erythrocytes *in vitro*, and these complexes caused enhanced microvascular obstruction compared to non-rosetting cytoadherent erythrocytes (188). PfEMP1 has also been shown to play a role in rosette formation, as have the parasite RIFIN and STEVOR proteins (189,190), and host IgM antibodies and CR1 (172,191,192). Furthermore, rosetting field isolates were found to favour either A or B blood group antigens, and to form larger rosettes with their preferred blood group (193). Interactions between platelets and parasitized erythrocytes may further contribute to vascular obstruction (172), and clumping can result in platelet activation and the production of inflammatory mediators (172). Parasitized erythrocytes are capable of binding to the platelet receptors CD36, P-selectin and gC1qR (186,194,195), but the parasite ligands mediating this interaction are currently unknown (172).

2.2 Microvascular Endothelial Dysfunction

Activated protein C plays a crucial role in regulating inflammation, apoptosis, vascular permeability and coagulation (196-198). Protein C is activated by thrombomodulin and thrombin, and this process is greatly enhanced by the presentation of protein C by EPCR (199,200). Cytoadherence of parasitized erythrocytes to the endothelium decreases the expression of thrombomodulin and EPCR (201) and inhibits the function of the residual EPCR (169,179,202-204), thereby resulting in reduced activation of protein C (199,200). Thus the parasite-induced attenuation of protein C activation may contribute to the endothelial dysfunction and coagulopathy observed during cerebral malaria (204) (Figure 3).

Binding of activated protein C to EPCR facilitates the activation of PAR-1, leading to the induction of cytoprotective pathways that suppress inflammation and apoptosis, alter gene expression, and stabilize the endothelial barrier (196,197,205). In this manner, activated protein C is able to reduce the expression of ICAM1 on endothelial cells (206), potentially attenuating the sequestration of parasitized erythrocytes within the brain. Furthermore, activated protein C-mediated signalling through PAR-1 was also shown to prevent apoptosis in brain endothelial cells following ischemic injury (207) and to protect neurons from NMDA-induced apoptosis (208). Importantly, activated protein C was found to be capable of stabilizing the endothelial barrier by upregulating the expression of angiopoietin-1 and Tie2 (209). Accordingly, the decreased activation of protein C resulting from the sequestration of parasitized erythrocytes may play a role in the loss of BBB integrity (169,202).

Furthermore, parasitized erythrocytes have been shown to induce the expression of tissue factor by endothelial cells (210), resulting in coagulation through the increased production of thrombin

(201). Activated protein C is able to inhibit coagulation by binding to protein S and inactivating FVa and FVIIIa, thereby preventing the production of thrombin (199). Autopsies of children who died of cerebral malaria demonstrated an absence of disseminated intravascular coagulopathy, and showed the colocalization of sequestered parasitized erythrocytes with fibrin deposits (201). Cerebral cytoadherence decreases the expression of EPCR (and thereby the production of activated protein C) in the vicinity of the sequestered parasitized erythrocytes, likely accounting for the localized microvascular thrombosis that occurs during cerebral malaria (201). Moreover, the low constitutive expression of both EPCR and thrombomodulin in the brain (211,212) may explain why the cerebral microvasculature is particularly vulnerable to the cytoadherence-mediated pathology.

Angiopoietin-2 and nitric oxide have also been demonstrated to play important opposing roles in the regulation of endothelial function (213,214) (Figure 3). Angiopoietin-2 levels are elevated in cerebral malaria compared to uncomplicated cases of malaria in Malawian and Ugandan children (215,216) and are associated with a fatal outcome in Ugandan children with cerebral malaria (217). Similarly, angiopoietin-2 was shown to be higher in Thai adults with cerebral malaria compared to uncomplicated cases of malaria and healthy controls (216,218), and was also increased in adult patients that succumbed to cerebral malaria compared to survivors in Bangladesh and India (219). Conversely, reduced nitric oxide production correlated with malaria severity in Tanzanian children (220), and exhaled nitric oxide levels were significantly decreased in Indonesian adults with severe malaria compared to moderately severe malaria (213).

Patients with cerebral malaria were found to have decreased plasma levels of L-arginine, the substrate for nitric oxide synthesis (213,221), indicating that hypoargininaemia may be partially responsible for the limited nitric oxide production. Nitric oxide bioavailability was also found to

be associated with the concentration of ADMA , a competitive inhibitor of nitric oxide synthase (222). Moreover, hemoglobin release following infection-induced hemolysis correlated with both the severity of malaria and nitric oxide bioavailability, suggesting that hemoglobin-mediated quenching may play a role in the low nitric oxide levels observed in severe malaria (223). Nitric oxide has been shown to attenuate cytokine-mediated endothelial activation (224), decrease cytoadherence of parasitized erythrocytes (225), and increase microvascular flow (226), suggesting possible explanations for its association with malaria severity.

Furthermore, nitric oxide has also been demonstrated to inhibit the release of angiopoietin-2 from activated endothelial cells by preventing the exocytosis of Weibel-Palade bodies (227,228). Angiopoietin-2 antagonizes the angiopoietin-1-mediated activation of the receptor Tie2, and this results in the increased expression of cell adhesion molecules, destabilization of endothelial cell tight junctions (229), and sensitization of endothelial cells to TNF (230). Accordingly, the levels of angiopoietin-1 were lower and the levels of soluble Tie2 were higher in patients with cerebral malaria compared to uncomplicated malaria (215-218), further highlighting the importance of the angiopoietin-1/Tie2 interaction in maintaining vascular quiescence and stability during malaria.

Finally, nitric oxide-mediated prevention of Weibel-Palade body exocytosis additionally prevents the release of von Willebrand factor (231), which is involved in platelet adhesion and aggregation (232) (Figure 3). The functional activity of von Willebrand factor is regulated by its multimeric composition; large multimers of von Willebrand factor have increased binding affinity for both collagen and platelets (233). The plasma levels of von Willebrand factor were shown to be markedly increased in children with severe malaria (215,234,235); in particular, severe malaria was shown to correlate with inhibited activity of the von Willebrand-cleaving protease ADAMTS13 and the accumulation of ultra-large von Willebrand multimers (235-237).

The increased platelet binding capacity of the ultra-large multimers may contribute to the increased adhesion of parasitized erythrocytes to activated endothelial cells and to the formation of thrombi in severe malaria (186,238,239).

2.3 Proinflammatory Immune Response

Elevated levels of multiple cytokines, including IFN γ , TNF, IL-6, IL-8, IL-10, and IL-12p70 have been associated with malaria infection (240-242). Moreover, certain cytokines, such as TNF, IL-6 and IL-10, have frequently been shown to correlate with the severe complications of *P. falciparum* infection in children, including cerebral malaria (243-247). Several studies also reported that TNF concentrations were the highest in children who subsequently died of cerebral malaria (243,245,246); although other studies did not find a significant correlation between serum TNF levels and disease severity or outcome (241). Furthermore, the association of severe complications during malaria infection with the serum levels of cytokines is much less clear in older individuals (240,248).

TNF is one of the most extensively studied cytokines in the context of malaria. TNF is able to induce the production of tissue factor by endothelial cells (249,250), and this effect was shown to be synergistically enhanced by concurrent stimulation with thrombin (251). Moreover, TNF can also decrease the expression of thrombomodulin and EPCR on endothelial cells (252). Consequently, TNF has the capacity to induce a procoagulant state by directly increasing thrombin levels, and by preventing the inhibition of thrombin production by activated protein C. Indeed, administration of TNF to healthy volunteers was shown to activate coagulation (253).

Thrombomodulin and EPCR have a low level of constitutive expression in the microvasculature of the brain (211,212), resulting in a decreased capacity to downregulate the TNF-mediated

increase in thrombin expression. In addition to playing an integral role in coagulation, thrombin can also upregulate the expression of cell adhesion molecules on activated endothelial cells (254), thus the surplus of thrombin following TNF stimulation may contribute to the preferential sequestration of parasites within the brain during cerebral malaria. Moreover, endothelial cells from patients with cerebral malaria were shown to have an increased responsiveness to TNF, leading to enhanced expression of inflammatory mediators, including the cell adhesion molecule ICAM1, following stimulation by this cytokine (255), potentially further augmenting the accumulation of parasitized erythrocytes (214).

While high levels of TNF have been associated with the incidence of cerebral malaria (241,246), elevated serum levels of TNF shortly following the initiation of chemotherapy were found to predict rapid clinical and parasitological resolution of both severe and uncomplicated malaria (256). These findings suggest a dual role for TNF, where the cytokine is required for parasite clearance, but where TNF can lead to neuropathology if the induced proinflammatory response is inappropriately regulated. As mentioned above, increased levels of the anti-inflammatory cytokine IL-10 are also associated with cerebral malaria (241,244). However, low IL-10:TNF ratios are observed in children with cerebral malaria (257), suggesting that the increased IL-10 may be indicative of a failed attempt to mitigate an excessive immune response.

Finally, in addition to cytokines, elevated levels of chemokines, particularly CXCL10, have also been associated with an increased risk of cerebral malaria. Indian patients with cerebral malaria had higher plasma levels of CXCL10 compared to patients with mild malaria (258), and both the serum and cerebrospinal fluid levels of CXCL10 were elevated in Ghanaian children with cerebral malaria compared to those with severe malarial anemia (259). CXCL10 can be induced by both IFN γ and TNF, and contributes to the chemotaxis of CXCR3-expressing lymphocytes

(260,261). Correspondingly, intravascular accumulation of mononuclear leukocytes has been observed in the brains of Ghanaian and Malawian children who succumbed to cerebral malaria, but the proportion of cases exhibiting mononuclear sequestration varied between studies (140,262-264). Finally, accumulation of mononuclear cells within the brain was also found in both children and adults in a study conducted in India (265).

2.4 Pathophysiological Features of Cerebral Malaria

Sequestration of parasitized erythrocytes within the cerebral microvasculature is highly heterogeneous, with capillaries containing parasitized erythrocytes adjacent to capillaries without sequestration (37,266). Moreover, accumulation of parasitized erythrocytes was observed to be associated with microvascular congestion in post-mortem studies of cerebral malaria (154,267), and both congestion and sequestration were shown to correlate with the depth of the pre-mortem coma and to be independently associated with a clinical diagnosis of cerebral malaria (267). Microvascular obstruction, as assessed by measuring the microcirculation in the rectal mucosa, was determined to be elevated in patients that succumbed to cerebral malaria compared to survivors (219). Attenuated microcirculation correlated with the estimated parasite biomass (*Pf*/HRP2 levels), but was not significantly associated (219) or was weakly associated (266) with the presence of coma.

In addition to cytoadherence, other adhesive phenotypes, such as rosetting and clumping, and the deformability of erythrocytes during *P. falciparum* infection, have also been implicated in microvascular obstruction. Rosetting was shown to enhance microvascular obstruction *in vitro* (188), and severe malaria has been associated with significantly higher levels of rosetting compared to non-severe hyperparasitemia and uncomplicated malaria, but no difference in

rosetting was observed between cerebral malaria and other forms of severe malaria (187,268). Additionally, polymorphisms that attenuate the ability of parasitized erythrocytes to form rosettes were found to confer protection against severe malaria (269,270).

Clumping may also contribute to microvascular obstruction, but the precise role of platelets in malaria pathology is unclear. Platelet accumulation was observed in the cerebral microvasculature of patients that died from cerebral malaria, but not in patients that died of severe malarial anemia (264). Moreover, platelet-mediated clumping was shown to be greater in severe malaria than in uncomplicated malaria in Kenyan and Malawian children (186,194), and was further elevated in cerebral malaria cases in the Malawian study (194). Contrastingly, clumping was determined to be associated with high parasitemia, but not with the severity of malaria in Malian children (271).

Finally, circulating erythrocytes, most of which are unparasitized, become rigid in patients with severe malaria (272), and are thought to contribute to decreased microcirculatory flow during severe malaria (273). Reduced deformability of erythrocytes was found to correlate with both disease severity and mortality in children with severe malaria (274). Several factors have been implicated in the impaired deformability of erythrocytes during malaria infection, including hemin-induced oxidative damage of the erythrocyte membrane (275) and the impaired bioavailability of nitric oxide that is observed during cerebral malaria (276,277).

Microvascular obstruction during malaria is associated with tissue hypoperfusion (154,219). Plasma lactate levels, indicative of tissue hypoperfusion, are higher in severe malaria than in mild malaria (214), and are associated with a fatal outcome (278,279) and elevated estimated parasite biomass (280). Lactic acidosis (blood lactate level $> 5.0\text{mM}$) is caused by the shift from

aerobic to anaerobic metabolism that results from hypoxia (281), and contributes to the overall metabolic acidosis associated with mortality in severe malaria (278,281,282). Lactic acidosis was shown to correlate with mortality in cerebral malaria, but not in severe malarial anemia (283). Increased lactate levels were found to be associated with the estimated parasite biomass in cerebral malaria, but primarily correlated with decreased hemoglobin levels in severe malarial anemia (283). Thus, lactic acidosis is related to factors that cause localized ischemia in cerebral malaria and factors that cause systemic hypoxia in severe malarial anemia (283).

In addition to microvascular obstruction, endothelial dysfunction has also been shown to correlate with tissue hypoperfusion during cerebral malaria (214,219). Levels of angiopoietin-2, an autocrine mediator of endothelial activation, were found to be associated with lactate levels, and with the severity and mortality of severe malaria (214,219). Angiopoietin-2 levels did not correlate with microvascular obstruction (219), demonstrating that endothelial dysfunction contributes to tissue hypoperfusion independently of obstruction. Beyond these two factors, hypovolemia (loss of intravascular volume) was also proposed to contribute to acidosis (284). Hypovolemia based on clinical signs is frequently observed in patients with severe malaria (285-287). However, extracellular water volume was not shown to correlate with lactate levels or disease severity in Gabonese children (288,289) and fluid boluses increased mortality in children with impaired perfusion (290). Thus, tissue hypoperfusion in severe malaria is likely mediated by microvascular obstruction and endothelial dysfunction, and not by hypovolemia.

Furthermore, brain swelling is commonly observed in both children (291-293) and adults (294,295) with cerebral malaria. Increased brain volume and intracranial hypertension were more frequent in children that died from cerebral malaria compared to survivors (291,296), but brain swelling was not found to be significantly associated with coma depth or mortality in adults

(294,295). Brain swelling during cerebral malaria may be the result of increased blood volume caused by the sequestration of parasitized erythrocytes, cytotoxic edema, and/or vasogenic edema. Ischemic injury from microvascular obstruction and endothelial dysfunction likely contributes to cytotoxic edema, while BBB disruption and the leakage of fluid into the perivascular space are likely responsible for vasogenic edema. Vasogenic edema does not appear to have a major role in the pathology of cerebral malaria in adults (295,297,298), as the prevalence of vasogenic edema was not significantly different between cerebral malaria and non-cerebral severe malaria in adults, nor did it correlate with pre-mortem coma (298). However, vasogenic edema is more common in pediatric cases, and may be at least partially responsible for the observed brain swelling (293,299).

Moreover, loss of BBB integrity, and diffuse axonal and myelin damage were shown to correlate with the sequestration of parasitized erythrocytes in Malawian children with cerebral malaria (300). Axonal and myelin damage were associated with ring hemorrhages and vascular thrombosis in the cerebral and cerebellar white matter and in the brainstem of these children (300). However, astrogliosis was not found to correlate with parasite sequestration, or myelin and axonal damage (300). Localized loss of vascular integrity was not found to be associated with pre-mortem coma in Vietnamese adults (298), but axonal injury was often associated with hemorrhages and areas of demyelination, and the frequency and extent of axonal injury was greater in patients that died due to cerebral malaria compared to non-cerebral malaria (301). In general, cerebral malaria appears to be associated with minimal changes in BBB integrity and mild intraparenchymal inflammatory responses compared to other neurological infections (297).

Focal reduction in the expression of the endothelial cell tight junction proteins occludin, vinculin and ZO-1 was observed in vessels with an accumulation of parasitized erythrocytes in both

children and adults with cerebral malaria (299,302), but their expression was not decreased in the brains of patients with non-cerebral malaria (302). Incubation of human umbilical vein endothelial cells with parasitized erythrocytes from patients with cerebral malaria decreased the expression of occludin, vinculin and ZO-1 to a greater extent than parasitized erythrocytes from patients with non-cerebral severe malaria or uncomplicated malaria (303). Thus, BBB disruption in cerebral malaria may be the result of the mitigated expression of tight junction proteins. Additionally, the adhesion of parasitized erythrocytes (304) and their release of soluble factors (305,306) have been shown to induce endothelial cell apoptosis *in vitro*, suggesting that apoptosis may also contribute to the loss of BBB integrity.

The localized and heterogeneous cerebral pathology observed during cerebral malaria, opposed to the widespread dysfunction observed in many other neurological infections, may account for the rapid reversibility of coma and the insidious nature of the long-term neurological sequelae associated with this disease. Coma depth, multiple convulsions and the duration of unconsciousness were found to be independent risk factors for neurological sequelae (307-311), whereas lactic acidosis, which correlates with the severity of malaria (214) and is a predictor of fatal outcome (278,279), was not found to be predicative of neurocognitive impairment (309). Consequently, mortality and neurological sequelae induced by cerebral malaria may be caused by different pathological mechanisms.

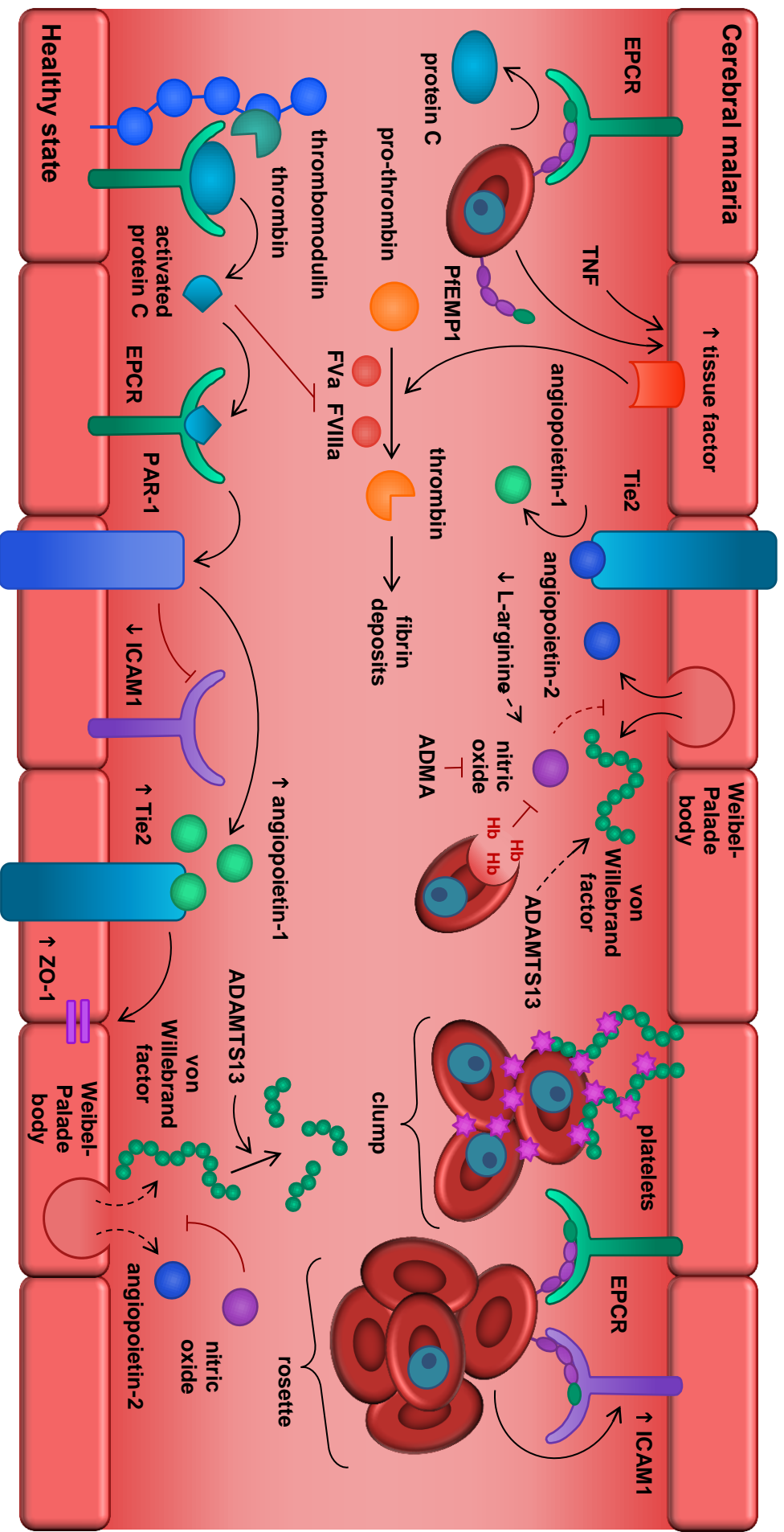


Figure 3. Overview of Cerebral Malaria Etiology. Cerebral malaria: Parasitized erythrocytes bind to endothelial cell receptors via PfEMP1 (severe complications associated with EPCR and DC8/DC13). Cytoadherence inhibits the activity of EPCR, resulting in decreased activation of protein C. Parasitized erythrocytes and TNF induce the production of tissue factor by endothelial cells, and this increases coagulation. Nitric oxide bioavailability is attenuated by reduced L-arginine levels, increased ADMA and hemoglobin-mediated quenching. The lack of nitric oxide allows the release on angiopoietin-2, which antagonizes the angiopoietin/Tie2 axis, and von Willebrand factor, which is involved in platelet aggregation. Moreover, decreased plasma ADAMTS13 causes the accumulation of ultra-large multimers of von Willebrand factor, potentially increasing the adhesion of parasitized erythrocytes. Parasitized erythrocytes bind to platelets to form clumps and to uninfected erythrocytes to form rosettes. Additionally, cytoadherence has the capacity to upregulate the expression of ICAM-1, potentially further increasing cerebral sequestration. **Healthy state:** Thrombomodulin, thrombin and EPCR activate protein C. Activated protein C reduces coagulation and thrombin production by inhibiting FVa and FVIII. Moreover, activated protein C and EPCR activate PAR-1, resulting in reduced expression of ICAM1, upregulation of angiopoietin-1 and Tie2, and stabilization of the endothelial barrier. Furthermore, nitric oxide prevents the exocytosis of Weibel-Palade bodies, thereby inhibiting the release of von Willebrand factor and angiopoietin-2. Figure generated by K.V.

3. Adjunctive Therapies for Cerebral Malaria

Increased implementation of preventive measures and the introduction of highly effective artemisinin-based combination therapies have resulted in a massive reduction in malaria transmission and mortality (10). However, if malaria is not treated rapidly following the initial onset of symptoms, uncomplicated malaria can rapidly progress to severe malaria, which has a case-fatality rate of 10-20% even under optimal conditions (53). Unlike the impressive decrease in malaria transmission that has occurred over the past decade, the mortality rate for severe malaria has remained relatively unchanged (53,312). Moreover, the prevalence of long-term neurocognitive impairments in patients that have survived cerebral malaria is becoming increasingly recognized (134,135).

Numerous adjunctive therapies that modify the pathological processes caused by cerebral malaria have been developed in the hopes of reducing mortality and neurological disability. The therapies are typically designed to either modulate the mechanisms that are thought to contribute to the pathophysiology of cerebral malaria or to alleviate the end-stage factors associated with poor clinical prognosis. None of the adjunctive therapies that have been assessed in clinical trials to date have resulted in a significant decrease in mortality and a few have been associated with a worsened clinical outcome. However, the majority of clinical studies have been insufficiently powered to detect the expected reduction in mortality that would be mediated by adjunctive treatment. A few recently developed adjuvant therapies have demonstrated promising results in murine cerebral malaria models and in clinical trials of uncomplicated malaria, and will hopefully prove to be effective at decreasing the mortality of severe malaria.

3.1 Cytoadherence and Microvascular Obstruction

Microvascular obstruction and endothelial activation resulting from the sequestration of parasites within the microvasculature of the brain is thought to play a central role in the pathology of cerebral malaria. Artemisinin-based combination therapies rapidly reduce the parasite burden (108); however, they do not appear to be able to quickly resolve parasite sequestration. Cytoadherence of parasitized erythrocytes was shown to continue for several hours following treatment (313), potentially due to the maintained presence of PfEMP1 on the surface of the drug-inactivated parasitized erythrocytes. Moreover, the rate of rosetting was also shown to be unaffected by anti-malarial treatment (314). Delayed restoration of the microcirculation may contribute to the ineffectiveness of artemisinin-based combination therapies against severe malaria; consequently the development of adjunctive therapies that rapidly release sequestered parasites may improve the case-fatality rate of cerebral malaria.

Levamisole is an alkaline-phosphatase inhibitor which has been shown to reduce the adhesion of parasitized erythrocytes to CD36 *in vitro* (315). A preliminary study of Thai adults with uncomplicated malaria found that adjunctive levamisole increased the frequency of mature-stage parasites in the peripheral circulation compared to patients that only received quinine, indicative of decreased sequestration (316). However, a randomized control trial in Bangladeshi adults with severe malaria demonstrated no significant changes in parasite sequestration or mortality between patients that received levamisole and those that only received artesunate (317).

It was hypothesized that the rapid onset of action and broad-stage specificity of artesunate compared to quinine (106) may have obscured the beneficial effect of levamisole (317). Additionally, brain endothelial cells have a limited expression of CD36 (155), suggesting that

other receptors may play a larger role in cerebral trophism, and cerebral malaria has been associated with PfEMP1 variants that do not bind to CD36 (164,166). Furthermore, parasites selected *in vitro* on human endothelial cells switched away from CD36-binding variants (170). Consequently, therapies aimed at interfering with binding to other endothelial receptors, particularly EPCR (202), may prove to be more effective.

Adjuvant therapies that target the disruption of rosettes have also been examined. A variety of sulphated glycoconjugate compounds, including heparin (318), curdlan sulphate (319) and fucosylated chondroitin sulphate (320), have been shown to be capable of rosette disruption. However, the anticoagulant properties of some of these compounds, particularly that of heparin, prevents their use in the treatment of severe malaria (53). Furthermore, certain field isolates were shown to be less sensitive to rosette-disruption by sulphated glycoconjugates (318,319,321), with blood group A rosettes being especially resistant to heparin-induced dispersion (314). A recent study determined that blood group A rosetting is mediated by RIFINs, rather than PfEMP1 (189), thus disruption of PfEMP1-heparin sulphate interactions would likely not be sufficient to disperse blood group A rosettes.

Low anticoagulant heparin was shown to disrupt cytoadherence, rosetting, and merozoite invasion *in vitro*, and to decrease sequestration in rat and macaque monkey models of severe malaria (321). Furthermore, low anticoagulant heparin was also able to disrupt rosettes in the majority of isolates from Cameroonian children with malaria (322). A study of the low anticoagulant heparin sevuparin in Thai adults with uncomplicated malaria did not meet the primary efficacy endpoint of an elevated number of mature parasitized erythrocytes in the peripheral blood over the first eleven hours following treatment, but the results did show a slight increase in late-stage parasites one hour after the first dose of sevuparin (323).

Curdlan sulphate was also found to decrease the formation of rosettes *in vitro* in clinical isolates from Kenyan children (319), and to limit the growth of *P. falciparum in vitro* by inhibiting merozoite invasion (324). One clinical trial found that curdlan sulphate treatment reduced the fever clearance time in Thai adults with severe malaria compared to patients that only received artesunate, but there was no significant difference in mortality between the two treatment groups (325), and no additional studies on the efficacy of curdlan sulphate have been completed to date.

Finally, in addition to cytoadherence and rosetting, reduced red cell deformability has also been shown to contribute to decreased microcirculatory flow during severe malaria (273). Impaired red cell deformability was demonstrated to be related to the severity of disease in Kenyan children with malaria, and exchange blood transfusion was found to restore deformability (274). A contemporaneous meta-analysis of eight studies found that exchange blood transfusion was not associated with an increased survival rate compared to antimalarial treatment alone, however the patients receiving a transfusion also had higher parasitemia and disease severity than the patients that did not receive a transfusion (326). A more recent study attempted to match reported cases based on severity, but also found no significant correlation between exchange blood transfusion and survival outcome (327). Furthermore, exchange blood transfusion requires expertise and intense monitoring, limiting its practicality in resource-limited settings.

3.2 Immunomodulation

A dysregulated inflammatory response has been associated with both the severity and clinical outcome of cerebral malaria. Inflammatory cytokines, particularly TNF, have been implicated in the induction and exacerbation of both endothelial dysfunction and parasite sequestration.

Appropriate regulation of the inflammatory response by adjunctive therapies may therefore limit the pathology resulting from the downstream effects of an unrestrained immune response.

Initially, treatment with monoclonal antibodies against TNF was observed to decrease fever in Gambian children with cerebral malaria, but the impact on mortality could not be accurately assessed as the study size was too small (328). A much larger subsequent study examining the efficacy of TNF depletion found no effect on mortality, and determined that treatment with monoclonal antibodies against TNF was associated with increased neurological sequelae (329). Inhibition of TNF release by adjunctive therapy with pentoxifylline has also been pursued. In addition to reducing TNF expression, pentoxifylline has also been shown to improve microcirculation by increasing red cell deformability and by preventing thrombosis (330). Pentoxifylline was able to attenuate TNF expression in the majority of studies that were conducted (331-334), but one study did not observe a significant effect on the serum levels of TNF (335). Treatment with pentoxifylline decreased the duration of coma and exhibited a trend toward decreased mortality in Burundian children (331) and Indian adults (333) with cerebral malaria, but failed to demonstrate significant clinical benefit in Kenyan children (332). Two studies in Thai and European adults that included non-cerebral severe malaria also observed no difference in disease severity compared to patients receiving anti-malarial treatment alone (334,335).

Additionally, inhibition of PPAR γ has been demonstrated to suppress the production of inflammatory cytokines (336,337), and to be neuroprotective against focal ischemic brain injury (338). Rosiglitazone, an agonist of PPAR γ , was shown to enhance the phagocytic clearance of parasitized erythrocytes *in vitro*, and to reduce inflammation and improve survival in a murine model of cerebral malaria (339). Moreover, adjunctive therapy with rosiglitazone at the onset of

neurological symptoms in mice with cerebral malaria increased survival and reduced neurocognitive impairment compared to artesunate treatment alone (340). The mice receiving rosiglitazone had elevated levels of angiopoietin-1, less BBB disruption and significantly fewer brain hemorrhages compared to mice only receiving artesunate (340). A study of rosiglitazone in Thai adults with uncomplicated malaria significantly decreased parasite clearance time and reduced the serum levels of the proinflammatory biomarkers IL-6 and MCP-1 (341). Moreover, the patients receiving the rosiglitazone adjunctive therapy also had a lower ratio of serum angiopoietin-2: angiopoietin-1 (340). A randomized control trial of rosiglitazone as adjunctive therapy for children with severe malaria is currently in progress (clinicaltrials.gov ID NCT02694874).

3.3 Augmentation of Nitric Oxide

Initially increased nitric oxide production was proposed to contribute to parasite clearance (342), and to mediate the development of cerebral malaria (343). A seminal study by Gramaglia, *et al.* in a murine model of cerebral malaria demonstrated that it was actually the low bioavailability of nitric oxide that was responsible for exacerbating neuropathology (344). Neither nitric oxide synthase deficiency nor exogenous nitric oxide was shown to affect the parasitemia of mice infected with *P. berghei* ANKA (344). Moreover, mice deficient for vascular nitric oxide synthase were not protected from ECM, whereas administration of a nitric oxide donor prevented neuropathogenesis (344). The increased bioavailability of nitric oxide in the treated mice was associated with reduced levels of proinflammatory biomarkers in the blood, decreased BBB disruption, and fewer petechial hemorrhages in the brain (344). Additionally, mice with ECM were shown to have attenuated levels of nitrate, increased free hemoglobin, and marked hypoargininaemia, all of which are indicative of low nitric oxide bioavailability (344).

Importantly, these results corroborated previous clinical studies that had found an association between low nitrate levels and cerebral malaria in Tanzanian children (220,221).

In addition to elevating nitric oxide levels using a nitric oxide donor, Gramaglia *et al.* also observed that inhaled nitric oxide similarly decreased mortality (344). Subsequent research by a different group found that adjunctive treatment with inhaled nitric oxide as late as 5.5 days post-infection decreased the incidence of cerebral malaria compared to artesunate alone (345). The inhaled nitric oxide was shown to be associated with a decreased systemic inflammatory response, reduced BBB disruption and fewer brain hemorrhages (345). Since inhaled nitric oxide had previously been approved for use in humans to treat other conditions (346) and is relatively simple to administer, it was thought to be a more attractive candidate for adjuvant therapy in cerebral malaria than a parenteral nitric oxide donor.

Two independent randomized clinical trials using inhaled nitric oxide to treat Ugandan children with cerebral malaria (347) and severe malaria (including cerebral malaria) (348) were conducted. Neither study observed a significant effect on mortality, the incidence of neurological sequelae or parasite clearance time in children receiving the inhaled nitric oxide compared to the control groups (347,348). However, the inhaled nitric oxide also failed to significantly affect the plasma levels of angiopoietin-2 (347,348). Thus the inability of the treatment method to induce a change in the vascular endothelium is likely responsible for the absence of an effect on the clinical outcome and suggests that an alternative method may be required to effectively augment the bioavailability of nitric oxide.

Decreased L-arginine has been implicated in the attenuation of nitric oxide levels during cerebral malaria (213,221). Moreover, recovery of endothelial function following successful treatment of

severe malaria, which is primarily dependent on nitric oxide produced by endothelial cells, was associated with increasing concentrations of L-arginine (349). Accordingly, L-arginine treatment of Indonesian adults with moderately severe malaria was observed to increase exhaled nitric oxide and to reverse the endothelial dysfunction mediated by *P. falciparum* infection (213). However, a pilot study of L-arginine infusion in Indonesia adults with severe malaria observed no change in the bioavailability of nitric oxide (350). It was postulated that other factors that are induced during severe malaria, including ADMA (222) and cell-free hemoglobin (223), may have contributed to the decreased vascular nitric oxide, necessitating the administration of larger doses of L-arginine in these patients. Clinical trials of higher doses of L-arginine to treat severe malaria are currently in progress (ACTRN12612000571875).

Finally, alternative methods of improving nitric oxide bioavailability remain as potential adjunctive therapies for severe malaria. Recently, treatment of mice with a hybrid compound of dihydroartemisinin and a nitric oxide donor was shown to decrease mortality compared to antimalarial drugs alone, even if administered after the development of clinical symptoms (351). Additionally, the angiotensin-1/Tie2 pathway is another possible target for novel therapies aimed at improving endothelial function during severe malaria. Low levels of angiotensin-1 have previously been associated with cerebral malaria (215,216,218), and administration of angiotensin-1 prevented the loss of BBB integrity and decreased the mortality of mice with cerebral malaria compared to artesunate alone (352).

3.4 Amelioration of Metabolic Acidosis

Lactic acidosis is associated with tissue hypoperfusion resulting from microvascular obstruction (154,219) and endothelial activation (214,219), and lactate levels were found to be higher in

cases of severe malaria (214) and capable of predicting fatal outcome in cerebral malaria (278,279). Dichloroacetate has been shown to ameliorate lactic acidosis by preventing the inhibition of pyruvate dehydrogenase, thereby increasing the oxidative removal of lactate (353,354). Dichloroacetate was demonstrated to decrease lactate levels (355) and reduce mortality (356) in rats infected with *P. berghei* ANKA. Furthermore, adjunctive treatment with dichloroacetate decreased lactate levels in Thai adults (357,358) and Ghanaian children (359) with severe malaria compared to quinine alone in open-labeled trials. Similarly, a randomized clinical trial found that in dichloroacetate mitigated lactic acidosis in Ghanaian children with severe malaria (360), but larger clinical trials are still required to accurately assess whether dichloroacetate is capable of reducing mortality.

Volume expansion has also been evaluated as an approach to reduce lactate levels by correcting hypovolemia. Volume depletion (based on clinical signs such as tachycardia and prolonged capillary refill time) was found to be present at admission in the majority of Kenyan children with severe malaria (287,361), and was thus postulated to contribute to the metabolic acidosis that is often observed in these patients. A small prospective study found that volume expansion with saline or albumin was associated with reduced acidosis in children with severe malaria (287). A subsequent open-label, randomized control trial comparing volume expansion with saline or albumin found no difference in the resolution of acidosis, but found that mortality was significantly reduced in children that received albumin (362). Additionally, results similar to that of saline were obtained for the adjunctive use of the synthetic colloid gelofusine when compared to albumin (363). However, the above studies did not include a maintenance fluid group and therefore were unable to resolve whether the administration of saline or gelofusine was detrimental compared to standard treatment.

Contemporaneously, another group observed that total body water (measured by bioelectrical impedance analysis) was lower in Gabonese children with severe malaria compared to moderate malaria, but found no association between total body water, extracellular water or intracellular water and lactate levels (288,289). Fluid volume depletion in patients with severe malaria was also shown to be mild compared to children with diarrhea, and was predominately accounted for by a decrease in intracellular water, with no significant changes in extracellular water (288). Hypovolemia is commonly accompanied by an increase in extracellular water, thus combined with the lack of association between volume changes and lactate levels, this group postulated that hypovolemia was unlikely to contribute to the pathophysiology of severe malaria (288).

A large clinical trial comparing volume expansion with albumin or saline to maintenance fluid in African children with severe febrile illness and impaired perfusion (including severe malaria) did not support the use of aggressive fluid resuscitation (290). Both the albumin-bolus and saline-bolus groups had a significantly increased risk of mortality at 48 hours, and increased risk of mortality and neurological sequelae at four weeks compared to maintenance fluid only (290). Unlike the previous small studies, no difference in mortality or sequelae was observed between the albumin-bolus and saline-bolus groups (290). Notably, the predicted adverse outcomes of fluid resuscitation (pulmonary edema and raised intracranial pressure) were determined to be rare occurrences (290).

Hypovolemia has also been observed in a large proportion of adults with severe malaria (285,286); however, retrospective analysis of fluid loading in Vietnamese adults with severe malaria found no evidence of improved acid-base status or clinical outcome in patients receiving fluid resuscitation (364). A small prospective study determined that lactic acidosis was associated with the sequestration of parasitized erythrocytes (assessed by erythrocyte flow

velocity) and not hypovolemia in Bangladeshi and Indian adults with severe malaria, and found that acid-base status was not improved by fluid loading (365). Furthermore, fluid resuscitation was shown to exacerbate pulmonary edema (365). Thus, hypovolemia in adults with severe malaria does not appear to contribute to pathophysiology, and volume expansion to resolve hypovolemia may actually exacerbate malaria-associated complications.

Finally, blood transfusion has also been suggested as an approach to reduce lactate levels in cerebral malaria, and was shown to resolve lactic acidosis in Kenyan children with severe malarial anemia (366,367). Elevated lactate levels were shown to be associated with decreased hemoglobin levels and systemic hypoxia in severe malarial anemia, but were found to be associated with parasite sequestration and localized ischemia in cerebral malaria (283). The differing pathophysiological correlates of lactic acidosis in severe malarial anemia and cerebral malaria suggest that blood transfusion would likely not be able to correct blood lactate levels in cerebral malaria patients.

3.5 Reduction of Brain Swelling

Brain swelling is commonly observed in children and adults with cerebral malaria (291-295), and is associated with poor outcome in children (291,296), but not in adults (294,295). Vasogenic edema does not appear to be responsible for the increased brain volume in adults (295,297,298), but may be at least partially responsible for brain swelling in children (293,299). Glucocorticoids (dexamethasone) and osmotic diuretics (mannitol) reverse vasogenic edema, thereby potentially reducing brain swelling and intracranial pressure. However, the etiology of brain swelling and whether it contributes to mortality or is merely an epiphenomenon is unclear.

Dexamethasone was used extensively in the treatment of cerebral malaria for over a decade, based on assumption that edema contributed to neuropathology and the results of a few small studies that did not use proper controls (368-371). A double-blind, placebo-controlled trial in Thai patients with cerebral malaria found that dexamethasone adjuvant treatment had no effect on mortality and significantly increased both coma duration and the incidence of complications, including pneumonia and gastrointestinal bleeding (372). Moreover, a subsequent study in Indonesians with cerebral malaria was also unable to show any change in mortality from dexamethasone treatment, but in contrast to the previous study, dexamethasone was not shown to affect the duration of coma or the incidence of complications (373).

Mannitol was also previously used in the treatment of cerebral malaria, based on the beneficial effect of this treatment in Reye's syndrome (374). In an uncontrolled clinical trial, mannitol was found to control intracranial pressure in Kenyan children with intermediate intracranial hypertension, but was unable to alleviate intracranial pressure in children with severe intracranial hypertension (296). However, a randomized, double-blind, placebo-controlled trial in Ugandan children with cerebral malaria determined that adjunctive therapy with mannitol did not significantly alter mortality or coma duration (375), and a randomized clinical trial in Indian adults with cerebral malaria and brain swelling found that mannitol adjuvant therapy showed a trend toward increased mortality and lengthened coma recovery time (294).

3.6 Neuroprotective Agents

Beyond the high case-fatality rate (53), cerebral malaria also causes neurocognitive impairment in approximately one-quarter of surviving children (134,135). Multiple convulsions, depth of coma and duration of unconsciousness have been shown to be independent risk factors for the

development of neurocognitive sequelae (307-311). Some deficits, such as blindness, were found to improve over time (134,309), while others, particularly speech and language impairments, were shown to persist long after recovery (134,308,376). Based on the prevalence and persistence of the neurocognitive impairments in survivors, successful treatment of cerebral malaria would require not only adjuvant therapies that decrease mortality, but also treatment that would preclude the development of sequelae.

Since seizures have been associated with the incidence of neurological sequelae following cerebral malaria, it was previously hypothesized that anticonvulsants, such as phenobarbital, might improve neurocognitive outcome. An early study found that a single dose of phenobarbital significantly decreased seizures in Thai patients with cerebral malaria, but had no effect on survival (377). A subsequent study in Kenyan children also observed a decrease in the incidence of seizures following phenobarbital treatment, and additionally determined that phenobarbital was associated with increased mortality, and did not significantly affect the frequency of neurocognitive sequelae at discharge or at three or twelve months post-discharge (378,379). Due to the increased mortality and failure to prevent neurocognitive impairment, the prophylactic use of phenobarbital is not currently recommended by the WHO (53).

Erythropoietin treatment was initially shown to be neuroprotective in rodent models of brain ischemia (380,381), and administration of erythropoietin at the onset of clinical symptoms in mice infected with *P. berghei* ANKA significantly decreased the incidence of cerebral malaria (382,383). Moreover, adjuvant therapy with erythropoietin was shown to increase the survival rate of mice compared to artesunate alone (384). Notably, elevated plasma levels of erythropoietin in Kenyan children with cerebral malaria were found to be associated with a decreased risk of mortality and acute neurological deficits (311), and erythropoietin therapy in

Malian children with cerebral malaria did not increase mortality compared to previous clinical studies (385).

Nevertheless, a larger subsequent study in Kenyan children with cerebral malaria did not observe a correlation between plasma erythropoietin and either acute or long-term neurological deficits, and determined that elevated plasma erythropoietin levels were associated with an increased risk of mortality and prolonged coma duration (386). Furthermore, erythropoietin levels were also shown to be increased in Indian adults with cerebral malaria compared to uncomplicated malaria, and further elevated in patients that died due to cerebral malaria compared to survivors (387). A randomized control trial aimed at assessing the safety and efficacy of erythropoietin adjuvant therapy in Malian children was started in 2008, but no results have been published so far (clinicaltrials.gov ID NCT00697164).

4. Experimental Cerebral Malaria

Clinical studies in humans have provided extensive information regarding the pathological correlates of disease severity in cerebral malaria, but mechanistic understanding of the etiology is lacking given the ethical limitations of human research. Murine models of malaria recapitulate a number of pathological processes associated with the human disease. Infection with *P. chabaudi* and *P. yoelii* are commonly used to study hyperparasitemia and anemia (388), while *P. berghei* NK65 and *P. berghei* ANKA have been used to examine hepatic (389) and cerebral pathology (390), respectively. However, the validity of these models to accurately portray the human disease, particularly the murine model of cerebral malaria, is a matter of some controversy (391).

Sequestration of parasitized erythrocytes in the microvasculature of the brain is a characteristic feature of human cerebral malaria (140,151,152), and the extent of this accumulation and its

contribution to pathology is the main area of debate in regard to the legitimacy of the mouse model (391). Parasite sequestration within the brain is substantially less prominent in ECM than in the human disease; however several studies have demonstrated that the accumulation of parasitized erythrocytes within the brain is required for neuropathogenesis in mice (392-395) and that non-ECM-causing parasite strains do not sequester within the brain to the same extent as *P. berghei* ANKA (393,396,397). Moreover, a recent study provided evidence for the cytoadherence of *P. berghei* ANKA *in vitro* under flow conditions (398). Nevertheless, the *P. berghei* ANKA genome does not contain any direct orthologues of PfEMP1 (399), the receptor responsible for the cytoadherence of *P. falciparum*, which likely precludes the study of anti-adhesive adjunctive therapies in the mouse model.

Estimated parasite biomass, indicative of parasite sequestration, has been shown to correlate with microvascular obstruction in humans (219), and microvascular obstruction is associated with elevated lactate levels (154,219), which is known to be a strong predictor of mortality (278,279). Thus, certain groups have postulated that vascular obstruction resulting from the sequestration of parasitized erythrocytes is the primary cause of neuropathology in cerebral malaria and that the ECM is thereby an unsuitable model due to the decreased brain sequestration of parasites (154,391). Contrarily, if mechanical obstruction were the main cause of cerebral malaria in humans, the pathophysiology of ECM would be fairly similar, as susceptible mice infected with *P. berghei* ANKA do have reduced cerebral blood flow and elevated lactate levels (400,401). Admittedly, the microvascular obstruction in mice is primarily caused by leukocytes rather than parasitized erythrocytes (154), but the subsequent complications arising from tissue hypoperfusion would essentially be the same.

In addition to microvascular obstruction, endothelial activation has been shown to independently correlate with elevated lactate levels in human cerebral malaria (219). Angiopoietin-2 and nitric oxide play important opposing roles in the regulation of endothelial function (213,214). Angiopoietin-2 antagonizes the angiopoietin-1/Tie2-mediated quiescence of the endothelial barrier (229), while nitric oxide inhibits the activation of endothelial cells (224), in part by preventing the release of angiopoietin-2 (227,228). The mouse model was instrumental in correcting the erroneous perception that nitric oxide contributed to neuropathology during cerebral malaria (344). Furthermore, mouse models have been utilized to optimize treatments aimed modulating angiopoietin-2 and nitric oxide levels, which have resulted in two of the most promising adjuvant therapies for cerebral malaria to date (clinicaltrials.gov ID NCT02694874 and ACTRN12612000571875). Thus, appropriate use of the mouse model to test adjuvant therapies (treatment given concomitantly with anti-malarial drugs at the onset of symptoms), does have the potential to identify viable therapies for the human disease.

Finally, CD8⁺ T cells have been shown to be critically required for neuropathogenesis in murine cerebral malaria (390), but the contribution of leukocytes to the human disease has been questioned (391). Accumulation of mononuclear cells within the brain of adults is infrequently observed (265), but a large proportion of children with cerebral malaria exhibit vascular pathology, including the sequestration of leukocytes (140,262-264). An effector role for CD8⁺ T cells in human cerebral malaria is often disregarded based on their paucity in brain autopsies (265); however, brain-sequestered CD8⁺ T cells are also difficult to identify in the murine model (390,402). Moreover, the chemokine CXCL10, which is involved in the chemotaxis of T cells, has been shown to be elevated in patients with cerebral malaria (258,259), and resistance to severe malaria in humans has been linked to certain human leukocyte antigen class I alleles

(403). Thus, the data support the possibility that CD8⁺ T cells contribute to pathology in human cerebral malaria and warrant further investigation.

4.1 The Role of T Cells

Infection of nude, SCID and RAG knock-out mice with *P. berghei* ANKA indicated a role for T cells in the pathogenesis of ECM (394,404-406). Nude mice, which do not have a thymus and cannot generate mature T cells, and SCID and RAG knock-out mice, which do not possess T or B cells, do not develop ECM (394,404-406). Further functional studies using antibody depletion and T cell deficient mice clearly demonstrated that T cells are required for ECM (390,394,395,405,407-409), whereas infection of B cell deficient mice with *P. berghei* ANKA determined that B cells are unlikely to have a critical role in the development of neuropathology (394,405). An early study suggested that CD4⁺ T cells, but not CD8⁺ T cells, were necessary for ECM (407). However, subsequent studies have demonstrated that both CD4⁺ and CD8⁺ T cells are critical to the development of ECM (390,394,395,405,406,408,409). The discrepant results of the former study are likely due to the efficiency of the antibody depletion; the number of CD8⁺ T cells in the lymph node was only decreased by two-thirds, and the remaining CD8⁺ T cells may have been sufficient to induce pathology (407).

Infiltration of leukocytes into the brain was observed to increase significantly on day 7 post-infection, upon the manifestation of neurological symptoms (390,410). Antibody depletion of CD4⁺ T cells on day 6 post-infection, failed to prevent the development of ECM, but depletion of CD8⁺ T cells completely protected mice from ECM, thereby assigning an effector role for CD8⁺ T cells and excluding one for the CD4⁺ T cells (390,395). Nevertheless, depletion of CD4⁺ T

cells early in the infection (day 0 and 4 post-infection) was able to prevent the development of ECM, indicating that CD4⁺ T cells have a role in the induction of pathology (390,394).

4.2 Induction of the T Cell Response

The spleen was identified as the initiation site of a cytotoxic immune response against *P. berghei* ANKA infection in a study that demonstrated complete protection from ECM in splenectomized mice (394). Based on accumulating evidence that established CD8⁺ T cells as the principal effector cells responsible for the neuropathology of ECM, work was conducted to determine whether the CD8⁺ T cell response was antigen-specific and the splenic cell type involved in antigen presentation. Mice lacking B cells and macrophages develop ECM following *P. berghei* ANKA infection, excluding an antigen presenting cell role for these cell types (394,395,405). Moreover, DCs had previously been determined to be essential for priming protective, antigen-specific T cell responses during both liver-stage and blood-stage malaria infection, suggesting that they may also be involved in the induction of a pathogenic T cell response in ECM (411).

There are four distinct populations of DCs in the murine spleen, three subtypes of cDCs (CD4⁺ DCs, CD8⁺ DCs and CD4⁻CD8⁻ DCs) and pDCs (412). *P. berghei* ANKA infection was shown to activate pDCs, as demonstrated by increased levels of type I IFN mRNA, but specific depletion of pDCs did not affect the susceptibility of mice to ECM (413). Additionally, a significant decrease in serum IFN γ was also measured in the pDC depleted mice, suggesting that pDCs may have a redundant contribution to inflammation in ECM (413). Depletion of cDCs using CD11c-DTR bone marrow transgenic mice markedly protected mice from ECM, establishing a critical role for cDCs in priming a pathogenic response during ECM (413).

The involvement of cDCs in the induction of the cytotoxic CD8⁺ T cell response was analyzed using transgenic *P. berghei* ANKA parasites that expressed model T cell epitopes, since no MHC class I-restricted antigens to blood-stage infection had been identified at the time (414). Transgenic CD8⁺ T cells specific for MHC class I-restricted epitopes were observed to proliferate *in vivo* in response to infection with the transgenic parasites (414) (Figure 4). Furthermore, infection with transgenic parasites increased the frequency of tetramer-specific CD8⁺ T cells and resulted in the specific lysis of transgenic peptide-pulsed splenocytes by endogenous cytotoxic T cells (414).

Following confirmation that cDCs induce parasite-specific CD8⁺ T cells, the specific subtype responsible was determined by co-culturing the subtypes isolated from transgenic parasite-infected mice with the requisite transgenic CD8⁺ T cells *in vitro* (414). CD8⁺ DC were shown to be superior in their presentation of transgenic antigens to CD8⁺ T cells, as measured by T cell proliferation, which is likely due to the ability of CD8⁺ DC to efficiently cross-present exogenous antigens using the MHC class I pathway (414,415). Furthermore, Clec9A-DTR mice, which allow efficient ablation of CD8⁺ DCs, were used to validate the essential antigen presenting cell role of these cells in the development of ECM *in vivo* (416).

Pattern recognition receptors play a central role in the initial detection of pathogens and in the activation of the innate immune response. A variety of receptors have been ascribed to DCs in the detection of malaria parasites, including TLRs, NLRs, CLRs and RLRs. TLR2 and TLR4 have been reported to recognize the GPI anchors present in *P. falciparum*, and malaria DNA bound to hemozoin has been described to activate DCs in a TLR9-dependent manner (417,418). Moreover, polymorphisms in TLR4 and TLR9 were shown to be associated with susceptibility to and severity of malaria in humans (419,420). Although TLR signalling has clearly been

demonstrated to contribute to the proinflammatory response in malaria infection, and genetic studies have shown that TLR polymorphisms correlate with the severity of disease, the exact role of TLRs in ECM is still inconclusive.

Mice deficient for MyD88, a downstream adaptor shared by most TLRs, were found to be partially protected from ECM in a number of studies (421-424), but others have observed no difference in their susceptibility compared to wild-type mice (425). The development of ECM pathology is likely independent of TLR4 (421,422,425,426); however, the contributions of TLR2 and TLR9 to ECM pathology are still an issue of controversy. Certain groups have determined that TLR2 (422) and TLR9 (421-423,427) deficient mice are partially protected from ECM, whereas other groups have demonstrated that TLR2 (421,425), TLR9 (425) and TLR2/4/9 (426) knock-out mice are just as susceptible to ECM as wild-type mice. Additionally, treatment of mice with E6446, which inhibits the activation of TLR9, was shown to protect mice from ECM (427). Interestingly, E6446 protected mice even when the treatment was administered five days post-infection, suggesting that the role of TLR-dependent signalling in ECM pathology may not be in the initial priming of the immune response.

The potential contribution of other pathogen recognition receptors in ECM has also been investigated, although not to the same extent as TLRs. *nod1nod2*^{-/-} mice infected with *P. berghei* ANKA demonstrated no difference in their susceptibility to ECM compared to wild-type mice (428). However, infection of the knock-out mice resulted in decreased levels of IL-1 β , KC and MCP-1, cytokines known to be induced by Nod1 and Nod2, indicating that malaria parasites have the capacity to activate NLRs (428). Hemozoin was also shown to be capable of inducing the production of IL-1 β through the activation of the NLRP3 inflammasome (429,430). While

NLRP3 knock-out mice were partially protected from ECM, mice deficient in ASC, caspase-1, IL-1 β and IL-1R were not, suggesting that the involvement of NLRP3 in ECM pathogenesis is independent of the inflammasome (424,430,431).

Additionally, the splenic and cerebral expression of CARD9, an adaptor molecule utilized by a number CLRs, was observed to be modulated by *P. berghei* ANKA infection, but CARD9^{-/-} mice developed ECM, excluding a pathogenic role for this adaptor (432). Contrastingly, mice deficient for the CLR DCIR and mice depleted of DCs expressing the CLR Clec9A were markedly protected from ECM, indicating that certain CLRs likely play a role in the pathogenesis of ECM (416,433). Finally, the RLR MDA5 was shown to recognize *P. berghei* ANKA RNA during liver-stage infection, and generate a MAVS-dependent, type I IFN response (434). IFN production was impaired to a greater extent in the MAVS^{-/-} mice compared to the MDA5^{-/-} mice, indicating that additional recognition mechanisms likely contribute to this response (434). Production of type I IFN was determined to limit liver parasite burden and parasitemia, but the impact of MDA5 on the mortality of ECM was not examined (434).

Beyond establishing the contribution of different pathogen recognition receptors in the induction of ECM, the identity of MHC class I-restricted epitopes was investigated to aid in further delineation of the pathogenic CD8⁺ T cell response. Transfer of CD8⁺ T cells from *P. berghei* ANKA infected mice into uninfected wild-type or RAG knock-out mice demonstrated that infection of the recipient mouse was required for pathology, negating a role for self-antigen (406,435). Furthermore, V β 8.1,2⁺ CD8⁺ T cells were observed to expand in the peripheral blood of infected mice exhibiting severe neurological symptoms (409). This subset and others bearing selected TCR β variant segments were found to be preferentially recruited to the brain of

mice with cerebral malaria, suggesting the existence of an immunodominant epitope or a small group of immunodominant epitopes (390,436).

Recently, several immunogenic blood-stage *P. berghei* ANKA epitopes were described. One of the inaugural studies examined the magnitude of the cytotoxic CD8⁺ T cell response by quantifying the expression of GzmB (a key effector molecule in ECM) and the induction of CD8^{int}CD11a^{hi} (antigen experienced) cells, and approximately 30% of splenic CD8⁺ T cells were found to be parasite specific at the peak of expansion (437). Moreover, this study identified five epitopes using *in silico* prediction of H2-K^b-restricted epitopes from the *P. berghei* ANKA proteome and subsequent evaluation of their ability to restimulate splenic CD8⁺ T cells from infected mice (437). The identified peptides were derived from putative activator-protein 2 transcription factor-like protein, ribonucleoside-diphosphate reductase, replication factor A1, putative replication factor C, and a hypothetical protein (437,438).

Additional epitopes were identified by a different group through screening of a *P. berghei* ANKA cDNA library expressed in EL4 cells against a NFAT-lacZ reporter cell line expressing TCR α and β chains derived from brain-sequestered CD8⁺ T cells (397,439). Positive EL4 clones were found to contain fragments of GAP50 and bergheilysin, and potential H2-D^b and H2-K^b epitopes were predicted using a computer algorithm and were used to generate peptide-MHC tetramers (397,439). In this manner, the H2-D^b-restricted epitope SQLLNAKYL (Pb1) and the H2-K^b-restricted epitope IITDFENL (Pb2) were identified (397,439). Furthermore, this group also created tetramers for all of the epitopes reported by the group mentioned above; however, only the H2-K^b-restricted epitope EIYIFTNI from replication factor A1 (F4) was able to label a subset of splenic CD8⁺ T cells (439). Accordingly, Pb1, Pb2 and F4 tetramer-positive cells were detected in both the spleen and brain of *P. berghei* ANKA-infected mice (397,439).

4.3 Chemotaxis of T Cells to the Brain

Priming of the pathogenic T cell response occurs in the spleen during ECM and sequestration of CD8⁺ T cells within the brain is required for the development of neuropathology. Furthermore, T cell sequestration in the brain was also observed in ECM-resistant perforin-deficient mice, indicating that T cell accumulation is an active process and not consequent of BBB disruption (406). Thus, the chemokine receptor expression of splenic and cerebral CD8⁺ T cells was examined to reveal the receptors involved in T cell migration during *P. berghei* ANKA infection (406). In both the spleen and the brain, mRNA expression of CCR2, CCR5, CXCR3 and CXCR4 were upregulated on activated CD8⁺ T cells, whereas naïve CD8⁺ T cells only expressed CXCR4 (406). Nitcheu *et al.* proposed that although CXCR4 was relevant to the chemotaxis of resting and activated T cells, only CCR2, CCR5 and CXCR3 were likely to be involved in the chemotaxis of peripheral T cells to the brain during ECM, and additional experiments clarifying the potential role of CXCR4 have not been conducted (406).

Further studies demonstrated that CCR2 is not necessary for the chemotaxis of pathogenic CD8⁺ T cells, as CCR2 deficient mice were not protected from ECM (440), whereas the extent to which CCR5 contributes to ECM pathogenesis is less clear (Figure 4). Belnoue *et al.* determined that greater than 80% of brain-sequestered CD8⁺ T cells were CCR5⁺, and that CCR5^{-/-} mice were markedly protected from ECM, with less than 20% developing neuropathology (440,441). Contrastingly, Nitcheu *et al.* found that CCR5 deficient mice displayed only a modest delay in the onset of ECM (406). The discordant results may be explained by the different mouse strains used by the aforementioned studies; the wild-type C57BL/6J x 129/Ola mice used by Belnoue *et al.* were only 70% susceptible to ECM, while 100% of the wild-type C57BL/6 mice used by Nitcheu *et al.* succumbed to ECM (406,441).

CXCR3 expression was found to have a significant effect on the incidence of ECM in every study that examined the impact of this chemokine receptor (Figure 4). Miu *et al.* found that CXCR3 deficient mice were markedly protected from ECM; 68% of the knock-out mice did not develop neuropathology (442). The augmented resistance of CXCR3^{-/-} mice was corroborated by Campanella *et al.*, who found that less than 30% of the knock-out mice were susceptible to ECM (443). Furthermore, the number of brain-sequestered CD4⁺ (442) and CD8⁺ T cells (442,443) in the CXCR3 deficient mice was markedly decreased compared to the wild-type mice on day 6 post-infection, validating the importance of CXCR3 expression in the chemotaxis of T cells to the brain during ECM.

The expression of both CCR5 and CXCR3 on splenic T cells was evaluated at different time points throughout *P. berghei* ANKA infection (444). CCR5 expression slightly increased from the onset of the infection to day 6 post-infection (1.75% to 10.8%), whereas CXCR3 expression was highly upregulated (21.7% to 55.8%) (444). Furthermore, on day 6 post-infection, Hansen *et al.* found that only 21.0% of brain-sequestered T cells expressed CCR5, compared to 89.5% of brain-sequestered T cells that were CXCR3⁺ (444). Similarly, Nie *et al.* determined that 7.69% and 66.9% of brain-sequestered T cells were CCR5⁺ and CXCR3⁺, respectively (445). Thus, CXCR3 expression in the spleen and the brain appear to correlate with T cell trafficking to the brain during ECM. However, while Miu *et al.* found that the total brain mRNA expression of both CXCR3 and CCR5 were significantly upregulated in infected mice, they did not observe a difference in the percentage of CXCR3⁺ CD8⁺ T cells within the brain of the infected mice compared to the uninfected mice (the percentage of CCR5⁺ CD8⁺ T cells was not examined) (442).

The requirement of CD8⁺ T cell-specific expression of CXCR3 for the development of ECM was confirmed by the adoptive transfer of wild-type CD8⁺ T cells from *P. berghei* ANKA-infected mice into CXCR3^{-/-} mice just before infection. Knock-out mice receiving CD8⁺ T cells were just as susceptible to ECM as wild-type mice (442,443), whereas the adoptive transfer of CD8⁻ cells had no effect on the incidence of ECM (442). Interestingly, the CXCR3-deficient mice that received wild-type CD8⁺ T cells also had an increase in the brain sequestration of CXCR3⁻CD8⁺ T cells compared to the knock-out mice that did not receive the wild-type cells (443). This result suggests that once in the brain, CXCR3⁺CD8⁺ T cells are able to induce the migration of additional CD8⁺ T cells in a CXCR3-independent manner.

In addition to chemokine receptors, the influence of the requisite chemokines on the development of neuropathology was also analyzed. At the onset of symptoms, the mRNA expression of CCL5 (CCR5), and CXCL9 and CXCL10 (CXCR3) in the brain were markedly increased (442,443,446) (Figure 4). Moreover, the protein levels of CXCL9 and CXCL10 were also significantly upregulated (443). (The protein level of CCL5 was not examined.) Using *in situ* RNA hybridization, Miu *et al.* detected CXCL9 expression in microglia and endothelial cells and CXCL10 expression in astrocytes and endothelial cells, whereas CCL5 was predominately expressed by infiltrating CD3⁺ lymphocytes (442). Campanella *et al.* also identified endothelial cells as a source of CXCL9 and CXCL10 using immunohistochemistry (443). Contrastingly, they found that neurons, and not astrocytes, expressed CXCL10 (443). The above results suggest that CCL5, CXCL9 and CXCL10 have distinct contributions to the pathogenesis of ECM. Moreover, the expression of CCL5 by sequestered T cells may potentially account for the increase in CXCR3-independent chemotaxis resulting from the accumulation of CXCR3⁺CD8⁺ T cells in the brain.

The roles of CXCL9 and CXCL10 in ECM neuropathology were confirmed by examining the impact of the respective knock-outs on the susceptibility of mice to *P. berghei* ANKA infection. Campanella *et al.* determined that CXCL9- and CXCL10-deficient mice were partially protected from ECM, with only 40% developing neuropathology (443). Nie *et al.* also found that CXCL10 deficiency protected mice from ECM; mice depleted of CXCL10 and CXCL10^{-/-} mice had an ECM incidence of less than 20% (445). Similar to the CXCR3^{-/-} mice, the brain sequestration of CD4⁺ and CD8⁺ T cells was significantly decreased in the CXCL10-deficient mice (445). Notably, the majority of the brain-sequestered T cells in the CXCL10^{-/-} mice were CXCR3⁺, which is likely due to the other CXCR3 chemokine CXCL9 (445).

Furthermore, the brain mRNA expression of IFN γ was shown to be elevated in *P. berghei* ANKA mice upon the onset of cerebral symptoms (446). CXCL9 and CXCL10 are IFN γ -inducible CXCR3 ligands (447-449); concordantly, the mRNA expression of CXCL9 and CXCL10 was greatly attenuated in the brains of *P. berghei* ANKA-infected IFN γ ^{-/-} BALB/c mice and IFN γ R^{-/-} DBA/1 mice (446). Moreover, IFN γ R^{-/-} 129P2Sv/Ev mice were shown to have reduced brain sequestration of T cells, particularly CD8⁺ T cells (450).

IFN γ has previously been shown to be necessary for the development of ECM (450-452), and the sequential production of IFN γ by NK cells and CD4⁺ T cells was shown to occur *in vitro* by challenging PBMCs with *P. falciparum* (453). NK cells were found to be the dominant cellular source of IFN γ in the brain up until day 5 post-infection, while CD4⁺ T cells were shown to be the dominant producers of IFN γ in the spleen throughout the infection (454). IFN γ production by CD4⁺ and CD8⁺ T cells in both the spleen and the brain was observed to be markedly increased on day 7 post-infection, and CD8⁺ T cells were found to replace NK cells as the major source of IFN γ in the brain at the onset of ECM symptoms (454).

Depletion of NK cells using anti-asialo GM1 significantly protected mice from ECM, and importantly, NK cell depletion also markedly reduced the sequestration of CD4⁺ and CD8⁺ T cells in the brain (444). Hansen *et al.* demonstrated that NK cells were recruited to the brain as early as day 4 post-infection, and that a high percentage of splenic NK cells were CXCR3⁺ (444). In corroboration, Campanella *et al.* found that the sequestration of NK cells within the brain was decreased 2-fold in CXCR3-deficient mice compared to wild-type (443). However, Miu *et al.* did not observe an increase in the brain accumulation of NK cells during *P. berghei* ANKA infection, nor did they detect a reduction in the number of NK cells in the brains of CXCR3^{-/-} mice (442). Interestingly, Hansen *et al.* demonstrated that NK cell depletion decreased the expression of CXCR3 and the chemotactic response of splenic T cells (444) (Figure 4). Notably, the adoptive transfer of wild-type NK cells, but not IFN γ ^{-/-} NK cells, into NK-depleted mice partially restored CXCR3 expression and the brain sequestration of T cells (444). Thus, NK cells appear to be an important early source of IFN γ and contribute to the CXCR3-mediated chemotaxis of T cells to the brain through their production of IFN γ .

The cellular sources of IFN γ required for ECM pathology were further characterized by the adoptive transfer of different cell populations from IFN γ -replete mice into IFN γ -deficient mice (454). Transfer of naïve splenocytes from wild-type mice into IFN γ ^{-/-} mice one day prior to infection resulted in the manifestation of prodromal signs of ECM, but none of the mice succumbed to cerebral complications (454). Disparately, transfer of naïve splenocytes from RAG knock-out mice failed to induce any signs of ECM, indicating that T cells are an essential source of IFN γ (454). Furthermore, transfer of infection-derived T cells (day 5 post-infection) into IFN γ ^{-/-} mice one day prior to infection, 5 days post-infection, or at both time points, caused ECM in 25%, 50% and 100% of the mice, respectively (454). Notably, transfer of infection-derived

CD4⁺ T cells, but not CD8⁺ T cells, one day prior to infection and 5 days post-infection induced ECM in 100% of the mice (454).

Based on the above results, Villegas-Mendez *et al.* concluded that only IFN γ production by CD4⁺ T cells was required for the development of neuropathology (454) (Figure 4); but, these results do not exclude an alternative early source of IFN γ . Adoptive transfer of CD4⁺ T cells was only able to cause ECM when the cells were isolated from mice 5 days post-infection, allowing ample time for IFN γ from other cells to influence the CD4⁺ T cells, and both Hansen *et al.* (444) and Villegas-Mendez *et al.* (454) have shown that NK cells are an early source of IFN γ . IFN γ depletion in the CD4⁺ T cell-transferred mice completely prevented the development of ECM, indicating that active secretion of IFN γ and not effector functions imprinted during IFN γ replete priming, was responsible for the ability of the wild-type CD4⁺ T cells to induce ECM (454). However, NK cell-derived IFN γ could still have affected the CD4⁺ T cells in other ways (*i.e.*, promote optimal IFN γ production or chemokine receptor expression), and importantly, the effect of infection-derived, wild-type NK cells on the incidence of ECM in the IFN γ ^{-/-} mice was not examined in this study.

Since CD8⁺ T cell accumulation within the brain is required for cerebral pathology during ECM, Villegas-Mendez *et al.* examined the effect of CD4⁺ T cell-derived IFN γ on the sequestration of CD8⁺ T cells (454). Adoptive transfer of wild-type CD4⁺ T cells into IFN γ ^{-/-} mice enhanced the brain mRNA levels of CXCL9 and CXCL10 compared to the control IFN γ ^{-/-} mice, and significantly increased the sequestration of CD8⁺ T cells within the brain (454). Moreover, a greater percentage of the brain-infiltrating CD8⁺ T cells were GzmB⁺ and KLRG1⁺ in the mice receiving the transfer, suggesting that CD4⁺ T cell-derived IFN γ also contributes to the terminal differentiation of brain-sequestered CD8⁺ T cells (454). Importantly, depletion of CD8⁺ T cells

mitigated the effect of the transferred wild-type CD4⁺ T cells, confirming that the IFN γ produced by the CD4⁺ T cells contributes to ECM pathology in a CD8⁺ T cell-dependent manner (454).

4.4 Effector Phase of the T Cell Response

The potential of antigen-specific CD8⁺ T cells to mediate BBB disruption during ECM was initially characterized using transgenic parasites, since MHC class I-restricted epitopes for blood-stage infection had not yet been identified. Using this approach, antigen-specific CD8⁺ T cells were shown to sequester in the brains of infected mice; however, it was unknown whether the immunodominant nature of the model T cell epitope would be representative of natural malaria antigens (414,455,456). Furthermore, the use of transgenic antigens prohibited comparative studies between the murine *Plasmodium* strains which differ in their ability to cause ECM.

The role of antigen-specific CD8⁺ T cells in mediating ECM was re-examined in greater depth upon the discovery of *P. berghei* ANKA-specific epitopes. Three epitopes were shown to be capable of eliciting an IFN γ response from splenocytes and the associated peptide-bound tetramer capable of labeling a subset of CD8⁺ T cells from infected mice: Pb1 (SQLLNAYYL from GAP50), Pb2 (IITDFENL from bergheilysin) and F4 (EIYIFTNI from replication factor A1) (397,439). Pb1-specific T cells were detected in the spleen on day 5 post-infection, and in the blood and brain on days 6 and 7 post-infection, respectively, corroborating earlier studies which determined that the T cell response is generated in the spleen, followed by chemotaxis of the T cells to the brain (397). Pb2- and F4- specific CD8⁺ T cells were also found in the spleen and brain of infected mice, but the timing of their appearance was not examined (439). No correlation was observed between the onset of Pb1-specific T cell sequestration within the brain

and the manifestation of ECM on day 7 post-infection, indicating that CD8⁺ T cells migrate to the brain before the development of symptoms (397).

Both perforin and GzmB have been shown to be required for the development of neuropathology in *P. berghei* ANKA-infected mice (406,456), and the induction of ECM following the adoptive transfer of wild-type CD8⁺ T cells into perforin- or GzmB-deficient mice, which are resistant to ECM, indicated that their pathogenicity was dependent on CD8⁺ T cell-specific production (406,456). The GzmB-deficient mice also required challenge with additional antigen to cause neuropathology, which is likely due to the decreased parasite burden in the brains of these mice compared to the wild-type mice, which will be discussed in greater detail below (456). Notably, while IFN γ is a marker of activated cytotoxic T cells, and has been shown to be necessary for the development of ECM, it was demonstrated that CD8⁺ T cell-derived IFN γ is not required for cerebral pathology (405,451,452,454,456).

After infection with *P. berghei* ANKA, at least 40% of Pb1-specific CD8⁺ T cells in the spleen and 70% of Pb1-specific CD8⁺ T cells in the brain were IFN γ ⁺GzmB⁺, and over 80% of Pb2- and F4-specific CD8⁺ T cells in both the spleen and brain were IFN γ ⁺GzmB⁺ (397,439). Since the production of GzmB by CD8⁺ T cells is necessary for the development of ECM, the capacity of the epitope-specific CD8⁺ T cells to kill splenocytes pulsed with the requisite peptides was examined using an *in vivo* cytotoxicity assay (397,439). Pb1-pulsed splenocytes transferred into *P. berghei* ANKA-infected mice were almost completely destroyed compared to unpulsed splenocytes, and Pb2- and F4-specific cells were shown to have moderate cytolytic activity (397,439). Furthermore, the epitope-specific cells were also determined to be positive for both CXCR3 and CCR5 (439), establishing that Pb1-, Pb2- and F4-specific CD8⁺ T cells are not only able of killing peptide-presenting cells, but are also capable of migrating to the brain.

All three of the epitopes identified in *P. berghei* ANKA are conserved in *P. berghei* NK65 and *P. yoelii*, which do not induce neuropathology (397,439). Pb1-, Pb2- and F4-specific CD8⁺ T cells were demonstrated to be induced in the spleen and accumulate within the brain of mice infected with the non-ECM-causing parasites (397,439). Indeed, Pb1 was found to be one of the most immunodominant epitopes in *P. yoelii*; greater than 15% of brain-sequestered CD8⁺ T cells in the *P. yoelii*-infected mice were Pb1-specific (397). Importantly, the epitope-specific cells generated in mice infected with *P. berghei* NK65 or *P. yoelii* were shown to be capable of cytolysis using the same *in vivo* cytolysis assay used in the *P. berghei* ANKA-infected mice (397,439).

It has been proposed that brain microvessel cells are activated during ECM, consequently allowing the cells to take-up and cross-present parasite material to CD8⁺ T cells, making them the targets of the CD8⁺ T cells (390,406,435) (Figure 4). Brain microvessel fragments isolated on day 7 post-infection from mice infected with the different strains were incubated with NFAT-lacZ reporter cells expressing the cognate TCR to compare antigen presentation between the different strains (397,439). The Pb1, Pb2 and F4 epitopes were only efficiently cross-presented by brain microvessels from mice infected with *P. berghei* ANKA, suggesting that cross-presentation in the brain is necessary for the development of neuropathology and may be a key difference between ECM-causing and non-ECM-causing parasites (397,439). Moreover, brain microvessel cross-presentation in *P. berghei* ANKA infected mice started to occur on day 6 post-infection, and only reached high levels on day 7 post-infection, when the clinical symptoms of ECM first appear, further reinforcing the idea that antigen-specific CD8⁺ T cells are responsible for the development of ECM (457).

Sequestration of parasites within the brain microvasculature was previously shown to strongly correlate with the onset of ECM and to be associated with host susceptibility (393-395). Amante *et al.* found that both CD4⁺ and CD8⁺ T cells contributed to whole-body parasite burden, while Claser *et al.* only observed a reduction in total parasite burden in mice deficient for CD8⁺ T cells (394,395). Furthermore, IFN γ ^{-/-} and LT α ^{-/-} mice were shown to have significantly attenuated parasite burdens, indicating that these two cytokines play a role in parasite tissue sequestration, and μ MT mice and mice receiving IL-10R-depleting antibodies had increased parasite burdens, suggesting that B cells and IL-10 production limit parasite accumulation (394). Alternatively, the impact of TNF on whole-body parasite burden varied from preventing to having no effect on sequestration, depending on the study (394,395).

The contribution of parasite tissue sequestration to the development of neuropathology was further examined by treating *P. berghei* ANKA-infected mice with anti-malarial drugs on day 6 post-infection. Treatment with artesunate or pyrimethamine prevented the development of ECM, and suppressed the associated increase in parasite biomass, but neither treatment attenuated the sequestration of CD8⁺ T cells within the brain (393,456). Furthermore, Haque *et al.*, found that treatment with artesunate significantly decreased the activation of the brain-accumulated CD8⁺ T cells, as indicated by reduced IFN γ production (456). Conversely, depletion of CD8⁺ T cells on day 6 post-infection substantially decreased parasite brain sequestration (393,456). These data suggest that CD8⁺ T cells augment the accumulation of parasites within the brain, and that CD8⁺ T cells require the concomitant presence of parasites for their activation and their ability to mediate ECM pathology.

McQuillan *et al.* also examined effect of parasite accumulation within the brain on the induction of ECM; parasite burden was decreased by the administration of quinine on days 4 to 6 post-

infection (392). The quinine treatment significantly decreased not only the parasite burden of the brain, but also the brain sequestration of CD8⁺ T cells (392). Furthermore, the quinine-treated mice were completely protected from ECM and succumbed to hyperparasitemia, compared to the pyrimethamine-treated mice which eventually developed ECM on days 13-15 post-infection, when their parasitemia was similar to that of the untreated mice on day 7 post-infection (392,393). (The artesunate-treated mice survived until at least day 12 post-infection, but whether they developed ECM after this time point was not indicated (456).) It is possible that there is a modest accumulation of parasites within the brain before day 6 post-infection that indirectly or directly causes the sequestration of CD8⁺ T cells within the brain by day 6 post-infection. And following a certain threshold, the CD8⁺ T cells are then able to accumulate within the brain in a parasite-independent manner, while the parasite burden increases in a CD8⁺ T cell-dependent manner. Thus minor differences in the timing of the antimalarial treatment may be responsible for whether the sequestration of CD8⁺ T cells was affected.

Furthermore, as mentioned above, the reduced parasite sequestration within the brain of the GzmB-deficient mice necessitated challenge with antigen in addition to the adoptive transfer of wild-type CD8⁺ T cells to induce ECM (456). Haque *et al.*, demonstrated that in the absence of GzmB, there was an enhanced anti-parasitic CD4⁺ T cell response that afforded improved control of the tissue parasite burden (456). The requirement of a critical threshold of parasite antigen for the development of neuropathology was confirmed by depletion of the anti-parasitic CD4⁺ T cells prior to the adoptive transfer of wild-type CD8⁺ T cells into GzmB-deficient mice, which resulted in an ECM incidence of 50% (456).

Based on the necessity of the concomitant sequestration of CD8⁺ T cells and parasites within the brain, it was postulated that the differing capacities of the brain microvessels to present antigen

may have been due to the varying tendencies toward the accumulation of the different parasite strains within the brain (397). Parasite sequestration was examined using luciferase-expressing lines of *P. berghei* ANKA and *P. yoelii* (397). On day 7 post-infection, when ECM symptoms typically start to appear in the *P. berghei* ANKA-infected mice, the parasitemia of the *P. yoelii*-infected mice was significantly higher, but the parasite burden in the perfused brains of the *P. berghei* ANKA-infected mice was much greater than in the *P. yoelii*-infected mice (397). Moreover, other studies reported significantly decreased parasite burdens in the brains of mice infected with *P. berghei* NK65 compared to *P. berghei* ANKA (393,396). Therefore, the reduced sequestration of parasites within the brain microvessels of mice infected with non-ECM-causing strains, and the consequent decreased availability of antigen, may partially explain the decreased cross-presentation of antigen to CD8⁺ T cells within the brain.

The necessity of parasite sequestration within the brain to induce neuropathology was extended to include the Pb1, Pb2 and F4 epitopes (397,439). *P. berghei* ANKA-infected mice were treated with anti-malarial drugs to eliminate parasite antigen within the brain and then given soluble antigen peptide to confirm that cross-presentation of parasite antigens to CD8⁺ T cells is required for the development of ECM (397). Pb1-treated mice displayed early symptoms of ECM, but did not progress to paralysis or coma, which is likely due to the Pb1-specific CD8⁺ T cells only accounting for approximately 9% of antigen-experienced CD8⁺ T cells in the brain (439). When the experiment was repeated with the addition of the neurotoxin folic acid, to increase the sensitivity of detecting BBB damage, greater than 80% of the mice given the Pb1 peptide died, compared to less than 20% of the mice given the control peptide (SIINFEKL from ovalbumin) (397).

Administration of Pb2 or F4 singularly after treatment with anti-malarial drugs did not increase the susceptibility of mice to folic acid-induced death; however, when both Pb2 and F4 were administered together, over 70% of the mice died (439). Given that Pb2- and F4-specific cells each only account for around 1% of antigen-experienced CD8⁺ T cells in the brain, it is logical to assume that the individual epitopes would not be as immunopathogenic as Pb1 (439). Furthermore, pulsing the brain microvasculature of *P. yoelii*-infected mice with Pb1 resulted in seven out of eight mice dying following folic acid challenge (397). This result supports the notion that access to and cross-presentation of parasite antigen by brain microvessels is required for the development of neuropathology. The necessity of antigen-specific CD8⁺ T cells in ECM was further validated by Lau *et al.*; transfer of CD8⁺ T cells from a MHCI-restricted TCR transgenic mouse specific for blood-stage *P. berghei* ANKA was shown to be capable of inducing ECM in mice depleted of endogenous CD8⁺ T cells (458).

Although the above studies clearly established that cross-presentation of parasite antigen to the cognate CD8⁺ T cell is necessary for the pathogenesis of ECM, the cell type responsible for antigen presentation was not identified. The multicellular microvessel fragments prevented analysis by flow cytometry and further digestion of the fragments to yield a single cell suspension significantly decreased cell viability (397). Nevertheless, myeloid cells were excluded as major antigen-presenting cells in *P. berghei* ANKA infection, since isolated brain leukocytes were found to stimulate the NFAT-lacZ reporter cells to a substantially smaller extent than the brain microvessel fragments, and no reduction in cross-presentation was observed in the microvessel fragments isolated from MAFIA mice (transgenic mice that allow the inducible apoptosis of macrophages and dendritic cells) (397). Furthermore, brain microvessel cross-presentation was dependent on collagenase digestion, indicating that the cells responsible for

cross-presentation were likely endothelial cells or pericytes, which are surrounded by the basal lamina (397)

Upon the optimization of a digestion protocol, single cell brain suspensions from *P. berghei* ANKA-infected mice were sorted into four populations: CD45⁺ microglia and leukocytes, CD45⁻CD31⁺ endothelial cells, CD45⁻CD140b⁺ pericytes, and CD45⁻CD31⁻CD140b⁻ astrocytes and neurons (457). Both the CD45⁺ microglia and leukocytes and the CD45⁻CD31⁺ endothelial cells were able to cross-present antigen when incubated with the NFAT-lacZ reporter cells (457). Further sorting of the CD45⁺ population into CD45^{int}CD11b⁺ microglia allowed the exclusion of microglia as a significant source of antigen presentation during *P. berghei* ANKA infection, as the isolated cells were unable to stimulate the reporter cells (457).

Cross-presentation by the isolated endothelial cells was observed to be markedly less than what had been shown for the microvessel fragments; however, the digestion method used had poor yields of endothelial cells (approximately 10% of other digestion methods that did not produce cells amenable to the assay) and the enzyme used in the digestion (papain) has previously been shown to cleave the heavy chain of MHC class I molecules (457). Nevertheless, normalization of cross-presentation by the cell input number demonstrated that endothelial cells were the most efficient at cross-presentation at the cellular level (457). Moreover, cell-to-cell interaction between CD8⁺ T cells and endothelial cells was observed *in situ* through immunofluorescence staining of olfactory bulb smears (457).

Subsequently, cross-presentation by brain endothelial cells was examined in greater detail *in vitro* using primary cultures of MBECs (457). Cross-presentation by brain microvessel fragments had previously been compared between wild-type mice and mice deficient for IFN γ , TNF α , and

LT α . IFN γ was shown to be necessary for cross-presentation in the brain, while TNF α and LT α were shown to be dispensable (457). Accordingly, concurrent stimulation with *P. berghei* ANKA parasitized erythrocytes and IFN γ was determined to be required for cross-presentation in MBECs from naïve mice (457). TNF α and LT α were neither able to induce cross-presentation by the MBECs nor enhance cross-presentation when used in conjunction with IFN γ (457). Additionally, substitution of the NFAT-lacZ reporter cells with CD8⁺ T cells from *P. berghei* ANKA-infected mice demonstrated that the cross-presenting MBECs were also able to be recognized for killing by parasite-specific CD8⁺ T cells (457).

Cross-presentation is thought to occur through two main pathways: the cytosolic pathway, which is sensitive to proteasome inhibitors and is TAP-dependent, and the vacuolar pathway, which requires endosome acidification and is TAP-independent (459). Antigen presentation was inhibited in MBECs from TAP-deficient mice and in MBECs treated with the proteasome inhibitor lactacystin, whereas treatment of MBECs with chloroquine, an inhibitor of endosome acidification, had no effect on cross-presentation, demonstrating that MBECs utilize the cytosolic pathway for cross-presentation (457). Additionally, examination of the co-localization of internalized parasites with acidic compartments revealed that merozoites were the primary source of antigen. The vast majority of phagosomes were not large enough to contain intact mature stages, and cross-presentation was found to be significantly more efficient when the MBECs were challenged with merozoites rather than mature parasitized erythrocytes (457).

The capacity of MBECs to capture and cross-present antigen from non-ECM-causing parasite strains to CD8⁺ T cells was also characterized, and both the internalization and the cross-presentation of antigen from *P. berghei* NK65 and *P. yoelii* were found to be markedly impaired compared to the cross-presentation of antigen from *P. berghei* ANKA (457). Therefore, the

inability of *P. berghei* NK65 and *P. yoelii* to cause ECM may be due to not only the mitigated sequestration of non-ECM-causing parasites within the brain, but also to the decreased cross-presentation efficiency of endothelial cells toward the non-ECM-causing strains.

As mentioned above, CD8⁺ T cell-mediated cytolysis of endothelial cells was previously proposed to be the dominant process responsible for the disruption of the BBB during ECM (390,406,435). Perforin and GzmB were shown to be necessary for the development of neuropathology (406,456) and parasite-specific CD8⁺ T cells were shown to be capable of recognizing cross-presenting brain endothelial cells for killing *in vitro* (457). The contribution of endothelial cell apoptosis to the pathogenesis of ECM has been corroborated (460) and disputed (396,461) by subsequent studies (Figure 4). Nevertheless, the high CD8⁺ T cell to endothelial cell ratio used *in vitro* is not indicative of the small number of CD8⁺ T cells that sequester within the brain *in vivo* (390), thus the strong killing of endothelial cells observed *in vitro* is unlikely to occur *in vivo*. Indeed, although CD8⁺ T cells were shown to colocalize with apoptotic endothelial cells *in vivo* using intravital imaging, apoptosis was demonstrated to be a rare event and therefore unlikely to play a large role in the loss of vascular integrity (396).

Olfactory bulb smears showed CD8⁺ T cells present on the luminal and abluminal faces of endothelial cells, and within the parenchyma (457), suggesting an alternative function for perforin and GzmB in ECM pathogenesis (Figure 4). Antigen-specific CD8⁺ T cells have been demonstrated to be capable of disrupting tight junctions between endothelial cells using a perforin-dependent mechanism (462), and to cross the BBB near endothelial cells presenting their cognate epitope (463), potentially through GzmB-mediated cleavage of the basement membrane (464). In this manner, cross-presentation of parasite antigen by endothelial cells may

result in apoptosis-independent BBB disruption, which ultimately leads to further pathological damage within the cerebral parenchyma (465).

CD8⁺ T cells have been shown to preferentially accumulate within post-capillary venules during ECM, rather than be homogeneously distributed throughout the brain (396,466). The cerebral microvasculature consists of two functionally distinct BBBs, the physiological BBB associated with capillaries (diameter $\leq 6\mu\text{m}$) and the neuroimmunological BBB associated with larger vessels (diameter 10-60 μm) (467). The physiological BBB is a single layer of endothelial cells, gliovascular membrane and astrocyte endfeet, while the neuroimmunological BBB consists of two layers, the vascular endothelial cells and their basement membrane and the basement membrane and astrocyte endfeet of the glia limitans, separated by the perivascular space (467). Nacer *et al.* observed that vascular leakage in ECM localized to the post-capillary venules (461), indicating that CD8⁺ T cells mediate disruption of the neuroimmunological BBB.

Intravital imaging studies revealed that antigen-specific CD8⁺ T cells were present on both the luminal and abluminal surfaces of cerebral endothelial cells *in vivo*, and that these cells exhibited arrested or sluggish movement (396,402). However, the relative importance of vascular and perivascular populations of CD8⁺ T cells differed between the two studies (396,402). Notably, the movement of the antigen-specific CD8⁺ T cells was reduced compared to bystander cells and was often found to be associated with significant vascular disruption (402). Furthermore, simultaneous blockade of the CD8⁺ T cell adhesion molecules LFA-1 and VLA-4 increased the velocity of the CD8⁺ T cells and prevented the development of neuropathology (402), indicating that vascular pathology in ECM is associated with the decreased movement of CD8⁺ T cells.

Notably, administration of an anti-peptide MHC I blocking antibody significantly increased the velocity of antigen-specific CD8⁺ T cells (402), demonstrating that an antigen-dependent interaction was responsible for the arrested movement of the CD8⁺ T cells. Furthermore, chimeric mice incapable of presenting MHC I peptides on endothelial cells and other stromal cells, but with normal hematopoietic presentation, were devoid of vascular pathology and markedly protected from ECM (402), further confirming that antigen-presentation by cerebral endothelial cells drives the CD8⁺ T cell-mediated disruption of the BBB *in vivo*.

Vascular leakage in these mice was associated with reduced expression of the tight junction protein claudin-5, suggesting an apoptosis-independent mechanism for BBB disruption (402). A prior study found that vascular leakage in ECM was not caused by decreased tight junction proteins by measuring the overall expression of tight junction proteins (466). However, vascular leakage in ECM is heterogeneous and localizes to certain areas of the cerebral microvasculature (461). Accordingly, Swanson *et al.* directly compared the tight junction protein expression in disrupted versus intact sections of the microvasculature and found that claudin-5 expression was significantly attenuated in areas of vascular leakage (402). Thus, BBB disruption was shown to be associated with antigen-specific CD8⁺ T cell interacting with cerebral endothelial cells and with mitigated expression of tight junction proteins.

Finally, the brainstem was shown to be a site of profound vascular leakage and cell death (402). Swanson *et al.* found that the vast majority of the dead cells in the brainstem were neurons, the extent of which was not observed in the other regions of the brain (402). Thus it was proposed that widespread, irreversible neuronal death in the brain stem was potentially the primary cause of mortality in ECM (402). Consistent with this observation, previous studies have shown that Fas- and FasL-deficient mice infected with *P. berghei* ANKA develop the clinical symptoms of

ECM, but ultimately resolve the cerebral symptoms (465,468), concurrent with the recovery of BBB integrity (468). However, this study determined that astrocytes, not neurons, accounted for the majority of apoptotic cells (465). Nevertheless, these results propose a model where BBB disruption is a critical step in the pathogenesis of ECM, but in which further pathology within the brain parenchyma is required for fatality.

4.5 Upregulation of CXCR3 Expression on T Cells

The chemokine receptor CXCR3 plays an integral role in the recruitment of pathogenic T cells to the brain during ECM (442-446); however, the factors that regulate the expression of CXCR3 following *P. berghei* ANKA infection remain undefined. In general, studies concerning chemokine receptors focus on the cellular distribution of their expression and on the response generated by the interaction with their requisite chemokines, while far fewer studies have examined the mechanisms underlying their induction. Thus, while it has been established that CXCR3 is highly expressed on NK cells and activated T cells, and that the chemokines CXCL9, CXCL10 and CXCL11 promote the chemotaxis of CXCR3-expressing cells (469), the processes controlling the upregulation of CXCR3 on naïve cells are much less well characterized.

CXCR3 induction has been shown to require reculture in the absence of exogenous stimulation following TCR-triggering (470); persistent TCR stimulation for an extended duration of time is unable to upregulate CXCR3 expression on T cells (470). Additionally, the production of IFN γ has also been shown to be essential to the induction of CXCR3; T cells deficient for IFN γ are unable to upregulate CXCR3 without the administration of exogenous IFN γ (470). Furthermore, unlike CCR5 (471,472), another chemokine receptor that is preferentially expressed on Th1 T cells, CXCR3 induction was found to not be dependent on the presence of IL-12 or STAT4

signalling, provided TCR stimulation was robust enough to induce IFN γ production independently of IL-12 co-stimulation (470).

Previously, IFN γ was shown to induce the expression of T-bet in a STAT1-dependent and STAT4-independent manner (473), and T-bet was found to transactivate the expression of IFN γ in CD4⁺ T cells (474,475), thereby forming a positive feedback loop. Accordingly, in addition to IFN γ blockade, CD4⁺ T cells deficient for STAT1 were also observed to be unable to upregulate the expression of CXCR3 following TCR triggering (476). Moreover, the attenuated expression of CXCR3 in STAT1^{-/-} CD4⁺ T cells was associated with impaired induction of T-bet (476), and the absence of T-bet also resulted in mitigated upregulation of CXCR3 on CD4⁺ T cells (477). Interestingly, Lord *et al.* determined that CXCR3 expression was completely independent of IFN γ production; CXCR3 expression was significantly induced when T-bet alone was transduced into T-bet^{-/-} x IFN γ ^{-/-} CD4⁺ T cells (477). This finding indicated that IFN γ is not directly responsible for CXCR3 expression in CD4⁺ T cells, rather IFN γ likely acts to induce the expression of T-bet, which then drives the upregulation of CXCR3 (477).

Contrastingly, neither the depletion of IFN γ nor the lack of STAT1 had an effect on CXCR3 expression on CD8⁺ T cells (476). Eomes, a master transcription factor of Th1 cells, is thought to play an integral role in the effector function of CD8⁺ T cells (478). CD8⁺ T cells from T-bet knock-out mice were observed to have normal expression of CXCR3, whereas CD8⁺ T cells from Eomes knock-out mice were observed to have markedly decreased expression of CXCR3 (479), suggesting that the regulation of CXCR3 expression in CD8⁺ T cells is Eomes-dependent and T-bet-independent. Additionally, while TCR signal transduction is crucial to the upregulation of CXCR3 on T cells in general, whether TCR signalling differentially effects the expression of CXCR3 on CD4⁺ and CD8⁺ T cells is unknown.

4.6 Regulatory CD4⁺ T Cells

In contrast to the involvement of CD8⁺ T cells in the pathogenesis of ECM, the role of regulatory CD4⁺ T cells is still a matter of contention. IL-10 is an important anti-inflammatory cytokine that is able to suppress the immune response to pathogens, and this can prevent infection-induced pathology (480), but it can also potentially impair parasite clearance (481). Depletion of IL-10 (482) and IL-10 receptor blockade (483) were shown to increase the incidence of ECM in resistant BALB/c mice, and exogenous IL-10 was found to significantly reduce neuropathology in susceptible CBA/J mice (482), suggesting that IL-10 plays a protective role in *P. berghei* ANKA infection. However, IL-10 deficiency (484) and treatment with anti-IL-10 receptor antibodies (394) were shown to have little to no effect on the susceptibility of C57BL/6 mice to ECM. Nevertheless, blockade of the IL-10 receptor in C57BL/6 mice did significantly augment their parasite burden (394).

Regulatory CD4⁺ T cells were shown to be the primary source of IL-10 during malaria infection in mice (481,485). And although the frequency of CD25⁺Foxp3⁺ CD4⁺ T cells (Tregs) in the spleen was shown to be unchanged or slightly decreased at the onset of ECM symptoms compared to naïve mice (484,486), the proportion of IL-10-producing CD25⁺CD4⁺ T cells was significantly increased (487). The potential role of Tregs in ECM was initially examined using CD25 depletion, as Foxp3, the exclusive marker of Tregs, is intracellular, and CD25 is highly expressed on these cells (484,486,487). Depletion of CD25 at the time of infection or 14 days prior to infection was demonstrated to markedly reduce the incidence of ECM (484,486,487). Protection was associated with a significant reduction in both the tissue parasite burden and brain sequestration of CD8⁺ T cells (484). Moreover, while CD25 depletion in wild-type mice was protective, IL-10 knock-out mice treated with anti-CD25 still succumbed to *P. berghei* ANKA

infection, leading Amante *et al.* to postulate that a non-Treg source of IL-10 was required to prevent neuropathogenesis (484).

However, at the onset of symptoms in the control mice, one study found that the percentage of splenic CD25⁺Foxp3⁺ CD4⁺ T cells in the CD25 depleted mice was significantly increased compared to the control mice (486), and another study found that the total number of splenic CD25⁺Foxp3⁺ CD4⁺ T cells in the CD25 depleted mice was the same as that of the control mice (484). DEREK mice express a DTR-eGFP fusion protein under the control of the *foxp3* gene locus that allows the diphtheria toxin-induced ablation of Foxp3⁺ Tregs (488). Specific depletion of Foxp3⁺ cells using DEREK mice had no effect on the incidence of ECM (488), further suggesting that the protection afforded by CD25-depletion was not caused by an absence of Tregs. Moreover, a study examining CD25-depletion during *P. yoelii* infection also found that there was a rapid recovery of splenic Tregs following CD25 depletion, which was determined to be due to the increased expression of CD25 on CD25⁻Foxp3⁺ cells (489).

Furthermore, the *in vivo* expansion of Tregs using IL-2/anti-IL-2 complexes significantly attenuated the incidence of ECM (490). The augmented population of Tregs expressed elevated levels of both IL-10 and CTLA-4, and was associated with significantly decreased sequestration of parasitized erythrocytes and CD8⁺ T cells within the brain (490). However, further examination determined that the protection afforded by the elevated number of Tregs was predominately dependent on CTLA-4 expression, rather than IL-10 production (490). IL-10 production by Foxp3⁻ regulatory CD4⁺ T cells has been shown to mitigate pathology in non-cerebral models of malaria (481,485), but the role of IL-10 produced by these cells in the pathogenesis of ECM is unknown.

Finally, IFN γ ⁺IL-10⁺ double-producing Foxp3⁻CD4⁺ T cells have also been shown to play a critical role in the regulation of *P. chabaudi*-induced immunopathology (485) and IL-10 single-producing Foxp3⁻CD4⁺ T cells were shown to be associated with impaired parasite clearance in *P. yoelii* infection (481). Additionally, IL-10 production by tissue-resident CD169⁺ macrophages was recently shown to limit immunopathology during *P. berghei* ANKA infection in BALB/c mice (491). Accordingly, IL-10 knock-out mice infected with either *P. yoelii* or *P. berghei* NK65 were better able to control their parasitemia, but exhibited significantly more hepatic pathology than wild-type mice (481,492). Liver damage has also been reported in *P. berghei* ANKA infected-C57BL/6 mice. One study indicated that high parasite burdens were responsible for hepatic pathology during ECM (493), while another demonstrated that liver injury was limited by CTLA-4-mediated attenuation of IL-12 and IFN γ production (494), but the effect of IL-10-producing regulatory T cells on hepatic pathology during ECM has not been examined.

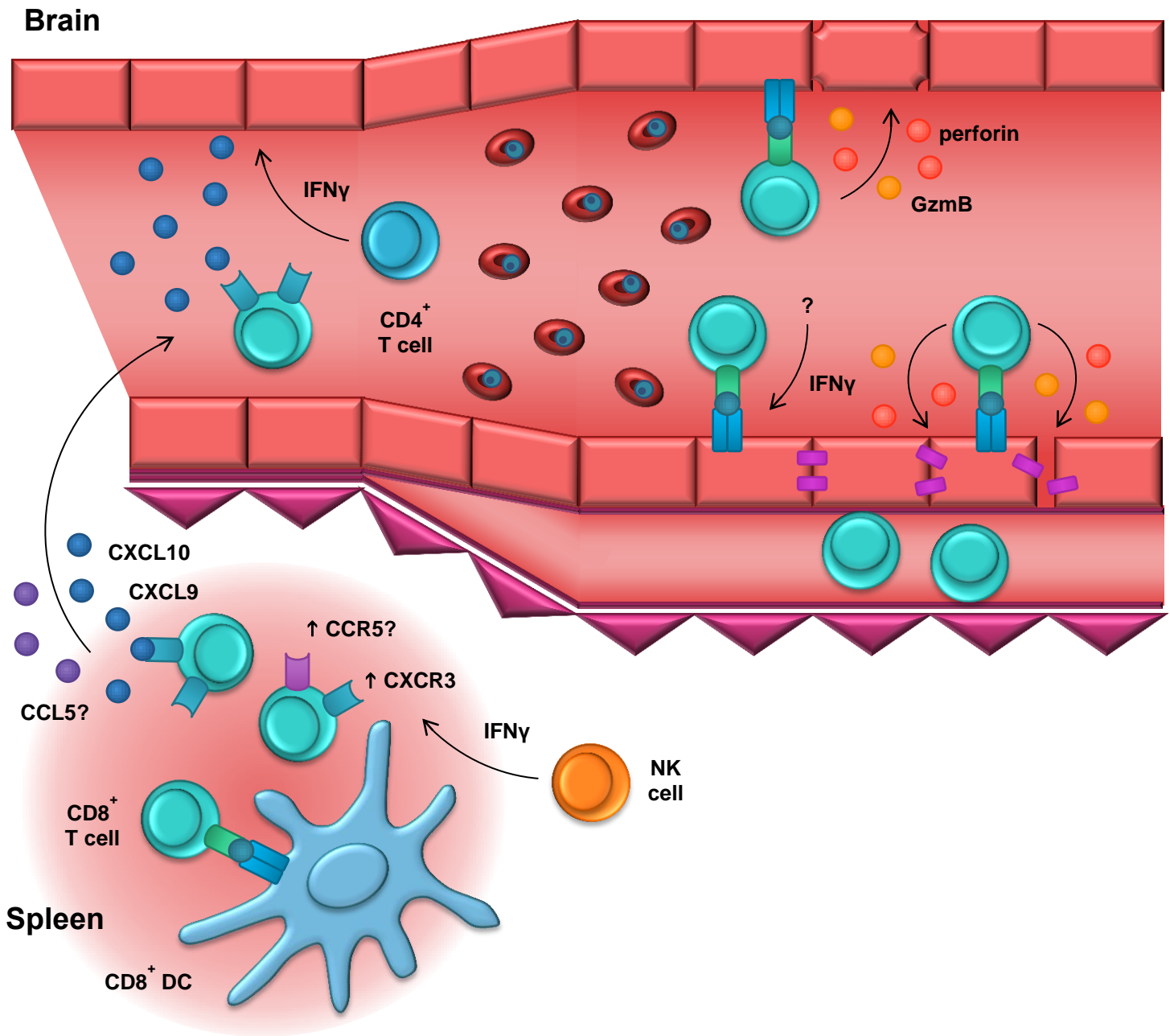


Figure 4. The Role of CD8⁺ T Cells in ECM. Parasite-specific CD8⁺ T cells are activated in the spleen by cross-presentation of parasite antigens by CD8⁺ DCs. Upon upregulation of the chemokine receptor CXCR3, CD8⁺ T cells migrate to the brain. IFN γ production by NK cells plays a role in T cell expression of CXCR3, and IFN γ production by CD4⁺ T cells increases the expression of CXCL9 and CXCL10. Activated brain microvessel cells (likely endothelial cells) take up parasite material and cross-present antigen to the brain-sequestered CD8⁺ T cells. IFN γ was shown to be necessary for cross-presentation in the brain, but the source was not identified. CD8⁺ T cell-mediated cytotoxicity was initially thought to be responsible for the breakdown of the BBB and the neuropathogenesis of ECM. Recently, other mechanisms have been proposed to explain the loss of vascular integrity. Antigen-specific CD8⁺ T cells are capable of disrupting tight junctions and cleave the basal lamina in a perforin- and GzmB-dependent manner, and the expression of tight junction proteins was shown to be attenuated in areas of vascular leakage during ECM. Figure generated by KV.

5. Malaria and Iron

Childhood anemia is a major public health problem in sub-Saharan Africa (495). Anemia is characterized by a reduced number of erythrocytes, often in conjunction with decreased hemoglobin levels and altered erythrocyte morphology, to an extent that tissue oxygen delivery is impaired (495,496). Iron deficiency is the primary cause of anemia, but malaria is also responsible for a large proportion of cases in many regions, particularly in western sub-Saharan Africa (495,497). Iron deficiency can be the result of a number of factors, including intestinal helminth infections, and inadequate intake or absorption from dietary sources (496). Iron deficiency anemia has been shown to correlate with suboptimal cognitive development in children (498), and iron supplementation has been consistently regarded as an effective intervention to decrease the prevalence of iron deficiency anemia (499,500). However, previous studies have indicated that iron deficiency may be protective against parasitemia and clinical malaria (501,502), and that iron supplementation may cause an increased risk of serious adverse events in areas that have a high transmission of malaria (503).

5.1 Systemic Iron Homeostasis

Iron levels within the body are primarily regulated at the level of intestinal absorption, as there is no excretory pathway (504). However, absorption by duodenal enterocytes only contributes to a small amount of the total circulating iron; the majority is obtained through macrophage-mediated recycling of iron from senescent erythrocytes (504) (Figure 5). Appropriate systemic availability of iron is maintained by hepcidin, which controls the release of iron into the circulatory system (504). Hepcidin causes the internalization and degradation of ferroportin, an iron transporter present on duodenal enterocytes, reticuloendothelial macrophages and hepatocytes, thereby preventing the export of iron from these cells (505) (Figure 5). A variety of factors, including

erythropoietic signals, iron concentration, and inflammation are capable of modulating the expression of hepcidin, and thereby adjusting the availability of iron to suit a diverse array of physiological conditions (504).

Ferrous iron and heme iron are the main forms of dietary iron that are absorbed by duodenal enterocytes. Duodenal cytochrome B contributes to the reduction of dietary ferric iron (Fe^{2+}) to ferrous iron (Fe^{3+}), but is not absolutely required for the import of ferric iron, suggesting the existence of additional ferric reductases (506-508). Following reduction, the ferrous iron is then transported into the cytoplasm of duodenal enterocytes by DMT1 (509). Less is known about the import of heme iron, but two possible candidates for intestinal heme transporters, HCP1 (510) and HRG1 (511), have been identified.

Macrophages predominately acquire iron through the phagocytosis and subsequent digestion of senescent erythrocytes and their hemoglobin (504). However the sequence of events following the release of heme iron from erythrocytes has not been determined with certainty. It has been proposed that the released heme is either degraded by HO-1 within the phagolysosome, freeing the iron to then be exported to the cytoplasm (512,513), or that the heme iron is first exported to the cytoplasm through one of the heme transporters mentioned above, and then degraded by HO-1 in the cytoplasm to release ferrous iron (514).

Once in the cytoplasm, the ferrous iron is either stored in ferritin following oxidation by the ferritin heavy chains to ferric iron (504), or the ferrous iron is exported from the cell into the bloodstream by ferroportin (515). Upon release into the circulation, the ferrous iron is converted to ferric iron by the ferroxidases hephaestin (516) and ceruloplasmin (517), and then loaded onto the iron-transport protein transferrin (504). Overall absorption of iron into the body is controlled

by hepcidin through the retention of iron within the duodenal enterocytes (518). Hepcidin induces the internalization and degradation of ferroportin, preventing the release of iron into the bloodstream (505). Enterocytes, and the iron contained within them, are sloughed off and removed from the body every two to five days, resulting in the excretion of excess iron (518).

Most cells in the body acquire iron through TfR1-mediated endocytosis of transferrin-bound iron (519) (Figure 5). Acidification of the endosomes following internalization induces conformational changes in both transferrin and TfR1, which releases the transferrin-bound iron (520). The ferric iron is then reduced to ferrous iron by STEAP metalloreductases and transported into the cytosol by DMT1, while transferrin and TfR1 are recycled back to the cell surface (519). The majority of iron within the body is incorporated in the hemoglobin of erythroid precursors and mature erythrocytes, and surplus iron is predominately stored within reticuloendothelial macrophages and hepatocytes to buffer fluxes in iron availability (521) (Figure 5). If the iron-binding capacity of transferrin is exceeded, non-transferrin-bound iron will start to accumulate (522). Circulating non-transferrin-bound iron mainly complexes with citrate or acetate, and can be taken up by a limited number of cell types, including hepatocytes (522).

As stated above, systemic iron availability is regulated by hepcidin, which is transcriptionally controlled by erythropoietic factors, iron concentration and inflammation (504). Initially, hypoxia and erythropoietin were thought to directly regulate hepcidin expression (523,524), but the preponderance of data now indicate that increased erythropoiesis following tissue hypoxia, anemia or erythropoietin administration is required for the induction of a hepcidin suppressor (525,526). Two BMP family members, GDF15 (527) and TWSG1 (528), were proposed as erythroid suppressors of hepcidin in thalassemia, but subsequent studies indicated that they were unlikely to contribute to hepcidin attenuation after hemorrhage (529). Recently erythroferrone

was shown to be produced by erythroblasts in response to erythropoietic stimulation and to be capable of mitigating hepcidin expression (530), suggesting that erythroferrone is the erythroid suppressor of hepcidin expression responsible for regulating the availability of iron in response to erythropoiesis (Figure 5).

Both iron stores and plasma iron concentrations are capable of modulating the production of hepcidin (531). Increased accumulation of iron-loaded ferritin within hepatocytes induces the production of BMP6 (532), predominately by other hepatic cell types, including sinusoidal endothelial cells and macrophages. The mechanism through which iron overload in hepatocytes increases the expression of BMP6 in other cell types is not currently known (533). BMP6 forms a complex with the heterodimeric BMP receptor and the co-receptor hemojuvelin, promoting signalling through the phosphorylation of SMAD1/5/8 and SMAD4 and causing the transcription of hepcidin (534-536) (Figure 5). TMPRSS6 attenuates BMP6-mediated signalling by cleaving hemojuvelin (537), and the upregulation of hepcidin through BMP/SMAD signalling further induces the expression of the negative feedback inhibitors SMAD7 (538) and Id1 (539). Additionally, hepcidin production is regulated by transferrin-bound iron through the receptors TfR2 and HFE (540) (Figure 5). TfR2 and HFE are thought to interact with the BMP receptor complex (531,541), but the downstream signalling cascade has not yet been characterized (533).

Finally, inflammation and infection are also capable of upregulating hepcidin production, primarily through IL-6-mediated STAT3 signalling (542,543) (Figure 5), but additional mediators, including type I IFN, have been shown to contribute (544). Elevated levels of hepcidin are responsible for the hypoferraemia that often accompanies infection (542), and can contribute to the development of anemia under conditions of prolonged inflammation by restricting the availability of iron for erythropoiesis (545). Iron deficiency resulting from the

inflammation-mediated induction of hepcidin is thought to be a host defense mechanism (533). Hypoferraemia decreases the hemoglobin content in erythrocytes (533) and iron deficiency has been shown to reduce the risk of parasitemia and hyperparasitemia during malaria (501). Erythrocytes from iron-deficient donors were found to be less efficiently parasitized by *P. falciparum* than erythrocytes from donors that were iron-replete, and iron supplementation in the iron-deficient donors abrogated the protection (546), potentially explaining the decreased risk of malaria-related pathology provided by iron deficiency.

Furthermore, elevated levels of inflammation and hepcidin resulting from malaria infection have been shown to cause a redistribution of iron within the body from hepatocytes to macrophages (547). This decreased storage of iron within hepatocytes mediated by blood-stage infection was found to inhibit the growth of sporozoites and prevent superinfection in a murine model (547), and was proposed to be a mechanism of innate immunity in young children in malaria-endemic regions. However hepcidin levels were observed to be lower in Nigerian and Kenyan children with severe malarial anemia compared to uncomplicated malaria (548,549). Hepcidin levels were associated with both IL-6 and IL-10 and were inversely correlated with hemoglobin levels (549). These findings suggest that erythropoietic-mediated suppression of hepcidin may outweigh inflammation-mediated induction of hepcidin in children with severe malarial anemia. Nevertheless, decreased hepcidin levels were also observed in children with cerebral malaria that were only mildly anemic (548), thus other factors likely contribute to hepcidin regulation during severe malaria.

5.2 Malaria and Iron Supplementation

Observational cohort studies have frequently found an association between iron deficiency and a reduced risk of malaria-related pathology. Nyakeriga *et al.* determined that the prevalence of clinical malaria was significantly lower in iron deficient Kenyan children compared to those that were iron replete (502), and Gwamaka *et al.*, observed that iron deficiency significantly decreased the risk of parasitemia, hyperparasitemia and severe malaria in Tanzanian children (501). However, accurate assessment of iron status in malaria endemic regions is problematic, because many of the typical measurements of systemic iron levels are also affected by inflammation (550). The above studies attempted to minimize the potential misclassification of iron status in several ways, including excluding children from analysis if they had evidence of inflammation or malaria infection when iron levels were measured (501,502). Nevertheless, it is possible that low levels of inflammation may have influenced the analysis of iron status.

Despite iron deficiency potentially offering protection from malaria, iron deficiency anemia is associated with impaired cognitive development (498), thus clinical trials of iron supplementation have been conducted in malaria-endemic regions to characterize the risk of iron administration in these areas. Pioneering studies in Tanzanian and Gambian children found that iron supplementation decreased the frequency of anemia and had no effect on the incidence of malaria (551,552). Moreover, antimalarial treatment alone was found to reduce the frequency of severe anemia (551). Contrastingly, a large subsequent study in Tanzania determined that iron supplementation significantly increased the risk of hospital admissions and serious adverse events (503). Furthermore, baseline iron status was shown to modify this effect on morbidity, as iron supplementation in children that were iron deficient/anaemic resulted in a significantly lower prevalence of adverse events compared to children that were iron replete (503).

The results of the study in Tanzania indicated that it might be necessary to limit iron supplementation to iron-deficient children; however, universal screening prior to administration of iron would be impractical in most malaria-endemic countries (553). Moreover, a sub-study of the Tanzanian trial failed to show a significant difference in the frequency of hospital admissions or adverse events between the placebo and iron supplementation groups (503). Sazawal *et al.* postulated that the disparity between the main study and the sub-study was likely due to increased diagnosis and management of children with malaria and other infections in the sub-study (503). Similarly, earlier iron supplementation studies also reported that iron was beneficial when combined with antimalarial treatment (552), and a subsequent trial conducted in Ghana found that iron supplementation did not increase the incidence of malaria when insecticide-treated nets and antimalarial treatment were provided to the participants (554).

Consequently, a systematic review of iron supplementation in infants and children living in malaria holo- or hyperendemic regions was performed to resolve these apparent discrepancies (555). Iron supplementation was found to be effective at improving hemoglobin levels and decreasing the frequency of anemia in regions with a high transmission of malaria (555). Furthermore, the analysis determined that iron supplementation did not cause a difference in the risk of clinical malaria compared to placebo or supplementation without iron (555). The risk of clinical malaria was lower in children receiving iron supplementation in studies that implemented malaria prevention and treatment programmes, and higher in children receiving iron supplementation in studies that did not include prevention and treatment strategies (555). Importantly, the risk of clinical malaria between the iron supplementation group and the control group was not affected by whether the children were baseline anaemic (555). Therefore, the systematic review concluded that iron supplementation is safe in malaria-endemic regions

without the need to screen for iron deficiency or anemia, provided that regular prevention and treatment services are available (555).

In addition to concerns regarding the safety of iron supplementation in malaria-endemic regions, there have also been concerns that iron supplementation may be less effective at ameliorating anemia in hyperendemic regions compared to non-malarious areas (556). Infection-induced inflammation is capable of inhibiting the absorption of iron from dietary sources by upregulating the expression of hepcidin (557,558), but the magnitude and duration of this effect are not fully understood. Iron incorporation was found to be decreased in Gambian children with post-malarial anemia compared to Gambian children with non-malarial anemia, and improved markedly following anti-malarial treatment (559). Interestingly, a significantly greater hemoglobin response was measured in the children with post-malarial anemia despite the attenuated incorporation of iron (559), which was hypothesized to be due to the release of sequestered iron following resolution of the infection.

Furthermore, asymptomatic parasitemia in young Beninese women was shown to reduce the absorption of dietary iron, but not to significantly alter systemic utilization of iron (560). The decreased intestinal absorption of iron observed in these women may be at least partially explained by the low level of inflammation and hepcidin that was induced by the parasitemia, despite the lack of clinical presentation (560). Correspondingly, Ivorian children with afebrile parasitemia were also shown to have increased inflammation and serum hepcidin levels prior to treatment with antimalarials, which was associated with decreased absorption, but not systemic utilization, of iron (561). Based on the above studies, it was hypothesized that effective iron incorporation in malaria-endemic areas may be dependent on the appropriate timing of iron supplementation with respect to antimalarial treatment.

Delaying iron supplementation in Ugandan children to four weeks after the initiation of antimalarial treatment resulted in a higher incorporation of iron into erythrocytes at four weeks post-treatment compared to children that received iron supplementation concomitantly (562). However, the iron status of the Ugandan children that received the delayed iron supplementation was demonstrated to be worse four weeks after the initiation of antimalarial treatment, and to be equivalent to the children that received iron supplementation concomitantly eight weeks after the initiation of antimalarial treatment (562). Thus delaying iron supplementation for four weeks increased iron incorporation into erythrocytes, but also postponed haematological recovery (562). Additionally, a study in Gambia that examined the effect of delaying iron supplementation for two weeks after the initiation of antimalarial treatment did not observe a difference in iron absorption or hemoglobin concentration in children that received the postponed iron supplementation compared to children that received concomitant administration of iron (563). Thus the data from these two studies do not demonstrate a benefit to delaying iron supplementation in children with malaria.

Finally, many malaria endemic regions have seasonal transmission, and it was hypothesized that differential rates of malaria transmission may result in iron supplementation being more efficacious at certain times of the year. In Gambian and Kenyan children, hepcidin levels were observed to be decreased and the prevalence of iron deficiency increased at the end of the malaria season (564). These data suggest that not only is there a greater need for iron supplementation at the end of the malaria season, but that iron incorporation would likely be higher at this time (564). However, iron incorporation and hemoglobin levels were not measured in this study, and the results obtained from the studies above suggest that relationship between malaria and iron is reliant on more factors than simply the level of hepcidin.

5.3 Iron and IFN γ Signalling

IFN γ is necessary for neuropathogenesis during *P. berghei* ANKA infection (394,450-452); mice deficient for IFN γ (394) or IFN γ R (450,451) have a markedly decreased incidence of ECM. IFN γ production induces the expression of the chemokines CXCL9 and CXCL10 (447-449), which promotes the chemotaxis of pathogenic T cells to the brain through the chemokine receptor CXCR3 (442,443). Accordingly, the mRNA expression of CXCL9 and CXCL10 were found to be reduced in mice deficient for IFN γ and IFN γ R (446), and the brain sequestration of T cell was attenuated in IFN γ R knock-out mice (450). Beyond decreasing the accumulation of pathogenic T cells in the brain by mitigating the expression of chemokines, the absence of IFN γ signalling likely also precludes the chemotaxis of CD4⁺ T cells by interfering with the upregulation of CXCR3. T cells deficient for IFN γ were shown to be unable to upregulate CXCR3 expression following TCR triggering (470). Interestingly, depletion of IFN γ did not affect the expression of CXCR3 on CD8⁺ T cells (476), indicating that CXCR3 is differentially regulated on CD4⁺ and CD8⁺ T cells.

TfR1-mediated uptake of iron was shown to induce the internalization of IFN γ R2 on T cells, thereby attenuating their responsiveness to IFN γ , as evidenced by the reduced phosphorylation of STAT1 (565). Moreover, treatment with the iron chelator deferoxamine was shown to cause the cell surface accumulation of IFN γ R2 and the induction of IFN γ -dependent apoptosis (565). The effect of iron on the expression of CXCR3 was not examined, but based on the data above the administration of iron would likely prevent the upregulation of CXCR3 on CD4⁺ T cells, but not on CD8⁺ T cells. Whether iron deficiency has the same effect on the T cell response as deferoxamine and whether IFN γ -mediated apoptosis is involved in the protection against malaria pathology provided by iron deficiency is unknown.

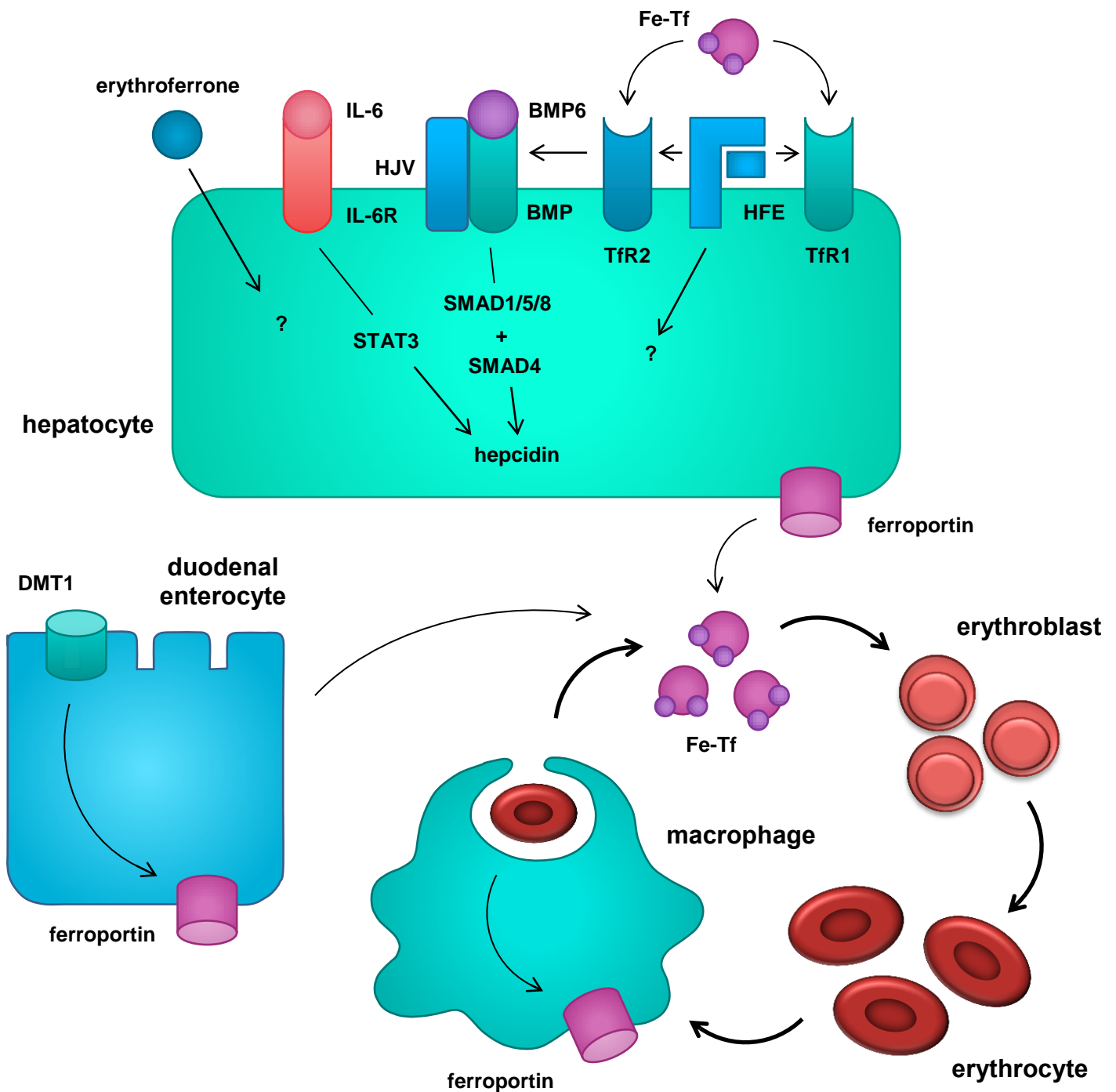


Figure 5. Systemic Iron Homeostasis. Hepcidin regulates the systemic availability of iron by causing the degradation of the iron transporter ferroportin. Hepcidin is transcriptionally controlled by erythropoietic signals (erythroferrone), inflammation (IL-6), and hepatic and plasma iron levels (BMP6 and transferrin-bound iron). The majority of iron within the body is derived from the heme of senescent erythrocytes, which are recycled by reticuloendothelial macrophages, while the absorption of dietary iron by duodenal enterocytes only contributes to a small amount of the total body iron. Iron released into the bloodstream by ferroportin is bound to transferrin, and transferrin is taken up by peripheral cells, particularly erythroid precursors. Surplus iron is stored within reticuloendothelial macrophages and hepatocytes to buffer fluxes in iron availability. Figure generated by KV.

6. Protein Tyrosine Phosphatases and the Immune Response

Tyrosine phosphorylation plays an integral role in signal transduction and contributes to the regulation of numerous cellular processes (566). The level and duration of tyrosine phosphorylation is controlled by the opposing actions of PTKs, which phosphorylate tyrosine residues, and PTPs, which dephosphorylate tyrosine residues (566). PTKs and PTPs can either positively or negatively regulate signal transduction depending on the particular protein, and both are required to appropriately modulate tyrosine phosphorylation during a physiological immune response. The role of PTKs in the regulation of TCR-mediated activation has long been appreciated; however, a specific and active role for PTPs in lymphocyte activation has only recently started to be recognized (567,568).

6.1 Regulation of Protein Tyrosine Phosphatase Activity

Class I, cysteine-based PTPs account for the majority of tyrosine phosphatases, and contain both the classical PTPs, which are tyrosine-specific, and the dual-specific PTPs, which have a broad range of substrate specificities (569). Class I PTPs share a common catalytic mechanism based on a conserved cysteine residue that forms a thiophosphate intermediate during catalysis (570-575). The nucleophilic cysteine disrupts the phosphorus-oxygen bond of the phosphatase group and an aspartate residue present in the active site of the phosphatase donates a proton to the OH-leaving group. This reaction results in the release of the dephosphorylated substrate and the formation of a phospho-cysteine intermediate, which is stabilized by an invariant arginine group. The thiophosphate intermediate is then hydrolyzed by the aspartate residue, which abstracts a proton from the newly formed water molecule, and provides it to the intermediate to form a free phosphate group.

Classical PTPs possess a phospho-tyrosine recognition domain that is responsible for their substrate specificity (576). The phospho-tyrosine domain defines the depth of the catalytic pocket, thereby selecting for the longer phospho-tyrosine substrates over the shorter phosphoserine and phospho-threonine substrates, which are unable to reach the catalytic residues (576). Substrate specificity is further defined by non-catalytic motifs that determine the cellular localization of the PTP or that allow binding to substrate proteins (577). Small changes in the microenvironment of the active site can affect the catalytic efficiencies toward different phospho-substrates (578,579), further selecting for the specificity of the phosphatase. For example, single amino acid substitutions in the phospho-tyrosine domain can restrain substrate binding within the active site so that phosphatase activity toward certain phospho-substrates is reduced (580,581) and substrate binding has been shown to cause conformational changes in the active site that effect catalytic activity (582,583).

PTP activity is regulated by numerous factors, including iron levels (584), phosphorylation (585,586), dimerization (587), and oxidation (588). While phosphorylation and dimerization have been shown to be specific to certain PTPs or PTP families, oxidation of the conserved cysteine in the active site is thought to be a general mechanism of PTP regulation (588). The catalytic cysteine has an unusually low pKa which renders it particularly susceptible to oxidation, and oxidation of the cysteine abrogates its nucleophilic capacity thereby inhibiting the phosphatase activity of the PTP (588). Oxidation of the cysteine is reversible if the cysteine is not oxidized further than sulphenic acid (S-OH), while oxidation to sulphinic acid (S-O₂H) or sulphonic acid (S-O₃H) is typically irreversible (588). However, dual-specificity phosphatases possess a second cysteine residue within their active site, which results in the formation of a

disulphide bond during oxidation, protecting the PTP from further oxidation and irreversible inactivation (589).

Peroxovanadium compounds, such as bpV(phen), are long-established inhibitors of protein tyrosine phosphatases (590), and attenuate PTP activity by irreversibly oxidizing the catalytic cysteine to sulphonic acid (591). Since peroxovanadium compounds target the conserved cysteine residue, they are unable to inhibit the activity of a particular PTP. Structural analysis has revealed differences in the surface topology and charge distribution in the regions surrounding the catalytic pocket (592) that could potentially be utilized to generate specific PTP inhibitors. Additionally, inhibitors that target allosteric sites on PTPs have also been proposed as a solution to the specificity problem. An allosteric inhibitor of the class I PTP PTP1B was shown to bind at a site on the side of the phosphatase opposite to the catalytic site (579). This inhibitor prevented the conformational changes required for the generation of the active form of the phosphatase, and importantly, did so by interacting with residues that are not conserved between PTPs (579). Identification of specific PTP inhibitors is currently an area of active research as aberrant tyrosine phosphorylation has been implicated in numerous pathologies, including leishmaniasis.

Inhibition of PTP activity by bpV(phen) was demonstrated to significantly reduce footpad swelling in a mouse model of cutaneous leishmaniasis, concomitant with a marked decrease in the accumulation of parasites in the draining lymph node (593). The protection provided by bpV(phen) was found to be dependent on the upregulation of nitric oxide production, as concurrent treatment with the inducible nitric oxide synthase inhibitor aminoguanidine abrogated control of the infection (594). Interestingly, administration of exogenous iron was also found to protect mice from footpad pathology during *Leishmania* infection (595). The iron-treated mice were shown to have a decreased parasite burden in the draining lymph node and increased

mRNA expression of inducible nitric oxide synthase (595). Since iron has been shown to be capable of attenuating PTP activity (584), these results suggest that PTP inhibition could be at least partially responsible for the protection provided by iron against cutaneous leishmaniasis.

6.2 Role of Lck and CD45 in Proximal TCR Signal Transduction

Signal transduction through the TCR is initiated by the recognition of cognate peptide bound to an MHC molecule. TCR engagement causes the dephosphorylation of the inhibitory tyrosine of the Src family kinase Lck. Activated Lck then phosphorylates the immunoreceptor tyrosine-based activation motifs located on the cytoplasmic tails of the TCR (596), leading to the recruitment of ZAP70 (597). TCR-bound ZAP70 is phosphorylated by Lck (598), which is followed by the phosphorylation of LAT (599) and SLP76 (600) by the activated ZAP70. This triggers a cascade of phosphorylation and activation of multiple downstream effectors, culminating in the activation of mitogen-activated protein kinase signalling, calcium mobilization, and transcriptional regulation.

Activation of Lck is controlled by the phosphorylation state of the inhibitory tyrosine (Y505) and the activatory tyrosine (Y394). Csk-mediated phosphorylation of the inhibitory tyrosine stabilizes Lck in a restrained, inactive conformation (601,602), while CD45-mediated dephosphorylation of the inhibitory tyrosine results in Lck adopting an open conformation that exposes the activatory tyrosine (603,604). Subsequent transphosphorylation of the activatory tyrosine stabilizes the catalytic pocket, enhancing the enzymatic activity of Lck (603,605). The activatory tyrosine can subsequently be dephosphorylated by various phosphatases, including CD45, SHP-1 and PTP-PEST, resulting in attenuated signalling capacity of Lck (606-608).

Treatment of Jurkat cells and human primary T cells with the PTP inhibitor pervanadate was found to induce patterns of tyrosine phosphorylation that were similar to the phosphorylation induced by TCR stimulation (609,610). Moreover, pervanadate treatment was shown to enhance the activity of Lck and to inhibit the activity of CD45, concomitant with increased phosphorylation of both the activating and inhibitory tyrosine of Lck (609). Pervanadate also augmented tyrosine phosphorylation and Lck activation in cells that were deficient for CD45, suggesting that the inhibition of CD45 was only partially responsible for the stimulatory effects of pervanadate (609). Overall, these results indicated that tyrosine phosphatase activity is required to limit basal PTK activity and to maintain a resting T cell phenotype. However, the impact of pervanadate compounds given concurrently with TCR stimulation is unknown. TCR signal transduction itself would likely change the tyrosine phosphorylation of proximal signalling molecules compared to naïve cells, which could potentially modulate the tyrosine residues available to be affected by PTP inhibition.

Rationale and Objectives

Malaria is an infectious, mosquito-borne disease caused by parasites of the *Plasmodium* genus, and was responsible for 212 million cases and 429,000 deaths in 2015 alone (10). Rapid and effective treatment of malaria with artemisinin-based combination therapy following parasitological confirmation typically results in a prompt and full recovery (53). However, if treatment is delayed or inadequate, uncomplicated *P. falciparum* malaria can quickly progress to severe complications, including cerebral malaria, which have a case-fatality rate of 10-20% even with effective anti-malarial treatment and supportive care (53). Thus, there is a need to develop adjunctive therapies to attenuate the pathological processes that contribute to death.

Clinical studies have revealed a number of pathological correlates of disease severity in cerebral malaria, but are unable to provide a mechanistic understanding of the etiology due to ethical limitations. Multiple mouse models have been employed to recapitulate and characterize the varying pathological processes associated with the human disease; in particular, infection of C57BL/6 mice with *P. berghei* ANKA has routinely been used to study cerebral malaria. In mice, the chemotaxis and subsequent sequestration of CD8⁺ T cells within the brain is required for the disruption of the BBB and the onset of neuropathology (390,406), but the contribution of leukocytes to human cerebral malaria has been questioned (391). Accumulation of leukocytes within the brain has been observed in a large proportion of children with cerebral malaria (140,262-264), and the chemokine CXCL10 has been shown to be elevated in patients with cerebral malaria (258,259). Thus, the data support the possibility that T cells may contribute to pathology in human cerebral malaria and warrant further investigation.

While the role of CXCR3 in the chemotaxis of T cells to the brain during ECM has been widely established (442-445), the factors that control the expression of this chemokine receptor following the induction of an immune response remain largely undefined. Thus, the objective of this thesis was to better characterize the processes that control the upregulation of CXCR3 on CD4⁺ and CD8⁺ T cells during cerebral malaria. Both the administration of iron and the inhibition of PTP activity during *P. berghei* ANKA infection were determined to prevent the development of neuropathology by attenuating the CXCR3-mediated chemotaxis of T cells to the brain. Consequently, IFN γ -responsiveness and TCR signal transduction, two factors thought to contribute to CXCR3 expression on T cells, were examined to characterize the mechanisms responsible for the expression of this chemokine receptor. A supplementary objective of these studies was to analyze the effect of iron and PTP inhibition on additional determinants known to contribute to cerebral and hepatic pathology during *P. berghei* ANKA infection, such as splenic regulatory CD4⁺ T cells and the production of proinflammatory and anti-inflammatory cytokines.

Chapter Two

Iron Prevents the Development of Experimental Cerebral Malaria by Attenuating CXCR3-mediated T Cell Chemotaxis

Preface

Iron status has been shown to affect the pathogenicity of malaria, with some studies suggesting that iron deficiency is protective against parasitemia and clinical malaria (501,502), and that iron supplementation may increase the risk of severe adverse events in areas that have a high transmission of malaria (503). However, iron deficiency anemia has also been associated with impaired cognitive development (498), thus an improved understanding of the interaction between iron and malaria is necessary to inform health care guidelines.

Several different methods were utilized to elevate the systemic levels of iron. Mice fed an iron-enriched diet for two weeks prior to infection with *P. berghei* ANKA and throughout the duration of the infection were not protected from developing neuropathology (Figure S1A). Similarly, *HJV^{-/-}* mice, which have an excessive accumulation of iron within their body due to their inability to upregulate hepcidin in response to BMP6, were also just as susceptible to ECM as the wild-type mice (Figure S1B). However, the incidence of ECM in mice treated with iron dextran was markedly decreased compared to the control mice (Figure 1A).

Following the conformation of cerebral malaria by analyzing the integrity of the BBB, and after excluding an antimalarial effect by comparing the parasitemia between the control and FeD mice, we examined the effect of iron supplementation on the immune response. Since the accumulation of CD8⁺ T cells within the brain is required for the development of ECM, we addressed the brain-sequestration of T cells and analyzed a number of factors known to be involved in the chemotaxis of T cells, including the expression of the chemokine receptor CXCR3. Additionally, we evaluated inflammation and other determinants that are thought to contribute to the neuropathology of *P. berghei* ANKA infection.

Iron Prevents the Development of Experimental Cerebral Malaria by Attenuating CXCR3-mediated T Cell Chemotaxis

Kristin M. Van Den Ham^{1,2}, Marina Tiemi Shio^{1,2,#}, Anthony Rainone¹, Sylvie Fournier¹, Connie M. Krawczyk¹ and Martin Olivier^{1,2*}

¹Department of Microbiology and Immunology, McGill University, Montréal, Québec, Canada

²McGill International TB Centre, Research Institute of the McGill University Health Centre, Montréal, Québec, Canada

[#]Current Address: Department of Microbiology, Immunology and Parasitology, Universidade Federal de São Paulo, São Paulo, São Paulo, Brazil

*Corresponding author: martin.olivier@mcgill.ca

(modified to include data for iron-enriched diet and HJV^{-/-} survival experiments)

Abstract

Cerebral malaria is a severe neurological complication of *Plasmodium falciparum* infection. Previous studies have suggested that iron overload can suppress the generation of a cytotoxic immune response; however, the effect of iron on ECM is yet unknown. Here we determined that the incidence of ECM was markedly reduced in mice treated with iron dextran. Protection was concomitant with a significant decrease in the sequestration of CD4⁺ and CD8⁺ T cells within the brain. CD4⁺ T cells demonstrated markedly decreased CXCR3 expression and had reduced IFN γ -responsiveness, as indicated by mitigated expression of IFN γ R2 and T-bet. Additional analysis of the splenic cell populations indicated that parenteral iron supplementation was also associated with a decrease in NK cells and increase in regulatory T cells. Altogether, these results suggest that iron is able to inhibit ECM pathology by attenuating the capacity of T cells to migrate to the brain.

Introduction

The processes contributing to the pathophysiology of ECM are multi-factorial and incompletely understood. Sequestration of immune cells and parasitized erythrocytes in the brain (410,611,612), activation of the inflammatory response (452,613), and the eventual loss of BBB integrity (614,615) have been shown to play integral roles in the development of the disease. Numerous studies have demonstrated that CD8⁺ T cells are the principal effector cells involved in the development of pathology(390,405,406); depletion of CD8⁺ T cells one day prior to the predicted onset of neurological symptoms results in 100% protection (390). Moreover, mice deficient in the chemokine receptor CXCR3, or its ligands CXCL9 and CXCL10, show a marked decrease in the incidence of ECM, coincident with reduced trafficking of CD8⁺ T cells to the

brain (443,446). Importantly, IFN γ produced by brain-sequestered CD4⁺ T cells is sufficient to induce the production of CXCL9 and CXCL10, thereby contributing to the accumulation of CXCR3-expressing CD8⁺ T cells within the brain (450,454).

The priming of *Plasmodium berghei* ANKA-specific T cell responses occurs in the spleen (390,616). MHC I-restricted antigens expressed by blood-stage parasites are captured by DCs and cross-presented to naïve CD8⁺ T cells, resulting in cell proliferation and the generation of cytotoxic T lymphocytes (413,414,416). The expression of CXCR3 on splenic T cells has been shown to increase during *P. berghei* ANKA infection (444). This upregulation is thought to be dependent on NK cells, as their depletion results in significantly reduced CXCR3 expression on splenic T cells and decreased accumulation of T cells within the brain (444). Additionally, the expansion of Tregs *in vivo* has been shown to attenuate the sequestration of conventional T cells within the brain and prevent the development of ECM (490). Further, adoptive transfer of Tregs has been demonstrated to attenuate CXCR3 expression on CD4⁺ T cells (617).

Previous studies have shown that iron overload can inhibit the production of effector cells (618). More recently, DCs have been observed to contribute to the generation of the reducing microenvironment required for T cell activation and proliferation (619). Thus, the resultant increase in oxidative radicals from parenteral iron supplementation may inhibit the development of an efficient immune response (620). Moreover, Tregs have also been shown to inhibit DC-mediated redox remodelling (621). However, the ability of iron to potentiate this specific attenuation and the other possible ramifications of augmented iron levels on T cells has not yet been fully elucidated, particularly in the context of a pathogenic disease.

Here we report that parenteral iron supplementation significantly decreased the incidence of ECM, concomitant with a marked reduction in the presence of CD4⁺ and CD8⁺ T cells in the brain. Splenic CD4⁺ and CD8⁺ T cells showed normal activation, but CD4⁺ T cells had decreased CXCR3 expression. Furthermore, CD4⁺ T cells demonstrated evidence of reduced IFN γ -responsiveness, characterized by attenuated IFN γ R2 and T-bet expression. Analysis of splenic populations revealed that iron supplementation increased Treg cell numbers and decreased NK cell numbers. Collectively these findings suggest that iron supplementation does not impair T cell activation, but rather alters the ability of T cells to migrate to the brain and cause pathology.

Results

Parenteral iron supplementation markedly protects mice from ECM

To determine the effect of parenteral iron supplementation on the pathology of ECM, we infected FeD mice with *P. berghei* ANKA. C57BL/6 mice infected with this parasite develop the clinical symptoms of ECM (i.e., hemi- or paraplegia, convulsions and coma) and succumb to the disease within 6 to 9 d post-infection (622,623). Dextran controls (with M_w = 5,000 kDa and 70,000 kDa) were included to establish if the dextran component itself was augmentative. PBS-treated (control) and dextran-treated mice developed ECM between days 7 and 11 post-infection, and their mortality was 100% (Figure 1A). In contrast, FeD mice were markedly protected, with a mortality of only 0-20% (Figure 1A). Additionally, further experiments revealed that iron supplementation provided a slight, but significant, protective effect when started up to 4 days post-infection (Figure S2). The level of parasitemia for control, dextran-treated and FeD mice was found to be similar through day 11 post-infection, by which time all control and dextran-treated mice had succumbed to ECM (Figure 1B). This result suggests that the protective effect

of iron dextran does not rely on the inhibition of parasitemia. FeD mice that did not develop ECM had increasing levels of parasitemia and either died due to the development of hyperparasitemia (parasitized erythrocytes > 80%) or were sacrificed on day 25 post-infection (Figure 1B). Since the mice treated with the dextran controls had the same clinical phenotype as the control mice, the iron-mediated protection was further investigated using only the control mice. ECM incidence was confirmed by analyzing the integrity of the BBB, which is a hallmark of ECM pathology (614). The uptake of EB into the brain parenchyma, which is indicative of BBB disruption, was evident in the infected control mice and was significantly reduced in the FeD mice (Figure 1C,D), indicating that iron supplementation prevented the loss of BBB integrity during ECM.

Organ sequestration of parasitized erythrocytes is decreased in FeD mice

Recent studies have shown that a rapid increase in tissue parasite burden, independent of parasitemia, is associated with the induction of clinical ECM (392-395,456). Parasite burden in the brain, spleen and liver were measured on day 7 post-infection using luciferase activity. Levels of parasitemia assessed using luciferase activity were similar to parasitemia as measured by counting blood smears, indicating that the two methods are comparable (Figure S3A). Although a significant difference in the parasitemia between the control and FeD mice was not observed before the development of symptoms in the control mice, a marked increase in tissue parasite burden was observed in the control mice upon the development of clinical symptoms (Figure 2A-C). An abrupt increase in the tissue parasite levels was not observed in FeD mice, as they did not become symptomatic. Since the tissue parasite burden in the control mice only increased upon the development of symptoms, the surge in parasites is likely associated with the onset of ECM pathology, which is in agreement with previous studies (392-395,456). In the

control mice the parasite burden increased to a greater extent in the brain compared to the spleen and the liver. However, parasite sequestration in the infected FeD mice and the infected control mice before the development of symptoms (as measured by the ratio of the RLU of the infected FeD mice or the infected control before the development of symptoms to the RLU of the uninfected mice) was much more extensive in the spleen (2250 fold increase) and liver (40 fold increase) than in the brain (3 fold increase) (Figure S3B-D). This large variance may account for the apparent lack of parasite sequestration detected in the brain of infected mice in some earlier studies (624).

FeD mice have an increased systemic inflammatory response

The activation of the inflammatory response by parasite antigens and immune cell adhesion has been shown to contribute to ECM pathology. Therefore, to discern the effect of parenteral iron supplementation on the systemic immune response, the concentrations of several cytokines in the serum were measured on day 7 post-infection. Overall, our data suggests that iron supplementation increased the proinflammatory response at late time points during *P. berghei* ANKA infection. Importantly, administration of iron dextran without infection did not appear to have a significant effect on most of the inflammatory mediators analyzed (Figure 3A-E). Surprisingly, IFN γ , which has been established to be integral to the development of ECM pathology (394,395,450,451,454), was observed to be significantly increased in the FeD mice compared to the control mice (Figure 3A). The FeD mice also had increased concentrations of TNF α (Figure 3B) and IL-10 (Figure 3C) after infection. TNF α and IL-10 have been shown to be associated with decreased tissue parasite accumulation during ECM (394,482), and this may account for the observed reduction in parasite burden in the FeD mice (Figure 2A-C). Furthermore, the FeD mice exhibited an increased serum concentration of IL-1 β (Figure 3D) and

IL-6 (Figure 3E), indicating a strong inflammatory response, but neither cytokine has been shown to play a role in the development of ECM (431,625). The levels of cytokines in the serum were also measured over the course of the infection. The serum concentration of IFN γ , TNF α , IL-10 and IL-6 only started to increase substantially on day 6 post-infection, and no apparent difference was observed in the serum levels of IL-1 β (Figure S4A-E). Interestingly, in contrast to the results obtained for the serum, the expression of inflammatory and immune response-related genes in the brain, spleen and liver of the FeD mice was predominately unchanged or reduced compared to the control mice (Table S1-3).

Expression of genes involved in T cell chemotaxis is attenuated in FeD mice

The expression of genes involved in the immune response was further profiled in the brain and the spleen on day 7 post-infection to develop a more comprehensive understanding of how parenteral iron supplementation may have been facilitating protection during ECM. Numerous studies have demonstrated that CD8⁺ T cell accumulation within the brain is necessary for the clinical onset of ECM (390,392-395,405,406,443,444,446,450,454,456,626). In the brain, it was observed that multiple genes involved in T cell trafficking were downregulated (Figure 4A). The mRNA expression of chemokines (CXCL10 and CCL5) and chemokine receptors (CXCR3 and CCR5) that have previously been determined to play a role in T cell trafficking and ECM pathogenesis were decreased (441,443,446). IFN γ production by CD4⁺ T cells has been shown to contribute to the accumulation of CD8⁺ T cells in the brain by inducing the expression of chemokines (450,454). Expression of IFN γ in the brain was also observed to be reduced in the FeD mice. Since T cell priming during ECM occurs in the spleen (390,616), we also analyzed the expression of genes involved in T cell trafficking in this organ (Figure 4B). In the spleen, a large increase in the expression of CXCL10 and a decrease in the expression of CXCR3 were

detected in FeD mice; whereas the expression of CCL5 and CCR5 were unchanged by iron supplementation. Additionally, the expression of IFN γ in the spleen was unchanged. This data suggests that CD4⁺ and CD8⁺ T cells in the FeD mice have an impaired ability to traffick to the brain during *P. berghei* ANKA infection.

Sequestration of CD4⁺ and CD8⁺ T cells in the brain is greatly reduced in FeD mice

The sequestration of CD4⁺ and CD8⁺ T cells to the brain was examined on day 7 post-infection to determine if the decreased expression of trafficking-associated genes correlated with a reduction in the chemotaxis of T cells to the brain. Infiltration of cells into the brain, as represented by the number of cells recovered after cell isolation, was significantly decreased in the FeD mice compared to the control mice after infection (Figure 5A). A slight increase in cell accumulation in the infected FeD mice compared to the uninfected FeD mice was measured, indicating that immune cell recruitment was not completely abrogated by parenteral iron supplementation. Furthermore, the infiltration of cells was not changed between the uninfected control and the uninfected FeD mice, suggesting that iron-mediated attenuation of immune cell sequestration only occurs after infection. There was a marked decrease in the number of accumulated CD8⁺ T cells in the FeD mice after infection, and no change between the control and FeD mice without infection (Figure 5B). Moreover, the number of CD8⁺ T cells was increased in the infected FeD mice compared to the uninfected FeD mice. Similar results were obtained for the percentage of CD8⁺ T cells (Figure 5C,D). A decrease in the total number of CD4⁺ T cells sequestered in the brain of the infected FeD mice compared to the infected control mice was observed (Figure 5E). No difference in the accumulation of CD4⁺ T cells was detected between the control and FeD mice without infection and a minor increase in the number of CD4⁺ T cells was measured in the infected FeD mice compared to the uninfected FeD mice. Iron

supplementation did not change the percentage of CD4⁺ T cells, but the percentage decreased during infection in the control mice (Figure 5D,F).

CXCR3 expression on CD4⁺ T cells in the spleen is significantly decreased in FeD mice

The above results indicated that parenteral iron supplementation prevented ECM pathology by reducing the sequestration of both CD4⁺ and CD8⁺ T cells within the brain. We hypothesized that the attenuated accumulation was due to either a deficiency in activation and/or expansion or to a defect in the chemotaxis of the T cells. The expansion of splenic CD4⁺ and CD8⁺ T cells was very similar between the control and FeD mice; only a minor delay in the proliferation of CD4⁺ T cells was observed (Figure S5A,B). Additionally, the percentage of activated CD4⁺ and CD8⁺ T cells in the spleen was slightly decreased in the FeD mice, except for the percentage of CD25⁺CD62L^{lo} CD4⁺ T cells, which was unchanged (Figure S6A,B). Splenic cDCs were also analyzed, since this subset of DCs is thought to be responsible for priming the T cell response during ECM (413,414,416). No difference in the percentage of cDCs or the MFI of CXCL10, CD40 or MHCII was observed in the FeD mice compared to the control mice (Figure S7B). Both CXCR3 and CCR5 have been implicated to play important roles in T cell migration during ECM, but previous studies have shown that a greater percentage of brain-infiltrating T cells express CXCR3 compared to CCR5 (444). Moreover, CXCR3 mRNA expression in the spleen was decreased in the FeD mice, whereas CCR5 expression was unchanged (Figure 4B). Therefore, the expression of CXCR3 on splenic CD4⁺ and CD8⁺ T cells was examined on day 7 post-infection to determine if iron supplementation was attenuating T cell chemotaxis. The percentage of CD4⁺ T cells expressing CXCR3 was markedly decreased in the iron supplemented mice (Figure 6A,B). Furthermore, the MFI of CXCR3 on CD4⁺CD44^{hi} T cells in the FeD mice was similarly reduced (Figure 6C,D). However, the percentage of CXCR3⁺ CD8⁺ T cells was

unchanged (Figure 6A,B), as was the MFI of CXCR3 on CD8⁺CD44^{hi} T cells (Figure 6C,D). The expression of CXCR3 on CD8⁺ T cells in the FeD mice trended toward a slight decrease, and a significant reduction was measured in some of the individual experiments, but overall, a significant difference was not observed (Figure 6A-D). The attenuated expression of CXCR3 on CD4⁺ T cells suggests that iron supplementation inhibits T cell sequestration within the brain by directly impairing the chemotactic capacity of only CD4⁺ T cells, and that the chemotaxis of CD8⁺ T cells to the brain is indirectly attenuated by the consequent decrease in the induction of chemokines by CD4⁺ T cells.

IFN γ R2 and T-bet expression in splenic T cells in FeD mice is attenuated during ECM

cDCs and CD4⁺ T cells in the spleen were analyzed on day 3 post-infection to determine if the cause of the attenuated expression of CXCR3 on CD4⁺ T cells was due to an early defect in activation or to impaired differentiation. No difference in the percentage of cDCs or the MFI of CXCL10 was observed, but a modest increase in the MFI of CD40 and MHCII was detected in the FeD mice (Figure S7A). Interestingly, on day 3 post-infection, a greater percentage of splenic CD4⁺ T cells in the FeD mice had an activated phenotype and expressed CXCR3 (Figure S8A-D). This result is in contrast to the status of CD4⁺ T cells on day 7 post-infection, at which time point CD4⁺ T cells from the FeD mice had a slight decrease in activation (Figure S6A,B) and a marked decrease in CXCR3 expression (Figure 6A-D). IFN γ signalling through the IFN γ R (IFN γ R1/IFN γ R2) induces T-bet, which subsequently transactivates both IFN γ and CXCR3 (627). The limiting factor in IFN γ -responsiveness is the expression of IFN γ R2, which has been shown to be downregulated by both IFN γ (628) and iron (565). Consequently, the expression of IFN γ R2 and T-bet was measured to develop a better understanding of CXCR3 induction in splenic CD4⁺ T cells.

On day 3 post-infection, IFN γ R2 was expressed on a low percentage of CD4⁺ T cells and the percentage of IFN γ R2⁺ CD4⁺ T cells was not significantly different in the FeD mice compared to the control mice (Figure 7A,B). The percentage of T-bet⁺ CD4⁺ T cells on day 3 post-infection was increased in the FeD mice (Figure 7C,D), concurring with the increased percentage of CXCR3⁺ CD4⁺ T cells observed on this day (Figure S8C,D). The percentages of IFN γ R2- and T-bet-expressing CD4⁺ T cells were increased in both groups on day 7 post-infection compared to day 3 post-infection; however, the percentages of IFN γ R2⁺ and T-bet⁺ CD4⁺ T cells were markedly reduced in the FeD mice on day 7 post-infection (Figure 7A-D). This result agrees with the decreased expression of CXCR3 measured on CD4⁺ T cells in the FeD mice on day 7 post-infection (Figure 6A-D). No differences were observed in the expression of IFN γ R2 or T-bet on CD8⁺ T cells on day 3 post-infection, but the expression of both IFN γ R2 and T-bet were significantly decreased in the FeD mice on day 7 post-infection (Figure S9A-D). However, this did not culminate in a decrease in CXCR3 expression (Figure 6A-D). IFN γ stimulation induces T-bet through the activation of STAT1 (627); therefore, the phosphorylation of STAT1 was examined to verify that iron supplementation was inhibiting IFN γ signalling in CD4⁺ T cells. The phosphorylation of STAT1 was notably reduced in CD4⁺ T cells in the FeD mice on day 7 post-infection (Figure S10). Thus, these results suggest that the attenuated expression of CXCR3 on splenic CD4⁺ T cells is dependent on the iron-mediated decrease in the IFN γ -responsiveness of CD4⁺ T cells.

FeD mice have a reduction in NK cells and an augmentation of Tregs in the spleen

Finally, we were interested in determining if iron supplementation affected other factors that might augment protection. Both NK cells and Tregs have been shown to influence the development of ECM. Depletion of NK cells using an anti-asialo GM1 antibody has been shown

to inhibit T cell chemotaxis to the brain by attenuating CXCR3 expression on splenic T cells (444). Additionally, the *in vivo* expansion of Tregs was observed to prevent conventional T cell accumulation in the brain during ECM through a CTLA-4-dependent mechanism (484). This study did not examine the expression of CXCR3 on conventional T cells; however, adoptive transfer of Tregs has previously been demonstrated to mitigate CXCR3 expression on CD4⁺ T cells (617). Therefore, the frequencies of splenic NK cells and Tregs were measured to determine if iron conferred protection by modulating the percentages of these cell types. On day 3 post-infection, the percentage of splenic NK cells was markedly decreased in the FeD mice (Figure 8A,B). The percentage of NK cells decreased in both groups from day 3 post-infection to day 7 post-infection and the percentage of NK cells in the FeD mice was the same as the control mice on day 7 post-infection (Figure 8A,B). The percentage of Tregs was increased in the FeD mice on day 3 post-infection (Figure 8C,D). This trend was also observed on day 7 post-infection; however, the difference was no longer significant (Figure 8C,D). Therefore, it appears that the modulated frequencies of NK cells and Tregs are associated with decreased ECM pathology in the FeD mice.

Discussion

Iron status has been shown to affect the pathogenicity of numerous infections, including malaria, with iron supplementation generally being associated with increased susceptibility (629). However, populations that have the greatest risk for developing malaria are also those that have an increased frequency of iron deficiency anemia. Moreover, malaria infection itself has been shown to contribute to iron deficiency by modulating the distribution and utilization of iron (630). Additionally, the complex relationship between host iron status and malaria infection also includes the proposed utilization of iron chelation as an ancillary therapy. Iron deficiency has

been previously observed to be associated with decreased risk of developing parasitemia and severe malaria (501). Anemic hosts have decreased reticulocyte production (the preferred host cell of *P. vivax*) (631) and phagocytize parasitized erythrocytes more efficiently (632).

However, inhibition of malaria by iron chelators is independent of host iron status, and instead relies on intracellular chelation of the labile iron pool within the parasitized erythrocytes (iron (III) chelators; *e.g.*, desferrioxamine B) or the formation of toxic complexes with iron (iron (II) chelators; *e.g.*, 2',2'-bipyridyl) (633-635). Furthermore, a review of the clinical trials using iron chelators found insufficient evidence to support the use of iron chelation as an adjunctive therapy for malaria (636). Nevertheless, an improved understanding of how *Plasmodium* parasites acquire iron and how host iron status affects the immune response during malaria infection would greatly aid iron supplementation guidelines in malaria endemic areas. Thus, we sought to determine the impact of parenteral iron supplementation on the development of severe malaria.

Mice treated with iron dextran had a markedly reduced incidence of cerebral malaria. The iron-mediated protection did not appear to be through an anti-malarial mechanism, as the parasitemia was not significantly different in the FeD mice compared to the control mice. However, the FeD mice had a reduced tissue parasite burden compared to the control mice that developed symptoms. Previous studies have shown that the accumulation of parasites in the brain and spleen is dependent on the sequestration of CD8⁺ T cells and the production of IFN γ and other inflammatory mediators (394,395). Therefore, the reduced tissue parasite burden observed in the FeD mice suggests that iron administration provided protection against ECM by attenuating CD8⁺ T cell sequestration and/or signalling by proinflammatory cytokines.

The sequestration of CD8⁺ T cells in the brain has been established to be essential to the development of ECM pathology, by both augmenting parasite accumulation (392-395,456) and by directly damaging the BBB (406,456,626). The total number of both CD4⁺ and CD8⁺ T cells sequestered in the brain was markedly decreased in the FeD mice, suggesting that iron supplementation was attenuating the expansion, activation or chemotactic capacity of the splenic T cells. Only a minor delay in proliferation of CD4⁺ T cells and a slight reduction in the activation of CD4⁺ and CD8⁺ T cells were observed in the FeD mice. However, the percentage of CXCR3⁺ CD4⁺ T cells was greatly reduced in the FeD mice, as was the MFI of CXCR3 on CD4⁺CD44⁺ T cells. Contrastingly, the expression of CXCR3 on CD8⁺ T cells was unchanged in the FeD mice compared to the control mice. Earlier studies demonstrated that IFN γ production by brain-sequestered CD4⁺ T cells promotes T cell chemotaxis to the brain by inducing the expression of CXCL9 and CXCL10 (450,454). Therefore, the reduced chemotactic capacity of splenic CD4⁺ T cells is likely responsible for the decreased expression of CXCL10 in the brain and the consequent reduction in the brain sequestration of CXCR3-expressing CD8⁺ T cells.

Moreover, IFN γ production has been established to be essential to the development of ECM pathology, as both IFN γ ^{-/-} and IFN γ R^{-/-} mice are completely protected from developing cerebral malaria (394,395,450,451,454). In an apparent contradiction to previous studies, the FeD mice had significantly higher concentrations of IFN γ in the blood than the control mice. However, IFN γ R^{-/-} mice also have increased concentrations of IFN γ in the blood compared to wild-type mice (451). It was proposed that the concentrations were higher in the knock-out mice because the IFN γ released into the blood could not bind to the receptor, and therefore was not as rapidly eliminated (451). The expression of IFN γ R2 on splenic CD4⁺ T cells was reduced on day 7 post-infection in the FeD mice. Previous studies have shown that the expression of the IFN γ R2 chain

can be downregulated by both iron (565) and IFN γ (628). Thus, the decreased expression of IFN γ R2 in the FeD mice was likely caused by the augmented level of iron and potentially reinforced by the increasing levels of IFN γ . Furthermore, IFN γ signalling has been demonstrated to be necessary for the induction of CXCR3 on CD4⁺ T cells, but not on CD8⁺ T cells (476,477). We observed that parenteral iron supplementation attenuated the expression of IFN γ R2 and T-bet on splenic CD4⁺ and CD8⁺ T cells, mitigating the IFN γ signalling capacity of these cells. The decrease in the IFN γ -responsiveness of the T cells may account for the expression of CXCR3 being significantly decreased on CD4⁺ T cells and relatively unaffected on CD8⁺ T cells.

Additionally, iron administration resulted in a decrease in NK cells and increase in Tregs in the spleen. The depletion of NK cells and the *in vivo* expansion of Tregs have both been shown to protect mice from developing ECM by attenuating T cell sequestration within the brain (444,484). The modulated frequencies of NK cells and Tregs in the FeD mice correlated with the decreased expression of CXCR3 on the splenic CD4⁺ T cells; however, these cell types could potentially be acting through mechanisms other than chemotaxis inhibition. Additionally, as dextran was not used as a control throughout the study, the ability to identify the changes induced by dextran itself is limited; however, it is unlikely that dextran plays a major role in the observed alterations. Previous studies have shown that iron treatment causes T cells to become refractory to IFN γ (565) and that IFN γ signalling is required for the induction of CXCR3 on CD4⁺ T cells (476). Thus, the iron component of iron dextran is presumably responsible for the vast majority of changes measured in the FeD mice, especially given that the dextran component itself did not prevent the development of ECM.

Finally, neither mice fed an iron-enriched diet nor HJV knock-out mice were protected from ECM. This lack of protection may be due to differences in the degree of iron loading, the

distribution of the iron within the body or the trafficking routes through which the iron is taken up. Parenteral iron can bypass the reticuloendothelial system and donate iron directly to transferrin (637), and the iron-induced internalization of the IFN γ R2 chain was previously shown to be caused by the TfR1-mediated uptake of iron (565). Thus, the protection provided by parenteral administration of iron dextran, but not by the iron-enriched diet or lack of HJV, may be the result of enhanced transferrin saturation in the FeD mice.

Altogether, we have demonstrated that parenteral iron supplementation significantly decreases the incidence of ECM by reducing the accumulation of CD4⁺ and CD8⁺ T cells in the brain. The decreased sequestration was associated with attenuated CXCR3 expression and reduced IFN γ -responsiveness of splenic CD4⁺ T cells. To the best of our knowledge, this is the first study to report the potential of iron supplementation to prevent the development of ECM. We believe that a better understanding of the cellular and molecular mechanisms underlying the iron-mediated, immunomodulatory protection could aid in the development of new therapeutic strategies to treat malaria-infected individuals prior to the onset of cerebral malaria pathology.

Materials and Methods

Mice

Female, C57BL/6 mice (6-8 weeks old) were purchased from Charles River Laboratories and Jackson Laboratories, and male and female HJV^{-/-} mice on a C57BL/6 background were obtained from Dr. Kostas Pantopoulos. All mice were kept in pathogen-free housing, and all research involving mice was carried out according to the regulations of the Canadian Council of Animal Care and was approved by the McGill University Animal Care Committee under ethics protocol

number 5925. Mice were euthanized at established humane endpoints using CO₂ asphyxiation followed by cervical dislocation or by using isoflurane if perfusion was performed.

Parasites and infection

In all experiments, red blood cells infected with *Plasmodium berghei* ANKA parasites expressing a GFP-luciferase fusion protein were used (Malaria Research and Reference Reagent Resource Center). C57BL/6 mice were infected by i.p. inoculation of 10⁴ parasitized erythrocytes. In all experiments other than late-stage survival and survival and disease assessment, mice received either PBS or 4 mg of iron dextran for five days before and five days after parasite inoculation (infected groups) or mock infection (uninfected groups) by i.p. injection. For late-stage survival, mice received either PBS or 4mg of iron dextran for five days (or until they succumbed to ECM), starting on day 4 post-infection or day 5 post-infection. Unless otherwise stated, mice were sacrificed on day 7 post-infection or post-mock infection, upon the development of ECM symptoms in the infected control group.

Survival and disease assessment

Mice were fed either standard chow containing 0.2g of iron/kg (TD.09521) or were fed an iron-enriched chow containing 20g of iron/kg (TD.00588) for fourteen days prior to infection, and then for the duration of the experiment. Alternatively, mice received PBS, 4.4 mg of dextran ($M_w = 5,000\text{kDa}$ or $M_w = 70,000\text{kDa}$), or 4 mg of iron dextran for five days before and five days after parasite inoculation by i.p. injection. Starting on day three post infection, tail-vein blood was collected daily. Blood smears were stained with Diff-Quik, and parasitemia was determined by counting at least 500 cells. Levels of parasitemia assessed using luciferase activity were determined using the Firefly Luciferase Assay Kit (Biotium, Inc.), according to the

manufacturer's protocol. Infected mice were monitored two to three times daily for clinical symptoms of ECM, including head deviation, hemi- or paraplegia, ataxia, convulsions and coma.

BBB integrity

Upon the development of clinical symptoms in the infected control group, mice were i.p. injected with 0.3 mL of 2% EB (Sigma-Aldrich). The mice were sacrificed 2 h thereafter, without perfusion, and brains and hearts were weighed and placed in formamide (Sigma-Aldrich) for 48 h at 37 °C to extract the dye. Absorbance was measured at 620nm. The concentration of EB in the brain was calculated using a standard curve prepared with known concentrations EB in formamide, and was normalized to the concentration in the heart.

Luciferase assay

Mice were perfused with PBS and organs were frozen immediately in liquid nitrogen. Organs were homogenized in PBS containing 0.1mg/mL aprotinin (Roche) 0.05mg/mL leupeptin (Roche) and 1X Firefly lysis buffer using a PRO200 Hand-held Homogenizer (Harvard Apparatus Canada). After lysing on ice, the mixture was centrifuged at 13,000 rpm for 30 min. The luciferase activity of the supernatant was measured using the Firefly Luciferase Assay Kit (Biotium, Inc.), according to the manufacturer's protocol.

Cytokine multiplex assay

Levels of the cytokines IFN γ , TNF α , IL-10, IL-1 β and IL-6 in serum samples were measured using a multiplex electrochemiluminescence assay (Meso Scale Discovery). Blood was collected from the saphenous vein. The serum samples were prepared and the assay was run according to

the manufacturer's protocol. The plate was read by an Imager 2400 plate reader (Meso Scale Discovery).

Quantitative real-time PCR array analysis

Genes associated with the host immune response were quantitated with the Mouse Innate and Adaptive Immune Responses RT² Profiler PCR Array (PAMM-052ZD, SABiosciences). Mice were perfused with PBS and organs were frozen immediately in liquid nitrogen. Total RNA was extracted from the spleen, liver and brain using TRIzol (Life Technologies), according to the manufacturer's protocol. Extracted RNA was treated with RQ1 RNase-free DNase (Promega) and purified using the RNeasy Mini Kit (Qiagen). The RNA was then concentrated via phenol-chloroform extraction and reverse transcribed using RevertAid H Minus Reverse Transcriptase (Thermo Scientific) using random hexamers (Invitrogen). A standardized amount of cDNA was mixed with the RT² SYBR Green qPCR Mastermix and added to the RT² Profiler PCR Array. The array was run using the recommended conditions on a CFX96 Touch Real-Time PCR Detection System.

Flow cytometric analysis of the brain

Flow cytometry was performed using a BD LSR Fortessa and results were analyzed using FlowJo version 9.6.2. Mice were perfused for the analysis of brain sequestered cells. Brains were digested in RPMI containing 1.6mg/mL collagenase (type IV; Sigma-Aldrich) and 200µg/mL DNase I (Sigma-Aldrich) at 37°C for 50 min. Cells were isolated using a Percoll gradient (GE Healthcare) and debris was filtered out using a 70µm nylon mesh. Cells were counted and labelled with LIVE/DEAD amine-reactive violet viability marker according to the manufacturer's protocol (Invitrogen). The cells were blocked and labeled with FITC anti-CD45

(eBioscience; 30-F11), PE anti-CD11b (BD Pharmingen; M1/70), APC anti-CD4 (eBioscience; RM4-5) and PerCP-Cy5.5 anti-CD8 (eBioscience; 53-6.7).

Flow cytometric analysis of the spleen

Flow cytometry was performed using a BD LSR Fortessa and a BD FACSCanto II and results were analyzed using FlowJo version 9.6.2. Mice were not perfused for the analysis of splenic cells. Splenocytes were isolated and erythrocytes were lysed in Tris-NH₄Cl buffer. Cells were counted, blocked with and labelled with PerCP-Cy5.5 anti-CD4 (BD Pharmingen; RM4-5), APC-eFluor780 anti-CD8 (eBioscience; 53-6.7), APC anti-CXCR3 (BioLegend; CXCR3-173), FITC anti-CD62L (eBioscience; MEL-14), FITC anti-Foxp3 (eBioscience; FJK-16s), FITC anti-CD8 (eBioscience; 53-6.7), FITC anti-CD3 (eBioscience; 145-2C11), PE anti-CD25 (BD Pharmingen; PC61) PE anti-T-bet (eBioscience; eBio4B10), PE anti-NK1.1 (BD Pharmingen; PK136), PE-Cy7 anti-CD44 (BD Pharmingen; IM7), PE anti-CD11b (eBioscience; M1/70), PerCP-Cy5.5 anti-CD11c (eBioscience; N418), FITC anti-MHCII (eBioscience; M5/114..15.2), APC anti-CD40 (BD Pharmingen; 3/23), biotin rabbit anti-mouse CXCL10 (Cedarlane; BAF466), purified hamster anti-mouse IFN γ R2 (BD Pharmingen; MOB-47), biotin mouse anti-Armenian and Syrian hamster (BD Pharmingen; 554010) and streptavidin APC-eFluor780 (eBioscience; 47-4317-82). Isolated splenocytes were labelled with CFSE and stimulated with 1 μ g/mL of anti-CD3 and 0.5 μ g/mL of anti-CD28. Cells were incubated at 37°C and collected on day 1 and 4 post stimulation. Cells were blocked and labelled with PerCP-Cy5.5 anti-CD4 (BD Pharmingen; RM4-5) and APC-eFluor780 anti-CD8 (eBioscience; 53-6.7).

IFN γ Stimulation and Western Blot

Splenic CD4⁺ T cells were isolated using the Stemcell Technologies EasySep Mouse CD4⁺ T Cell Enrichment Kit, according to the manufacturer's protocol. 1 x 10⁶ CD4⁺ T cells were stimulated with 1000U/mL of recombinant murine IFN γ (Invitrogen) for 0, 15, 30 and 60 minutes. Cells were lysed (50mM Tris (pH 7.0), 0.1 mM EDTA, 0.1 mM EGTA, 0.1% 2-mercaptoethanol, 1% IGEPAL, complete protease inhibitor (Roche), 1mM Na₃VO₄ and 50 mM NaF) and run on a SDS-PAGE gel. Proteins were detected using antibodies against pSTAT1 (Cell Signalling; D4A7) and STAT1 (Cell Signalling; 42H3). Anti-rabbit antibodies conjugated to horse-radish peroxidase (Amersham) were used as secondary antibodies. Membranes were visualised using the Pierce ECL Western Blotting Substrate (Thermo Fischer Scientific).

Statistical analysis

Statistical analyses were performed using the unpaired Student's t-test. Error bars represent S.E.M. The log-rank was used for all experiments in which survival was assessed as an endpoint. The data were analyzed using GraphPad Prism software (version 5.0). * P < 0.05, ** P < 0.01, and *** P < 0.001.

Acknowledgements

We thank the McGill University Flow Cytometry and Cell Sorting Facility and the McGill University Multiplexing, Peptide and SPR Facilities.

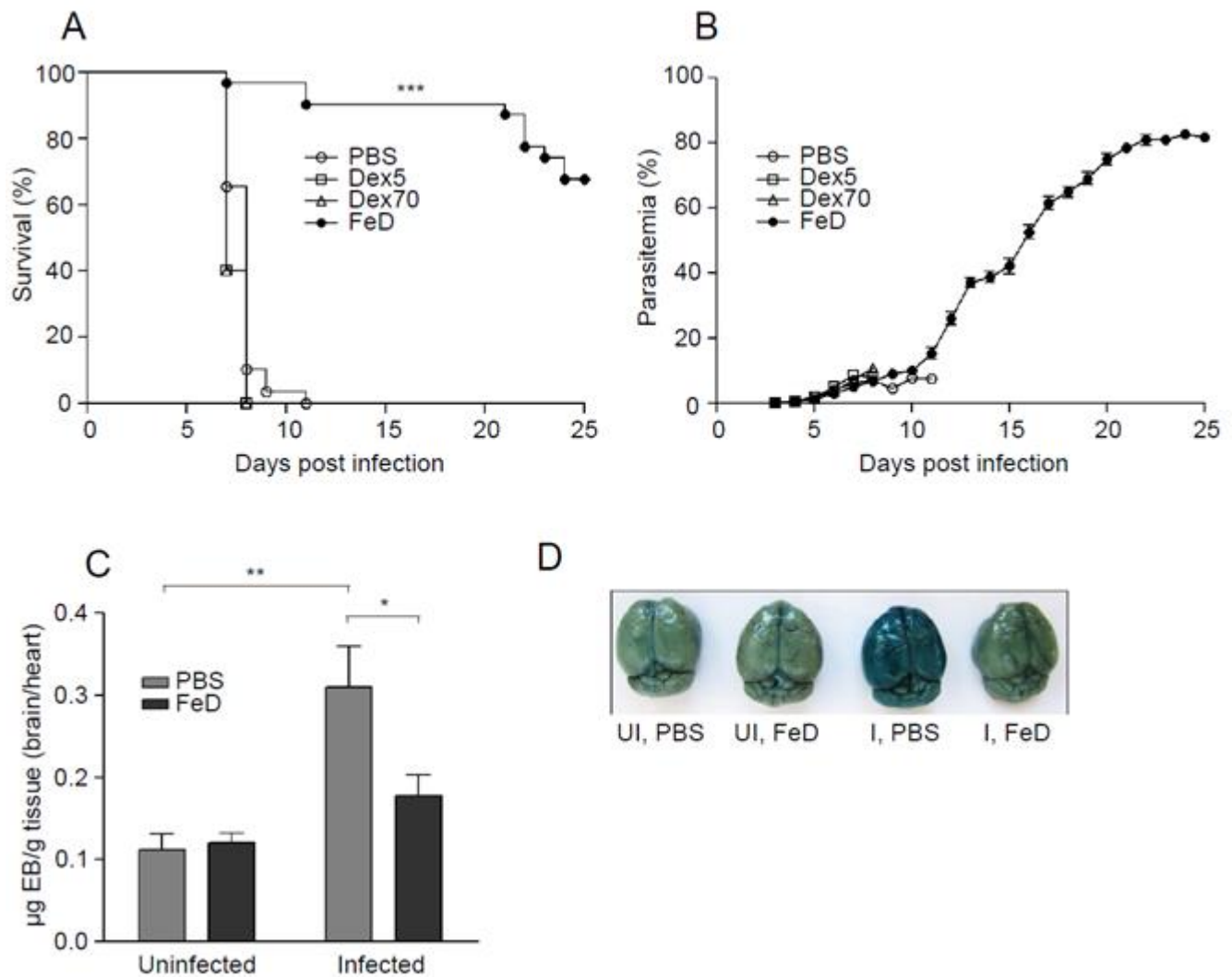


Figure 1. Iron Dextran Prevents the Development of ECM. Survival (A) and mean parasitemia (B) of infected mice treated with iron dextran, dextran M_w 5kDa and dextran M_w 70kDa. PBS-treated mice were used as a control. BBB disruption was assessed using EB. EB (C) is shown as mean μg of EB per g of brain tissue normalized to mean μg of EB per g of heart tissue. Representative picture of EB-stained brains (D). For survival: $n = 29$ for control mice, $n = 31$ for FeD mice and $n = 5$ for Dex5 and Dex70 mice. The average of four individual experiments is shown for the control and FeD mice. For parasitemia: $n = 20$ for control and FeD mice and $n = 5$ for Dex5 and Dex70. The average of three individual experiments is shown for the control and FeD mice. For EB: $n = 5$ for control, uninfected and infected mice, and $n = 6$ for FeD, uninfected and infected mice. PBS = control, Dex5 = dextran M_w 5kDa, Dex70 = dextran M_w 70kDa, FeD = iron dextran, UI = uninfected, I = infected. Statistically significant differences, shown by asterisks (* $P < 0.05$, ** $P < 0.01$, and *** $P < 0.001$), were determined by log-rank test (survival) and unpaired Student's t-test (BBB disruption).

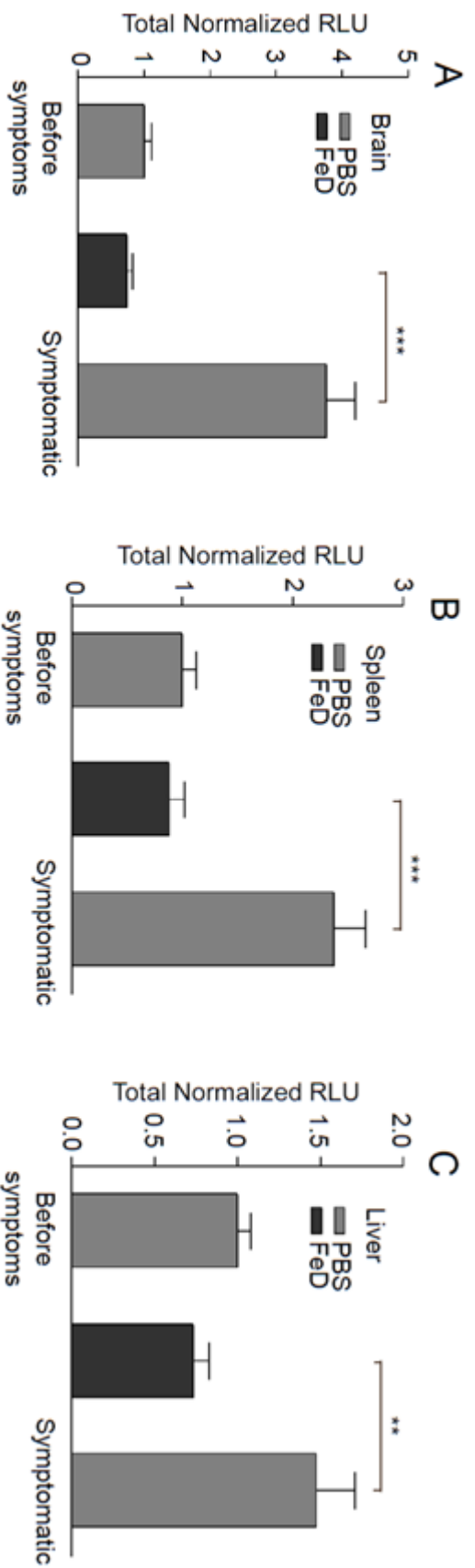


Figure 2. Tissue parasite sequestration is inhibited by parenteral iron supplementation. Parasite levels in the brain (A), spleen (B) and liver (C) on day 7 post-infection. Luciferase activity is shown as the total RLU per organ normalized to the total RLU in the control mice before symptoms. $n = 8$ for the control mice before symptoms, $n = 8$ for the control, symptomatic mice and $n = 12$ for the FeD mice. FeD = iron dextran, PBS = control. Statistically significant differences, shown by asterisks (** $P < 0.01$ and *** $P < 0.001$), were determined by unpaired Student's t-test.

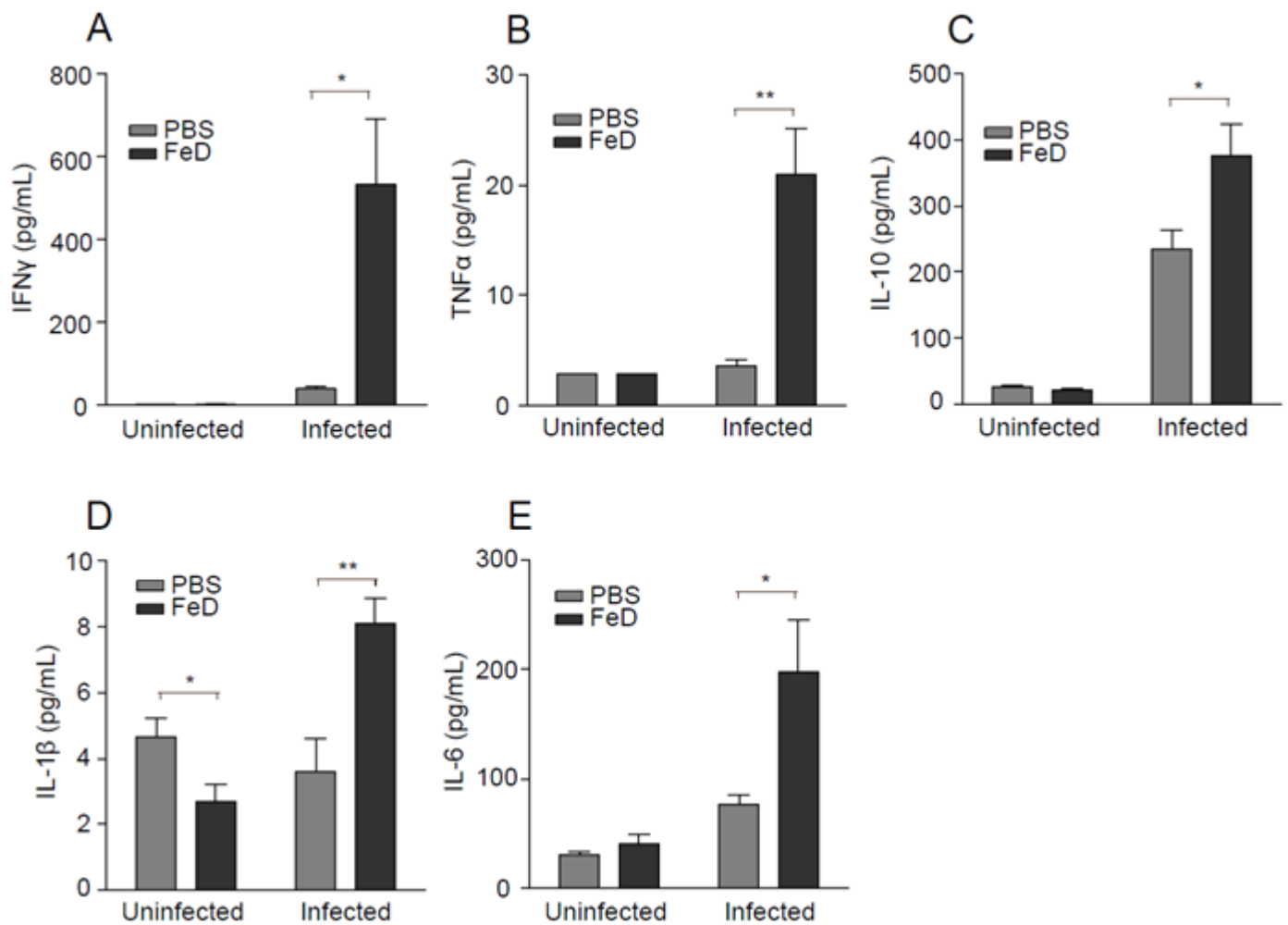


Figure 3. Systemic Inflammation is Augmented in FeD Mice. Concentration of IFN γ (A), TNF α (B), IL-10 (C), IL-1 β (D) and IL-6 (E) in the serum on day 7 post-infection. $n = 5$ for the control, uninfected group mice and $n = 6$ for all other groups. Levels of TNF α are below the limit of detection in the uninfected groups. FeD = iron dextran, PBS = control. Statistically significant differences, shown by asterisks (* $P < 0.05$ and ** $P < 0.01$), were determined by unpaired Student's t-test.

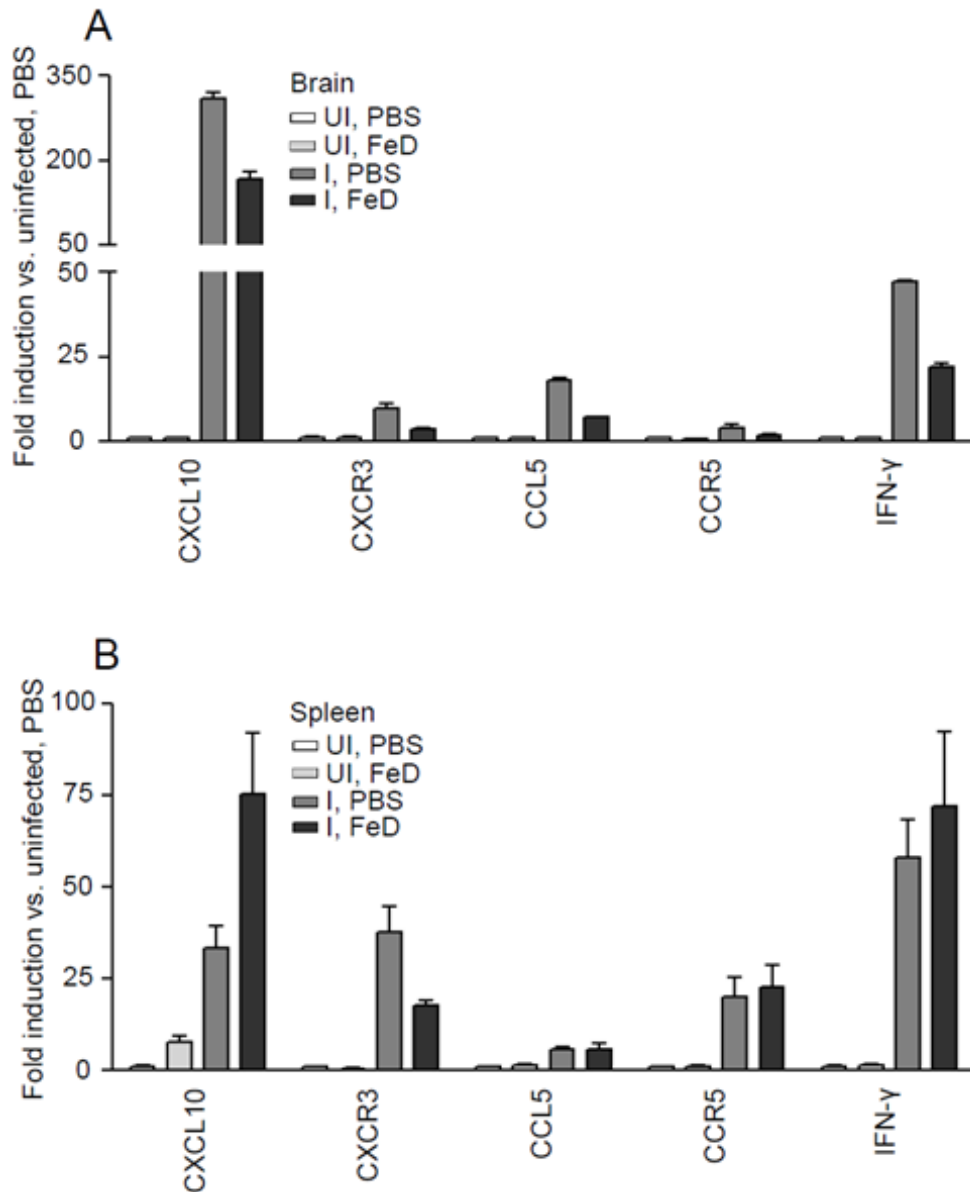


Figure 4. The Expression of Genes Involved in T Cell Chemotaxis are Attenuated by Parenteral Iron Supplementation. The expression of genes involved in T cell chemotaxis is shown for the brain (A) and the spleen (B) on day 7 post-infection. mRNA levels were normalized to *Gusb*. 2 samples pooled from 6 mice (3 mice per sample) were used for each group. UI = uninfected, I = infected, FeD = iron dextran, PBS = control.

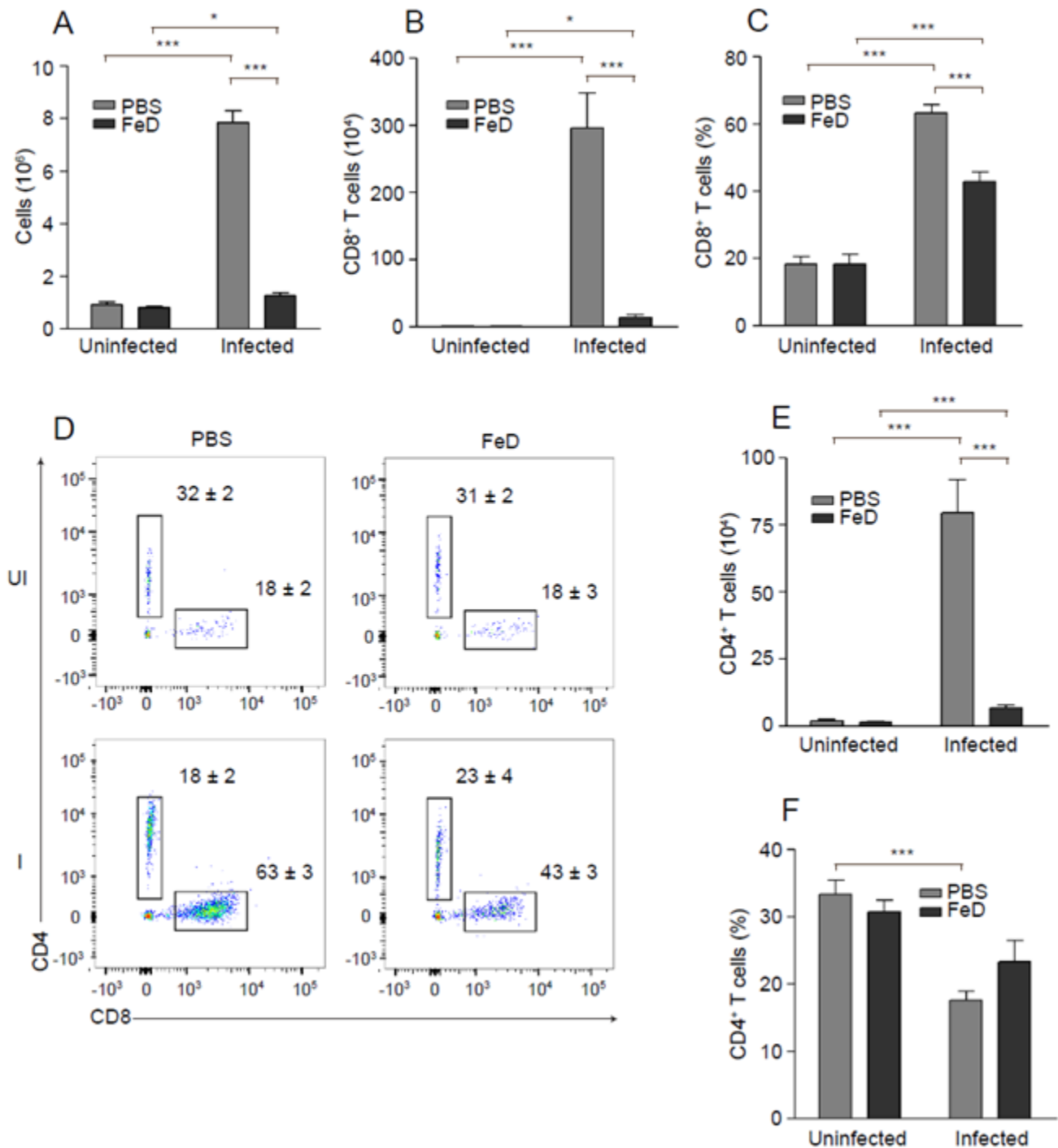


Figure 5. Sequestration of CD4⁺ and CD8⁺ T Cells in the Brain is Reduced in FeD Mice. The total number of cells recovered after isolation (A), the total number (B) and percentage (C) of CD8⁺ T cells after gating on infiltrating leukocytes (CD45⁺CD11b^{lo-hi}), representative flow cytometric dot plots of CD4⁺ and CD8⁺ T cells after gating on infiltrating leukocytes (D), and the total number (E) and percentage (F) of CD4⁺ T cells after gating on infiltrating leukocytes, on day 7 post-infection. The numbers shown on the dot plots indicate the mean percentage of cells inside the gate \pm S.E.M. $n = 5$ mice were used for each group. UI = uninfected, I = infected, FeD = iron dextran, PBS = control. Statistically significant differences, shown by asterisks (* $P < 0.05$ and *** $P < 0.001$), were determined by unpaired Student's t-test.

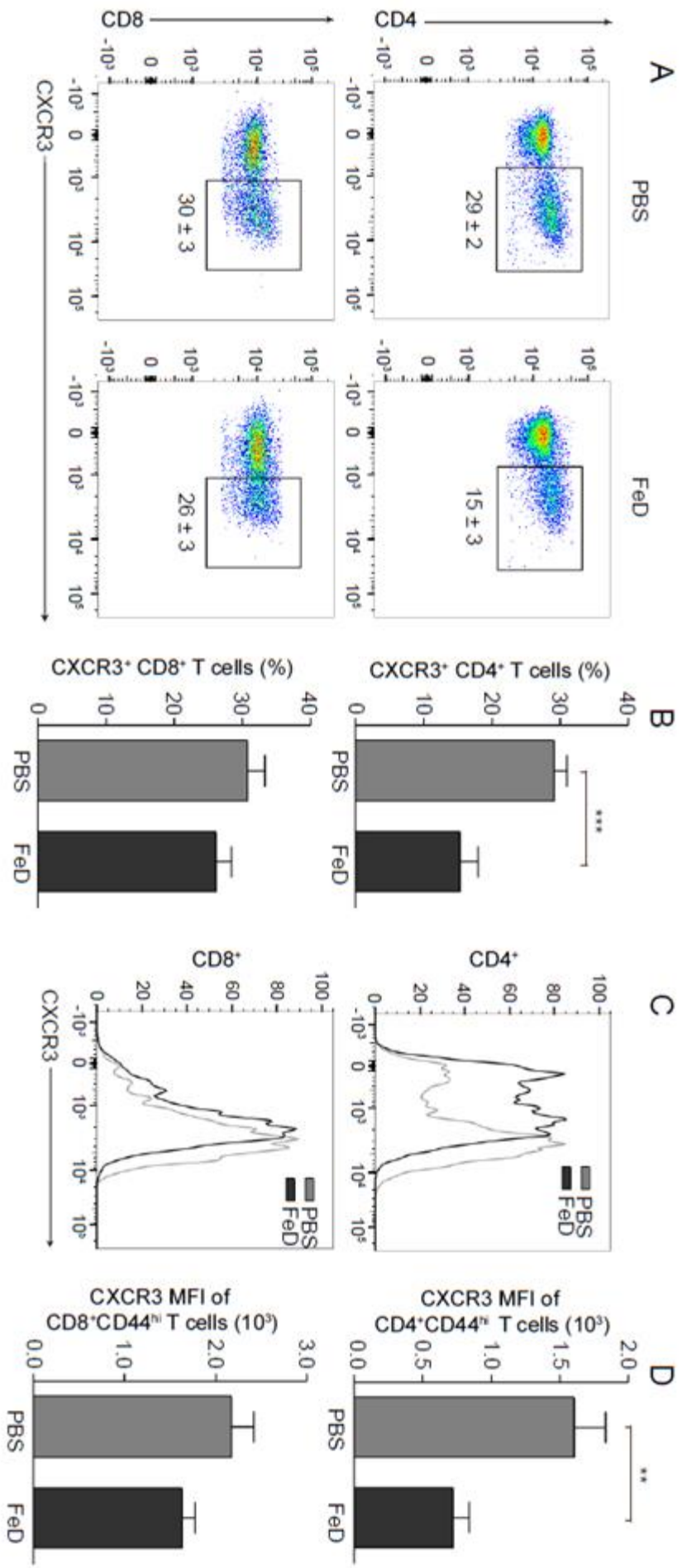


Figure 6. The Expression of CXCR3 on Splenic CD4⁺ T Cells is Decreased by Parenteral Iron Supplementation. Representative flow cytometric dot plots of CXCR3⁺ CD4⁺ and CD8⁺ T cells (A) and the percentage of CXCR3⁺ cells after gating on CD4⁺ or CD8⁺ T cells (B). Representative flow cytometric histograms of CXCR3 (C) and the MFI of CXCR3 (D) after gating on CD4⁺ CD44^{hi} or CD8⁺ CD44^{hi} T cells. All experiments were performed on day 7 post-infection. The numbers shown on the dot plots indicate the mean percentage of cells inside the gate ± S.E.M. $n = 13$ for all groups. The average of two individual experiments is shown. FeD = iron dextran, PBS = control. Statistically significant differences, shown by asterisks (** $P < 0.01$ and *** $P < 0.001$), were determined by unpaired Student's t-test.

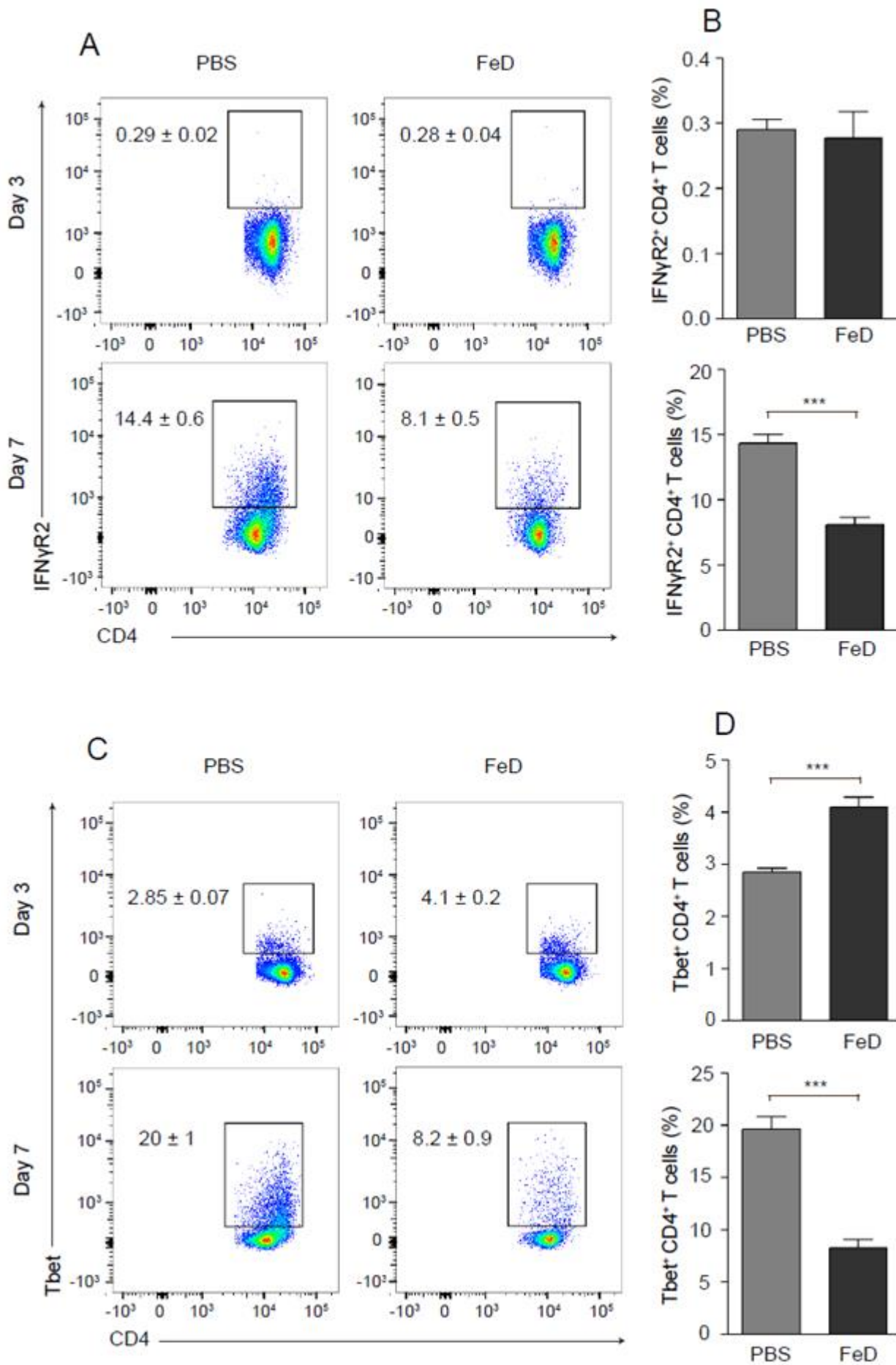


Figure 7. Iron Dextran Mitigates the Upregulation of IFN γ R2 and T-bet on CD4⁺ T Cells in the Spleen. Representative flow cytometric dot plots for IFN γ R2⁺ CD4⁺ T cells (**A**) and the percentage of IFN γ R2⁺ cells (**B**) after gating on CD4⁺ T cells on day 3 and day 7 post-infection. Representative flow cytometric dot plots for T-bet⁺ CD4⁺ T cells (**C**) and the percentage of T-bet⁺ cells (**D**) after gating on CD4⁺ T cells on day 3 and 7 post-infection. The numbers shown on the dot plots indicate the mean percentage of cells inside the gate \pm S.E.M. On day 3 post-infection, $n = 6$ for control mice and $n = 5$ for FeD mice. On day 7 post-infection, $n = 6$ for control mice and $n = 6$ for FeD mice. FeD = iron dextran, PBS = control. Statistically significant differences, shown by asterisks (***) $P < 0.001$, were determined by unpaired Student's t-test.

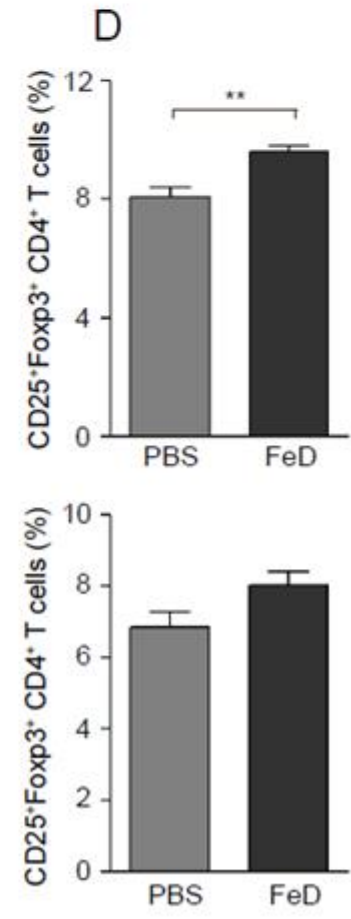
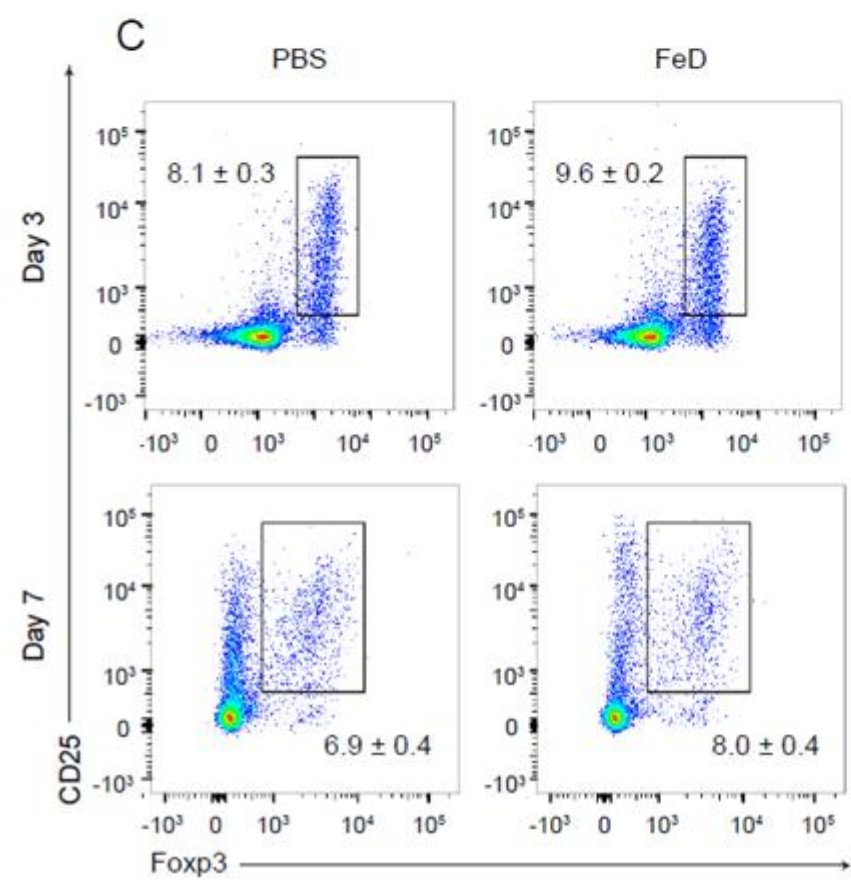
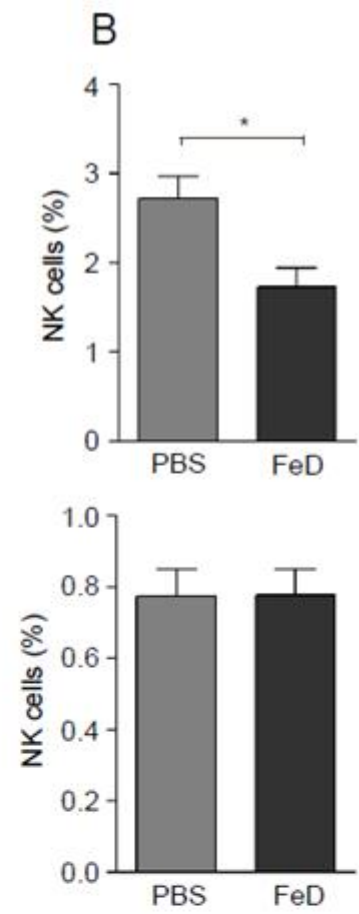
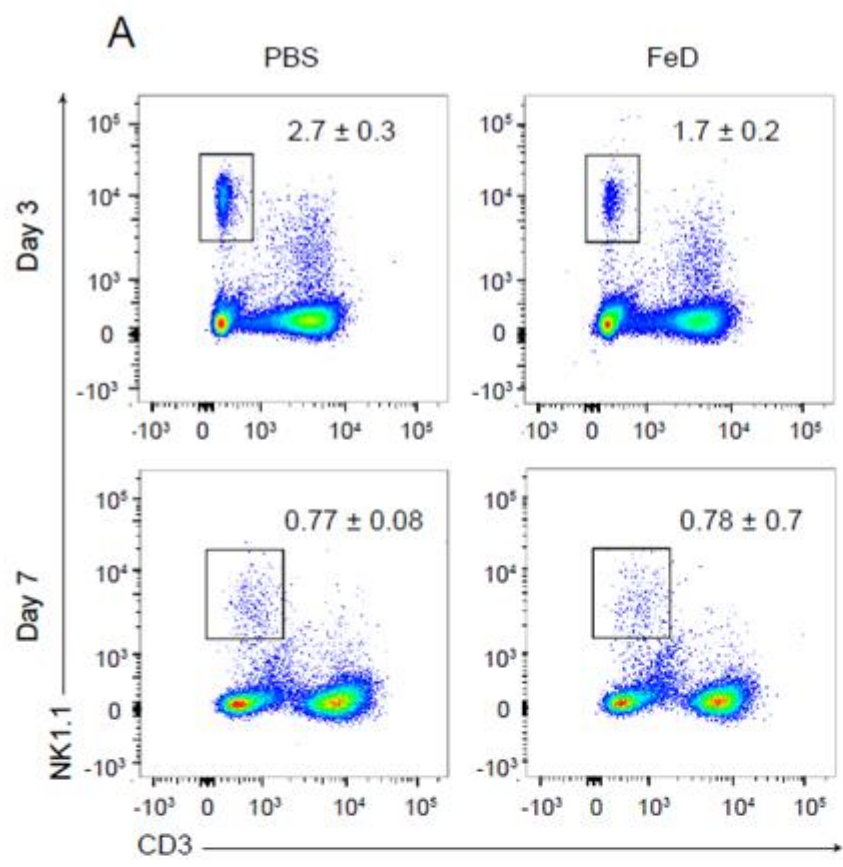
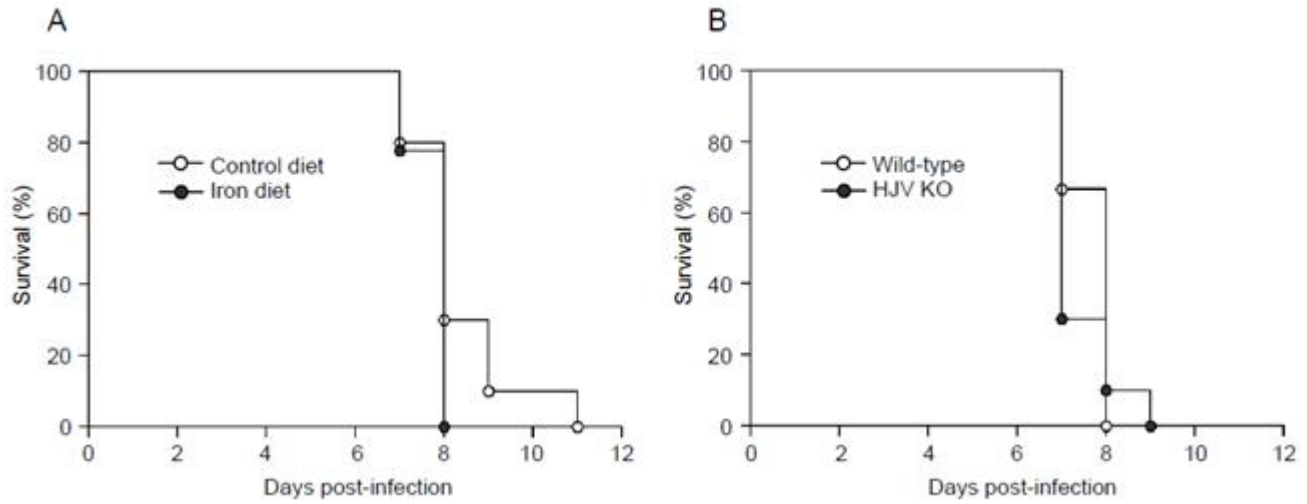
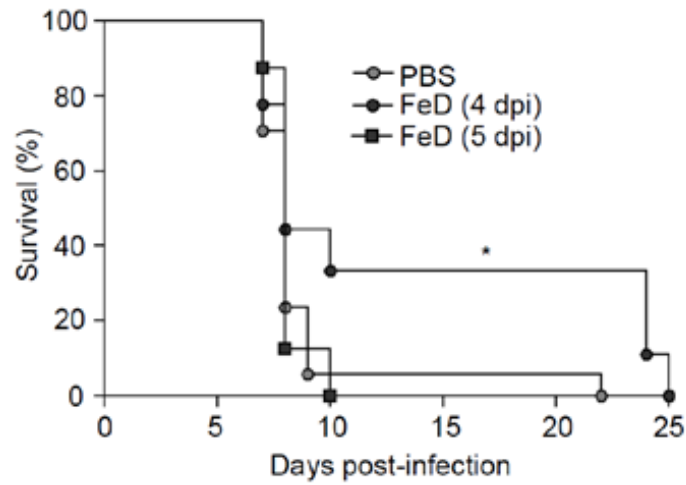


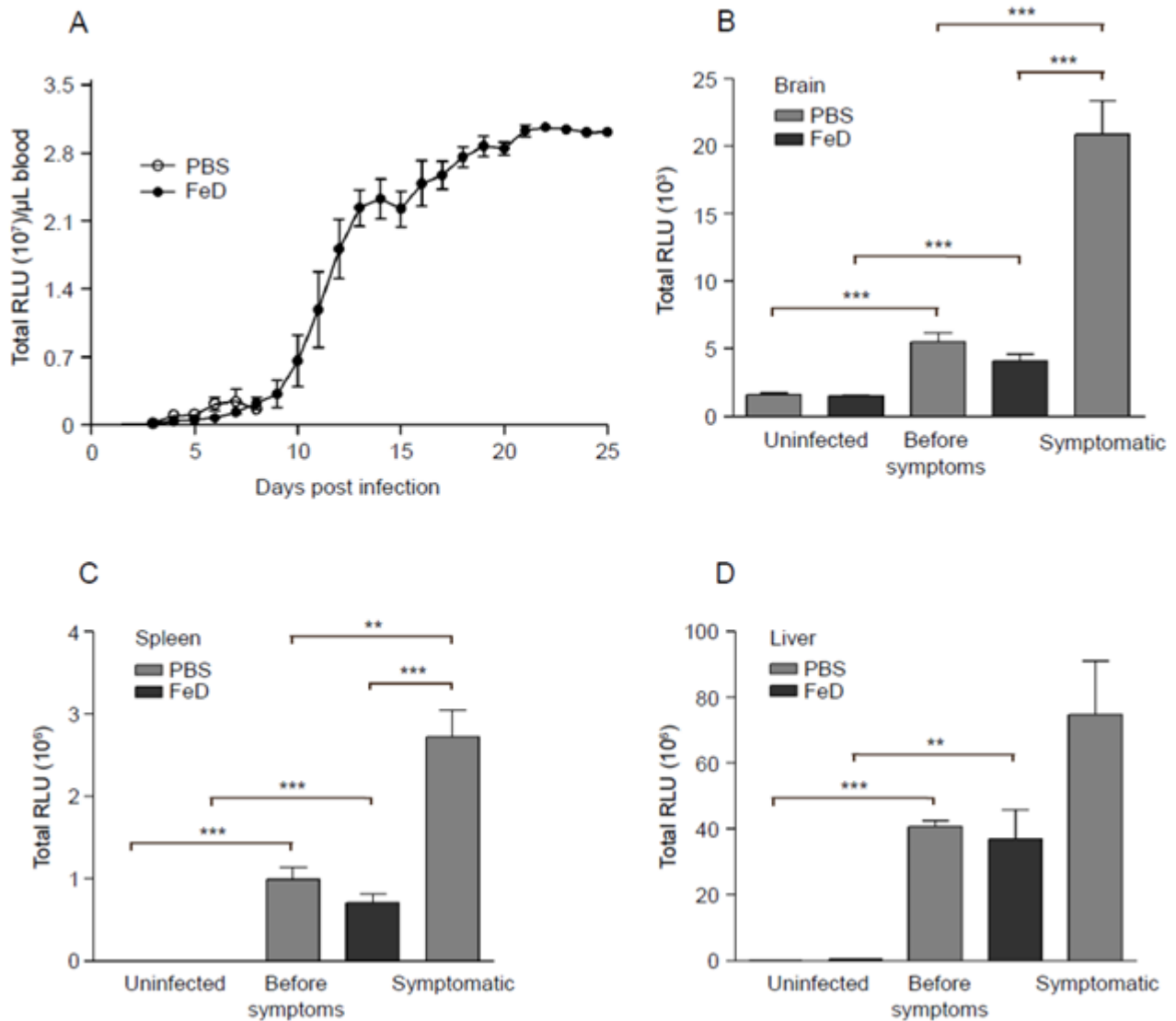
Figure 8. FeD Mice have Modulated Frequencies of Splenic NK Cells and Tregs Early During the Infection. Representative flow cytometric dot plots of NK cells (**A**) and the percentage of NK cells (**B**) on day 3 and day 7 post-infection. Representative flow cytometric dot plots of Tregs (**C**) and the percentage of Tregs after gating on CD4⁺ T cells (**D**) on day 3 and day 7 post-infection. The numbers shown on the dot plots indicate the mean percentage of cells inside the gate \pm S.E.M. On day 3 post-infection, $n = 6$ for control mice and $n = 5$ for FeD mice, except for Tregs, where $n = 5$ for the control mice. On day 7 post-infection, $n = 6$ for control mice and $n = 6$ for FeD mice. FeD = iron dextran, PBS = control. Statistically significant differences, shown by asterisks (* $P < 0.05$ ** $P < 0.01$), were determined by unpaired Student's t-test.



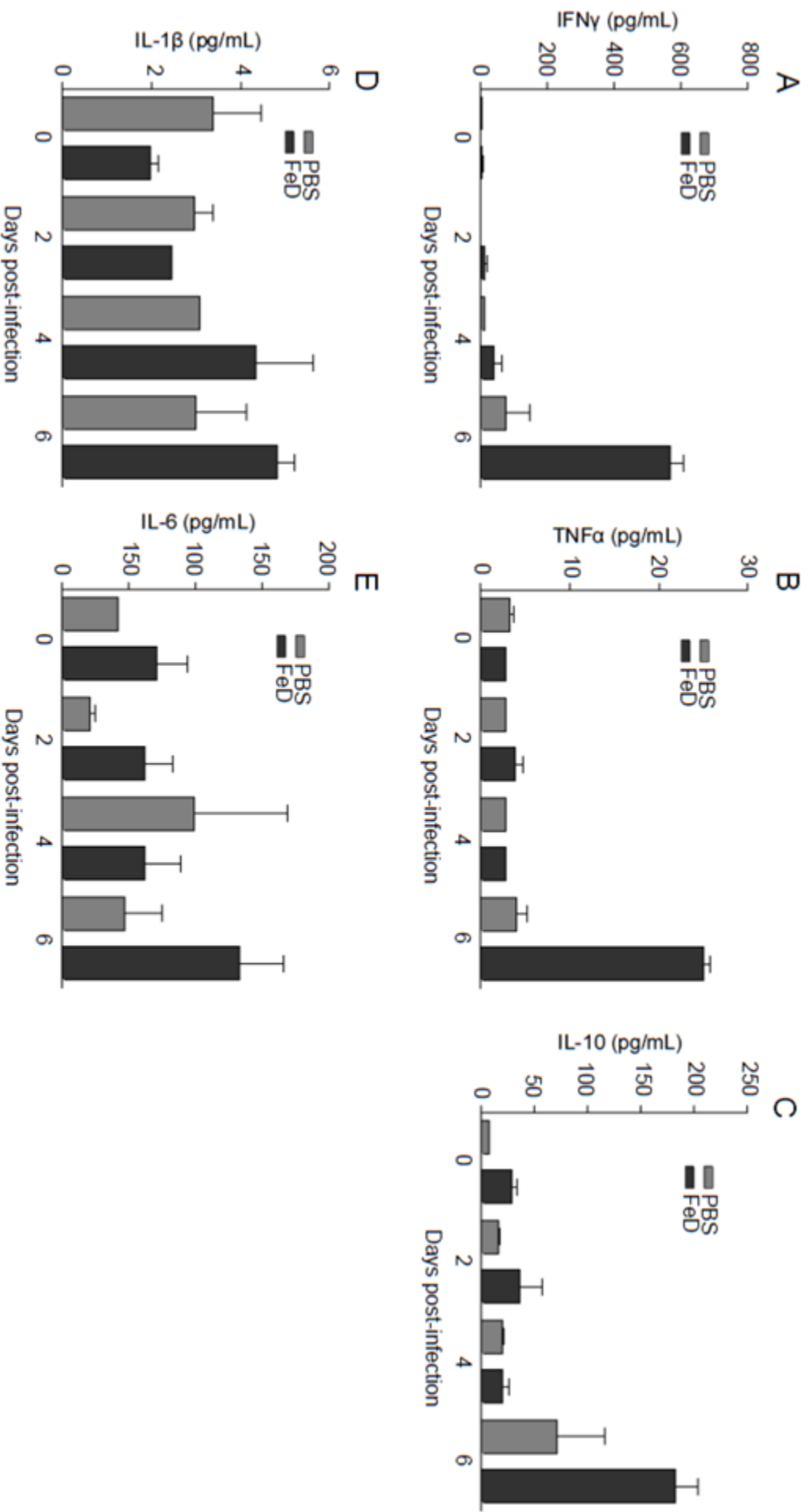
Supplementary Figure 1. Mice Fed an Iron-enriched Diet and HJV^{-/-} Mice are not Protected from ECM. Survival of mice fed an iron-enriched diet (A) and of HJV^{-/-} mice (B). $n = 10$ for mice fed a standard diet, $n = 9$ for mice fed an iron enriched diet, $n = 9$ for wild-type mice and $n = 10$ for HJV^{-/-} mice. No statistical difference in survival as determined by the log-rank test.



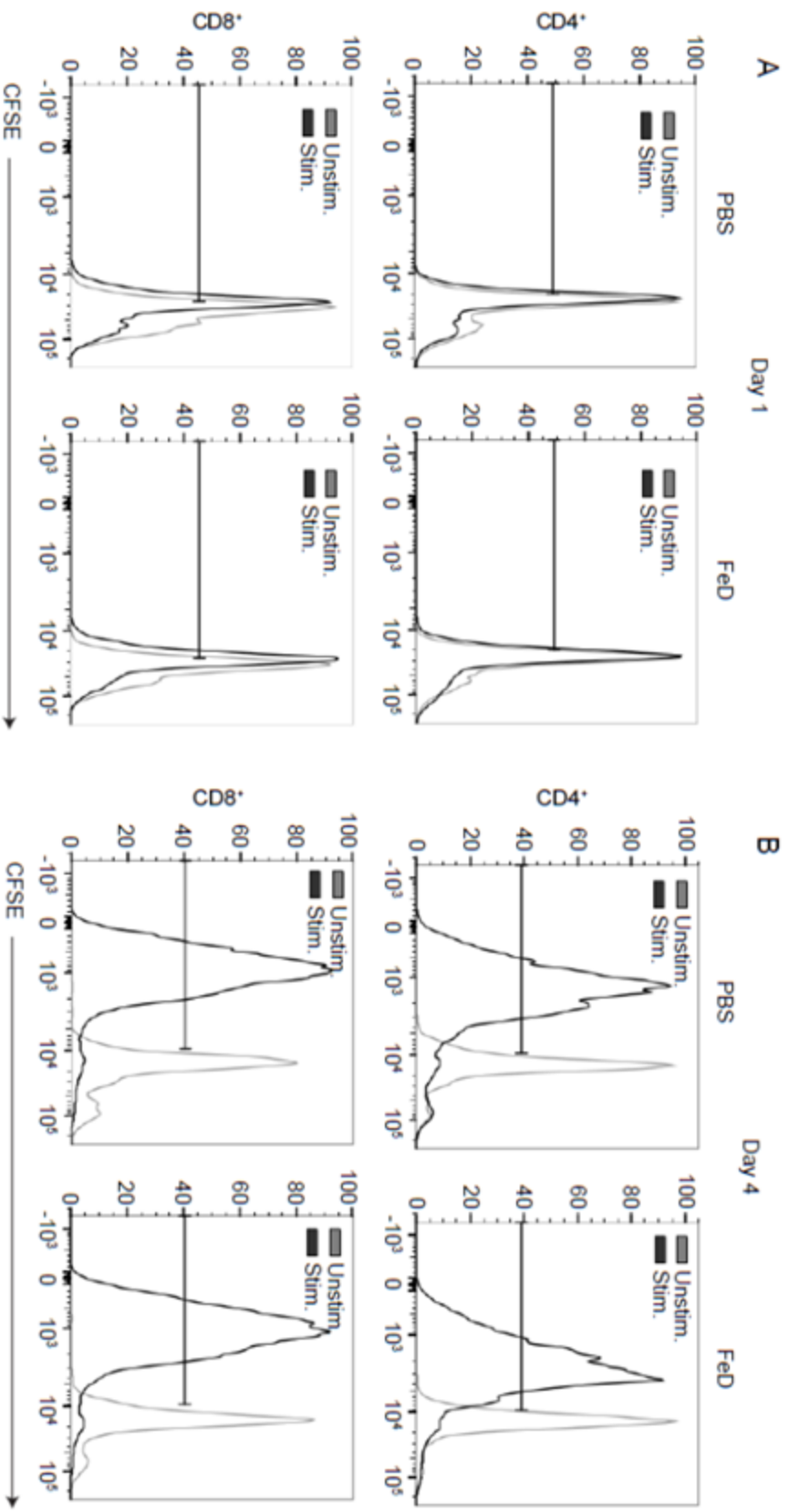
Supplementary Figure 2. Iron Dextran Administered after Infection can Prevent the Development of ECM. Survival of mice treated with PBS or iron dextran starting 4 or 5 days post-infection. The average of two individual experiments is shown. $n = 17$ for PBS mice; $n = 9$ for FeD mice, 4 days post-infection; and $n = 8$ for FeD mice, 5 days post-infection. PBS = control, FeD = iron dextran. Statistically significant differences, shown by asterisks ($* P < 0.05$), were determined by log-rank test.



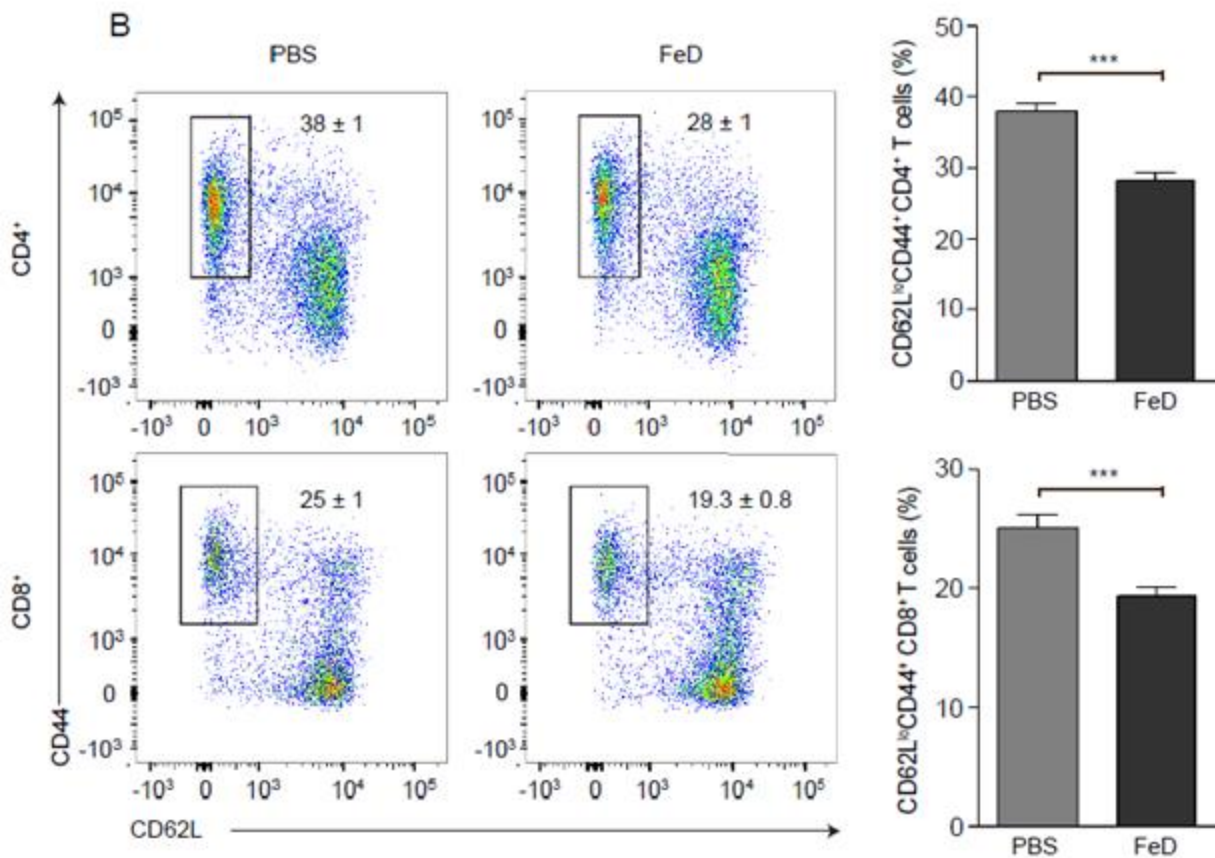
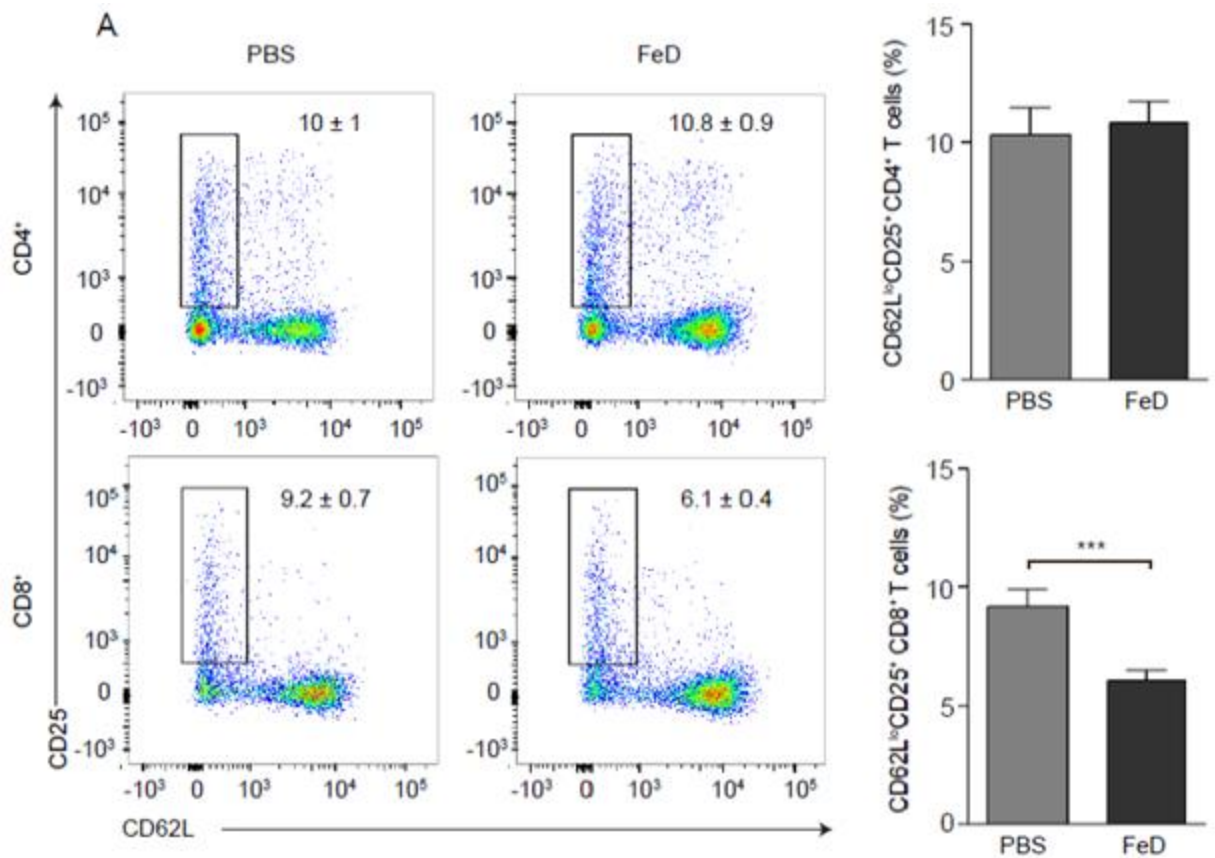
Supplementary Figure 3. RLU Measured in the Blood, Brain, Spleen and Liver. Parasitemia was determined by measuring relative luminescence units (RLU) per μL of blood in infected FeD mice and control mice (A). Parasite levels in the brain (B), spleen (C) and liver (D) on day 7 post-infection were determined by measuring RLU. For parasitemia: $n = 10$ for the control and FeD mice. For tissue parasite burden: $n = 6$ for all groups, except for the control, unsymptomatic mice ($n = 4$) and the control, symptomatic mice ($n = 4$). Shown on the graphs are the average \pm S.E.M. FeD = iron dextran, PBS = control. Statistically significant differences, shown by asterisks (** $P < 0.01$ and *** $P < 0.001$), were determined by unpaired Student's t-test.



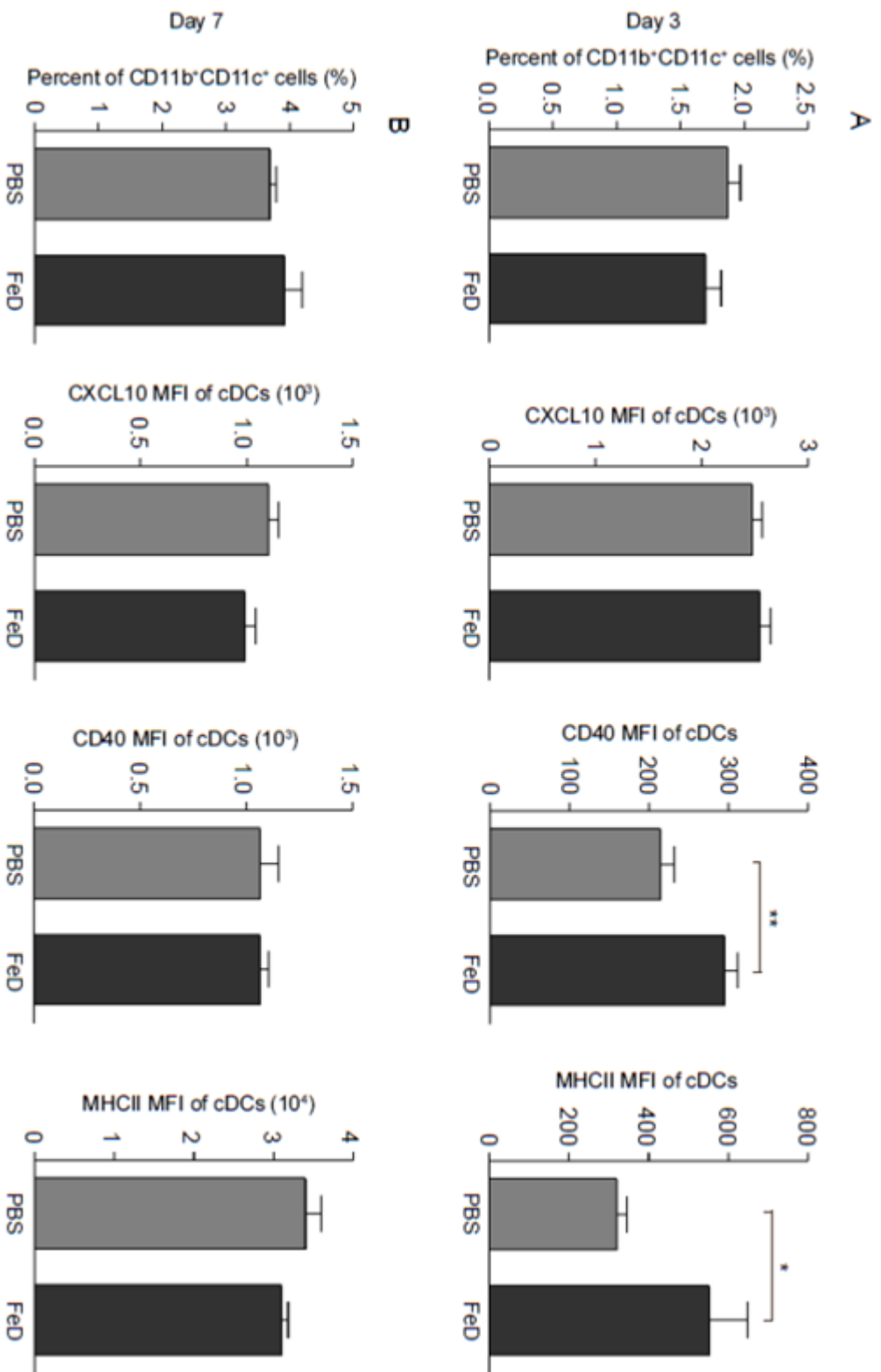
Supplementary Figure 4. Systemic Inflammation in FeD Mice is Increased Only Late during the Infection. Concentration of IFN γ (A), TNF α (B), IL-10 (C), IL-1 β (D) and IL-6 (E) in the serum. $n = 2$ for all groups. FeD = iron dextran, PBS = control.



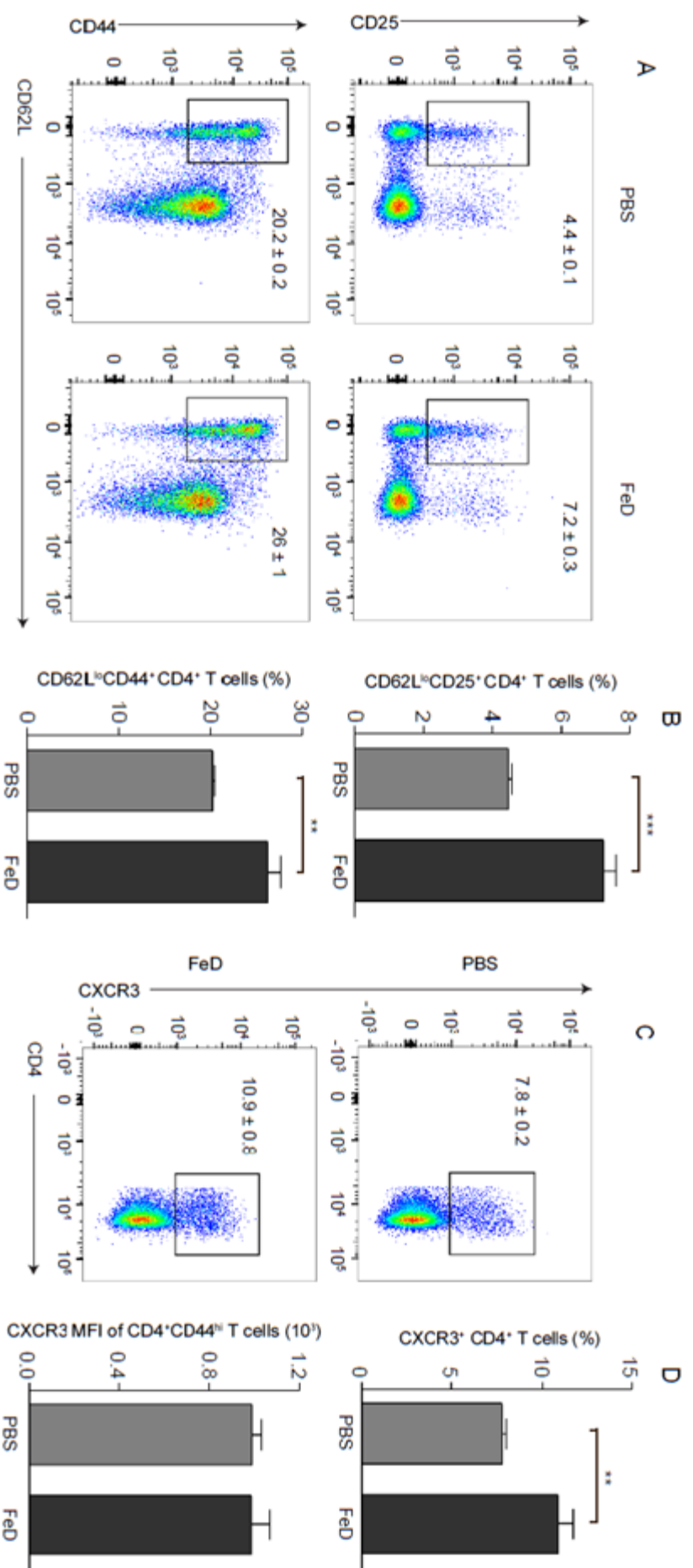
Supplementary Figure 5. Iron Dextran Causes a Minor Delay in the Proliferation of Splenic CD4⁺ T Cells. Representative flow cytometric histograms of CFSE after gating on CD4⁺ or CD8⁺ T cells on day 1 (A) and day 4 (B) after *ex vivo* stimulation. Splenic cells were isolated on day 7 post-infection. *n* = 6 for control mice and *n* = 7 for FeD mice. FeD = iron dextran, PBS = control.



Supplementary Figure 6. Percentage of Activated CD4⁺ and CD8⁺ T Cells in the Spleen is Slightly Decreased in the FeD Mice. Representative flow cytometric dot plots and the percentage of CD62L^{lo}CD25⁺ cells (**A**) and representative flow cytometric dot plots and the percentage of CD62L^{lo}CD44⁺ cells (**B**) after gating on CD4⁺ or CD8⁺ T cells. All experiments were performed on day 7 post-infection. The numbers shown on the dot plots indicate the mean percentage of cells inside the gate \pm S.E.M. Shown on the graphs are the average \pm S.E.M $n = 20$ for all groups. The average of three individual experiments is shown. FeD = iron dextran, PBS = control. Statistically significant differences, shown by asterisks (***) $P < 0.001$, were determined by unpaired Student's t-test.

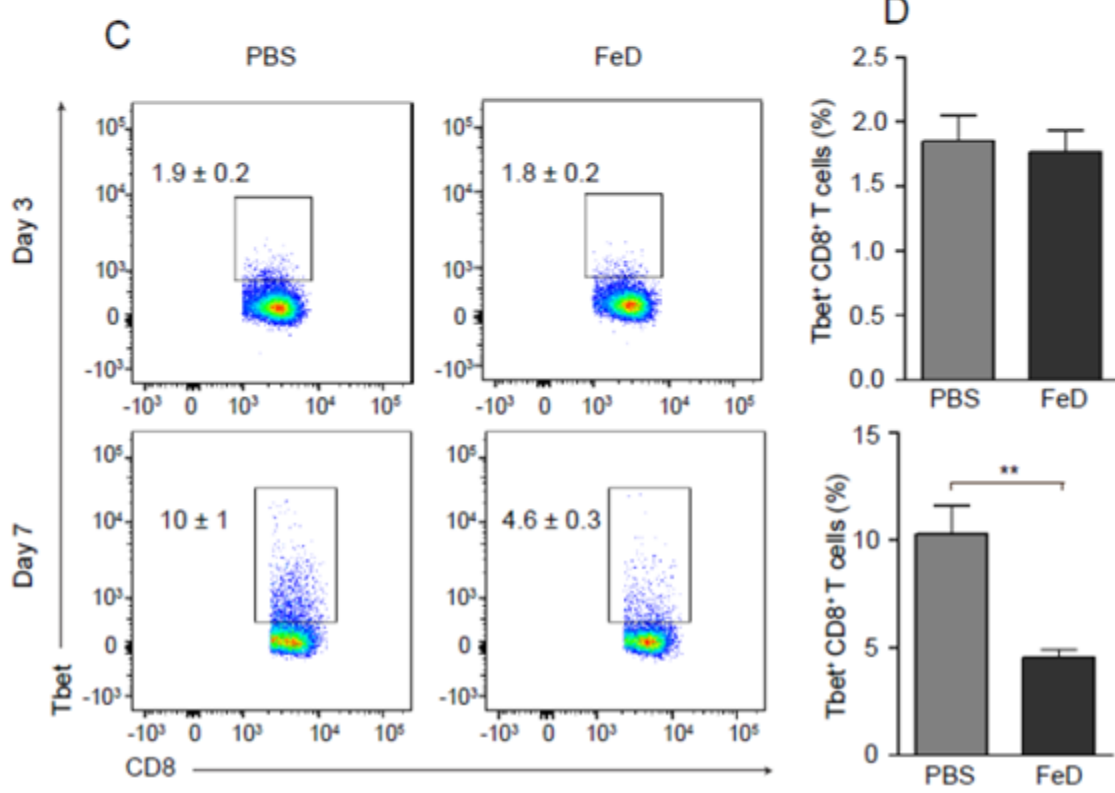
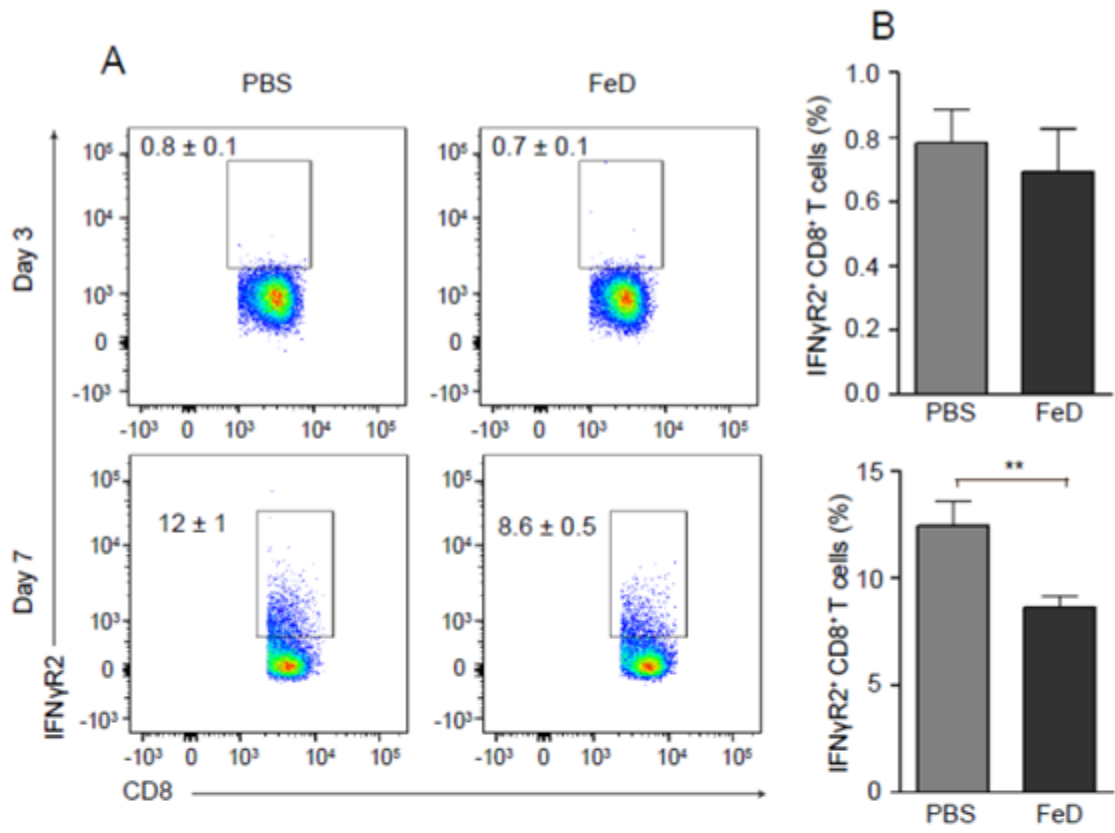


Supplementary Figure 7. Iron Supplementation Results in a Slight Increase in the Priming Capacity of Splenic cDCs. The percentage of CD11b⁺CD11c⁺ cells, and the MFI of CXCL10, CD40 and MHCII after gating on CD11b⁺CD11c⁺ cells on day 3 (A) and day 7 post-infection (B). On day 3 post-infection, $n = 6$ for control mice and $n = 5$ for FeD mice. On day 7 post-infection, $n = 6$ for control mice and $n = 6$ for FeD mice. Shown on the graphs are the average \pm S.E.M FeD = iron dextran, PBS = control. Statistically significant differences, shown by asterisks (* $P < 0.05$ and ** $P < 0.01$), were determined by unpaired Student's t-test

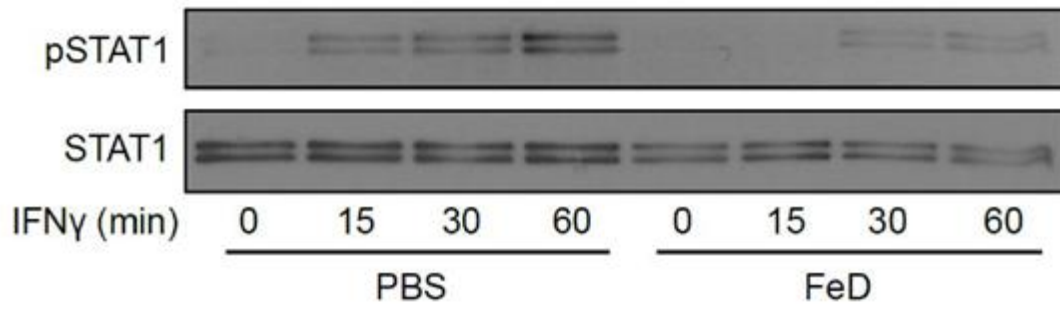


Supplementary Figure 8. A Greater Percentage of Splenic CD4⁺ T Cells in FeD Mice Show an Activated Phenotype and Express

CXCR3 on Day 3. Representative flow cytometric dot plots of CD62L^{lo}CD25⁺ and CD62L^{lo}CD44⁺ cells (A) and the percentage of CD62L^{lo}CD25⁺ and CD62L^{lo}CD44⁺ cells (B) after gating on CD4⁺ T cells. Representative flow cytometric dot plots of CXCR3⁺CD4⁺ T cells (C), and the percentage of CXCR3⁺ cells and the MFI of CXCR3 (D) after gating on CD4⁺ T cells. All experiments were performed on day 3 post-infection. The numbers shown on the dot plots indicate the mean percentage of cells inside the gate ± S.E.M. Shown on the graphs are the average ± S.E.M $n = 6$ for control mice and $n = 5$ for FeD mice. FeD = iron dextran, PBS = control. Statistically significant differences, shown by asterisks (** $P < 0.01$ and *** $P < 0.001$), were determined by unpaired Student's t-test.



Supplementary Figure 9. Attenuated Expression of IFN γ R2 and T-bet does not Result in Decreased Expression of CXCR3 on Splenic CD8⁺ T Cells. Representative flow cytometric dot plots for IFN γ R2⁺ CD8⁺ T cells (**A**) and the percentage of IFN γ R2⁺ cells (**B**) after gating on CD8⁺ T cells on day 3 and day 7 post-infection. Representative flow cytometric dot plots for T-bet⁺ CD8⁺ T cells (**C**) and the percentage of T-bet⁺ cells (**D**) after gating on CD8⁺ T cells on day 3 and day 7 post-infection. The numbers shown on the dot plots indicate the mean percentage of cells inside the gate \pm S.E.M. On day 3, $n = 6$ for control mice and $n = 5$ for FeD mice. On day 7, $n = 6$ for control mice and $n = 6$ for FeD mice. FeD = iron dextran, PBS = control. Statistically significant differences, shown by asterisks (** $P < 0.01$), were determined by unpaired Student's t-test.



Supplementary Figure 10. Iron Supplementation Decreases STAT1 Phosphorylation in Splenic CD4⁺ T cells in FeD Mice. Representative western blot of pSTAT1 and STAT1. *n* = 2 for all groups. FeD = iron dextran, PBS = control.

gene	UI, PBS	UI, Fed	I, PBS	I, Fed	gene	UI, PBS	UI, Fed	I, PBS	I, Fed	gene	UI, PBS	UI, Fed	I, PBS	I, Fed
APCS	1.00	1.12	1.02	0.73	IFNA1	1.19	1.52	1.39	1.06	MX1	1.14	1.15	26.73	6.91
C3	1.47	0.40	3.63	2.02	IFNAR1	1.00	1.02	1.09	0.89	MYD88	1.04	1.20	3.75	2.29
CSF1	1.02	1.19	4.58	3.77	IFNB1	1.18	1.65	1.58	1.09	NFkB1	1.00	1.15	2.09	1.14
CASP1	1.00	1.01	3.95	1.63	IFNG	1.00	1.12	47.21	22.23	IKKB	1.02	1.05	2.62	1.44
CCL12	1.05	1.31	20.81	30.46	IFNGR1	1.00	1.05	2.15	1.36	NLRP3	1.02	0.75	2.37	1.31
CCL5	1.01	1.06	18.20	7.15	IL-10	1.00	1.12	12.55	2.64	NOD1	1.04	1.17	2.76	2.16
CCR4	1.16	1.66	2.33	1.17	IL-13	1.02	1.50	1.67	1.10	NOD2	1.29	2.12	3.19	2.09
CCR5	1.03	1.20	4.23	2.01	IL-17A	1.01	1.11	1.60	1.10	RAG1	1.03	2.26	0.98	1.90
CCR6	1.10	1.73	0.92	1.35	IL-18	1.00	0.87	1.32	0.95	RORC	1.00	1.22	1.77	1.09
CCR8	1.00	1.12	1.06	0.73	IL-1 α	1.04	0.84	2.88	1.71	SLC11A1	1.00	0.92	2.00	1.63
CD14	1.01	1.02	16.83	2.09	IL-1 β	1.06	1.16	3.23	2.11	STAT1	1.00	0.94	12.71	7.54
CD4	1.00	0.68	1.12	0.80	IL-1R1	1.03	1.25	1.69	1.16	STAT3	1.00	1.01	3.28	1.71
CD40	1.01	1.00	1.73	1.71	IL-2	1.15	1.58	1.51	1.30	STAT4	1.03	0.77	1.77	0.96
CD40L	1.00	1.12	2.36	1.35	IL-23A	1.01	0.94	1.30	1.13	STAT6	1.00	1.14	1.67	1.23
CD80	1.00	0.61	4.82	1.37	IL-4	1.09	1.52	1.28	0.74	TBX21	1.00	1.12	2.91	1.11
CD86	1.00	0.79	4.71	1.95	IL-5	1.04	1.21	2.74	1.21	TTCAM1	1.01	1.07	1.74	1.46
CD8 α	1.13	1.37	34.56	17.01	IL-6	1.00	1.49	9.19	2.22	TLR1	1.00	0.82	3.76	2.80
CRP	1.49	0.43	0.54	1.07	IRAK1	1.00	1.04	1.03	0.76	TLR2	1.05	0.99	7.27	3.83
GM-CSF	1.24	1.33	2.51	1.35	IRF3	1.00	1.08	0.92	0.95	TLR3	1.00	1.08	3.14	1.73
CXCL10	1.01	1.01	308.53	166.16	IRF7	1.00	1.35	36.26	12.37	TLR4	1.00	0.87	2.16	1.72
CXCR3	1.05	1.16	9.84	3.81	ITGAM	1.00	0.72	1.17	0.99	TLR5	1.00	0.97	0.89	0.74
DDX58	1.00	1.00	8.71	4.36	JAK2	1.00	0.96	1.47	1.18	TLR6	1.03	0.93	1.85	1.35
FASL	1.00	1.12	1.34	0.73	LY96	1.00	0.44	1.34	0.98	TLR7	1.00	1.18	4.76	2.59
FOXP3	1.01	1.68	1.29	1.16	LYZ2	1.01	1.23	7.76	6.07	TLR8	1.15	1.65	3.91	2.36
GATA3	1.09	1.24	1.78	1.15	ERK2	1.00	0.91	1.18	0.79	TLR9	1.01	0.81	2.25	1.97
H2-Q10	1.25	0.49	0.83	0.61	JNK1	1.00	0.95	1.06	0.76	TNF	1.00	1.25	29.96	15.52
H2-T23	1.00	1.01	11.83	5.96	MBL2	1.39	1.85	1.28	1.17	TRAF6	1.02	1.06	1.67	1.24
ICAM1	1.08	1.58	14.34	9.25	MPO	1.00	0.81	1.11	0.74	TYK2	1.01	0.90	1.20	1.16

Supplementary Table 1. Immune Response-related Gene Expression in the Brain is Mostly Reduced or Unchanged in FeD Mice. The mRNA expression of immune related genes was determined in the brain on day 7 post-infection. mRNA levels were normalized to *Gusb*. 2 samples pooled from 6 mice (3 mice per sample) were used for each group. Shown in the table are the averages UI = uninfected, I = infected, FeD = iron dextran, PBS = control.

gene	UI, PBS	UI, Fed	I, PBS	I, Fed	gene	UI, PBS	UI, Fed	I, PBS	I, Fed	gene	UI, PBS	UI, Fed	I, PBS	I, Fed
APCS	1.00	4.41	2.01	1.44	IFNA1	1.01	4.97	7.28	7.49	MX1	1.01	0.42	4.96	1.79
C3	1.00	3.52	12.94	5.33	IFNAR1	1.00	3.57	7.40	3.97	MYD88	1.00	5.72	48.24	32.66
C5R1	1.02	24.57	327.10	285.60	IFNB1	1.00	5.19	5.42	5.49	NFKB1	1.00	2.06	2.39	2.51
CASP1	1.00	0.61	0.47	0.96	IFNG	1.09	1.35	58.21	72.15	IKKB	1.00	0.45	1.09	0.77
CCL12	1.00	0.32	1.22	4.25	IFNGR1	1.00	1.53	5.30	2.78	NLRP3	1.00	2.95	16.39	13.07
CCL5	1.00	1.44	5.60	5.71	IL-10	1.06	9.22	144.40	164.27	NOD1	1.01	1.77	7.65	3.77
CCR4	1.00	3.09	3.14	2.49	IL-13	1.00	4.41	1.31	5.26	NOD2	1.01	6.53	5.71	5.08
CCR5	1.00	0.93	20.17	22.63	IL-17A	1.00	4.41	0.70	1.44	RAG1	1.00	4.41	0.70	1.44
CCR6	1.00	0.72	1.09	0.68	IL-18	1.00	1.16	6.43	2.42	RORC	1.00	5.63	1.85	1.60
CCR8	1.02	4.38	6.86	11.06	IL-1 α	1.00	2.08	5.95	5.14	SLC11A1	1.00	9.38	31.46	31.09
CD14	1.00	0.76	2.85	1.31	IL-1 β	1.00	1.39	0.90	0.88	STAT1	1.00	1.36	3.47	4.48
CD4	1.00	8.87	18.14	8.19	IL-1R1	1.00	5.82	9.47	5.18	STAT3	1.00	3.86	10.48	7.10
CD40	1.00	0.69	0.42	0.50	IL-2	1.00	2.74	5.03	2.03	STAT4	1.01	2.40	3.81	4.33
CD40L	1.00	7.95	8.62	19.63	IL-23A	1.00	4.41	5.13	3.06	STAT6	1.00	5.32	12.27	7.69
CD80	1.00	1.38	4.02	1.46	IL-4	1.00	0.56	0.38	0.54	TBX21	1.00	7.33	32.61	65.27
CD86	1.00	1.83	2.25	2.07	IL-5	1.00	4.41	11.05	2.71	TTCAM1	1.02	9.23	38.66	17.39
CD8 α	1.00	7.70	6.98	11.14	IL-6	1.00	4.41	7.33	5.52	TLR1	1.00	0.82	0.89	0.75
CRP	1.00	4.41	1.06	2.57	IRAK1	1.00	1.01	3.34	1.55	TLR2	1.00	2.56	5.16	3.03
GM-CSF	1.00	19.67	11.01	34.70	IRF3	1.00	1.25	0.81	1.12	TLR3	1.00	0.57	1.54	0.95
CXCL10	1.04	7.76	33.25	75.46	IFRF7	1.01	7.02	37.11	41.92	TLR4	1.00	2.48	10.79	6.84
CXCR3	1.00	1.86	37.33	17.77	ITGAM	1.00	17.05	19.99	28.03	TLR5	1.01	1.37	1.87	0.56
DDX58	1.00	1.48	3.18	1.99	JAK2	1.00	1.12	1.62	1.22	TLR6	1.01	1.57	11.51	4.82
FASL	1.00	0.17	0.40	0.27	LY96	1.00	2.42	6.22	3.26	TLR7	1.00	1.19	11.33	3.34
FOXP3	1.00	7.46	6.51	2.54	LYZ2	1.00	0.93	1.57	1.17	TLR8	1.07	1.90	31.28	7.65
GATA3	1.01	3.82	3.37	7.53	ERK2	1.00	2.31	3.44	2.62	TLR9	1.00	9.59	16.23	12.36
H2-Q10	1.12	2.61	2.81	3.04	JNK1	1.00	3.62	3.47	2.62	TNF	1.00	8.79	20.32	13.16
H2-T23	1.00	0.59	0.74	0.89	MBL2	1.00	4.41	0.86	1.44	TRAF6	1.00	1.88	15.28	3.07
ICAM1	1.00	2.53	6.88	5.96	MPO	1.32	5.08	15.66	9.75	TYK2	1.00	5.30	4.73	4.37

Supplementary Table 2. Immune Response-related Gene Expression in the Spleen is Mostly Reduced or Unchanged in FeD Mice. The mRNA expression of immune related genes was determined in the spleen on day 7 post-infection. mRNA levels were normalized to *Gusb*. 2 samples pooled from 6 mice (3 mice per sample) were used for each group. Shown in the table are the averages. UI = uninfected, I = infected, FeD = iron dextran, PBS = control

gene	UI, PBS	UI, Fed	I, PBS	I, Fed	gene	UI, PBS	UI, Fed	I, PBS	I, Fed	gene	UI, PBS	UI, Fed	I, PBS	I, Fed
APCS	1.00	0.32	2.63	1.05	IFNA1	1.00	0.76	1.42	0.22	MX1	1.06	0.70	5.59	2.52
C3	1.05	0.56	1.24	0.51	IFNAR1	1.00	0.91	1.27	0.58	MYD88	1.03	0.69	3.85	1.58
CSF1	1.06	1.41	8.08	285	IFNB1	1.00	0.50	1.40	0.14	NFKB1	1.00	0.89	1.34	1.19
CASP1	1.00	1.83	6.80	9.79	IFNG	1.00	1.63	110.15	77.47	IKKBK	1.04	0.79	1.56	0.99
CCL12	1.01	1.52	11.30	31.70	IFNGR1	1.00	0.97	2.66	1.27	NLRP3	1.00	1.04	8.34	4.08
CCL5	1.02	1.42	22.37	18.45	IL-10	1.01	0.32	35.11	12.36	NOD1	1.00	1.01	3.06	1.58
CCR4	1.02	1.70	2.41	1.73	IL-13	1.01	1.26	1.38	1.03	NOD2	1.00	0.68	1.99	1.43
CCR5	1.00	0.20	8.57	3.88	IL-17A	1.01	1.26	1.38	1.03	RAG1	1.01	1.26	1.38	1.03
CCR6	1.02	0.39	0.91	0.28	IL-18	1.00	0.90	1.50	0.67	RORC	1.01	0.91	2.72	0.20
CCR8	1.01	1.26	5.83	4.21	IL-1 α	1.00	0.90	1.21	0.91	SLC11A1	1.01	3.70	9.40	8.86
CD14	1.00	0.35	2.12	1.63	IL-1 β	1.04	0.28	0.39	0.61	STAT1	1.00	1.05	5.23	6.57
CD4	1.04	3.68	9.88	5.27	IL-1R1	1.07	0.57	5.04	1.08	STAT3	1.00	0.89	1.94	1.11
CD40	1.01	1.15	4.77	6.96	IL-2	1.00	1.00	2.12	0.82	STAT4	1.00	0.87	9.77	7.55
CD40L	1.00	1.55	19.51	13.53	IL-23A	1.01	0.89	1.58	0.45	STAT6	1.02	0.72	1.22	0.78
CD80	1.00	1.92	8.79	3.35	IL-4	1.00	0.56	1.33	0.30	TBX21	1.00	1.23	10.39	9.69
CD86	1.00	0.82	3.96	2.36	IL-5	1.00	0.59	2.35	0.38	TICAM1	1.03	0.74	1.41	0.39
CD8 α	1.00	1.45	32.42	26.48	IL-6	3.41	0.12	0.16	0.14	TLR1	1.01	2.51	10.83	6.20
CRP	1.00	0.33	0.67	0.29	IRAK1	1.00	1.24	1.38	0.51	TLR2	1.00	1.03	3.47	6.49
GM-CSF	1.10	0.86	1.25	0.40	IRF3	1.00	0.88	0.76	0.64	TLR3	1.01	0.66	2.01	1.15
CXCL10	1.00	2.99	10.36	18.44	IRF7	1.00	1.67	5.94	3.31	TLR4	1.00	1.72	5.91	3.16
CXCR3	1.01	0.85	11.11	5.54	ITGAM	1.00	1.37	16.35	8.27	TLR5	1.01	0.30	4.04	0.12
DDX58	1.00	0.90	1.13	0.80	JAK2	1.01	1.03	2.27	1.45	TLR6	1.00	1.03	4.72	2.15
FASL	1.01	1.26	4.02	1.65	LY96	1.00	0.64	1.45	0.65	TLR7	1.02	1.17	5.57	1.37
FOXP3	1.00	1.40	2.71	1.18	LYZ2	1.01	3.18	1.35	2.51	TLR8	1.01	2.04	8.94	2.32
GATA3	1.00	2.35	2.98	2.63	ERK2	1.00	0.72	1.09	0.59	TLR9	1.00	2.14	12.89	8.52
H2-Q10	1.00	0.84	0.54	0.26	JNK1	1.00	0.68	1.86	0.51	TNF	1.00	2.39	11.39	10.74
H2-T23	1.00	0.94	3.69	2.43	MBL2	1.01	0.51	0.33	0.32	TRAF6	1.00	1.09	3.17	0.56
ICAM1	1.00	1.69	5.24	4.99	MPO	1.01	1.40	2.38	2.17	TYK2	1.00	0.92	1.17	0.88

Supplementary Table 3. Immune Response-related Gene Expression in the Liver is Mostly Reduced or Unchanged in FeD Mice. The mRNA expression of immune related genes was determined in the liver on day 7 post-infection. mRNA levels were normalized to *Hsp90*. 2 samples pooled from 6 mice (3 mice per sample) were used for each group. Shown in the table are the averages. UI = uninfected, I = infected, FeD = iron dextran, PBS = control.

Chapter Three

Protein Tyrosine Phosphatase Inhibition Prevents Experimental Cerebral Malaria by Precluding CXCR3 Expression on T Cells

Preface

Previous studies have demonstrated that PTP activity can be attenuated by numerous physiological factors, including iron levels (584). Notably, the administration of exogenous iron and the inhibition of PTP activity by bpV(phen) were both shown to significantly reduce footpad swelling in a mouse model of cutaneous leishmaniasis, with both treatments decreasing the parasite burden in the draining lymph node and increasing the production of nitric oxide (593-595). Altogether, the results of the above studies suggested that the iron-mediated protection from leishmaniasis may have been at least partially due to the inhibition of PTP activity.

Since we had recently demonstrated that iron supplementation markedly reduced the development of neuropathology in mice infected with *P. berghei* ANKA (638), we were interested in the potential effect of direct PTP inhibition on ECM. Mice treated with the PTP inhibitor bpV(phen) exhibited a significant reduction in the incidence of ECM and had parasitemia similar to that of the control mice. Based on the necessity of T cell accumulation within the brain to induce neuropathology and the attenuation of T cell chemotaxis caused by iron dextran, we examined the impact of bpV(phen) on CXCR3 expression. Additionally, non-cerebral malaria mouse models have demonstrated that IL-10 plays a role in limiting hepatic pathology and we observed that the bpV(phen)-treated mice had enhanced production of IL-10. Thus we also analysed the effect of IL-10 and PTP inhibition on liver injury.

Protein Tyrosine Phosphatase Inhibition Prevents Experimental Cerebral Malaria by Precluding CXCR3 Expression on T Cells

Kristin M. Van Den Ham^{1,3}, Logan K. Smith^{1,2}, Martin J. Richer^{1,2*} and Martin Olivier^{1,3*}

¹Department of Microbiology and Immunology, McGill University, Montréal, QC, H3A 0G4, Canada, ²Microbiome and Disease Tolerance Centre and Associate Member, Goodman Cancer Research Centre, McGill University, Montréal, QC, H3A 2B4, Canada, ³Infectious Diseases and Immunity in Global Health Program, Research Institute of the McGill University Health Centre, Montréal, QC, H4A 3J1, Canada.

*Corresponding authors: martin.olivier@mcgill.ca, martin.j.richer@mcgill.ca

Abstract

Cerebral malaria induced by *Plasmodium berghei* ANKA infection is dependent on the sequestration of cytotoxic T cells within the brain and augmentation of the inflammatory response. Herein, we demonstrate that inhibition of PTP activity significantly attenuates T cell sequestration within the brain and prevents the development of neuropathology. Mechanistically, the initial upregulation of CXCR3 on splenic T cells upon T cell receptor stimulation was critically decreased through the reduction of T cell-intrinsic PTP activity. Furthermore, PTP inhibition markedly increased IL-10 production by splenic CD4⁺ T cells by enhancing the frequency of LAG-3⁺CD49b⁺ type 1 regulatory cells. Overall, these findings demonstrate that modulation of PTP activity could possibly be utilized in the treatment of cerebral malaria and other CXCR3-mediated diseases.

Introduction

Nearly half of the world's population is at risk of malaria, a mosquito-borne, infectious disease caused by *Plasmodium* parasites. Notably, infection with *P. falciparum* can cause severe complications that often result in death (10). Multiple mouse models have been employed to recapitulate and characterize the varying pathologies. Infection with *Plasmodium berghei* NK65 induces immune-mediated liver damage (389), while infection with *P. berghei* ANKA results in a neuropathology referred to as ECM (390). Additionally, liver damage has also been reported in this model (493,494).

Sequestration of cytotoxic CD8⁺ T cells within the brain is required for the disruption of the BBB and the development of cerebral damage during *P. berghei* ANKA infection (390,406). The CD8⁺ T cell response is primed in the spleen (394) through the cross-presentation of antigen by

dendritic cells (414), and the resulting upregulation of the chemokine receptor CXCR3 is necessary for the chemotaxis of T cells to the brain (442-445). Furthermore, while a potent inflammatory response is required to control parasitemia and resolve the infection, inappropriate regulation of cytokine production can promote fatal hepatic and cerebral pathology.

The role of inflammation in ECM is poorly defined. IL-10 is an important immune regulator that can suppress inflammation (480). Depletion of IL-10 in resistant BALB/c mice was shown to increase the incidence of ECM, and exogenous IL-10 decreased neuropathology in susceptible CBA/J mice (482). However, in C57BL/6 mice, depletion of the IL-10 receptor did not affect susceptibility to ECM, but did significantly increase parasite burden (394). Furthermore, IL-10 production by Foxp3⁻ regulatory CD4⁺ T cells has been shown to mitigate pathology in non-cerebral murine malaria (481,485). Tr1 cells suppress effector T cell responses through the production of high levels of IL-10 (639), and the surface markers CD49b and LAG-3 were recently shown to be able to non-ambiguously identify Tr1 cells (640).

Trafficking of T cells to the brain has been established to be absolutely critical in the development of ECM (442-445). Induction of CXCR3 requires transient TCR stimulation (470); however the subsequent pathways that control its expression are unclear. Signal transduction downstream of TCR stimulation relies on a dynamic tyrosine phosphorylation cascade, regulated by the opposing activities of PTKs and PTPs (567). For example, the PTP CD45 is crucially involved in promoting proximal TCR signalling by dephosphorylating the inhibitory tyrosine of Lck (Y505) (567). Inhibition of PTP activity has been shown to cause at least partial T cell activation (609,610), but the impact of PTP inhibition in conjunction with TCR stimulation is unknown.

PTP activity is regulated by a variety of physiological mechanisms, including dimerization (587), oxidation (588) and increased systemic levels of iron (584). Furthermore, PTP inhibition has been shown to reduce pathology in models of asthma (641), cancer (642) and leishmaniasis (593). However, the underlying pathological mechanisms that are modulated by tyrosine phosphorylation are largely undefined, thus we were interested in examining the impact of direct PTP inhibition on the T cell response and on the regulation of infection-induced inflammation during ECM.

We determined that treatment with the PTP inhibitor bpV(phen), precluded the development of hepatic and cerebral damage in ECM. PTP inhibition significantly decreased the brain sequestration of CD4⁺ and CD8⁺ T cells, concomitant with a marked decrease in the expression of CXCR3 on splenic T cells. bpV(phen) prevented the initial upregulation of CXCR3, which was associated with differential tyrosine phosphorylation of the proximal TCR-signalling molecule Lck. Moreover, PTP inhibition greatly augmented the frequency of IL-10-producing regulatory CD4⁺ T cells, and both bpV(phen) and IL-10 were shown to limit hepatic pathology. Thus, we have demonstrated that modulation of PTP activity has the potential to be utilized in the development of novel adjunctive therapies for malaria.

Results

Inhibition of PTP activity prevents the development of ECM

To determine the impact of reduced tyrosine phosphatase activity on the pathology of ECM, mice were treated with the PTP inhibitor, bpV(phen), daily from 3 days before to 12 days after infection with *P. berghei* ANKA. bpV(phen) targets a conserved catalytic cysteine, resulting in a general inhibition of PTP activity (590,591). While 100% of the control mice succumbed to

ECM, the bpV(phen)-treated mice were markedly protected, with an overall ECM incidence of less than 13% (Figure 1A). Furthermore, the parasitemia of the control and bpV(phen)-treated mice was similar until the control mice succumbed to the infection, indicating that the protective effect of PTP inhibition did not rely on the increased clearance of parasites (Figure 1B). The bpV(phen)-treated mice that did not develop ECM had increasing levels of parasitemia and either succumbed to hyperparasitemia or were sacrificed on day 23 post-infection. The incidence of ECM was confirmed by examining the integrity of the BBB using EB. The uptake of the dye into the brain parenchyma, indicative of BBB disruption, was significantly decreased in the infected bpV(phen)-treated mice (Figure 1C,D). Moreover, the control mice developed definite symptoms of neuropathology, but PTP inhibition prevented the clinical manifestation of cerebral malaria (Figure S1). Therefore, inhibition of PTP activity is capable of protecting mice from ECM by preventing the development of neuropathology.

bpV(phen) treatment enhances IL-10 production by splenic regulatory CD4⁺ T cells

PTP inhibition using bpV(phen) has been shown to modulate the inflammatory response during leishmaniasis, asthma and cancer (594,641,642), and previously IL-10 was shown to afford protection against ECM (482). The effect of Tregs on the cerebral pathology induced by *P. berghei* ANKA infection is still uncertain (484,486-488,490), but IL-10 production by Foxp3⁺ CD4⁺ T cells has been reported to decrease pathology in non-cerebral murine malaria (481,485). Thus, we asked whether PTP inhibition protected mice from ECM by modulating immunoregulatory mechanisms.

The percentage of IL-10⁺CD4⁺ T cells in the spleen increased with both infection and bpV(phen) treatment (Figure 2A). PTP inhibition caused a slight increase in the percentage of Foxp3⁺ CD4⁺

T cells in both the uninfected and infected mice (Figure 2B,D). However, Tregs only accounted for approximately 10% of the total IL-10⁺CD4⁺ T cells in the uninfected mice and slightly more than 15% of the total IL-10⁺CD4⁺ T cells in the infected mice, congruous with an infection-dependent increase in IL-10 production by Foxp3⁺CD4⁺ T cells (Figure S2A). Thus, despite being positively regulated by PTP inhibition, Foxp3⁺CD4⁺ T cells only represented a small fraction of the enhanced IL-10 production induced by bpV(phen) treatment.

Next, we examined the impact of PTP inhibition on splenic Tr1 cells. The frequency of CD4⁺ T cells expressing both LAG-3 and CD49b (Tr1 cells) increased with infection and was further enhanced by bpV(phen) treatment (Figure 2C,E). Importantly, Tr1 cells accounted for the majority of the IL-10 producing CD4⁺ T cells; greater than 75% of the IL-10⁺CD4⁺ T cells also expressed LAG-3 and CD49b (Figure S2B). Thus, the bpV(phen)-mediated increase in IL-10 production by splenic CD4⁺ T cells is likely the result of the concomitant increase in the frequency of LAG-3⁺CD49b⁺ Tr1 cells.

IFN γ /IL-10 co-producing cells were shown to be the principal source of IL-10 during *P. chabaudi* infection (485), and adoptive transfer of IL-10 producing regulatory B cells has been shown to decrease the incidence of ECM (643), thus we examined the frequency of double positive CD4⁺ T cells and IL-10⁺ B cells. The percentage of IFN γ ⁺IL-10⁺ CD4⁺ T cells increased with infection, but PTP inhibition caused a trend toward a reduction in the frequency of double-producing CD4⁺ T cells in the infected mice, but this difference did not reach statistical significance (Figure S2C). Moreover, infection also increased the production of IL-10 by B cells in the spleen, but PTP inhibition had no effect on the percentage of IL-10⁺ B cells (Figure S2D). Taken together, this data suggests that although *P. berghei* ANKA infection increases the

expression of IL-10 by other cellular sources, IL-10 production by these cell subsets is not positively regulated by PTP inhibition.

IL-10 reduces mortality from P. berghei ANKA infection independently of cerebral pathology

To determine if the bpV(phen)-mediated protection from ECM was IL-10 dependent, IL-10 knock-out mice were treated with bpV(phen) following the same protocol that was used with the wild-type mice. The onset and clinical manifestation of ECM in the untreated wild-type and IL-10 knock-out mice was not significantly different, suggesting that IL-10 does not have an essential role in the development of cerebral pathology during *P. berghei* ANKA infection (Figure 3A; Figure S3A).

bpV(phen)-treated IL-10 knock-out mice were partially protected, with nearly 40% of the mice surviving until 3 weeks post-infection. The parasitemia of the bpV(phen)-treated wild-type and IL-10 knock-out mice was similar until 11 days post-infection; and as the infection progressed, the surviving, bpV(phen)-treated IL-10 knock-out mice demonstrated superior control of their blood parasite levels (Figure 3B). Importantly, the bpV(phen)-treated IL-10 knock-out mice that succumbed to the infection did not present with any of the typical clinical symptoms of cerebral malaria, such as paralysis or coma, but instead developed weakness, hypothermia and pallor (Figure S3B). The absence of cerebral symptoms in the bpV(phen)-treated IL-10 knock-out mice demonstrates that IL-10 is not required to preclude the development of neuropathology following PTP inhibition; however, the increased percentage of IL-10 knock-out mice succumbing to the infection at early time points indicates that IL-10 has a key role in limiting *P. berghei* ANKA-induced pathology.

bpV(phen) and IL-10 attenuate ECM-induced liver injury

In addition to cerebral damage, severe malaria can also present as hyperparasitemia-induced anemia and immune-mediated liver injury. Since the parasitemia of the bpV(phen)-treated IL-10 knock-out mice was similar to the bpV(phen)-treated wild-type mice when they died (days 9 to 12 post-infection), we examined whether IL-10 was involved in controlling liver injury by measuring the serum levels of ALT and AST (Figure 4A,B). Control wild-type and IL-10 knock-out mice were analyzed 7 days post-infection, upon the onset of neurological symptoms in both groups, and the bpV(phen)-treated wild-type and IL-10 knock-out mice were evaluated on day 10 post-infection, when the IL-10 knock-out mice began to develop weakness, pallor and hypothermia. PTP inhibition had no effect on the serum levels of ALT or AST in the uninfected mice. The absence of IL-10 markedly increased liver injury in both the control and bpV(phen)-treated mice, while treatment with bpV(phen) significantly decreased the serum levels of ALT and AST in the IL-10 knock-out mice and further attenuated hepatic pathology in the wild-type mice.

Large parasite burdens were previously associated with liver damage during *P. berghei* ANKA infection (493), and IL-10 has been shown to limit parasite sequestration during ECM (394), therefore we examined liver parasite burden as a possible source of liver damage in our model. The parasite burden was measured as both RLU/mg tissue and total RLU per liver (Figure S4A-D), as the bpV(phen)-treated wild-type and IL-10 knock-out mice had slightly enlarged livers compared to the control mice. Neither bpV(phen) treatment nor the presence of IL-10 affected the liver parasite burden. Moreover, the accumulation of parasites within the liver did not appear to be directly responsible for increased hepatic pathology, but rather occurred subsequent to

cerebral damage. This data demonstrates that PTP inhibition and IL-10 are capable of attenuating liver injury independently of liver parasite burden.

PTP inhibition significantly decreases the brain sequestration of CD4⁺ and CD8⁺ T cells

Sequestration of cytotoxic CD8⁺ T cells within the brain microvasculature is required for the development of neuropathology during *P. berghei* ANKA infection (390,406). Strikingly, bpV(phen) treatment inhibited the infection-induced infiltration of cells into the brain (Figure 5A). The percentage of sequestered cells that were CD4⁺ or CD8⁺ T cells was not affected by bpV(phen), but infection reduced the percentage of CD4⁺ T cells and increased the percentage of CD8⁺ T cells (Figure 5B-5D). Importantly the total number of CD4⁺ and CD8⁺ T cells that accumulated within the brain was markedly decreased by PTP inhibition in the infected mice (Figure 5E,F). These results indicate that PTP inhibition prevents the development of neuropathology by preventing the sequestration of both CD4⁺ and CD8⁺ T cells within the brain.

bpV(phen) decreases CXCR3 expression on splenic T cells

T cell priming occurs in the spleen (394) and the chemokine receptor CXCR3 plays an integral role in T cell migration to the brain during *P. berghei* ANKA infection (442-445). As our data highlighted a near complete reduction in cell sequestration with the brain, we analyzed the splenic CD4⁺ and CD8⁺ T cell populations to determine how PTP inhibition modulated the T cell response during *Plasmodium* infection in order to preclude T cell sequestration within the brain. While infection caused a significant increase in the frequency of CXCR3⁺ CD4⁺ and CD8⁺ T cells in the spleen of control mice, bpV(phen) treatment completely abrogated the upregulation of CXCR3 on T cells following infection (Figure 6A-6D).

PTP inhibition did not affect the activation of splenic CD4⁺ T cells, but the percentage of activated CD8⁺ T cells in the spleen was significantly decreased in the infected, bpV(phen)-treated mice (Figure S5A-D). Consequently, the expression of CXCR3 on activated T cells was examined to determine if the attenuated activation was responsible for the reduced frequency of CXCR3⁺ cells. The percentage of CD62L^{lo}CD44⁺ CD4⁺ and CD8⁺ T cells that expressed CXCR3 was decreased by bpV(phen) treatment in a similar manner to what was observed for total CD4⁺ and CD8⁺ T cells (Figure S6A,B). Thus PTP inhibition is able to decrease the expression of CXCR3 on T cells on both total and activated splenic T cells, suggesting that bpV(phen) decreases the expression of this chemokine receptor independently of T cell activation.

Since PTP inhibition markedly decreased the activation of splenic CD8⁺ T cells, we were interested in determining if bpV(phen) treatment also affected the frequency or total number of antigen-experienced CD8⁺ T cells. We examined the total population of splenic CD8⁺ T cells exhibiting an antigen-experienced phenotype by measuring the percentage of CD8⁺ T cells that were CD11a^{hi}CD8^{lo} at the onset of symptoms in the control mice (644). bpV(phen) did not affect the frequency or total number of antigen-experienced CD8⁺ T cells induced by *P. berghei* ANKA infection (Figure S6C,D). Thus downregulation of CXCR3 expression on both CD4⁺ and CD8⁺ T cells, and the consequent attenuation of T cell chemotaxis to the brain, rather than decreased numbers of responding T cells, appears to be the main mechanism through which PTP inhibition prevents neuropathogenesis.

PTP inhibition prevents CXCR3 upregulation by attenuating TCR signal transduction

Since the attenuated activation of T cells was not responsible for the decreased percentage of CXCR3⁺ T cells, we were interested in identifying the mechanism used by bpV(phen) to prevent the upregulation of this chemokine receptor. Previous studies have demonstrated that CXCR3 induction requires transient TCR stimulation (470), but the subsequent pathways that regulate CXCR3 expression are uncertain. Isolated splenic CD4⁺ and CD8⁺ T cells were stimulated with anti-CD3/anti-CD28 and then allowed to recover in the absence of stimulation to upregulate CXCR3 expression *ex vivo*. bpV(phen) significantly suppressed the induction of CXCR3 on both CD4⁺ and CD8⁺ T cells (Figure 7A-7C). CXCR3 expression was markedly reduced by PTP inhibition when bpV(phen) was present during TCR stimulation, whereas the addition of bpV(phen) during the recovery incubation did not affect the expression of CXCR3 on CD4⁺ T cells and only caused a partial decrease in CXCR3 expression on CD8⁺ T cells (Figure S7A-C).

TCR signal transduction is dependent on the concerted actions of PTKs and PTPs (567). Lck is one of the first kinases recruited upon TCR stimulation, and the activity of this kinase is modulated by the phosphorylation of a negative regulatory tyrosine (Y505) and an opposing positive regulatory tyrosine (Y394). CD45-dependent dephosphorylation of the negative regulatory site is required for efficient TCR-mediated signalling. Following the same stimulation protocol used above, the effect of bpV(phen) on TCR signal transduction was further examined in CD8⁺ T cells. bpV(phen) treatment caused an increase in the phosphorylation of the negative regulatory tyrosine of Lck following CD3 cross-linking (Figure 7D,F). This resulted in a decrease in the phosphorylation of the downstream kinases ERK1/2, with phospho-ERK1/2 being almost entirely lost after 5 minutes of stimulation (Figure 7E,G). Thus, PTP inhibition attenuates the TCR signalling capacity of T cells by preventing the dephosphorylation of the

Y505 residue on Lck, and this decreased signalling is likely responsible for the reduced expression of CXCR3 on T cells.

Discussion

The development of ECM requires the accumulation of cytotoxic CD8⁺ T cells within the brain and dysregulation of the proinflammatory response. bpV(phen) has been shown to modulate the inflammatory response during *Leishmania* infection (593,594), but the impact of PTP inhibition on the T cell response has not previously been investigated. Herein, we demonstrate that bpV(phen) treatment throughout the infection precludes the development of cerebral and hepatic pathology during *P. berghei* ANKA infection and rescues infected animals from ECM-induced mortality. PTP inhibition attenuated cerebral damage by preventing the TCR-dependent upregulation of CXCR3 expression on splenic T cells and reduced liver injury using a mechanism that was independent of liver parasite sequestration.

PTP inhibition prevented the disruption of the BBB and the consequent development of neuropathology by markedly decreasing the sequestration of both CD4⁺ and CD8⁺ T cells within the brain. The chemokine receptor CXCR3 has been shown to play an integral role in the trafficking of pathogenic T cells to the brain during *P. berghei* ANKA infection (442-445). We observed that bpV(phen) treatment significantly reduced the expression of CXCR3 on CD4⁺ and CD8⁺ T cells in the spleen. PTP inhibition attenuated the activation of splenic CD8⁺ T cells, but had no impact on the activation of CD4⁺ T cells, but the percentage of activated T cells that expressed CXCR3 was also reduced by bpV(phen), indicating that PTP inhibition is sufficient to decrease CXCR3 even on activated T cells and that the decreased expression of CXCR3 was not resultant of attenuated T cell activation.

The mechanism used by PTP inhibition to reduce CXCR3 expression was further examined by analyzing the effect of bpV(phen) on isolated splenic T cells. The presence of bpV(phen) during TCR stimulation precluded the initial upregulation of CXCR3 on both CD4⁺ and CD8⁺ T cells. PTP inhibition during the recovery period following stimulation did not affect the expression of CXCR3 on CD4⁺ T cells and had only an intermediate effect on CXCR3 expression on CD8⁺ T cells. These results demonstrate that the underlying mechanisms controlling CXCR3 expression on CD4⁺ and CD8⁺ T cells are differentially regulated by tyrosine phosphorylation. For both cell types, PTP inhibition had the largest impact on CXCR3 expression during TCR stimulation, indicating that bpV(phen) predominately decreases CXCR3 expression by inhibiting a PTP involved in TCR signal transduction. Notably, PTP inhibition during the recovery phase partially decreased CXCR3 expression on CD8⁺ T cells, but the reduction was not synergistic with the decrease caused by bpV(phen) during TCR stimulation. Thus, it appears that CD8⁺ T cells have redundant, PTP-mediated mechanisms that control CXCR3 expression.

Based on the finding that PTP inhibition had the greatest effect on CXCR3 expression during TCR stimulation, the impact of bpV(phen) on TCR signal transduction was further examined. PTP inhibition increased the phosphorylation of the negative regulatory tyrosine of Lck following TCR triggering. The effect of the increased phosphorylation of Lck Y505 on TCR signalling was analyzed by measuring the phosphorylation of the downstream ERK pathway. The phosphorylation of the kinases ERK1/2 were reduced by bpV(phen), with phosphorylation being almost entirely lost 5 minutes after stimulation. Based on these results, bpV(phen) treatment is likely attenuating the TCR signalling capacity of T cells by preventing the dephosphorylation of Lck Y505 and the subsequent activation of this kinase. Dephosphorylation of the negative regulatory site of Lck is controlled by the tyrosine phosphatase CD45 (567), thus

bpV(phen) is presumably precluding the expression of CXCR3 on splenic CD4⁺ and CD8⁺ T cells by inhibiting the activity of this PTP. Nevertheless, bpV(phen) causes a general inhibition of PTP activity, thus further studies will be required to determine whether other PTPs are involved in the pathogenesis of ECM.

In addition to preventing the development of neuropathology, we demonstrated that bpV(phen) is also able to modulate the inflammatory response. CD4⁺ T cells have previously been shown to be the dominant source of IL-10 during both *P. chabaudi* and *P. yoelii* infection (481,485). We found that the frequency of IL-10-producing CD4⁺ T cells was increased by both infection and PTP inhibition. Similar to the non-cerebral malaria infections, the majority of the IL-10⁺CD4⁺ T cells were Foxp3⁻ Tr1 cells. However, the criteria used to designate the regulatory CD4⁺ T cells as Tr1 cells differed between our studies, as the previous work was published before the identification of LAG-3 and CD49b as selective surface markers (640). Following the determination of Tr1 cells as the dominant source of IL-10 induced by bpV(phen) treatment during *P. berghei* ANKA infection, we examined whether IL-10 contributed to the protection afforded by PTP inhibition.

Depletion of the IL-10 receptor (394) and IL-10 deficiency (484) in C57BL/6 mice were previously shown to have little to no effect on the incidence of ECM, and we observed that the control IL-10 knock-out mice were not significantly protected compared to the control wild-type mice. PTP inhibition prevented the development of neuropathology in the IL-10 knock-out mice, evidenced by the lack of cerebral malaria symptoms exhibited by these mice, indicating that bpV(phen)-mediated protection from ECM is not IL-10 dependent. Notably, the bpV(phen)-treated IL-10 knock-out mice that survived past 2 weeks post-infection displayed far superior control of their parasitemia compared to the bpV(phen)-treated wild-type mice. IL-10 knock-out

mice have also been shown to have decreased parasitemia compared to wild-type mice in *P. yoelii* and *P. berghei* NK65 infection (481,492). The decreased parasitemia in these studies correlated with an increased serum concentration of IFN γ (481). IFN γ is critically involved in the induction of ECM (454); thus the prevention of neuropathology by bpV(phen) treatment may have bypassed the IFN γ -mediated pathology of this disease and allowed the increased IFN γ production of the IL-10 knock-out mice to better control their parasitemia.

Approximately two-thirds of the bpV(phen)-treated IL-10 knock-out succumbed to the infection nearly two weeks before the majority of the bpV(phen)-treated wild-type mice. Since the parasitemia of the IL-10 knock-out and wild-type mice was similar during this period of time, the impact of both bpV(phen) and IL-10 on hepatic pathology was analyzed. Both PTP inhibition and the presence of IL-10 were found to reduce liver injury. A previous study associated liver damage with a high liver parasite burden (493). Half of our control wild-type mice were symptomatic on day 7 post-infection, and the onset of neurological symptoms markedly increased the accumulation of parasites within the liver, but had no effect on hepatic pathology. Furthermore the non-symptomatic, control wild-type mice and the bpV(phen)-treated wild-type mice had a similar parasite burden, even though the non-symptomatic, control wild-type mice had increased liver damage. Thus, our results indicate that liver parasite burden is not directly responsible for hepatic pathology.

Furthermore, depletion of the IL-10 receptor was previously linked to increased tissue parasite burden (394), suggesting that IL-10 may limit tissue sequestration. In our study, the presence of IL-10 decreased liver damage, but did not appear to have an effect on the liver parasite burden. There was a slight, but not significant, increase in parasite accumulation in the bpV(phen)-treated IL-10 knock-out mice compared to the bpV(phen)-treated wild-type mice, but this is

likely not caused by the lack of IL-10 production. This assumption is supported by the control mice, as there was no difference in the liver parasite burden between the symptomatic, control wild-type mice and the control IL-10 knock-out (all of which were symptomatic), despite the difference in IL-10 expression. Therefore our results do not indicate that the presence of IL-10 decreases the sequestration of parasites in the liver. Furthermore, the liver parasite burden in control wild-type mice increased significantly upon the onset of symptoms, suggesting that parasite sequestration within this organ is dependent on the onset of cerebral pathology.

While ECM and human cerebral malaria share similar pathological mechanisms, the role of CD8⁺ T cells in the human disease remains indeterminate. A pathological role for CD8⁺ T cells has often been disregarded based on their paucity in human cerebral malaria (265); however, intravascular CD8⁺ T cells are also difficult to identify in murine brains (390,402). Moreover, resistance to severe malaria in humans has been linked to certain human leukocyte antigen class I alleles (403) and the expression of CXCL10, a chemokine for CXCR3, has been linked to disease severity (258,259). Thus, the data support the possibility that CD8⁺ T cells may contribute to pathology in human cerebral malaria and warrant further investigation.

Overall, our study supports earlier work which demonstrated that hepatic pathology also occurs in the *P. berghei* ANKA model and that liver injury is independent of cerebral pathology. However, we found that liver damage did not correlate with a high parasite burden and that the presence of IL-10 did not limit liver parasite burden. Moreover, our results also support the crucial role of CXCR3 and the consequent brain sequestration of T cells in the development of neuropathology. The factors influencing the expression of CXCR3 remain poorly defined, particularly during infection. We determined that T cell-intrinsic PTP(s) are critically involved in the initial upregulation of CXCR3 on T cells in ECM, and that PTP inhibition was sufficient to

prevent the sequestration of pathogenic T cells within the brain. Recently, increased systemic iron levels were also shown to prevent the development of ECM by modulating the chemotactic T cell response (638). Elevated iron levels decreased CXCR3 expression only on CD4⁺ T cells by interfering with IFN γ signalling (638), in contrast to PTP inhibition, which reduced CXCR3 expression on both CD4⁺ and CD8⁺ T cells, likely through the modulation of TCR signal transduction.

In conclusion, we have established that regulation of tyrosine phosphorylation plays an essential role in both hepatic and cerebral pathology during *P. berghei* ANKA infection and that an improved understanding of PTP regulation and that further characterization of the specific PTPs that contribute to the pathogenesis of ECM may be beneficial to the design of novel immunotherapies for malaria. Moreover, a better understanding of the factors influencing CXCR3 expression would likely also be advantageous for other CXCR3-mediated diseases, such as graft-versus-host disease, rheumatoid arthritis and multiple sclerosis (645-650).

Materials and Methods

Mice

C57BL/6 mice (6-8 weeks old) were purchased from Charles River Laboratories and IL-10 knock-out mice on a C57BL/6 background (6-8 weeks) were purchased from The Jackson Laboratory. All mice were maintained under specific pathogen-free conditions. All research involving mice was carried out according to the regulations of the Canadian Council of Animal Care and was approved by the McGill University Animal Care Committee under ethics protocol number 5925 and the Research Institute of the McGill University Health Centre Animal Care Committee under ethics protocol number 7607. Mice were euthanized at established humane

endpoints using CO₂ asphyxiation followed by cervical dislocation or by using isoflurane if perfusion was performed.

Parasites and infection

In all experiments, red blood cells infected with *P. berghei* ANKA parasites expressing a GFP-luciferase fusion protein were used (Malaria Research and Reference Reagent Resource Center). Wild-type and IL-10 knock-out C57BL/6 mice were infected by i.p. inoculation of 10⁴ infected red blood cells. In all experiments mice received either PBS or 1.5 μmol/18g body weight of bpV(phen) daily from 3 days before to 12 days after parasite inoculation (infected groups) or mock infection (uninfected groups), or up until the experimental endpoint (day 7 or 10 post-infection), by subcutaneous injection. Starting on day 3 post-infection of all survival experiments, tail-vein blood was collected daily. Blood smears were stained with Diff-Quik, and parasitemia was determined by counting at least 500 cells.

BBB integrity analysis

Mice were i.p. injected with 0.3 mL of 2% EB (Sigma-Aldrich). The mice were sacrificed 2 h thereafter, without perfusion, and brains were weighed and placed in formamide (Sigma-Aldrich) for 48 h at 37 °C to extract the dye. Absorbance was measured at 620nm. The concentration of EB in the brain was calculated using a standard curve prepared with known concentrations of EB in formamide.

Flow cytometric analysis of the brain

Brains were digested in RPMI containing 1.6mg/mL collagenase (type IV; Sigma-Aldrich) and 200 μg/mL DNase I (Sigma-Aldrich) at 37°C for 50 min. Cells were isolated using a Percoll

gradient (GE Healthcare) and debris was filtered out using a 70µm nylon mesh. Cells were counted and labelled with LIVE/DEAD amine-reactive violet viability marker according to the manufacturer's protocol (Invitrogen). Cells were labeled with FITC anti-CD45 (eBioscience; 30-F11), PE anti-CD11b (BD Pharmingen; M1/70), PerCP-Cy5.5 anti-CD4 (eBioscience; RM4-5) and APC-eFluor780 anti-CD8 (eBioscience; 53-6.7). Flow cytometry was performed using a BD LSR Fortessa and results were analyzed using FlowJo version 9.6.2. Mice were perfused for the analysis of brain sequestered cells.

Flow cytometric analysis of the spleen

Splenocytes were isolated and erythrocytes were lysed in Tris-NH₄Cl buffer. To analyze cytokine production by T cells, isolated splenocytes were stimulated with 50ng/mL PMA and 500ng/mL ionomycin for 5 h at 37°C. Brefeldin A (eBioscience) was added for the entire duration of the experiment. For the analysis of cytokine production by B cells, isolated splenocytes were stimulated with 50ng/mL PMA, 500ng/mL ionomycin and 10µg/mL LPS (Sigma) for 5 h at 37°C. Monensin (eBioscience) was added for the entire duration of the experiment. *Ex vivo* stimulation was performed in IMDM supplemented with 10% FBS (Invitrogen), 100 U/mL penicillin, 100 µg/mL streptomycin and 2 mM L-glutamine (Wisent), and 50 µM 2β-mercaptoethanol (Sigma-Aldrich). Cells were counted and labelled with PerCP-Cy5.5 anti-CD4 (eBioscience; RM4-5), APC-eFluor780 anti-CD8 (eBioscience; 53-6.7), APC anti-CXCR3 (eBioscience; CXCR3-173), FITC anti-CD62L (eBioscience; MEL-14), PE-Cy7 anti-CD44 (eBioscience; IM7), FITC anti-IL-10 (BD Pharmingen, JES5-16E3), BV785 anti-IFNγ (BioLegend; XMG1.2), PE anti-CD223 (LAG-3) (eBioscience; eBioC9B7W), APC anti-Foxp3 (eBioscience; FJK-16s), eFluor 450 anti-CD49b (integrin α2; DX5), and PE anti-CD19

(eBioscience; eBio1D3). Flow cytometry was performed using a BD LSR Fortessa and a BD FACSCanto II and results were analyzed using FlowJo version 9.6.2.

Ex vivo induction of CXCR3 on splenic T cells

CD4⁺ and CD8⁺ T cells were isolated from total splenocytes using the EasySepTM Mouse CD4⁺ T Cell Isolation Kit and the EasySepTM Mouse CD8⁺ T cell Isolation Kit, respectively, according to the manufacturer's protocol (Stemcell). 5 µg/mL anti-CD3 (eBioscience; 145-2C11) and 2 µg/mL anti-CD28 (eBioscience; 37.51) were co-immobilized on 24-well plates overnight at 4°C and wells were washed 3 times with PBS prior to T cell stimulation. 1.5 x 10⁶ CD4⁺ or CD8⁺ T cells were incubated at 37°C for 48 h in RPMI supplemented with 10% FBS (Invitrogen/Wisent), 100 U/mL penicillin, 100 µg/mL streptomycin and 2 mM L-glutamine (Wisent/Sigma), with or without 1 µM bpV(phen). Cells were collected and incubated for an additional 24 h in the absence of anti-CD3 and anti-CD28 in RPMI with or without 1 µM bpV(phen). Cells were counted and labelled with PerCP-Cy5.5 anti-CD4 (eBioscience; RM4-5), APC-eFluor780 anti-CD8 (eBioscience; 53-6.7), and APC anti-CXCR3 (eBioscience; CXCR3-173). Flow cytometry was performed using a BD LSR Fortessa and results were analyzed using FlowJo version 9.6.2.

CD3 cross-linking of splenic CD8 T cells

Splenic CD8⁺ T cells were isolated as described above and 2.0-10.0 x 10⁶ CD8⁺ T cells were stimulated on 6-well plates using the same protocol that was utilized for the *ex vivo* induction of CXCR3 on splenic T cells. 0.5-10.0 x 10⁶ cells were incubated on ice with 10 µg/mL biotinylated CD3 (eBioscience; 145-2C11) and cross-linked with streptavidin for the indicated times at 37°C. Cells were washed with ice cold PBS and lysed in NP40 buffer (20 mM HEPES, pH 7.9; 100 mM NaCl; 5 mM EDTA; 0.5 mM CaCl₂; 1% Nonidet p-40; 1mM PMSF; 10 µg/mL

leupeptin; 5 µg/mL pepstatin; and 1 mM Na₃VO₄). 5-15 µg of protein was resolved by SDS-PAGE, transferred to a methanol-activated PVDF membrane, and probed with antibodies as indicated. Antibodies were detected with goat anti-rabbit conjugated to horseradish peroxidase (Santa Cruz; sc-2054) and HyGlo (Denville Scientific). Images were quantified with ImageJ software. Phosphorylation quantification is presented as the ratio of signal intensity of the phosphorylated protein of interest to the signal intensity of total protein, and was normalized to the maximal phosphorylation.

Quantification of alanine and aspartate transferase

Blood samples were collected by cardiac puncture and the serum samples were analyzed by the McGill University Comparative Medicine and Animal Resources Centre.

Quantification of liver parasite burden

Pieces of liver were homogenized in PBS containing 0.1mg/mL aprotinin (Roche), 0.05mg/mL leupeptin (Roche) and 1X Firefly lysis buffer using a PRO200 Hand-held Homogenizer (Harvard Apparatus Canada), and lysed on ice. The homogenate was centrifuged at 13,000 rpm for 30 min and the luciferase activity of the supernatant was measured using the Firefly Luciferase Assay Kit (Biotium, Inc.), according to the manufacturer's protocol.

Statistical analysis

Statistical analyses were performed using the unpaired Student's *t*-test (two-tailed) or one-way ANOVA and Tukey's multiple comparisons test. Error bars represent S.E.M. The log-rank test was used for all experiments in which survival was assessed as an endpoint. The data were analyzed using GraphPad Prism software.

Acknowledgements

We thank the McGill University Flow Cytometry and Cell Sorting Facility, the Research Institute of the McGill University Health Centre Immunophenotyping Platform, and the McGill University Comparative Medicine and Animal Resources Centre.

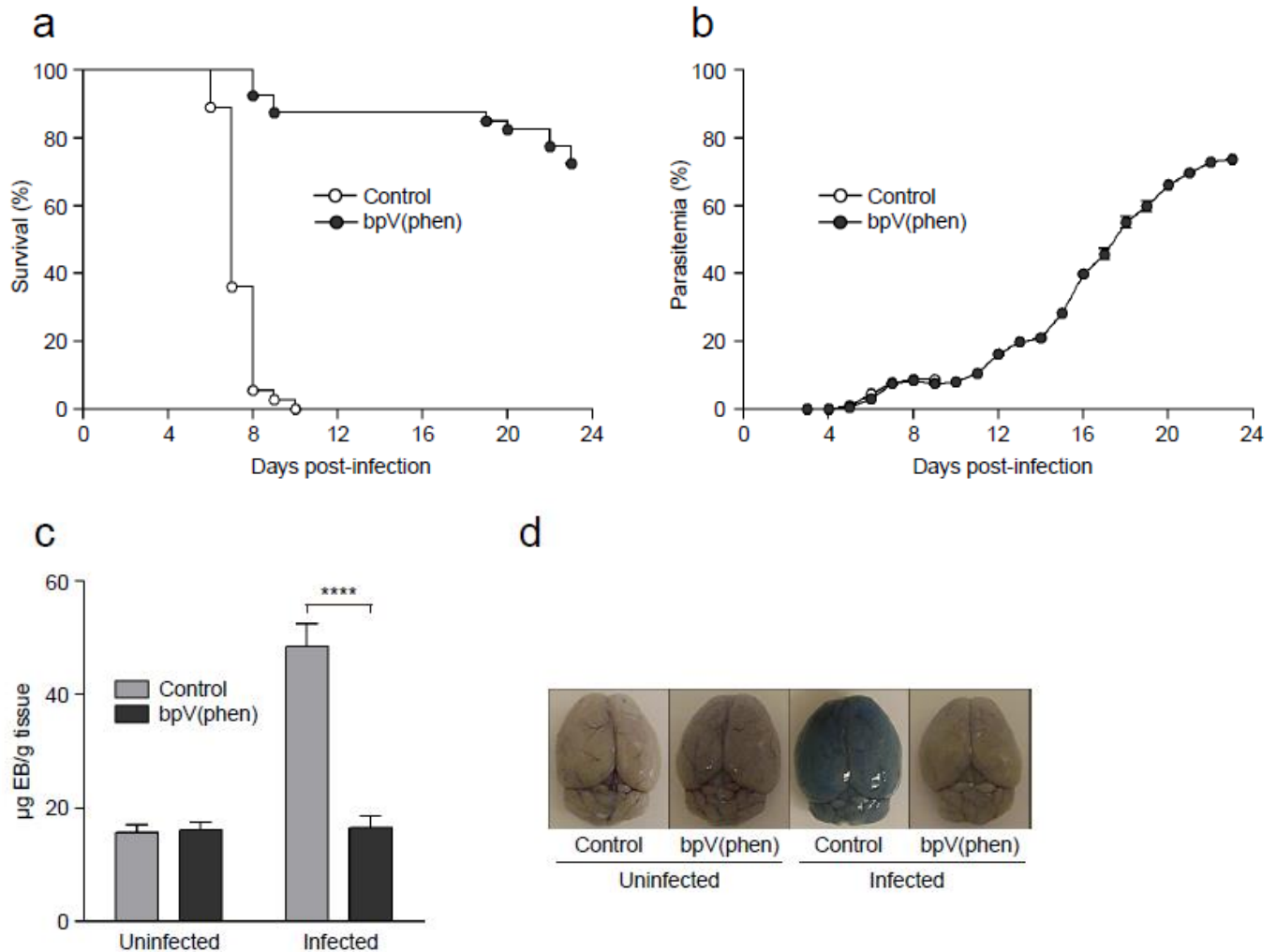


Figure 1. PTP inhibition prevents the development of ECM. (A) Survival and (B) parasitemia of bpV(phen)-treated mice infected with *P. berghei* ANKA, (C) graph of EB accumulation within the brain and (D) representative picture of EB-stained brains. For survival and parasitemia, the cumulative average of six independent experiments is shown. $n = 36$ for control mice and $n = 40$ for bpV(phen)-treated mice. $P < 0.0001$ using the log-rank test. EB assay was performed on day 7 post-infection. $n = 5$ for uninfected, control mice, $n = 4$ for uninfected, bpV(phen)-treated mice, $n = 7$ for infected, control mice and $n = 5$ for infected, bpV(phen)-treated mice for the EB assay. **** $P < 0.0001$ using a one-way ANOVA and Tukey's multiple comparisons test.

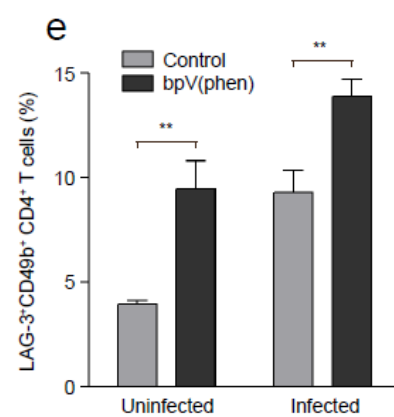
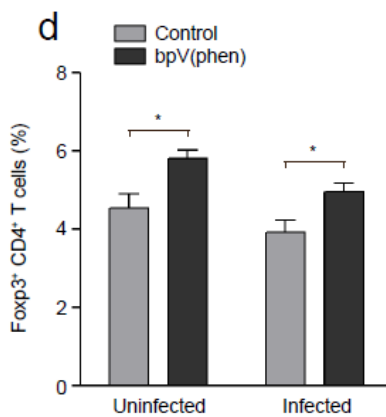
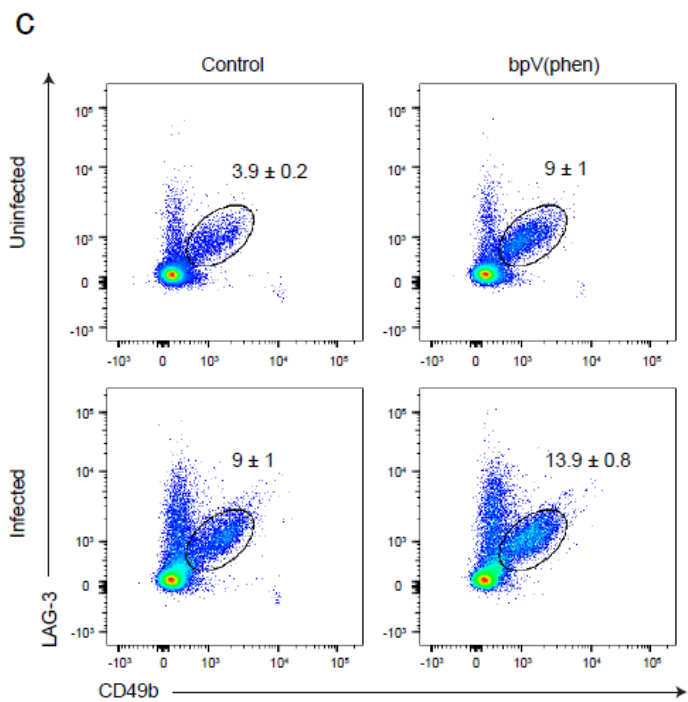
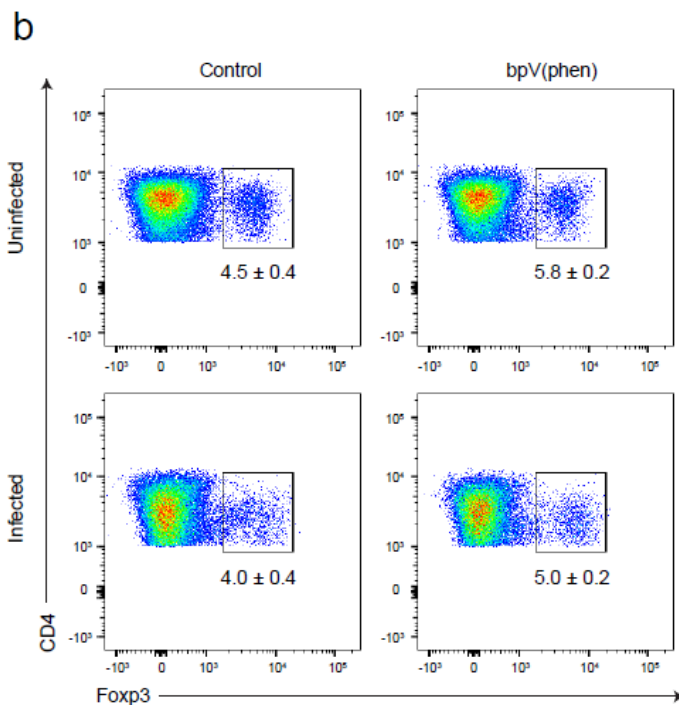
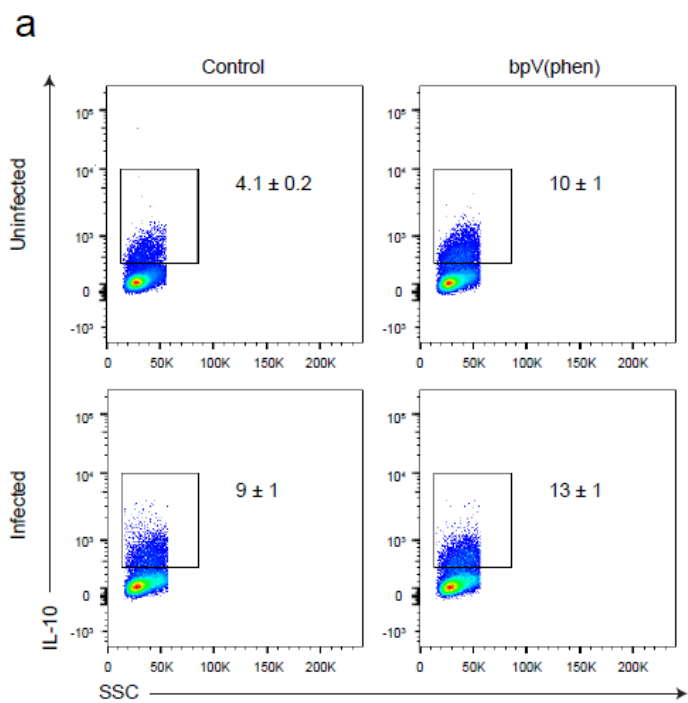


Figure 2. bpV(phen) treatment increases the frequency of regulatory CD4⁺ T cells in the spleen. Representative flow cytometry plots of (A) IL-10⁺ CD4⁺ T cells, (B) Foxp3⁺ and (C) LAG-3⁺CD49b⁺ CD4⁺ T cells, and the percentage of (D) Foxp3⁺ and (E) LAG-3⁺CD49b⁺ CD4⁺ T cells measured on day 7 post-infection after PMA/ionomycin stimulation. The numbers shown on the flow cytometry plots indicate the mean percentage of cells inside the gate ± S.E.M. The cumulative average of 2 independent experiments is shown. *n* = 9 for uninfected, control mice, *n* = 9 for uninfected, bpV(phen)-treated mice, *n* = 11 for infected, control mice, and *n* = 11 for infected, bpV(phen)-treated mice. For the IL-10⁺CD4⁺ T cells, *P* = 0.0047 for the uninfected control and bpV(phen)-treated mice, and *P* = 0.0263 of the infected control and bpV(phen)-treated mice. * *P* < 0.05 and ** *P* < 0.01. Statistical significance was determined using a one-way ANOVA and Tukey's multiple comparisons test.

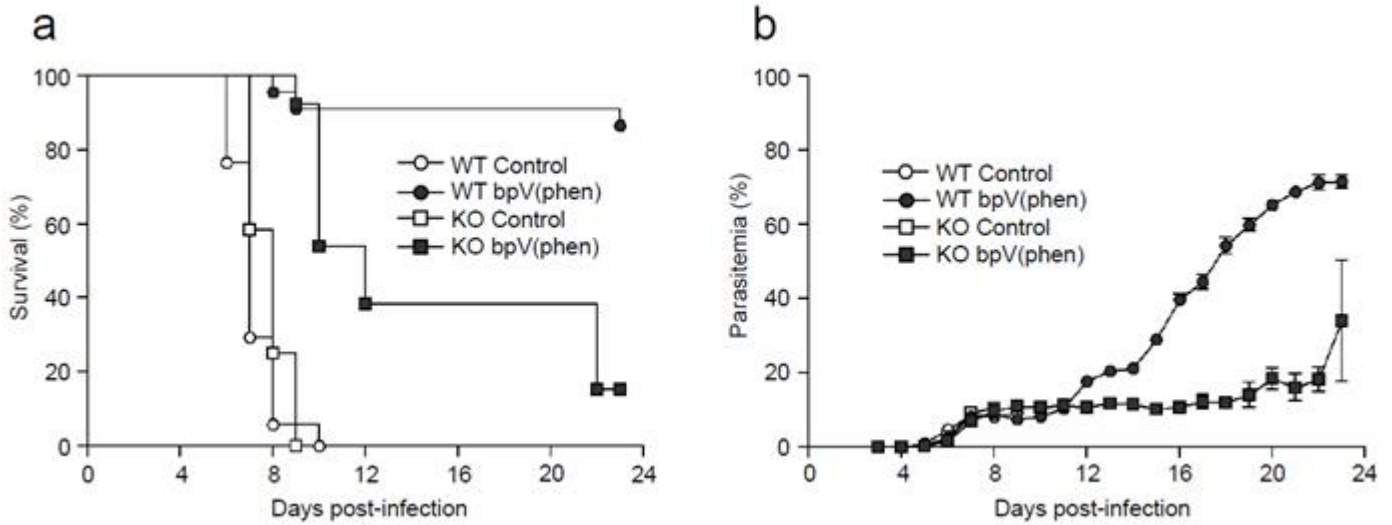


Figure 3. PTP Inhibition Partially Protects IL-10 Knock-out Mice from *P. berghei* ANKA Infection.

(A) Survival and (B) parasitemia graph of bpV(phen)-treated wild-type and IL-10 knock-out mice infected with *P. berghei* ANKA. The cumulative average of 4 independent experiments is shown. $n = 17$ for control, wild-type mice, $n = 22$ for bpV(phen)-treated, wild-type mice, $n = 12$ for control, IL-10 knock-out mice and $n = 13$ for bpV(phen)-treated, IL-10 knock-out mice. For bpV(phen)-treated, wild-type mice versus bpV(phen)-treated IL-10 knock-out mice, $P < 0.0001$, and for control, IL-10 knock-out mice versus bpV(phen)-treated IL-10 knock-out mice, $P < 0.0001$, using the log-rank test.

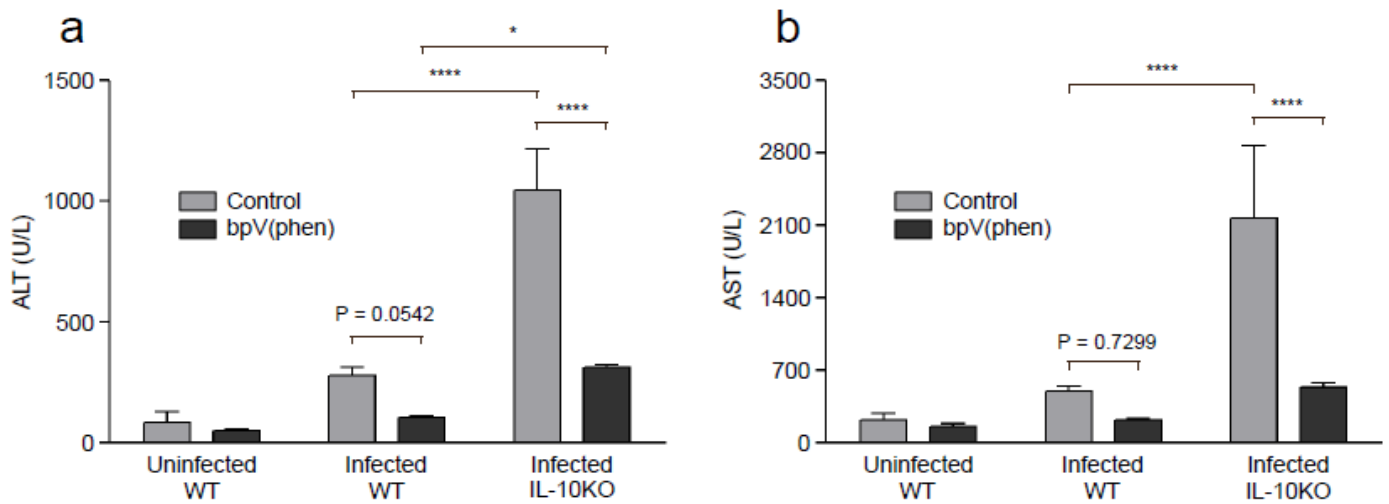


Figure 4. bpV(phen) treatment and IL-10 mitigate ECM-induced liver damage. Serum levels of (A) ALT and (B) AST measured on day 7 (control wild-type and IL-10 knock-out mice) and day 10 (bpV(phen)-treated wild-type and IL-10 knock-out mice) post-infection. $n = 5$ for control, wild-type mice, $n = 8$ for bpV(phen)-treated, wild-type mice, $n = 4$ for control, IL-10 knock-out mice and $n = 4$ for bpV(phen)-treated, IL-10 knock-out mice. * $P < 0.05$ and **** $P < 0.0001$ using a one-way ANOVA and Tukey's multiple comparisons test.

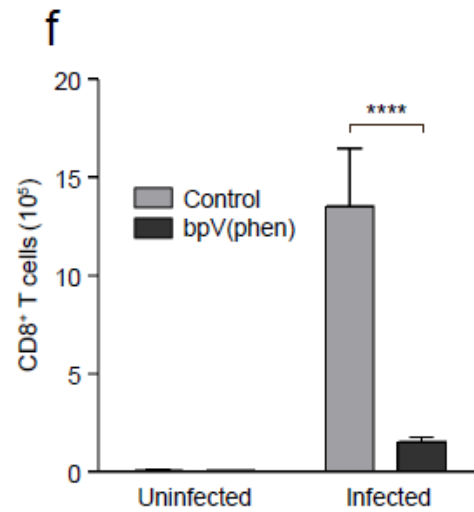
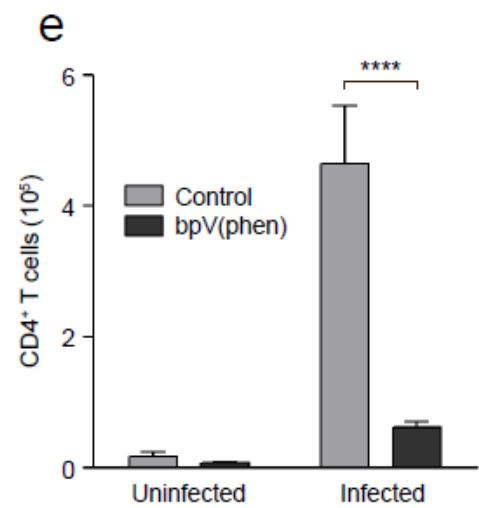
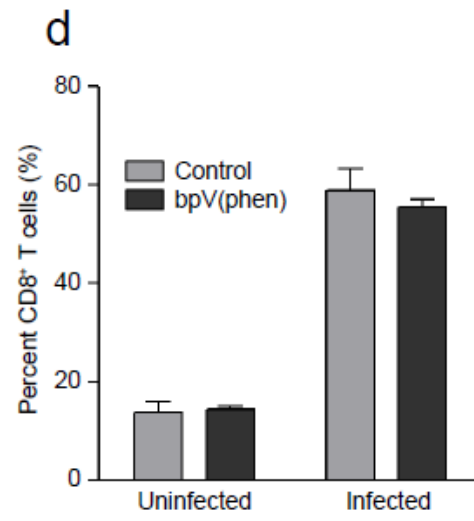
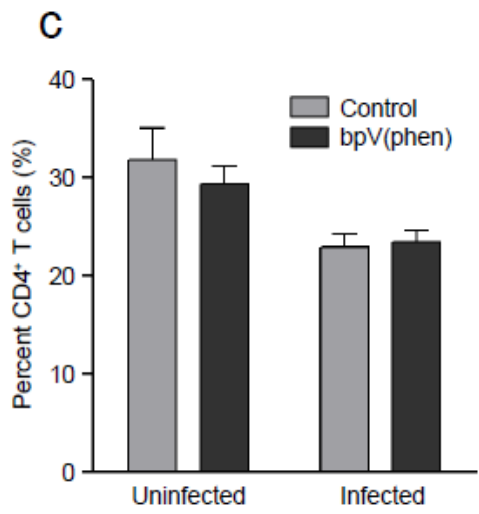
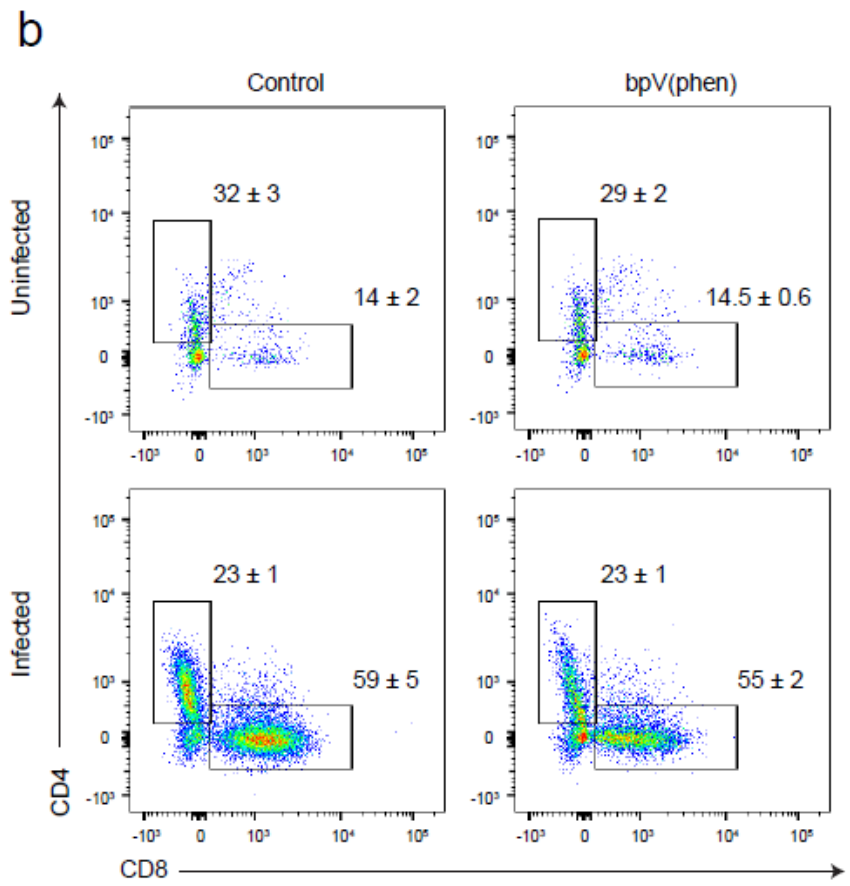
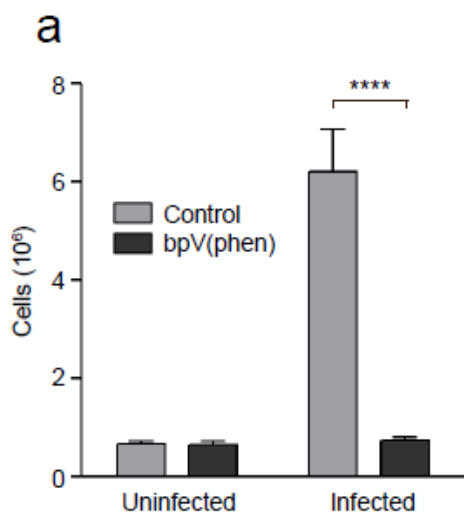


Figure 5. PTP inhibition prevents the brain sequestration of CD4⁺ and CD8⁺ T cells. (A) Total cells sequestered in the brain, (B) representative flow cytometry plots of CD4⁺ and CD8⁺ T cells, percentage of brain-infiltrating leukocytes that are (C) CD4⁺ T cells and (D) CD8⁺ T cells, and total brain-sequestered (E) CD4⁺ T cells and (F) CD8⁺ T cells measured on day 7 post-infection. Infiltrating leukocytes are defined as CD11b^{lo-hi}CD45⁺ cells. The numbers shown on the flow cytometry plots indicate the mean percentage of cells inside the gate \pm S.E.M. $n = 5$ for uninfected, control mice, $n = 5$ for uninfected, bpV(phen)-treated mice, $n = 5$ for infected, control mice and $n = 8$ for infected, bpV(phen)-treated mice. **** P < 0.0001 using a one-way ANOVA and Tukey's multiple comparisons test.

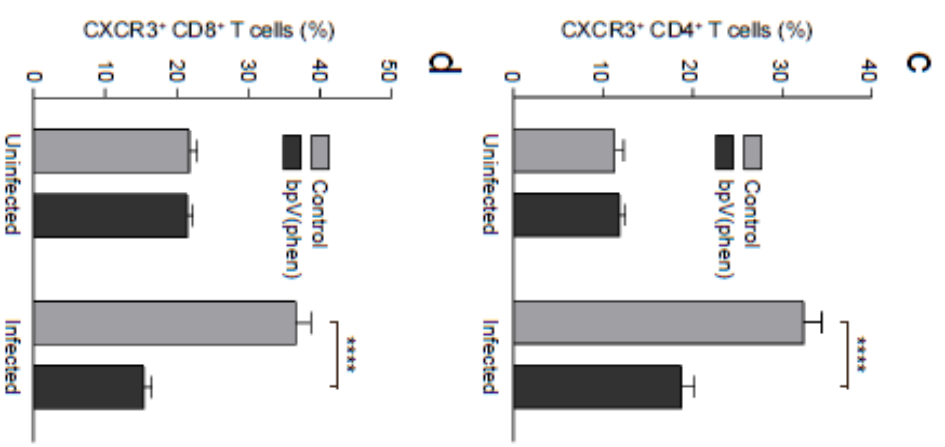
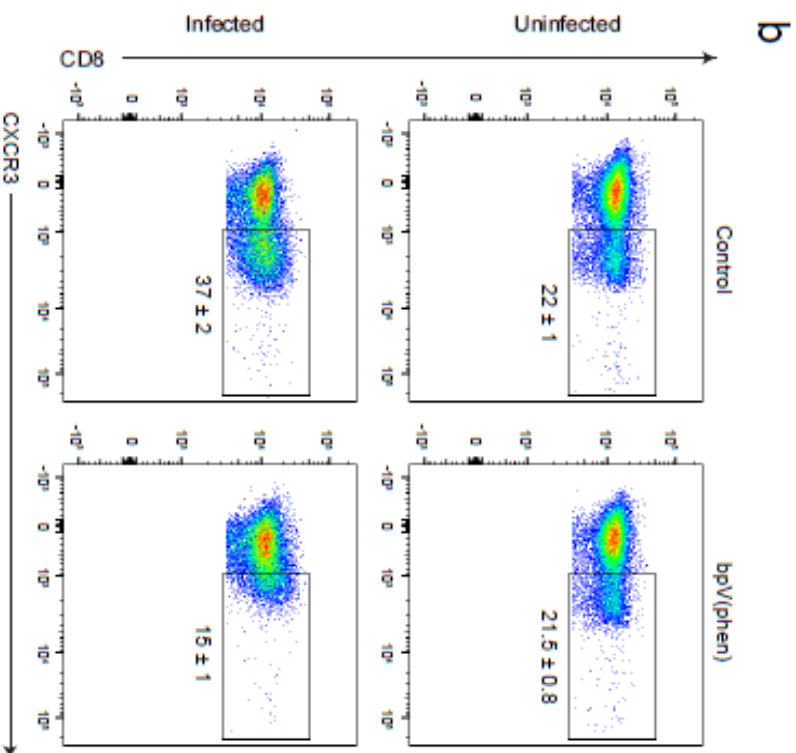
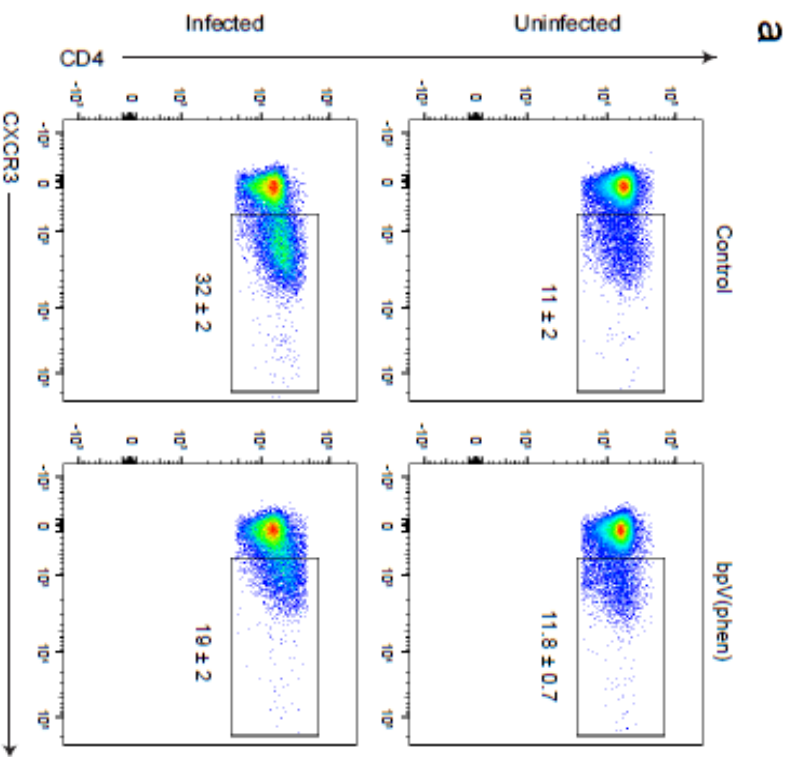


Figure 6. bpV(phen) treatment attenuates the expression of CXCR3 on splenic CD4⁺ and CD8⁺ T cells. Representative flow cytometry plots of CXCR3⁺ (A) CD4⁺ and (B) CD8⁺ T cells, and the percentage of CXCR3⁺ (C) CD4⁺ and (D) CD8⁺ T cells measured on day 7 post-infection. The numbers shown on the flow cytometry plots indicate the mean percentage of cells inside the gate ± S.E.M. The cumulative average of 2 independent experiments is shown. $n = 9$ for uninfected, control mice, $n = 10$ for uninfected, bpV(phen)-treated mice, $n = 9$ for infected, control mice, and $n = 9$ for infected, bpV(phen)-treated mice. **** $P < 0.0001$ using a one-way ANOVA and Tukey's multiple comparisons test.

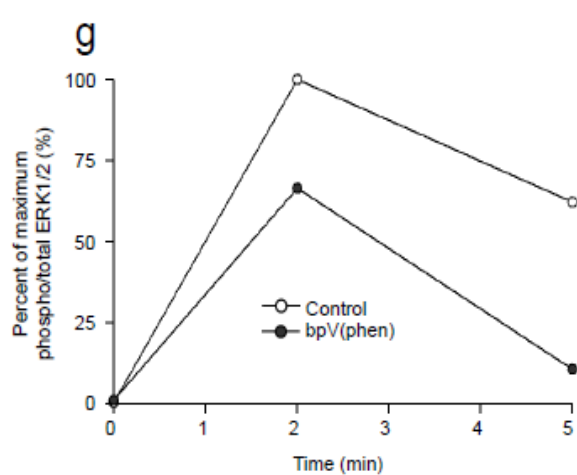
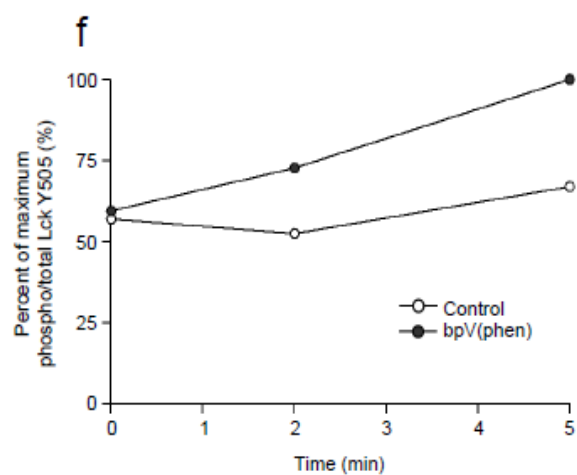
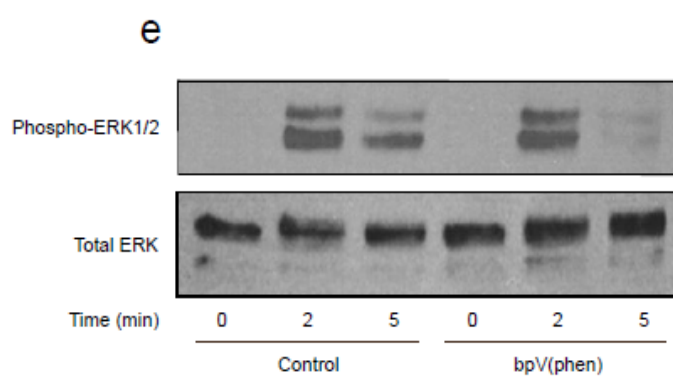
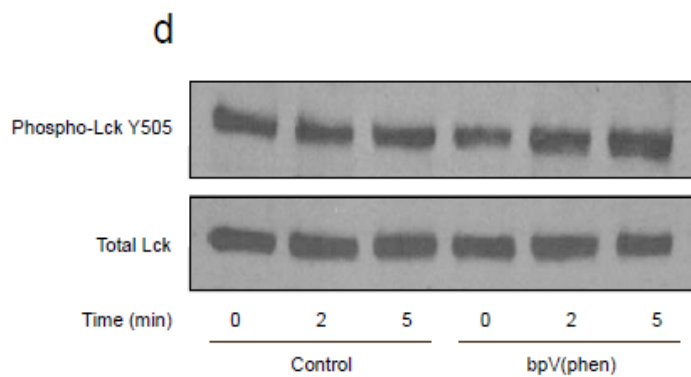
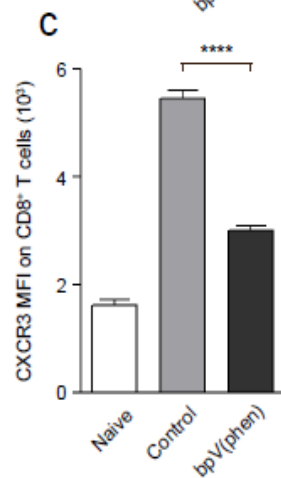
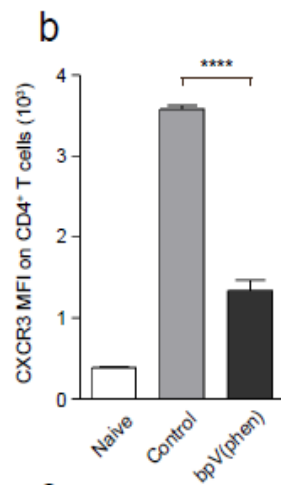
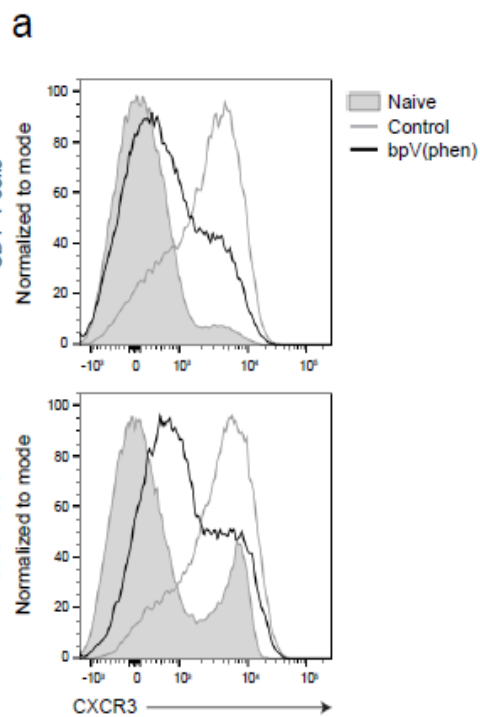
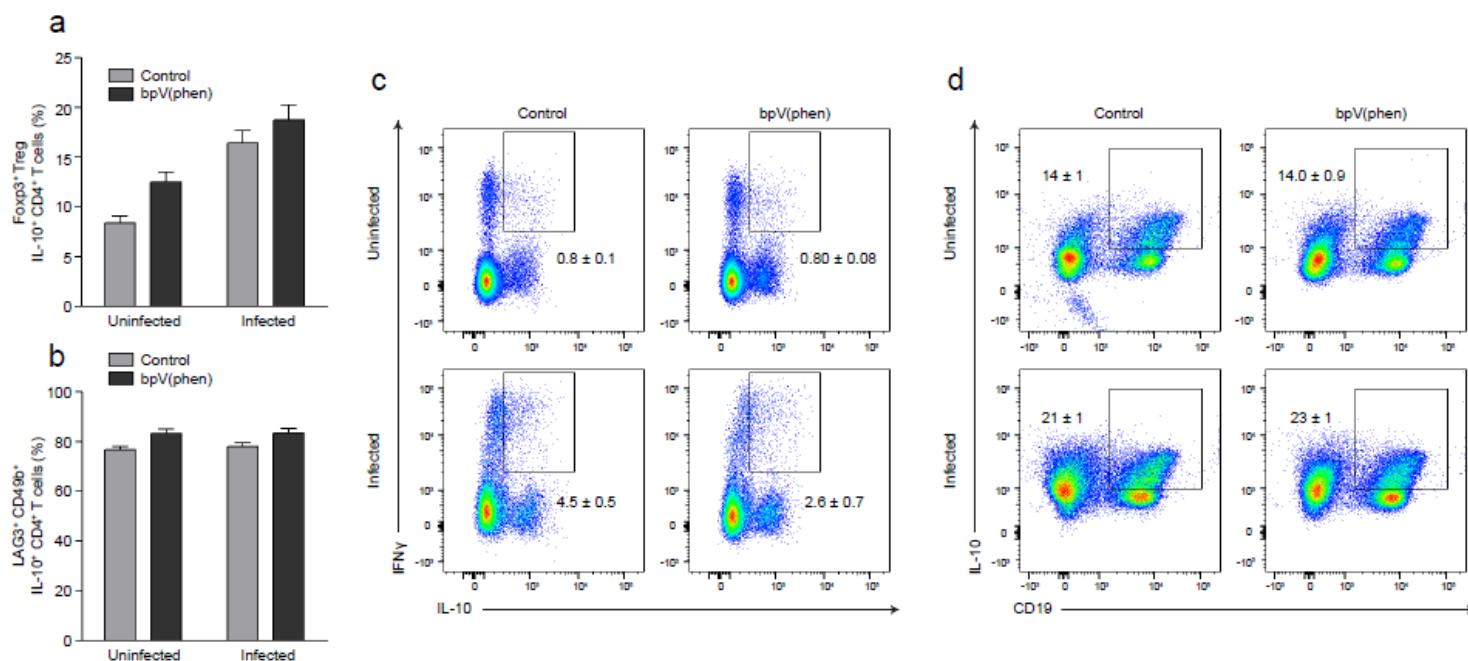
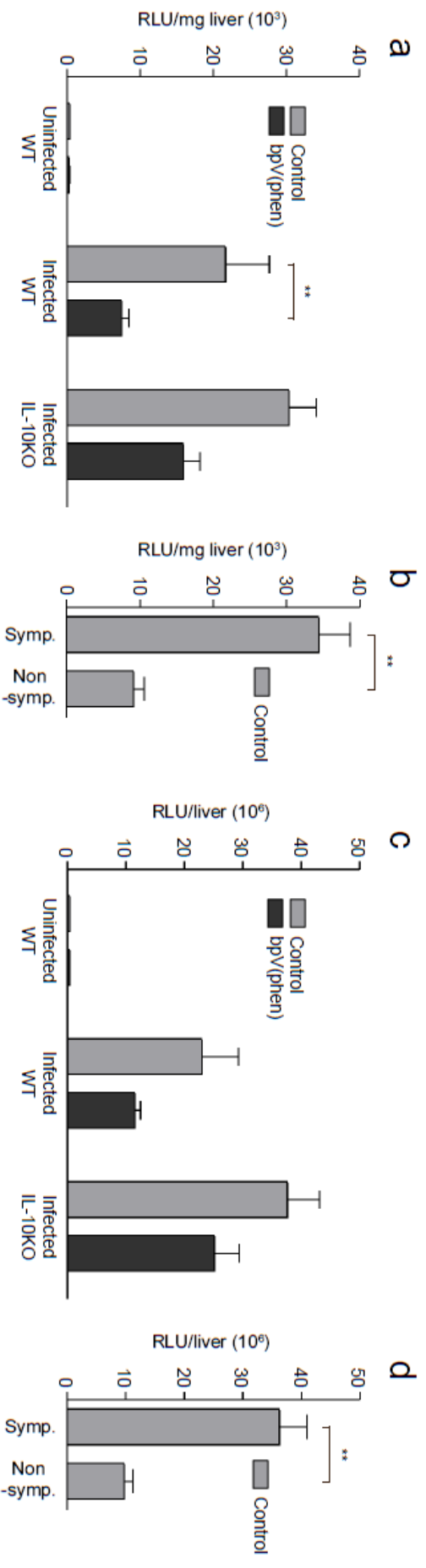


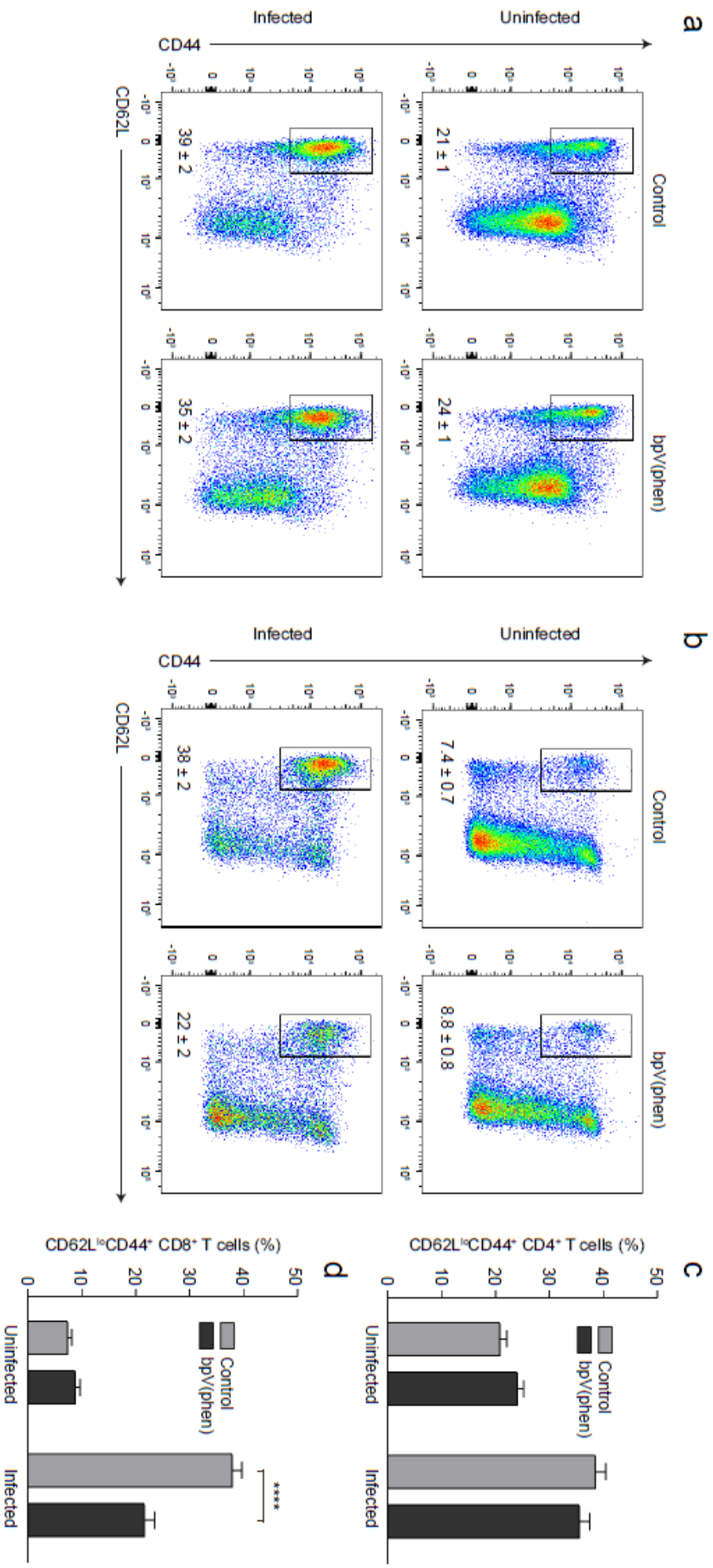
Figure 7. PTP inhibition prevents the upregulation of CXCR3 and attenuates TCR-mediated signalling in splenic T cells. (A) Representative histograms of CXCR3 expression on bpV(phen)-treated CD4⁺ and CD8⁺ T cells and the MFI of CXCR3 on bpV(phen)-treated (B) CD4⁺ and (C) CD8⁺ T cells following anti-CD3/anti-CD28 stimulation. **** P < 0.0001 using a one-way ANOVA and Tukey's multiple comparisons test. The cumulative average of 3 independent experiments is shown. Representative western blots of (D) phospho- and total Lck Y505 and (E) phospho- and total ERK1/2, and densitometry graphs of (F) phospho-LckY505 and (G) phospho-ERK1/2. The western blots and densitometry graphs are representative of 3 independent experiments.



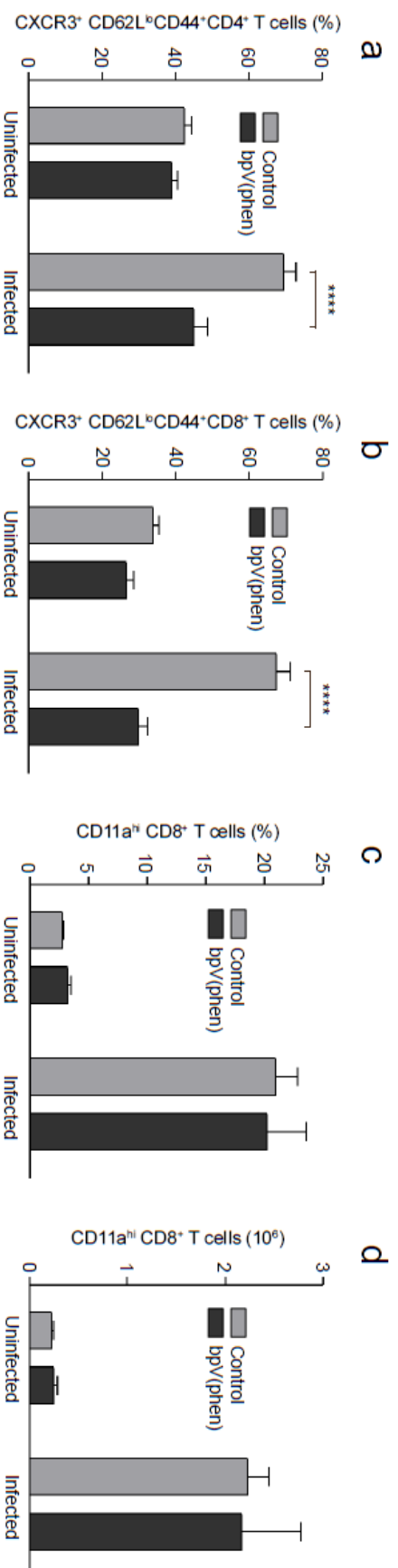
Supplementary Figure S2. IL-10 production by CD4⁺ T cells and B cells. Percentage of IL-10⁺ CD4⁺ T cells that (A) Foxp3⁺ and (B) LAG3⁺CD49⁺, and representative flow cytometry plots of (C) IFNγ⁺IL-10⁺ CD4⁺ T cells measured on day 7 post-infection after PMA/ionomycin stimulation. Representative flow cytometry plots of (D) IL-10⁺ B cells measured on day 7 post-infection after PMA/ionomycin/LPS stimulation. The numbers shown on the flow cytometry plots indicate the mean percentage of cells inside the gate ± S.E.M. For the graphs, the cumulative average of 2 independent experiments is shown; *n* = 9 for uninfected, control mice, *n* = 9 for uninfected, bpV(phen)-treated mice, *n* = 11 for infected, control mice, and *n* = 11 for infected, bpV(phen)-treated mice. For the IFNγ⁺IL-10⁺ CD4⁺ T cells, *n* = 5 for uninfected, control mice, *n* = 4 for uninfected, bpV(phen)-treated mice, *n* = 5 for infected, control mice, and *n* = 4 for infected, bpV(phen)-treated mice. For the IL-10⁺CD19⁺ cells, *n* = 5 for all groups.



Supplementary Figure S4. Liver parasite load is dependent on the onset of cerebral symptoms. **(A)** RLU per milligram of liver of wild-type and IL-10 knock-out mice and **(B)** RLU per milligram of liver of symptomatic and non-symptomatic control, wild-type mice. **(C)** Total liver RLU of wild-type and IL-10 knock-out mice and **(D)** total liver RLU of symptomatic and non-symptomatic control, wild-type mice. Liver parasite burden was measured on day 7 (control wild-type and IL-10 knock-out mice) and day 10 (bpV(phen)-treated wild-type and IL-10 knock-out mice) post-infection. ** $P < 0.01$ using a one-way ANOVA and Tukey's multiple comparisons test **(A)** and using the unpaired t-test **(B and D)**. $n = 5$ for control, wild-type mice, $n = 8$ for bpV(phen)-treated, wild-type mice, $n = 4$ for control, IL-10 knock-out mice and $n = 4$ for bpV(phen)-treated, IL-10 knock-out mice.

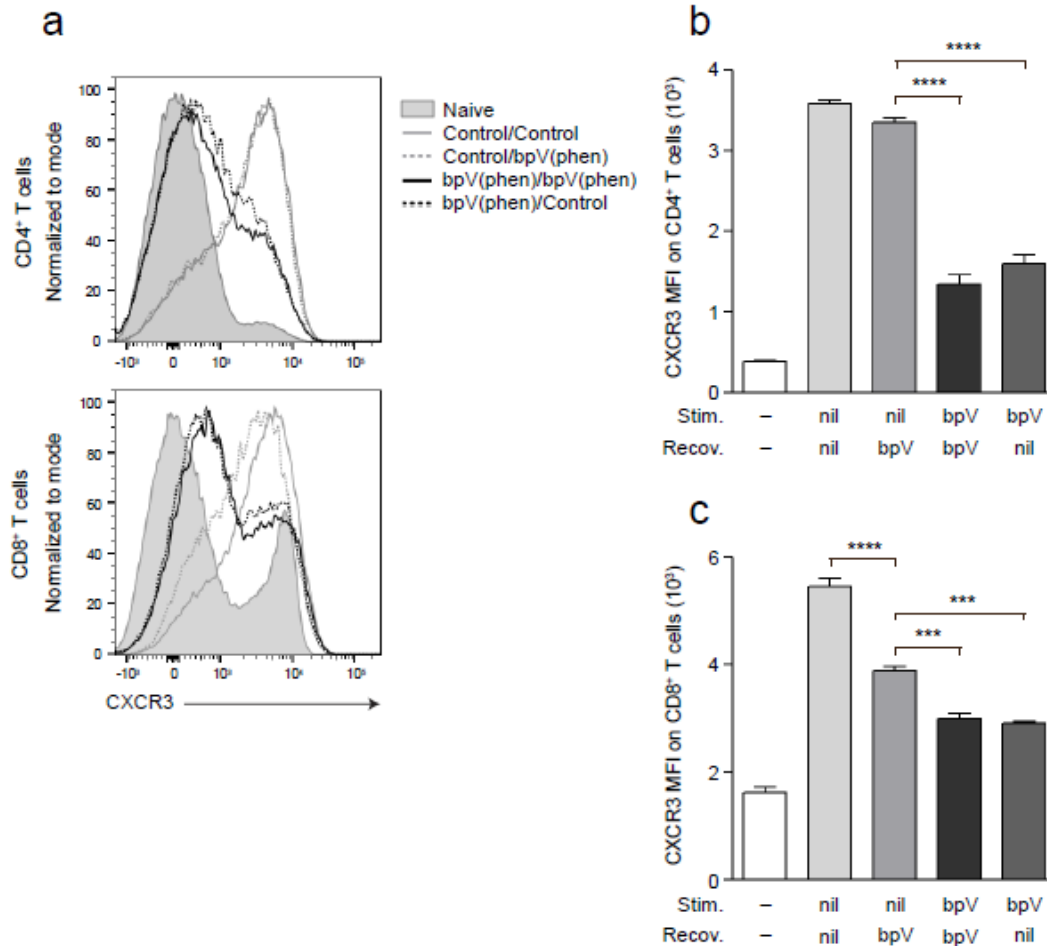


Supplementary Figure S5. PTP inhibition decreases the activation of splenic CD8⁺ T cells. Representative flow cytometry plots of CD62L^{lo}CD44⁺ (A) CD4⁺ T cells and (B) CD8⁺ T cells, and the percentage of CD62L^{lo}CD44⁺ (C) CD4⁺ T cells and (D) CD8⁺ T cells measured on day 7 post-infection. The numbers shown on the flow cytometry plots indicate the mean percentage of cells inside the gate ± S.E.M. The cumulative average of 2 independent experiments is shown. $n = 9$ for uninfected, control mice, $n = 10$ for uninfected, bpV(phen)-treated mice, $n = 9$ for infected, control mice, and $n = 9$ for infected, bpV(phen)-treated mice. **** $P < 0.0001$ for the percentage of CD62L^{lo}CD44⁺CD8⁺ T cells using a one-way ANOVA and Tukey's multiple comparisons test.



Supplementary Figure S6. bpV(phen) decreases CXCR3 on activated T cells, but does not affect the antigen experience of CD8⁺

T cells. The percentage of CXCR3⁺ CD62L^{lo}CD44⁺ CD4⁺ T cells and **(B)** CD8⁺ T cells, and the **(C)** percentage and **(D)** total number of antigen-experienced (CD11a^{Hi}CD8⁺) CD8⁺ T cells measured on day 7 post-infection. The cumulative average of 2 independent experiments is shown; $n = 9$ for uninfected, control mice, $n = 10$ for uninfected, bpV(phen)-treated mice, $n = 9$ for infected, control mice, and $n = 9$ for infected, bpV(phen)-treated mice (A and B), $n = 6$ for uninfected, control mice, $n = 6$ for uninfected, bpV(phen)-treated mice, $n = 11$ for infected, control mice, and $n = 7$ for infected, bpV(phen)-treated mice (C and D). **** $P < 0.0001$ using a one-way ANOVA and Tukey's multiple comparisons test.



Supplementary Figure 7. PTP inhibition attenuates CXCR3 expression to a greater extent during stimulation compared to recovery. (A) Representative histograms of CXCR3 expression on bpV(phen)-treated CD4⁺ and CD8⁺ T cells following anti-CD3/anti-CD28 stimulation, and the mean fluorescence intensity (MFI) of CXCR3 on bpV(phen)-treated (B) CD4⁺ and (C) CD8⁺ T cells following stimulation. The cumulative average of 3 independent experiments is shown. *** P < 0.001 and **** P < 0.0001 using a one-way ANOVA and Tukey's multiple comparisons test.

Chapter Four

Final Discussion and Conclusions

Introduction

Malaria has caused pathology in humans for thousands of years (1-3), and is still responsible for over four hundred thousand deaths per year despite decades of research and intervention programmes (10,20). Renewed global interest in malaria elimination and the resulting campaigns to deliver insecticide-treated nets substantially decreased the incidence of malaria between 2000-2015 (20). Furthermore, the increased frequency of parasitological confirmation allowed by the introduction of rapid diagnostic tests and the use of highly effective artemisinin-based combination therapies have further reduced the transmission of malaria and have helped to prevent the manifestation of severe symptoms (10,20). However, if treatment is delayed or inefficacious, *P. falciparum* infection can develop into severe malaria, which has a high case-fatality rate (53) and carries a considerable risk of long-term neurological sequelae (134,135).

The mortality rate and the severity of the sequelae caused by severe malaria is dependent on the clinical manifestation, with cerebral malaria having both a high case-fatality rate and a substantial risk of developing long-term neurocognitive impairments (53). Many adjunctive therapies have been developed in an attempt to reduce the morbidity and mortality resulting from cerebral malaria, but so far none have proved to be capable of significantly improving the outcome of patients (53). Clinical studies have provided extensive information regarding the correlates of disease severity in cerebral malaria, but a mechanistic understanding of the factors that contribute to cerebral pathology is lacking due to the ethical limitations of human research. Murine models of malaria recapitulate a number of pathological processes associated with the human disease, affording a more in depth examination of the underlying etiology of the disease that may inform the design of effective adjunctive therapies.

The validity of mouse models to accurately portray human cerebral malaria is a matter of controversy (391), particularly the importance of T cells to the development of neuropathology. Sequestration of T cells within the brain is absolutely required for the onset of neurological symptoms in ECM (390), whereas the role of T cells in human cerebral malaria is unknown, with some researchers suggesting that they are not involved at all. However, the sequestration of leukocytes within the brain has been observed in a large proportion of children with cerebral malaria (140,262-264), and the chemokine CXCL10, which contributes to the chemotaxis of T cells in ECM, is elevated in patients with cerebral malaria (258,259). Thus, the available data support the possibility that T cells play a role in the neuropathogenesis of human cerebral malaria and warrant further investigation.

Beyond the generation of effective adjunctive therapies, a better understanding of the factors that cause severe malaria would also inform healthcare guidelines for geographically overlapping issues. Iron deficiency anemia is associated with suboptimal cognitive development in children (498); however, iron supplementation may increase the risk of serious adverse events in areas that have a high transmission of malaria in the absence of regular prevention and treatment services (503,555). Based on the above, we sought to better define the relationship of systemic iron levels and the neuropathogenesis of cerebral malaria using the mouse model. As shown in Chapter Two, we determined that the administration of iron dextran to mice markedly decreased the incidence of ECM without affecting the parasitemia.

Additionally, iron has been shown to be capable of attenuating PTP activity (584), and both exogenous iron and the inhibition of PTP activity were shown to protect mice from cutaneous leishmaniasis by modulating the same mechanisms (593-595). Accordingly, we examined the impact of direct PTP inhibition on ECM pathology using the PTP inhibitor bpV(phen). As

demonstrated in Chapter Three, we found that similar to iron dextran, bpV(phen) protected mice from ECM without affecting parasitemia. Since neither the administration of iron dextran nor PTP inhibition displayed an antimalarial effect, we subsequently characterized the impact of both iron dextran and bpV(phen) on immunological mechanisms that have been associated with pathology during *P. berghei* ANKA infection.

CXCR3-mediated Chemotaxis of T Cells

Sequestration of T cells within the brain is required for the disruption of the BBB and the development of ECM (390). Mice given either iron dextran or bpV(phen) had a marked decrease in the accumulation of T cells within their brain, retained the integrity of their BBB, and did not exhibit any of the typical clinical symptoms of cerebral malaria, such as paralysis or coma. Since the chemokine receptor CXCR3 has been shown to play an integral role in the trafficking of pathogenic T cells to the brain during ECM (442-445), we examined whether the CXCR3-mediated chemotaxis of CD4⁺ and CD8⁺ T cells was modulated by iron or PTP inhibition.

Iron significantly decreased the expression of CXCR3 on CD4⁺ T cells, but the expression of CXCR3 on CD8⁺ T cells was not affected by the administration of iron (Figure 1). Previous studies have shown that CXCR3 expression on CD4⁺ T cells requires the IFN γ -mediated induction of the transcription factor T-bet (477). Accordingly, we observed that CD4⁺ T cells from FeD mice had attenuated expression of IFN γ R2 and T-bet, and reduced phosphorylation of STAT1, indicating that the CD4⁺ T cells had a reduced capacity to respond to IFN γ . TfR1-mediated uptake of iron has previously been shown to cause the internalization of IFN γ R2 on T cells (565), and this process is likely responsible for the decreased IFN γ -responsiveness that we observed in the CD4⁺ T cells from the FeD mice.

Despite the expression of CXCR3 on CD8⁺ T cells being unaffected by the administration of exogenous iron, the sequestration of CD8⁺ T cells in the brain was also significantly decreased. CD4⁺ T cells have been shown to enhance the expression of the requisite chemokines of CXCR3 in the brain, thereby increasing the accumulation of CXCR3-expressing T cells (454). We observed that mice given iron dextran had reduced brain expression of CXCL10, thus iron dextran appears to have decreased the sequestration of CD8⁺ T cells indirectly by inhibiting the ability of CD4⁺ T cells to induce the production of chemokines within the brain. However, the attenuated brain sequestration of CD8⁺ T cells may have also been affected by ligand-mediated desensitization of CXCR3 (651,652), since the iron dextran-treated mice had increased levels of CXCL10 in the spleen compared to the control mice.

Contrastingly, PTP inhibition significantly decreased the expression of CXCR3 on both CD4⁺ and CD8⁺ T cells (Figure 1). Upregulation of CXCR3 requires the release of T cells from persistent TCR stimulation, thus we examined the impact of PTP inhibition during both TCR stimulation and during the recovery period following stimulation. bpV(phen) had the greatest effect on CXCR3 expression on both CD4⁺ and CD8⁺ T cells when the inhibitor was present during TCR stimulation. PTP inhibition during the recovery period did not affect the expression of CXCR3 on CD4⁺ T cells and only caused a partial decrease in CXCR3 expression on CD8⁺ T cells, demonstrating that the role of tyrosine phosphorylation in the upregulation of CXCR3 occurs predominately during TCR stimulation and differentially effects CD4⁺ and CD8⁺ T cells.

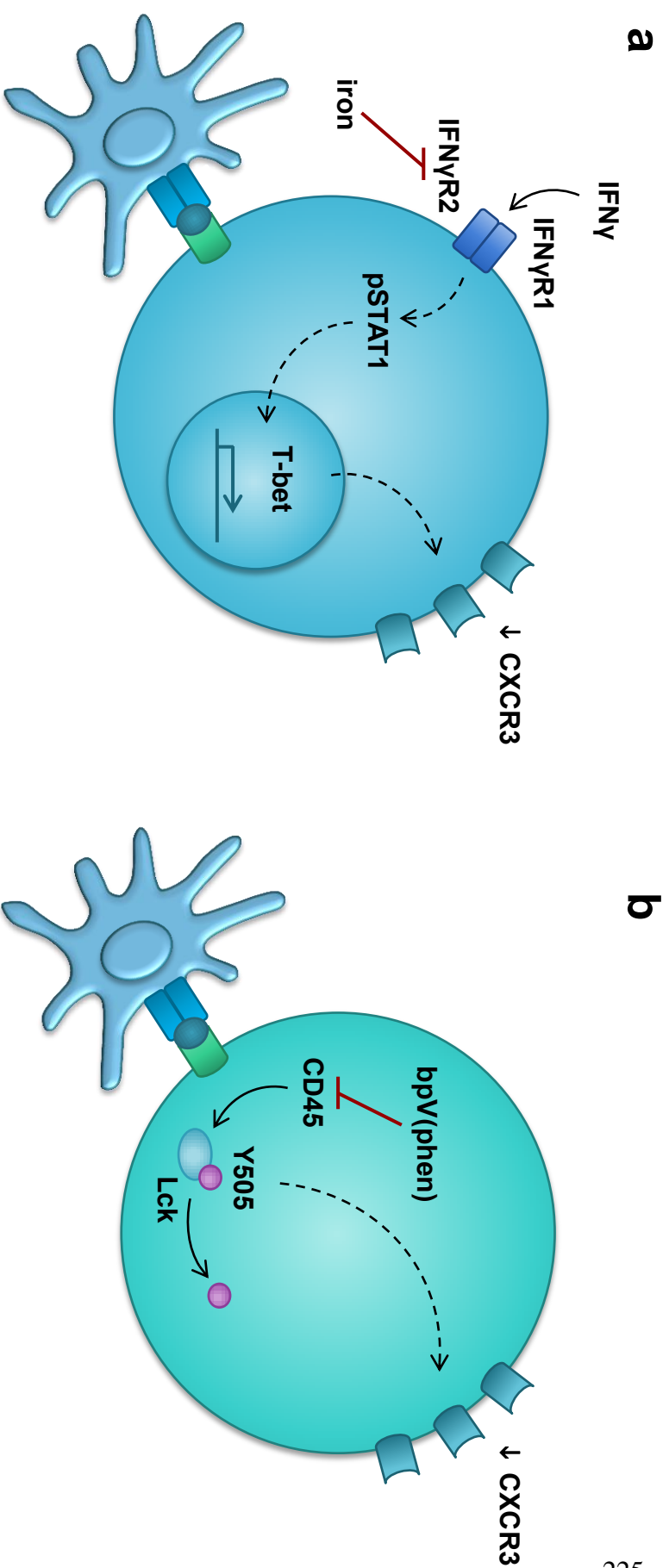


Figure 1. Modulation of CXCR3 Expression on T Cells by Iron and bpV(phen). (A) CXCR3 expression on CD4⁺ T cells requires the induction of T-bet. IFN γ stimulation through the IFN γ R promotes T-bet expression through STAT-1-mediated signalling, and T-bet transactivates the expression of CXCR3. Notably, IFN γ depletion or STAT1 deficiency does not affect the upregulation of CXCR3 on CD8⁺ T cells, and CD8⁺ T cells from T-bet knock-out mice were shown to have normal CXCR3 expression. TfR1-mediated uptake of iron was previously shown to induce the internalization of IFN γ R2 on T cells. We demonstrated that exogenous iron is able to attenuate the IFN γ -responsiveness and the expression of CXCR3 on CD4⁺ T cells *in vivo*, thereby protecting mice from ECM by preventing the chemotaxis of T cells to the brain. (B) CXCR3 expression on T cells requires release from persistent TCR stimulation, but the downstream mechanisms involved in the upregulation of CXCR3 and whether TCR signalling differentially affects the expression of CXCR3 on CD4⁺ and CD8⁺ T cells is unknown. TCR signal transduction results in a cascade of tyrosine phosphorylation, and we determined that PTP inhibition precluded the dephosphorylation of the inhibitory tyrosine of Lck (Y505), likely through the inhibition of CD45. Moreover, CXCR3 expression was affected the most when PTP activity was inhibited during TCR stimulation, and PTP inhibition during the recovery period affected CXCR3 expression to a greater extent on CD8⁺ T cell than CD4⁺ T cells. Figure generated by KV.

Since PTP inhibition had the largest impact on CXCR3 expression during TCR stimulation, we postulated that the main target of bpV(phen) responsible for the attenuated CXCR3 expression was likely to be a PTP involved in TCR signal transduction. We found that PTP inhibition increased the phosphorylation of the inhibitory tyrosine of Lck (Y505) and reduced downstream signalling, as evidenced by decreased phosphorylation of the kinases ERK1/2. Based on these results, we concluded that bpV(phen) predominantly prevented the upregulation of CXCR3 on CD4⁺ and CD8⁺ T cells by inhibiting CD45, which is known to dephosphorylate Y505.

NK Cells and CD4⁺ Regulatory Cells

Beyond effector T cells, NK cells and regulatory CD4⁺ T cells have also been demonstrated to play a role in ECM pathology. NK cells are thought to enhance the sequestration of pathogenic T cells in the brain by increasing the T cell expression of CXCR3 (444). We found that FeD mice had a reduced frequency of NK cells early in the infection, which may have potentially contributed to the decreased percentage of CXCR3-expressing CD4⁺ T cells. Tregs have also been implicated in limiting the brain sequestration of T cells during ECM (484), and we observed a trend toward an increased percentage of Tregs in the spleen of the FeD mice, but the difference was not significant.

In addition to mitigating brain sequestration of pathogenic T cells, CD4⁺ regulatory T cells have also been shown to be the dominant source of IL-10 in non-cerebral mouse models of malaria (481,485). We found that both infection and bpV(phen) treatment increased the frequency of IL-10-producing CD4⁺ T cells, and similar to the non-cerebral malaria infections, the majority of the IL-10-producing CD4⁺ T cells were Foxp3⁻ Tr1 cells. IL-10 knock-out mice given bpV(phen) did not develop neuropathology, demonstrating that the bpV(phen)-mediated protection from ECM

was not dependent on an increased production of IL-10. The bpV(phen)-treated, IL-10 knock-out mice that survived for greater than two weeks post-infection had significantly reduced parasitemia compared to the bpV(phen)-treated wild-type mice. This may be due to the bpV(phen)-mediated protection from ECM allowing the normally pathogenic IFN γ response, enhanced by the lack of IL-10, to better control the parasitemia.

Hepatic Injury

A large proportion of the bpV(phen)-treated IL-10 knock-out mice succumbed to the *P. berghei* ANKA infection nearly two weeks before the bpV(phen)-treated wild type mice, and did so without displaying cerebral symptoms and without having a substantially different parasitemia compared to the wild-type mice. In addition to neuropathology and hyperparasitemia, malaria infection can also cause hepatic pathology (481,492,493), severe anemia (388) and lung injury (653). Since IL-10 knock-out mice infected with either *P. yoelii* or *P. berghei* NK65 exhibited significantly more hepatic pathology than wild-type mice (481,492) we examined whether the bpV(phen)-treated IL-10 knock-out mice also had enhanced hepatic pathology. We observed that both the presence of IL-10 and PTP inhibition reduced liver injury. PTP inhibition significantly decreased hepatic pathology in the IL-10 knock-out mice, indicating that bpV(phen) is capable of attenuating liver damage independently of IL-10, but without necessarily excluding the possibility that bpV(phen) may also reduce liver injury in an IL-10-dependent manner.

A previous study determined that liver damage in ECM was caused by a high parasite burden (493), but we did not observe an association between the liver parasite burden and hepatic pathology. For example, on day 7 post-infection half of our control wild-type mice were symptomatic and half had yet to develop cerebral symptoms. The symptomatic mice had a

markedly increased accumulation of parasites within the liver compared to the non-symptomatic mice, but the two groups of mice had no difference in liver damage. Additionally, IL-10 has been proposed to limit the tissue parasite burden in ECM (394), but our study did not demonstrate an association between the liver parasite burden and the presence of IL-10. There was no difference in the liver parasite burden of the control IL-10 knock-out mice (all of which were symptomatic) and the symptomatic, control wild-type mice, despite the difference in the expression of IL-10. However, as mentioned above, the presence or absence of cerebral symptoms again appeared to correlate with the parasite burden of the liver.

Conclusions

Overall, this thesis supports previous work which demonstrated that liver damage occurs during *P. berghei* ANKA infection independently of cerebral pathology. However, we did not observe an association between the tissue parasite burden and hepatic pathology (493), nor did we find that IL-10 plays a role in limiting the liver parasite burden (394). Instead our data suggests that IL-10 is able to attenuate liver damage independently of the tissue parasite burden and that PTP inhibition prevents liver damage using a mechanism that appears to be independent of IL-10.

Furthermore, we demonstrated that the majority of the IL-10-producing CD4⁺ T cells in ECM were Foxp3⁻ Tr1 cells, similar to what has been observed in non-cerebral murine malaria models (481,485). PTP inhibition was shown to enhance the production of IL-10 by splenic CD4⁺ T cells by increasing the frequency of Tr1 cells, and iron dextran caused a trend toward an increase in the percentage of splenic regulatory cells, but the difference was not significant.

Importantly, we determined that both iron dextran and bpV(phen) are able to prevent neuropathology during *P. berghei* ANKA infection by reducing the expression of CXCR3 on T

cells, thereby attenuating the sequestration of CD4⁺ and CD8⁺ T cells within the brain. These findings support the integral role of CXCR3-mediated chemotaxis to the induction of cerebral injury in ECM (442-445) and improve our understanding of the underlying factors responsible for the upregulation of CXCR3 on T cells, which has previously been poorly defined.

Prior studies found that iron sulphate is able to decrease the IFN γ -responsiveness of T cells *in vitro* by inducing the internalization of IFN γ R2 (565), and that IFN γ signalling is required for the upregulation of CXCR3 on CD4⁺ T cells *in vitro* due to the consequent increase in the expression of T-bet (476,477). Here we determined that the administration of iron dextran to mice infected with *P. berghei* ANKA downregulates the expression of IFN γ R2 and attenuates the IFN γ -responsiveness of CD4⁺ T cells, culminating in reduced expression of CXCR3 *in vivo*.

Furthermore, while it has been demonstrated that the upregulation of CXCR3 requires release from persistent TCR stimulation (470), the downstream factors responsible for CXCR3 expression and any potential differences in the requirements of TCR stimulation between CD4⁺ and CD8⁺ T cells was unknown. We determined that inhibition of PTP activity during TCR stimulation significantly decreased the upregulation of CXCR3 on both CD4⁺ and CD8⁺ T cells, and that PTP inhibition after the removal of TCR stimulation only substantially affected CXCR3 expression on CD8⁺ T cells. Prevention of CXCR3 upregulation during TCR stimulation is likely due to the inhibition of CD45 activity, as we observed that bpV(phen)-treated T cells had increased phosphorylation of the inhibitory tyrosine of Lck.

In conclusion, the results of this thesis provide insight into the underlying mechanisms that are responsible for pathology during ECM, particularly those that control the expression of CXCR3 on T cells. Improved understanding of the factors that modulate the upregulation of this

chemokine receptor would not only be beneficial to the design of novel adjuvant therapies for malaria, but could be useful for other diseases in which CXCR3-mediated chemotaxis contributes to pathology, such as graft-versus-host disease, rheumatoid arthritis and multiple sclerosis (645-650).

References

1. Liu W, Li Y, Learn GH, Rudicell RS, Robertson JD, et al. Origin of the human malaria parasite *Plasmodium falciparum* in gorillas. *Nature*. 2010;467(7314):420-425.
2. Liu W, Li Y, Shaw KS, Learn GH, Plenderleith LJ, et al. African origin of the malaria parasite *Plasmodium vivax*. *Nat Commun*. 2014;5:3346.
3. Sundararaman SA, Plenderleith LJ, Liu W, Loy DE, Learn GH, et al. Genomes of cryptic chimpanzee *Plasmodium* species reveal key evolutionary events leading to human malaria. *Nat Commun*. 2016;7:11078.
4. Kwiatkowski DP. How malaria has affected the human genome and what human genetics can teach us about malaria. *Am J Hum Genet*. 2005;77(2):171-192.
5. Carter R and Mendis KN. Evolutionary and historical aspects of the burden of malaria. *Clin Microbiol Rev*. 2002;15(4):564-594.
6. Hedrick PW. Population genetics of malaria resistance in humans. *Heredity*. 2011;107(4):283-304.
7. Allison AC. Protection afforded by sickle-cell trait against subtertian malarial infection. *Br Med J*. 1954;1(4857):290-294.
8. Flint J, Hill AV, Bowden DK, Oppenheimer SJ, Sill PR, et al. High frequencies of alpha-thalassaemia are the result of natural selection by malaria. *Nature*. 1986;321(6072):744-50.
9. Tishkoff SA, Varkonyi R, Cahinhinan N, Abbas S, Argyropoulos G, et al. Haplotype diversity and linkage disequilibrium at human G6PD: recent origin of alleles that confer malarial resistance. *Science*. 2001;293(5529):455-62.
10. WHO 2016. World malaria report 2016. Geneva, Switzerland: World Health Organization.

11. Singh B, Kim Sung L, Matusop A, Radhakrishnan A, Shamsul SS, et al. A large focus of naturally acquired *Plasmodium knowlesi* infections in human beings. *Lancet*. 2004;363(9414):1017-24.
12. Ta TH, Hisam S, Lanza M, Jiram AI, Ismail N, et al. First case of a naturally acquired human infection with *Plasmodium cynomolgi*. *Malar J*. 2014;13:68.
13. White NJ. Determinants of relapse periodicity in *Plasmodium vivax* malaria. *Malar J*. 2011;10:297.
14. White NJ, Pukrittayakamee S, Hien TT, Faiz MA, Mokuolu OA, et al. Malaria. *Lancet*. 2014;383(9918):723-35.
15. Crutcher JMH, S.L. 1996. Malaria. In: Baron, S. (ed.) *Medical Microbiology*. 4th ed. Galveston, Texas: University of Texas Medical Branch at Galveston.
16. Price RN, Tjitra E, Guerra CA, Yeung S, White NJ, et al. *Vivax* malaria: neglected and not benign. *Am J Trop Med Hyg*. 2007;77(6 Suppl):79-87.
17. Cox-Singh J, Davis TM, Lee KS, Shamsul SS, Matusop A, et al. *Plasmodium knowlesi* malaria in humans is widely distributed and potentially life threatening. *Clin Infect Dis*. 2008;46(2):165-71.
18. Doolan DL, Dobaño C and Baird JK. Acquired immunity to malaria. *Clin Microbiol Rev*. 2009;22(1):13-36.
19. Langhorne J, Ndungu FM, Sponaas A-M and Marsh K. Immunity to malaria: more questions than answers. *Nat Immunol*. 2008;9(7):725-732.
20. WHO 2015. World malaria report 2015. Geneva, Switzerland: World Health Organization.
21. Kitchen AD and Chiodini PL. Malaria and blood transfusion. *Vox Sang*. 2006;90(2):77-84.
22. Kaushik KS, Kapila K and Praharaj AK. Shooting up: the interface of microbial infections and drug abuse. *J Med Microbiol*. 2011;60(Pt 4):408-22.
23. Schantz-Dunn J and Nour NM. Malaria and pregnancy: a global health perspective. *Rev Obstet Gynecol*. 2009;2(3):186-192.
24. Sidjanski S and Vanderberg JP. Delayed migration of *Plasmodium* sporozoites from the mosquito bite site to the blood. *Am J Trop Med Hyg*. 1997;57(4):426-9.

25. Medica DL and Sinnis P. Quantitative dynamics of *Plasmodium yoelii* sporozoite transmission by infected anopheline mosquitoes. *Infect Immun*. 2005;73(7):4363-4369.
26. Verhage DF, Telgt DS, Bousema JT, Hermesen CC, van Gemert GJ, et al. Clinical outcome of experimental human malaria induced by *Plasmodium falciparum*-infected mosquitoes. *Neth J Med*. 2005;63(2):52-8.
27. Yamauchi LM, Coppi A, Snounou G and Sinnis P. *Plasmodium* sporozoites trickle out of the injection site. *Cell Microbiol*. 2007;9(5):1215-1222.
28. Amino R, Thiberge S, Martin B, Celli S, Shorte S, et al. Quantitative imaging of *Plasmodium* transmission from mosquito to mammal. *Nat Med*. 2006;12(2):220-224.
29. Ishino T, Yano K, Chinzei Y and Yuda M. Cell-passage activity is required for the malarial parasite to cross the liver sinusoidal cell layer. *PLOS Biol*. 2004;2(1):e4.
30. Frevert U, Engelmann S, Zougbedé S, Stange J, Ng B, et al. Intravital observation of *Plasmodium berghei* sporozoite infection of the liver. *PLOS Biol*. 2005;3(6):e192.
31. Mota MM, Hafalla JCR and Rodriguez A. Migration through host cells activates *Plasmodium* sporozoites for infection. *Nat Med*. 2002;8(11):1318-1322.
32. Mota MM, Pradel G, Vanderberg JP, Hafalla JC, Frevert U, et al. Migration of *Plasmodium* sporozoites through cells before infection. *Science*. 2001;291(5501):141-4.
33. Sturm A, Amino R, van de Sand C, Regen T, Retzlaff S, et al. Manipulation of host hepatocytes by the malaria parasite for delivery into liver sinusoids. *Science*. 2006;313(5791):1287-90.
34. Karunaweera ND, Wijesekera SK, Wanasekera D, Mendis KN and Carter R. The paroxysm of *Plasmodium vivax* malaria. *Trends Parasitol*. 2003;19(4):188-93.
35. Cowman AF, Berry D and Baum J. The cellular and molecular basis for malaria parasite invasion of the human red blood cell. *J Cell Biol*. 2012;198(6):961.
36. Cranston HA, Boylan CW, Carroll GL, Suter SP, Williamson JR, et al. *Plasmodium falciparum* maturation abolishes physiologic red cell deformability. *Science*. 1984;223(4634):400-3.
37. Silamut K, Phu NH, Whitty C, Turner GD, Louwrier K, et al. A quantitative analysis of the microvascular sequestration of malaria parasites in the human brain. *Am J Pathol*. 1999;155(2):395-410.

38. Suwanarusk R, Cooke BM, Dondorp AM, Silamut K, Sattabongkot J, et al. The deformability of red blood cells parasitized by *Plasmodium falciparum* and *P. vivax*. *J Infect Dis.* 2004;189(2):190-194.
39. Aly ASI, Vaughan AM and Kappe SHI. Malaria parasite development in the mosquito and infection of the mammalian host. *Annu Rev Microbiol.* 2009;63:195-221.
40. Matuschewski K. Getting infectious: formation and maturation of *Plasmodium* sporozoites in the *Anopheles* vector. *Cell Microbiol.* 2006;8(10):1547-56.
41. WHO 2007. Insecticide-treated mosquito nets: a WHO position statement. Geneva, Switzerland: World Health Organization.
42. Killeen GF, Smith TA, Ferguson HM, Mshinda H, Abdulla S, et al. Preventing childhood malaria in Africa by protecting adults from mosquitoes with insecticide-treated nets. *PLOS Med.* 2007;4(7):e229.
43. WHO 2015. Indoor residual spraying: an operational manual for indoor residual spraying (IRS) for malaria transmission control and elimination. 2nd ed. Geneva, Switzerland: World Health Organization.
44. WHO 2006. Indoor residual spraying: use of indoor residual spraying for scaling up global malaria control and elimination. Geneva, Switzerland: World Health Organization.
45. Hemingway J. The role of vector control in stopping the transmission of malaria: threats and opportunities. *Philos Trans R Soc Lond B Biol Sci.* 2014;369(1645):20130431.
46. Soderlund D 2005. Sodium Channels. In: GILBERT, L., IATROU, K. & GILL, S. (eds.) *Comprehensive molecular insect science*. New York: Elsevier.
47. Ranson H, N'Guessan R, Lines J, Moiroux N, Nkuni Z, et al. Pyrethroid resistance in African anopheline mosquitoes: what are the implications for malaria control? *Trends Parasitol.* 2011;27(2):91-8.
48. Riveron JM, Irving H, Ndula M, Barnes KG, Ibrahim SS, et al. Directionally selected cytochrome P450 alleles are driving the spread of pyrethroid resistance in the major malaria vector *Anopheles funestus*. *Proc Natl Acad Sci USA.* 2013;110(1):252-257.
49. Muller P, Warr E, Stevenson BJ, Pignatelli PM, Morgan JC, et al. Field-caught permethrin-resistant *Anopheles gambiae* overexpress CYP6P3, a P450 that metabolises pyrethroids. *PLOS Genet.* 2008;4(11):e1000286.

50. Sharp BL, Kleinschmidt I, Streat E, Maharaj R, Barnes KI, et al. Seven years of regional malaria control collaboration-Mozambique, South Africa, and Swaziland. *Am J Trop Med Hyg.* 2007;76(1):42-7.
51. WHO 2012. Interim position statement: the role of larviciding for malaria control in sub-Saharan Africa. Geneva, Switzerland: World Health Organization.
52. WHO 2013. Larval source management: a supplementary measure for malaria vector control. Geneva, Switzerland: World Health Organization.
53. WHO 2015. Guidelines for the treatment of malaria. Geneva, Switzerland: World Health Organization.
54. WHO 2013. Seasonal malaria chemoprevention with sulfadoxine-pyrimethamine plus amodiaquine in children: a field guide. Geneva, Switzerland: World Health Organization.
55. WHO 2014. WHO policy brief for the implementation of intermittent preventive treatment of malaria in pregnancy using sulfadoxine-pyrimethamine (IPTp-SP). Geneva, Switzerland: World Health Organization.
56. WHO 2011. Intermittent preventive treatment for infants using sulfadoxine-pyrimethamine (SP-IPTi) for malaria control in Africa: implementation field guide. Geneva, Switzerland: World Health Organization.
57. Sibley CH, Hyde JE, Sims PFG, Plowe CV, Kublin JG, et al. Pyrimethamine-sulfadoxine resistance in *Plasmodium falciparum*: what next? *Trends Parasitol.* 2001;17(12):582-588.
58. Peters PJ, Thigpen MC, Parise ME and Newman RD. Safety and toxicity of sulfadoxine/pyrimethamine: implications for malaria prevention in pregnancy using intermittent preventive Treatment. *Drug Saf.* 2007;30(6):481-501.
59. Hernandez-Diaz S, Werler MM, Walker AM and Mitchell AA. Neural tube defects in relation to use of folic acid antagonists during pregnancy. *Am J Epidemiol.* 2001;153(10):961-8.
60. Hernandez-Diaz S, Werler MM, Walker AM and Mitchell AA. Folic acid antagonists during pregnancy and the risk of birth defects. *N Engl J Med.* 2000;343(22):1608-14.
61. Ouma P, Parise ME, Hamel MJ, Ter Kuile FO, Otieno K, et al. A randomized controlled trial of folate supplementation when treating malaria in pregnancy with sulfadoxine-pyrimethamine. *PLOS Clin Trials.* 2006;1(6):e28.

62. Mbaye A, Richardson K, Balajo B, Dunyo S, Shulman C, et al. Lack of inhibition of the anti-malarial action of sulfadoxine-pyrimethamine by folic acid supplementation when used for intermittent preventive treatment in Gambian primigravidae. *Am J Trop Med Hyg.* 2006;74(6):960-4.
63. Sokhna C, Cisse B, Ba el H, Milligan P, Hallett R, et al. A trial of the efficacy, safety and impact on drug resistance of four drug regimens for seasonal intermittent preventive treatment for malaria in Senegalese children. *PLOS ONE.* 2008;3(1):e1471.
64. WHO 2010. Global report on antimalarial drug efficacy and drug resistance: 2000-2010. Geneva, Switzerland: World Health Organization.
65. Petersen I, Eastman R and Lanzer M. Drug-resistant malaria: molecular mechanisms and implications for public health. *FEBS Lett.* 2011;585(11):1551-1562.
66. Clerk CA, Bruce J, Affipunguh PK, Mensah N, Hodgson A, et al. A randomized, controlled trial of intermittent preventive treatment with sulfadoxine-pyrimethamine, amodiaquine, or the combination in pregnant women in Ghana. *J Infect Dis.* 2008;198(8):1202-11.
67. Tagbor H, Bruce J, Browne E, Randal A, Greenwood B, et al. Efficacy, safety, and tolerability of amodiaquine plus sulphadoxine-pyrimethamine used alone or in combination for malaria treatment in pregnancy: a randomised trial. *Lancet.* 2006;368(9544):1349-56.
68. Massaga JJ, Kitua AY, Lemnge MM, Akida JA, Malle LN, et al. Effect of intermittent treatment with amodiaquine on anaemia and malarial fevers in infants in Tanzania: a randomised placebo-controlled trial. *Lancet.* 2003;361(9372):1853-1860.
69. Cairns M, Cisse B, Sokhna C, Cames C, Simondon K, et al. Amodiaquine dosage and tolerability for intermittent preventive treatment to prevent malaria in children. *Antimicrob Agents Chemother.* 2010;54(3):1265-74.
70. Desai M, ter Kuile FO, Nosten F, McGready R, Asamoah K, et al. Epidemiology and burden of malaria in pregnancy. *Lancet Infect Dis.* 2007;7(2):93-104.
71. Eisele TP, Larsen DA, Anglewicz PA, Keating J, Yukich J, et al. Malaria prevention in pregnancy, birthweight, and neonatal mortality: a meta-analysis of 32 national cross-sectional datasets in Africa. *Lancet Infect Dis.* 2012;12(12):942-9.

72. ter Kuile FO, van Eijk AM and Filler SJ. Effect of sulfadoxine-pyrimethamine resistance on the efficacy of intermittent preventive therapy for malaria control during pregnancy: a systematic review. *JAMA*. 2007;297(23):2603-16.
73. Kayentao K, Garner P, van Eijk AM, Naidoo I, Roper C, et al. Intermittent preventive therapy for malaria during pregnancy using 2 vs 3 or more doses of sulfadoxine-pyrimethamine and risk of low birth weight in Africa: systematic review and meta-analysis. *JAMA*. 2013;309(6):594-604.
74. Desai M, Gutman J, Taylor SM, Wiegand RE, Khairallah C, et al. Impact of sulfadoxine-pyrimethamine resistance on effectiveness of intermittent preventive therapy for malaria in pregnancy at clearing infections and preventing low birth weight. *Clin Infect Dis*. 2016;62(3):323-33.
75. Harrington WE, Mutabingwa TK, Muehlenbachs A, Sorensen B, Bolla MC, et al. Competitive facilitation of drug-resistant *Plasmodium falciparum* malaria parasites in pregnant women who receive preventive treatment. *Proc Natl Acad Sci USA*. 2009;106(22):9027-9032.
76. WHO 2010. WHO policy recommendation on intermittent preventive treatment during infancy with sulfadoxine-pyrimethamine (SP-IPTi) for *Plasmodium falciparum* malaria control in Africa. Geneva, Switzerland: World Health Organization.
77. Naidoo I and Roper C. Drug resistance maps to guide intermittent preventive treatment of malaria in African infants. *Parasitology*. 2011;138(12):1469-79.
78. Naidoo I and Roper C. Mapping 'partially resistant', 'fully resistant', and 'super resistant' malaria. *Trends Parasitol*. 2013;29(10):505-15.
79. Aponte JJ, Schellenberg D, Egan A, Breckenridge A, Carneiro I, et al. Efficacy and safety of intermittent preventive treatment with sulfadoxine-pyrimethamine for malaria in African infants: a pooled analysis of six randomised, placebo-controlled trials. *Lancet*. 2009;374(9700):1533-42.
80. Macete E, Aide P, Aponte JJ, Sanz S, Mandomando I, et al. Intermittent preventive treatment for malaria control administered at the time of routine vaccinations in Mozambican infants: a randomized, placebo-controlled trial. *J Infect Dis*. 2006;194(3):276-85.

81. WHO 2012. WHO policy recommendation: seasonal malaria chemoprevention (SMC) for *Plasmodium falciparum* malaria control in highly seasonal transmission areas of the Sahel Sub-region in Africa. Geneva, Switzerland: World Health Organization.
82. Meremikwu MM, Donegan S, Sinclair D, Esu E and Oringanje C. Intermittent preventive treatment for malaria in children living in areas with seasonal transmission. *Cochrane Database Syst Rev.* 2012(2):Cd003756.
83. Consortium M 2016. Making the case for seasonal malaria chemoprevention. London, United Kingdom: Malaria Consortium.
84. Cisse B, Ba EH, Sokhna C, JL ND, Gomis JF, et al. Effectiveness of seasonal malaria chemoprevention in children under ten years of age in Senegal: a stepped-wedge cluster-randomised trial. *PLOS Med.* 2016;13(11):e1002175.
85. Cohen J, Nussenzweig V, Nussenzweig R, Vekemans J and Leach A. From the circumsporozoite protein to the RTS, S/AS candidate vaccine. *Hum Vaccin.* 2010;6(1):90-6.
86. Secretariat JTEGoMVJaW 2015. Background paper on the RTS,S/AS01 malaria vaccine.
87. Olotu A, Fegan G, Wambua J, Nyangweso G, Leach A, et al. Seven-year efficacy of RTS,S/AS01 malaria vaccine among young african children. *N Engl J Med.* 2016;374(26):2519-2529.
88. RTS SCTP. Efficacy and safety of RTS,S/AS01 malaria vaccine with or without a booster dose in infants and children in Africa: final results of a phase 3, individually randomised, controlled trial. *Lancet.* 2015;386(9988):31-45.
89. WHO. Malaria vaccine: WHO position paper. *Wkly Epidemiol Rec.* 2016;91(4):33-51.
90. WHO 2011. Universal access to malaria diagnostic testing: an operational manual. Geneva, Switzerland: World Health Organization.
91. Bell D, Wongsrichanalai C and Barnwell JW. Ensuring quality and access for malaria diagnosis: how can it be achieved? *Nat Rev Micro.* 2006;4(9):682-695.
92. WHO 2015. Malaria rapid diagnostic test performance. Results of WHO product testing of malaria RDTs: round 6 (2014-2015). Geneva, Switzerland: World Health Organization.

93. d'Acremont V, Malila A, Swai N, Tillya R, Kahama-Marro J, et al. Withholding antimalarials in febrile children who have a negative result for a rapid diagnostic test. *Clin Infect Dis*. 2010;51(5):506-511.
94. Kyabayinze DJ, Asiimwe C, Nakanjako D, Nabakooza J, Counihan H, et al. Use of RDTs to improve malaria diagnosis and fever case management at primary health care facilities in Uganda. *Malar J*. 2010;9:200.
95. Uzochukwu BSC, Onwujekwe E, Ezuma NN, Ezeoke OP, Ajuba MO, et al. Improving rational treatment of malaria: perceptions and influence of RDTs on prescribing behaviour of health workers in southeast Nigeria. *PLOS ONE*. 2011;6(1):e14627.
96. Hamer DH, Ndhlovu M, Zurovac D, Fox M, Yeboah-Antwi K, et al. Improved diagnostic testing and malaria treatment practices in Zambia. *JAMA*. 2007;297(20):2227-31.
97. O'Neill PM and Posner GH. A medicinal chemistry perspective on artemisinin and related endoperoxides. *J Med Chem*. 2004;47(12):2945-64.
98. Gautam A, Ahmed T, Batra V and Paliwal J. Pharmacokinetics and pharmacodynamics of endoperoxide antimalarials. *Curr Drug Metab*. 2009;10(3):289-306.
99. Meunier B and Robert A. Heme as trigger and target for trioxane-containing antimalarial drugs. *Acc Chem Res*. 2010;43(11):1444-51.
100. Meshnick SR, Yang YZ, Lima V, Kuypers F, Kamchonwongpaisan S, et al. Iron-dependent free radical generation from the antimalarial agent artemisinin (qinghaosu). *Antimicrob Agents Chemother*. 1993;37(5):1108-1114.
101. O'Neill PM, Barton VE and Ward SA. The molecular mechanism of action of artemisinin—the debate continues. *Molecules*. 2010;15(3):1705-21.
102. Wang J, Zhang C-J, Chia WN, Loh CCY, Li Z, et al. Haem-activated promiscuous targeting of artemisinin in *Plasmodium falciparum*. *Nat Commun*. 2015;6:10111.
103. Asawamahasakda W, Ittarat I, Pu YM, Ziffer H and Meshnick SR. Reaction of antimalarial endoperoxides with specific parasite proteins. *Antimicrob Agents Chemother*. 1994;38(8):1854-1858.
104. Eckstein-Ludwig U, Webb RJ, van Goethem IDA, East JM, Lee AG, et al. Artemisinins target the SERCA of *Plasmodium falciparum*. *Nature*. 2003;424(6951):957-961.

105. Klonis N, Crespo-Ortiz MP, Bottova I, Abu-Bakar N, Kenny S, et al. Artemisinin activity against *Plasmodium falciparum* requires hemoglobin uptake and digestion. Proc Natl Acad Sci USA. 2011;108(28):11405-11410.
106. ter Kuile F, White NJ, Holloway P, Pasvol G and Krishna S. *Plasmodium falciparum*: *in vitro* studies of the pharmacodynamic properties of drugs used for the treatment of severe malaria. Exp Parasitol. 1993;76(1):85-95.
107. Kumar N and Zheng H. Stage-specific gametocytocidal effect *in vitro* of the antimalarial drug qinghaosu on *Plasmodium falciparum*. Parasitol Res. 1990;76(3):214-8.
108. White NJ. Assessment of the pharmacodynamic properties of antimalarial drugs *in vivo*. Antimicrob Agents Chemother. 1997;41(7):1413-1422.
109. Looareesuwan S. Overview of clinical studies on artemisinin derivatives in Thailand. Trans R Soc Trop Med Hyg. 1994;88 Suppl 1:S9-11.
110. Foley M and Tilley L. Quinoline antimalarials: mechanisms of action and resistance and prospects for new agents. Pharmacol Ther. 1998;79(1):55-87.
111. Combrinck JM, Mabothe TE, Ncokazi KK, Ambele MA, Taylor D, et al. Insights into the role of heme in the mechanism of action of antimalarials. ACS Chem Biol. 2013;8(1):133-137.
112. Davis TM, Hung TY, Sim IK, Karunajeewa HA and Ilett KF. Piperaquine: a resurgent antimalarial drug. Drugs. 2005;65(1):75-87.
113. Raynes K, Foley M, Tilley L and Deady LW. Novel bisquinoline antimalarials. Synthesis, antimalarial activity, and inhibition of haem polymerisation. Biochem Pharmacol. 1996;52(4):551-9.
114. Warhurst DC, Adagu IS, Beck HP, Duraisingh MT, Kirby GC, et al. Mode of action of artemether lumefantrine (COARTEM): the sole, fixed, oral ADCC and its role in combating multidrug resistance. Southeast Asian J Trop Med Public Health. 2001;32(1):4-8.
115. Kirby GC, Wright CW and Warhurst DC. The mode of action of benflumetol. 1997.
116. Brockman A, Price RN, van Vugt M, Heppner DG, Walsh D, et al. *Plasmodium falciparum* antimalarial drug susceptibility on the north-western border of Thailand during five years of extensive use of artesunate-mefloquine. Trans R Soc Trop Med Hyg. 2000;94(5):537-544.

117. Weidekamm E, Plozza-Nottebrock H, Forgo I and Dubach UC. Plasma concentrations of pyrimethamine and sulfadoxine and evaluation of pharmacokinetic data by computerized curve fitting. *Bull World Health Organ.* 1982;60(1):115-122.
118. Hombhanje FW, Hwaihwanje I, Tsukahara T, Saruwatari J, Nakagawa M, et al. The disposition of oral amodiaquine in Papua New Guinean children with *falciparum* malaria. *Br J Clin Pharmacol.* 2005;59(3):298-301.
119. Tarning J, Ashley EA, Lindegardh N, Stepniewska K, Phaiphun L, et al. Population pharmacokinetics of piperazine after two different treatment regimens with dihydroartemisinin-piperazine in patients with *Plasmodium falciparum* malaria in Thailand. *Antimicrob Agents Chemother.* 2008;52(3):1052-1061.
120. White NJ. Antimalarial drug resistance. *J Clin Invest.* 2004;113(8):1084-1092.
121. WHO 2016. Artemisinin and artemisinin-based combination therapy resistance. Geneva, Switzerland: World Health Organization Global Malaria Programme.
122. Veiga MI, Dhingra SK, Henrich PP, Straimer J, Gnädig N, et al. Globally prevalent PfMDR1 mutations modulate *Plasmodium falciparum* susceptibility to artemisinin-based combination therapies. *Nat Commun.* 2016;7:11553.
123. Ecker A, Lehane AM and Fidock DA 2012. Molecular markers of *Plasmodium* resistance to antimalarials. In: STAINES, H. M. & KRISHNA, S. (eds.) *Treatment and prevention of malaria - antimalarial drug chemistry, action and use.* Springer.
124. Price RN, Uhlemann A-C, Brockman A, McGready R, Ashley E, et al. Mefloquine resistance in *Plasmodium falciparum* and increased pfmdr1 gene copy number. *Lancet.* 2004;364(9432):438-447.
125. Cowman AF, Galatis D and Thompson JK. Selection for mefloquine resistance in *Plasmodium falciparum* is linked to amplification of the pfmdr1 gene and cross-resistance to halofantrine and quinine. *Proc Natl Acad Sci USA.* 1994;91(3):1143-1147.
126. Price RN, Uhlemann A-C, van Vugt M, Al B, Hutagalung R, et al. Molecular and pharmacological determinants of the therapeutic response to artemether-lumefantrine in multidrug-resistant *Plasmodium falciparum* malaria. *Clin Infect Dis.* 2006;42(11):1570-1577.

127. Amato R, Lim P, Miotto O, Amaratunga C, Dek D, et al. Genetic markers associated with dihydroartemisinin-piperazine failure in *Plasmodium falciparum* malaria in Cambodia: a genotype-phenotype association study. *Lancet Infect Dis.* 2017;17(2):164-173.
128. Witkowski B, Duru V, Khim N, Ross LS, Saintpierre B, et al. A surrogate marker of piperazine-resistant *Plasmodium falciparum* malaria: a phenotype-genotype association study. *Lancet Infect Dis.* 2017;17(2):174-183.
129. Sinclair D, Zani B, Donegan S, Olliaro P and Garner P. Artemisinin-based combination therapy for treating uncomplicated malaria. *Cochrane Database Syst Rev.* 2009(3):Cd007483.
130. Galappaththy GN, Tharyan P and Kirubakaran R. Primaquine for preventing relapse in people with *Plasmodium vivax* malaria treated with chloroquine. *Cochrane Database Syst Rev.* 2013(10):Cd004389.
131. Zhang J, Krugliak M and Ginsburg H. The fate of ferriprotophyrin IX in malaria infected erythrocytes in conjunction with the mode of action of antimalarial drugs. *Mol Biochem Parasitol.* 1999;99(1):129-41.
132. Sidhu ABS, Verdier-Pinard D and Fidock DA. Chloroquine resistance in *Plasmodium falciparum* malaria parasites conferred by pfprt mutations. *Science.* 2002;298(5591):210-213.
133. Gogtay N, Kannan S, Thatte UM, Olliaro PL and Sinclair D. Artemisinin-based combination therapy for treating uncomplicated *Plasmodium vivax* malaria. *Cochrane Database Syst Rev.* 2013(10).
134. Idro R, Kakooza-Mwesige A, Balyejjussa S, Mirembe G, Mugasha C, et al. Severe neurological sequelae and behaviour problems after cerebral malaria in Ugandan children. *BMC Res Notes.* 2010;3(1):104.
135. John CC, Bangirana P, Byarugaba J, Opoka RO, Idro R, et al. Cerebral malaria in children is associated with long-term cognitive impairment. *Pediatrics.* 2008;122.
136. Sinclair D, Donegan S, Isba R and Lalloo DG. Artesunate versus quinine for treating severe malaria. *Cochrane Database Syst Rev.* 2012(6):Cd005967.
137. Dondorp AM, Fanello CI, Hendriksen IC, Gomes E, Seni A, et al. Artesunate versus quinine in the treatment of severe *falciparum* malaria in African children (AQUAMAT): an open-label, randomised trial. *Lancet.* 2010;376(9753):1647-57.

138. Dondorp A, Nosten F, Stepniewska K, Day N and White N. Artesunate versus quinine for treatment of severe *falciparum* malaria: a randomised trial. *Lancet*. 2005;366(9487):717-25.
139. Esu E, Effa EE, Opie ON, Uwaoma A and Meremikwu MM. Artemether for severe malaria. *Cochrane Database Syst Rev*. 2014(9):1-83.
140. Taylor TE, Fu WJ, Carr RA, Whitten RO, Mueller JS, et al. Differentiating the pathologies of cerebral malaria by postmortem parasite counts. *Nat Med*. 2004;10(2):143-5.
141. Okubadejo NU and Danesi MA. Diagnostic issues in cerebral malaria: a study of 112 adolescents and adults in Lagos, Nigeria. *Niger Postgrad Med J*. 2004;11(1):10-4.
142. Greiner J, Dorovini-Zis K, Taylor TE, Molyneux ME, Beare NAV, et al. Correlation of hemorrhage, axonal damage, and blood-tissue barrier disruption in brain and retina of Malawian children with fatal cerebral malaria. *Front Cell Infect Microbiol*. 2015;5:18.
143. White VA, Lewallen S, Beare N, Kayira K, Carr RA, et al. Correlation of retinal haemorrhages with brain haemorrhages in children dying of cerebral malaria in Malawi. *Trans R Soc Trop Med Hyg*. 2001;95(6):618-21.
144. Lewallen S, Bakker H, Taylor TE, Wills BA, Courtright P, et al. Retinal findings predictive of outcome in cerebral malaria. *Trans R Soc Trop Med Hyg*. 1996;90(2):144-6.
145. Beare NA, Southern C, Chalira C, Taylor TE, Molyneux ME, et al. Prognostic significance and course of retinopathy in children with severe malaria. *Arch Ophthalmol*. 2004;122(8):1141-7.
146. Lewallen S, Bronzan RN, Beare NA, Harding SP, Molyneux ME, et al. Using malarial retinopathy to improve the classification of children with cerebral malaria. *Trans R Soc Trop Med Hyg*. 2008;102(11):1089-1094.
147. Beare NAV, Taylor TE, Harding SP, Lewallen S and Molyneux ME. Malarial retinopathy: a newly established diagnostic sign of severe malaria. *Am J Trop Med Hyg*. 2006;75(5):790-797.
148. Looareesuwan S, Warrell DA, White NJ, Chanthavanich P, Warrell MJ, et al. Retinal hemorrhage, a common sign of prognostic significance in cerebral malaria. *Am J Trop Med Hyg*. 1983;32(5):911-5.

149. Kochar DK, Shubhakaran, Kumawat BL and Vyas SP. Prognostic significance of eye changes in cerebral malaria. *J Assoc Physicians India*. 2000;48(5):473-7.
150. Kochar DK, Shubhakaran, Kumawat BL, Thanvi I, Joshi A, et al. Ophthalmoscopic abnormalities in adults with *falciparum* malaria. *QJM*. 1998;91(12):845-52.
151. MacPherson GG, Warrell MJ, White NJ, Looareesuwan S and Warrell DA. Human cerebral malaria. A quantitative ultrastructural analysis of parasitized erythrocyte sequestration. *Am J Pathol*. 1985;119(3):385-401.
152. Milner DA, Whitten RO, Kamiza S, Carr R, Liomba G, et al. The systemic pathology of cerebral malaria in African children. *Front Cell Infect Microbiol*. 2014;4:104.
153. Maier AG, Cooke BM, Cowman AF and Tilley L. Malaria parasite proteins that remodel the host erythrocyte. *Nat Rev Micro*. 2009;7(5):341-354.
154. White NJ, Turner GD, Day NP and Dondorp AM. Lethal malaria: Marchiafava and Bignami were right. *J Infect Dis*. 2013;208(2):192-8.
155. Turner GD, Morrison H, Jones M, Davis TM, Looareesuwan S, et al. An immunohistochemical study of the pathology of fatal malaria. Evidence for widespread endothelial activation and a potential role for intercellular adhesion molecule-1 in cerebral sequestration. *Am J Pathol*. 1994;145(5):1057-69.
156. Clark IA and Alleva LM. Is human malarial coma caused, or merely deepened, by sequestration? *Trends Parasitol*. 2009;25(7):314-8.
157. Storm J and Craig AG. Pathogenesis of cerebral malaria— inflammation and cytoadherence. *Front Cell Infect Microbiol*. 2014;4:100.
158. Crabb BS, Cooke BM, Reeder JC, Waller RF, Caruana SR, et al. Targeted gene disruption shows that knobs enable malaria-infected red cells to cytoadhere under physiological shear stress. *Cell*. 1997;89(2):287-96.
159. Baruch DI, Pasloske BL, Singh HB, Bi X, Ma XC, et al. Cloning the *P. falciparum* gene encoding PfEMP1, a malarial variant antigen and adherence receptor on the surface of parasitized human erythrocytes. *Cell*. 1995;82(1):77-87.
160. Su XZ, Heatwole VM, Wertheimer SP, Guinet F, Herrfeldt JA, et al. The large diverse gene family *var* encodes proteins involved in cytoadherence and antigenic variation of *Plasmodium falciparum*-infected erythrocytes. *Cell*. 1995;82(1):89-100.

161. Smith JD, Chitnis CE, Craig AG, Roberts DJ, Hudson-Taylor DE, et al. Switches in expression of *Plasmodium falciparum* var genes correlate with changes in antigenic and cytoadherent phenotypes of infected erythrocytes. *Cell*. 1995;82(1):101-10.
162. Grau GE and Craig AG. Cerebral malaria pathogenesis: revisiting parasite and host contributions. *Future Microbiol*. 2012;7(2):291-302.
163. Arap W, Kolonin MG, Trepel M, Lahdenranta J, Cardo-Vila M, et al. Steps toward mapping the human vasculature by phage display. *Nat Med*. 2002;8(2):121-7.
164. Kyriacou HM, Stone GN, Challis RJ, Raza A, Lyke KE, et al. Differential var gene transcription in *Plasmodium falciparum* isolates from patients with cerebral malaria compared to hyperparasitaemia. *Mol Biochem Parasitol*. 2006;150(2-4):211-218.
165. Nielsen MA, Staalsoe T, Kurtzhals JA, Goka BQ, Dodoo D, et al. *Plasmodium falciparum* variant surface antigen expression varies between isolates causing severe and nonsevere malaria and is modified by acquired immunity. *J Immunol*. 2002;168(7):3444-50.
166. Jensen AT, Magistrado P, Sharp S, Joergensen L, Lavstsen T, et al. *Plasmodium falciparum* associated with severe childhood malaria preferentially expresses PfEMP1 encoded by group A var genes. *J Exp Med*. 2004;199(9):1179-90.
167. Jespersen JS, Wang CW, Mkumbaye SI, Minja DT, Petersen B, et al. *Plasmodium falciparum* var genes expressed in children with severe malaria encode CIDR α 1 domains. *EMBO Mol Med*. 2016;8(8):839-850.
168. Lavstsen T, Turner L, Saguti F, Magistrado P, Rask TS, et al. *Plasmodium falciparum* erythrocyte membrane protein 1 domain cassettes 8 and 13 are associated with severe malaria in children. *Proc Natl Acad Sci USA*. 2012;109(26):E1791-800.
169. Bernabeu M, Danziger SA, Avril M, Vaz M, Babar PH, et al. Severe adult malaria is associated with specific PfEMP1 adhesion types and high parasite biomass. *Proc Natl Acad Sci USA*. 2016;113(23):E3270-9.
170. Avril M, Tripathi AK, Brazier AJ, Andisi C, Janes JH, et al. A restricted subset of var genes mediates adherence of *Plasmodium falciparum*-infected erythrocytes to brain endothelial cells. *Proc Natl Acad Sci USA*. 2012;109(26):E1782-E1790.
171. Claessens A, Adams Y, Ghumra A, Lindergard G, Buchan CC, et al. A subset of group A-like var genes encodes the malaria parasite ligands for binding to human brain endothelial cells. *Proc Natl Acad Sci USA*. 2012;109(26):E1772-81.

172. Rowe JA, Claessens A, Corrigan RA and Arman M. Adhesion of *Plasmodium falciparum*-infected erythrocytes to human cells: molecular mechanisms and therapeutic implications. *Expert Rev Mol Med*. 2009;11:e16.
173. Magistrado P, Salanti A, Tuikue Ndam NG, Mwakalinga SB, Resende M, et al. VAR2CSA expression on the surface of placenta-derived *Plasmodium falciparum*-infected erythrocytes. *J Infect Dis*. 2008;198(7):1071-4.
174. Roberts DJ, Craig AG, Berendt AR, Pinches R, Nash G, et al. Rapid switching to multiple antigenic and adhesive phenotypes in malaria. *Nature*. 1992;357(6380):689-92.
175. Rogerson SJ, Tembenu R, Dobano C, Plitt S, Taylor TE, et al. Cytoadherence characteristics of *Plasmodium falciparum*-infected erythrocytes from Malawian children with severe and uncomplicated malaria. *Am J Trop Med Hyg*. 1999;61(3):467-72.
176. McCormick CJ, Craig A, Roberts D, Newbold CI and Berendt AR. Intercellular adhesion molecule-1 and CD36 synergize to mediate adherence of *Plasmodium falciparum*-infected erythrocytes to cultured human microvascular endothelial cells. *J Clin Invest*. 1997;100(10):2521-2529.
177. Udomsangpetch R, Reinhardt PH, Schollaardt T, Elliott JF, Kubes P, et al. Promiscuity of clinical *Plasmodium falciparum* isolates for multiple adhesion molecules under flow conditions. *J Immunol*. 1997;158(9):4358-64.
178. Rask TS, Hansen DA, Theander TG, Gorm Pedersen A and Lavstsen T. *Plasmodium falciparum* erythrocyte membrane protein 1 diversity in seven genomes – divide and conquer. *PLOS Comput Biol*. 2010;6(9):e1000933.
179. Turner L, Lavstsen T, Berger SS, Wang CW, Petersen JEV, et al. Severe malaria is associated with parasite binding to endothelial protein C receptor. *Nature*. 2013;498(7455):502-505.
180. Naka I, Patarapotikul J, Hananantachai H, Imai H and Ohashi J. Association of the endothelial protein C receptor (PROCR) rs867186-G allele with protection from severe malaria. *Malar J*. 2014;13(1):105.
181. Tripathi AK, Sullivan DJ and Stins MF. *Plasmodium falciparum*-infected erythrocytes increase intercellular adhesion molecule 1 expression on brain endothelium through NF- κ B. *Infect Immun*. 2006;74(6):3262-70.

182. Hviid L and Jensen ATR 2015. Chapter two - PfEMP1 – A parasite protein family of key importance in *Plasmodium falciparum* malaria immunity and pathogenesis. In: ROLLINSON, D. & STOTHARD, J. R. (eds.) *Advances in Parasitology*. Academic Press.
183. Avril M, Bernabeu M, Benjamin M, Brazier AJ and Smith JD. Interaction between endothelial protein C receptor and intercellular adhesion molecule 1 to mediate binding of *Plasmodium falciparum*-infected erythrocytes to endothelial cells. *MBio*. 2016;7(4).
184. Bengtsson A, Joergensen L, Rask TS, Olsen RW, Andersen MA, et al. A novel domain cassette identifies *Plasmodium falciparum* PfEMP1 proteins binding ICAM-1 and is a target of cross-reactive, adhesion-inhibitory antibodies. *J Immunol*. 2013;190(1):240-9.
185. David PH, Handunnetti SM, Leech JH, Gamage P and Mendis KN. Rosetting: a new cytoadherence property of malaria-infected erythrocytes. *Am J Trop Med Hyg*. 1988;38(2):289-97.
186. Pain A, Ferguson DJ, Kai O, Urban BC, Lowe B, et al. Platelet-mediated clumping of *Plasmodium falciparum*-infected erythrocytes is a common adhesive phenotype and is associated with severe malaria. *Proc Natl Acad Sci USA*. 2001;98(4):1805-10.
187. Rowe A, Obeiro J, Newbold CI and Marsh K. *Plasmodium falciparum* rosetting is associated with malaria severity in Kenya. *Infect Immun*. 1995;63(6):2323-2326.
188. Kaul DK, Roth EF, Jr., Nagel RL, Howard RJ and Handunnetti SM. Rosetting of *Plasmodium falciparum*-infected red blood cells with uninfected red blood cells enhances microvascular obstruction under flow conditions. *Blood*. 1991;78(3):812-9.
189. Goel S, Palmkvist M, Moll K, Joannin N, Lara P, et al. RIFINs are adhesins implicated in severe *Plasmodium falciparum* malaria. *Nat Med*. 2015;21(4):314-317.
190. Niang M, Bei AK, Madnani KG, Pelly S, Dankwa S, et al. STEVOR is a *Plasmodium falciparum* erythrocyte binding protein that mediates merozoite invasion and rosetting. *Cell Host Microbe*. 2014;16(1):81-93.
191. Rowe JA, Moulds JM, Newbold CI and Miller LH. *P. falciparum* rosetting mediated by a parasite-variant erythrocyte membrane protein and complement-receptor 1. *Nature*. 1997;388(6639):292-5.

192. Rowe JA, Shafi J, Kai OK, Marsh K and Raza A. Nonimmune IgM, but not IgG binds to the surface of *Plasmodium falciparum*-infected erythrocytes and correlates with rosetting and severe malaria. *Am J Trop Med Hyg.* 2002;66(6):692-9.
193. Carlson J and Wahlgren M. *Plasmodium falciparum* erythrocyte rosetting is mediated by promiscuous lectin-like interactions. *J Exp Med.* 1992;176(5):1311-7.
194. Wassmer SC, Taylor T, MacLennan CA, Kanjala M, Mukaka M, et al. Platelet-induced clumping of *Plasmodium falciparum*-infected erythrocytes from Malawian patients with cerebral malaria-possible modulation *in vivo* by thrombocytopenia. *J Infect Dis.* 2008;197(1):72-78.
195. Biswas AK, Hafiz A, Banerjee B, Kim KS, Datta K, et al. *Plasmodium falciparum* uses gC1qR/HABP1/p32 as a receptor to bind to vascular endothelium and for platelet-mediated clumping. *PLOS Pathog.* 2007;3(9):1271-80.
196. Schuepbach RA, Feistritzer C, Fernandez JA, Griffin JH and Riewald M. Protection of vascular barrier integrity by activated protein C in murine models depends on protease-activated receptor-1. *Thromb Haemost.* 2009;101(4):724-33.
197. Gleeson EM, O'Donnell JS and Preston RJ. The endothelial cell protein C receptor: cell surface conductor of cytoprotective coagulation factor signaling. *Cell Mol Life Sci.* 2012;69(5):717-26.
198. Mosnier LO, Zlokovic BV and Griffin JH. The cytoprotective protein C pathway. *Blood.* 2007;109(8):3161-72.
199. Esmon CT. The protein C pathway. *Chest.* 2003;124(3 Suppl):26s-32s.
200. Stearns-Kurosawa DJ, Kurosawa S, Mollica JS, Ferrell GL and Esmon CT. The endothelial cell protein C receptor augments protein C activation by the thrombin-thrombomodulin complex. *Proc Natl Acad Sci USA.* 1996;93(19):10212-6.
201. Moxon CA, Wassmer SC, Milner DA, Chisala NV, Taylor TE, et al. Loss of endothelial protein C receptors links coagulation and inflammation to parasite sequestration in cerebral malaria in African children. *Blood.* 2013;122(5):842.
202. Petersen JE, Bouwens EA, Tamayo I, Turner L, Wang CW, et al. Protein C system defects inflicted by the malaria parasite protein PfEMP1 can be overcome by a soluble EPCR variant. *Thromb Haemost.* 2015;114(5):1038-48.

203. Sampath S, Brazier AJ, Avril M, Bernabeu M, Vigdorovich V, et al. *Plasmodium falciparum* adhesion domains linked to severe malaria differ in blockade of endothelial protein C receptor. *Cell Microbiol.* 2015;17(12):1868-82.
204. Gillrie MR, Avril M, Brazier AJ, Davis SP, Stins MF, et al. Diverse functional outcomes of *Plasmodium falciparum* ligation of EPCR: potential implications for malarial pathogenesis. *Cell Microbiol.* 2015;17(12):1883-99.
205. Aird WC, Mosnier LO and Fairhurst RM. *Plasmodium falciparum* picks (on) EPCR. *Blood.* 2014;123(2):163-7.
206. Joyce DE, Gelbert L, Ciaccia A, DeHoff B and Grinnell BW. Gene expression profile of antithrombotic protein c defines new mechanisms modulating inflammation and apoptosis. *J Biol Chem.* 2001;276(14):11199-203.
207. Cheng T, Liu D, Griffin JH, Fernandez JA, Castellino F, et al. Activated protein C blocks p53-mediated apoptosis in ischemic human brain endothelium and is neuroprotective. *Nat Med.* 2003;9(3):338-342.
208. Guo H, Liu D, Gelbard H, Cheng T, Insalaco R, et al. Activated protein C prevents neuronal apoptosis via protease activated receptors 1 and 3. *Neuron.* 2004;41(4):563-72.
209. Minhas N, Xue M, Fukudome K and Jackson CJ. Activated protein C utilizes the angiopoietin/Tie2 axis to promote endothelial barrier function. *FASEB J.* 2010;24(3):873-81.
210. Francischetti IM, Seydel KB, Monteiro RQ, Whitten RO, Erexson CR, et al. *Plasmodium falciparum*-infected erythrocytes induce tissue factor expression in endothelial cells and support the assembly of multimolecular coagulation complexes. *J Thromb Haemost.* 2007;5(1):155-65.
211. Wong VL, Hofman FM, Ishii H and Fisher M. Regional distribution of thrombomodulin in human brain. *Brain Res.* 1991;556(1):1-5.
212. Laszik Z, Mitro A, Taylor FB, Jr., Ferrell G and Esmon CT. Human protein C receptor is present primarily on endothelium of large blood vessels: implications for the control of the protein C pathway. *Circulation.* 1997;96(10):3633-40.
213. Yeo TW, Lampah DA, Gitawati R, Tjitra E, Kenangalem E, et al. Impaired nitric oxide bioavailability and l-arginine-reversible endothelial dysfunction in adults with *falciparum* malaria. *J Exp Med.* 2007;204(11):2693-2704.

214. Yeo TW, Lampah DA, Gitawati R, Tjitra E, Kenangalem E, et al. Angiotensin-converting enzyme 2 is associated with decreased endothelial nitric oxide and poor clinical outcome in severe *falciparum* malaria. *Proc Natl Acad Sci USA*. 2008;105(44):17097-102.
215. Conroy AL, Phiri H, Hawkes M, Glover S, Mallewa M, et al. Endothelium-based biomarkers are associated with cerebral malaria in Malawian children: a retrospective case-control study. *PLOS ONE*. 2011;5(12):e15291.
216. Lovegrove FE, Tangpukdee N, Opoka RO, Lafferty EI, Rajwans N, et al. Serum angiotensin-converting enzyme 1 and -2 levels discriminate cerebral malaria from uncomplicated malaria and predict clinical outcome in African children. *PLOS One*. 2009;4(3):e4912.
217. Erdman LK, Dhabangi A, Musoke C, Conroy AL, Hawkes M, et al. Combinations of host biomarkers predict mortality among Ugandan children with severe malaria: a retrospective case-control study. *PLOS ONE*. 2011;6(2):e17440.
218. Conroy AL, Lafferty EI, Lovegrove FE, Krudsood S, Tangpukdee N, et al. Whole blood angiotensin-converting enzyme 1 and -2 levels discriminate cerebral and severe (non-cerebral) malaria from uncomplicated malaria. *Malar J*. 2009;8:295.
219. Hanson J, Lee SJ, Hossain MA, Anstey NM, Charunwatthana P, et al. Microvascular obstruction and endothelial activation are independently associated with the clinical manifestations of severe *falciparum* malaria in adults: an observational study. *BMC Med*. 2015;13(1):122.
220. Anstey NM, Weinberg JB, Hassanali MY, Mwaikambo ED, Manyenga D, et al. Nitric oxide in Tanzanian children with malaria: inverse relationship between malaria severity and nitric oxide production/nitric oxide synthase type 2 expression. *J Exp Med*. 1996;184(2):557-67.
221. Lopansri BK, Anstey NM, Weinberg JB, Stoddard GJ, Hobbs MR, et al. Low plasma arginine concentrations in children with cerebral malaria and decreased nitric oxide production. *Lancet*. 2003;361(9358):676-8.
222. Yeo TW, Lampah DA, Tjitra E, Gitawati R, Darcy CJ, et al. Increased asymmetric dimethylarginine in severe *falciparum* malaria: association with impaired nitric oxide bioavailability and fatal outcome. *PLOS Pathog*. 2010;6(4):e1000868.

223. Yeo TW, Lampah DA, Tjitra E, Gitawati R, Kenangalem E, et al. Relationship of cell-free hemoglobin to impaired endothelial nitric oxide bioavailability and perfusion in severe *falciparum* malaria. *J Infect Dis.* 2009;200(10):1522-9.
224. De Caterina R, Libby P, Peng HB, Thannickal VJ, Rajavashisth TB, et al. Nitric oxide decreases cytokine-induced endothelial activation. Nitric oxide selectively reduces endothelial expression of adhesion molecules and proinflammatory cytokines. *J Clin Invest.* 1995;96(1):60-68.
225. Serirom S, Raharjo WH, Chotivanich K, Loareesuwan S, Kubes P, et al. Anti-adhesive effect of nitric oxide on *Plasmodium falciparum* cytoadherence under flow. *Am J Pathol.* 2003;162(5):1651-1660.
226. Vaughn MW, Kuo L and Liao JC. Effective diffusion distance of nitric oxide in the microcirculation. *Am J Physiol.* 1998;274(5 Pt 2):H1705-14.
227. Matsushita K, Morrell CN, Cambien B, Yang SX, Yamakuchi M, et al. Nitric oxide regulates exocytosis by S-nitrosylation of N-ethylmaleimide-sensitive factor. *Cell.* 2003;115(2):139-50.
228. Fiedler U, Scharpfenecker M, Koidl S, Hegen A, Grunow V, et al. The Tie-2 ligand angiopoietin-2 is stored in and rapidly released upon stimulation from endothelial cell Weibel-Palade bodies. *Blood.* 2004;103(11):4150-6.
229. Carvalho LJdM, Moreira AdS, Daniel-Ribeiro CT and Martins YC. Vascular dysfunction as a target for adjuvant therapy in cerebral malaria. *Mem Inst Oswaldo Cruz.* 2014;109(5):577-588.
230. Fiedler U, Reiss Y, Scharpfenecker M, Grunow V, Koidl S, et al. Angiopoietin-2 sensitizes endothelial cells to TNF-alpha and has a crucial role in the induction of inflammation. *Nat Med.* 2006;12(2):235-9.
231. Wagner DD. The Weibel-Palade body: the storage granule for von Willebrand factor and P-selectin. *Thromb Haemost.* 1993;70(1):105-10.
232. Ruggeri ZM. Structure and function of von Willebrand factor. *Thromb Haemost.* 1999;82(2):576-84.
233. Lenting PJ, Christophe OD and Denis CV. von Willebrand factor biosynthesis, secretion, and clearance: connecting the far ends. *Blood.* 2015;125(13):2019-28.

234. Hollestelle MJ, Donkor C, Mantey EA, Chakravorty SJ, Craig A, et al. von Willebrand factor propeptide in malaria: evidence of acute endothelial cell activation. *Br J Haematol.* 2006;133(5):562-9.
235. Larkin D, de Laat B, Jenkins PV, Bunn J, Craig AG, et al. Severe *Plasmodium falciparum* malaria is associated with circulating ultra-large von Willebrand multimers and ADAMTS13 inhibition. *PLOS Pathog.* 2009;5(3):e1000349.
236. de Mast Q, Groot E, Asih PB, Syafruddin D, Oosting M, et al. ADAMTS13 deficiency with elevated levels of ultra-large and active von Willebrand Factor in *P. falciparum* and *P. vivax* malaria. *Am J Trop Med Hyg.* 2009;80(3):492-498.
237. Lowenberg EC, Charunwatthana P, Cohen S, van den Born BJ, Meijers JC, et al. Severe malaria is associated with a deficiency of von Willebrand factor cleaving protease, ADAMTS13. *Thromb Haemost.* 2010;103(1):181-7.
238. Wassmer SC, Lepolard C, Traore B, Pouvelle B, Gysin J, et al. Platelets reorient *Plasmodium falciparum*-infected erythrocyte cytoadhesion to activated endothelial cells. *J Infect Dis.* 2004;189(2):180-9.
239. Bridges DJ, Bunn J, van Mourik JA, Grau G, Preston RJ, et al. Rapid activation of endothelial cells enables *Plasmodium falciparum* adhesion to platelet-decorated von Willebrand factor strings. *Blood.* 2010;115(7):1472-4.
240. Dieye Y, Mbengue B, Dagamajalu S, Fall MM, Loke MF, et al. Cytokine response during non-cerebral and cerebral malaria: evidence of a failure to control inflammation as a cause of death in African adults. *PeerJ.* 2016;4:e1965.
241. Lyke KE, Burges R, Cissoko Y, Sangare L, Dao M, et al. Serum levels of the proinflammatory cytokines interleukin-1 beta (IL-1 β), IL-6, IL-8, IL-10, tumor necrosis factor alpha, and IL-12(p70) in Malian children with severe *Plasmodium falciparum* malaria and matched uncomplicated malaria or healthy controls. *Infect Immun.* 2004;72(10):5630-5637.
242. Mshana RN, Boulandi J, Mshana NM, Mayombo J and Mendome G. Cytokines in the pathogenesis of malaria: levels of IL-1 beta, IL-4, IL-6, TNF-alpha and IFN-gamma in plasma of healthy individuals and malaria patients in a holoendemic area. *J Clin Lab Immunol.* 1991;34(3):131-9.

243. Grau GE, Taylor TE, Molyneux ME, Wirima JJ, Vassalli P, et al. Tumor necrosis factor and disease severity in children with *falciparum* malaria. *N Engl J Med*. 1989;320(24):1586-91.
244. Peyron F, Burdin N, Ringwald P, Vuillez JP, Rousset F, et al. High levels of circulating IL-10 in human malaria. *Clin Exp Immunol*. 1994;95(2):300-303.
245. Jakobsen PH, McKay V, Morris-Jones SD, McGuire W, van Hensbroek MB, et al. Increased concentrations of interleukin-6 and interleukin-1 receptor antagonist and decreased concentrations of beta-2-glycoprotein I in Gambian children with cerebral malaria. *Infect Immun*. 1994;62(10):4374-4379.
246. Kwiatkowski D, Hill AV, Sambou I, Twumasi P, Castracane J, et al. TNF concentration in fatal cerebral, non-fatal cerebral, and uncomplicated *Plasmodium falciparum* malaria. *Lancet*. 1990;336(8725):1201-4.
247. Kern P, Hemmer CJ, Van Damme J, Gruss HJ and Dietrich M. Elevated tumor necrosis factor alpha and interleukin-6 serum levels as markers for complicated *Plasmodium falciparum* malaria. *Am J Med*. 1989;87(2):139-43.
248. Day NP, Hien TT, Schollaardt T, Loc PP, Chuong LV, et al. The prognostic and pathophysiologic role of pro- and anti-inflammatory cytokines in severe malaria. *J Infect Dis*. 1999;180(4):1288-97.
249. Parry GCN and Mackman N. Transcriptional regulation of tissue factor expression in human endothelial cells. *Arterioscler Thromb Vasc Biol*. 1995;15(5):612.
250. Bierhaus A, Zhang Y, Deng Y, Mackman N, Quehenberger P, et al. Mechanism of the tumor necrosis factor alpha-mediated induction of endothelial tissue factor. *J Biol Chem*. 1995;270(44):26419-32.
251. Liu Y, Pelekanakis K and Woolkalis MJ. Thrombin and tumor necrosis factor alpha synergistically stimulate tissue factor expression in human endothelial cells: regulation through c-Fos and c-Jun. *J Biol Chem*. 2004;279(34):36142-7.
252. Nan B, Lin P, Lumsden AB, Yao Q and Chen C. Effects of TNF-alpha and curcumin on the expression of thrombomodulin and endothelial protein C receptor in human endothelial cells. *Thromb Res*. 2005;115(5):417-26.

253. van der Poll T, Buller HR, ten Cate H, Wortel CH, Bauer KA, et al. Activation of coagulation after administration of tumor necrosis factor to normal subjects. *N Engl J Med.* 1990;322(23):1622-7.
254. Clark IA, Alleva LM, Budd AC and Cowden WB. Understanding the role of inflammatory cytokines in malaria and related diseases. *Travel Med Infect Dis.* 2008;6(1–2):67-81.
255. Wassmer SC, Moxon CA, Taylor T, Grau GE, Molyneux ME, et al. Vascular endothelial cells cultured from patients with cerebral or uncomplicated malaria exhibit differential reactivity to TNF. *Cell Microbiol.* 2011;13(2):198-209.
256. Kremsner PG, Winkler S, Brandts C, Wildling E, Jenne L, et al. Prediction of accelerated cure in *Plasmodium falciparum* malaria by the elevated capacity of tumor necrosis factor production. *Am J Trop Med Hyg.* 1995;53(5):532-538.
257. May J, Lell B, Luty AJ, Meyer CG and Kremsner PG. Plasma interleukin-10: tumor necrosis factor (TNF)-alpha ratio is associated with TNF promoter variants and predicts malarial complications. *J Infect Dis.* 2000;182(5):1570-3.
258. Jain V, Armah HB, Tongren JE, Ned RM, Wilson NO, et al. Plasma IP-10, apoptotic and angiogenic factors associated with fatal cerebral malaria in India. *Malar J.* 2008;7:83-83.
259. Armah HB, Wilson NO, Sarfo BY, Powell MD, Bond VC, et al. Cerebrospinal fluid and serum biomarkers of cerebral malaria mortality in Ghanaian children. *Malar J.* 2007;6:147-147.
260. Groom JR and Luster AD. CXCR3 ligands: redundant, collaborative and antagonistic functions. *Immunol Cell Biol.* 2011;89(2):207-15.
261. Harris DP, Bandyopadhyay S, Maxwell TJ, Willard B and DiCorleto PE. Tumor necrosis factor (TNF)-alpha induction of CXCL10 in endothelial cells requires protein arginine methyltransferase 5 (PRMT5)-mediated nuclear factor (NF)-kappaB p65 methylation. *J Biol Chem.* 2014;289(22):15328-39.
262. Clark IA, Awburn MM, Whitten RO, Harper CG, Liomba NG, et al. Tissue distribution of migration inhibitory factor and inducible nitric oxide synthase in *falciparum* malaria and sepsis in African children. *Malaria Journal.* 2003;2(1):6.

263. Armah H, Doodoo AK, Wiredu EK, Stiles JK, Adjei AA, et al. High-level cerebellar expression of cytokines and adhesion molecules in fatal, paediatric, cerebral malaria. *Ann Trop Med Parasitol.* 2005;99(7):629-47.
264. Grau GE, Mackenzie CD, Carr RA, Redard M, Pizzolato G, et al. Platelet accumulation in brain microvessels in fatal pediatric cerebral malaria. *J Infect Dis.* 2003;187(3):461-6.
265. Patnaik JK, Das BS, Mishra SK, Mohanty S, Satpathy SK, et al. Vascular clogging, mononuclear cell margination, and enhanced vascular permeability in the pathogenesis of human cerebral malaria. *Am J Trop Med Hyg.* 1994;51(5):642-7.
266. Dondorp AM, Ince C, Charunwatthana P, Hanson J, van Kuijen A, et al. Direct *in vivo* assessment of microcirculatory dysfunction in severe *falciparum* malaria. *J Infect Dis.* 2008;197(1):79-84.
267. Ponsford MJ, Medana IM, Prapansilp P, Hien TT, Lee SJ, et al. Sequestration and microvascular congestion are associated with coma in human cerebral malaria. *J Infect Dis.* 2012;205(4):663-671.
268. Doumbo OK, Thera MA, Kone AK, Raza A, Tempest LJ, et al. High levels of *Plasmodium falciparum* rosetting in all clinical forms of severe malaria in African children. *Am J Trop Med Hyg.* 2009;81(6):987-93.
269. Cockburn IA, Mackinnon MJ, O'Donnell A, Allen SJ, Moulds JM, et al. A human complement receptor 1 polymorphism that reduces *Plasmodium falciparum* rosetting confers protection against severe malaria. *Proc Natl Acad Sci USA.* 2004;101(1):272-7.
270. Rowe JA, Handel IG, Thera MA, Deans A-M, Lyke KE, et al. Blood group O protects against severe *Plasmodium falciparum* malaria through the mechanism of reduced rosetting. *Proc Natl Acad Sci USA.* 2007;104(44):17471-17476.
271. Arman M, Raza A, Tempest LJ, Lyke KE, Thera MA, et al. Platelet-mediated clumping of *Plasmodium falciparum* infected erythrocytes is associated with high parasitemia but not severe clinical manifestations of malaria in African children. *Am J Trop Med Hyg.* 2007;77(5):943-946.
272. Dondorp AM, Angus BJ, Hardeman MR, Chotivanich KT, Silamut K, et al. Prognostic significance of reduced red blood cell deformability in severe *falciparum* malaria. *Am J Trop Med Hyg.* 1997;57(5):507-11.

273. Ishioka H, Ghose A, Charunwatthana P, Maude R, Plewes K, et al. Sequestration and red cell deformability as determinants of hyperlactatemia in *falciparum* malaria. *J Infect Dis.* 2016;213(5):788-793.
274. Dondorp AM, Nyanoti M, Kager PA, Mithwani S, Vreeken J, et al. The role of reduced red cell deformability in the pathogenesis of severe *falciparum* malaria and its restoration by blood transfusion. *Trans R Soc Trop Med Hyg.* 2002;96(3):282-6.
275. Nuchsongsin F, Chotivanich K, Charunwatthana P, Fausta O-S, Taramelli D, et al. Effects of malaria heme products on red blood cell deformability. *Am J Trop Med Hyg.* 2007;77(4):617-622.
276. Bor-Kucukatay M, Wenby RB, Meiselman HJ and Baskurt OK. Effects of nitric oxide on red blood cell deformability. *Am J Physiol Heart Circ Physiol.* 2003;284(5):H1577-84.
277. Rey J, Buffet PA, Ciceron L, Milon G, Mercereau-Puijalon O, et al. Reduced erythrocyte deformability associated with hypoargininemia during *Plasmodium falciparum* malaria. *Sci Rep.* 2014;4:3767.
278. Day NP, Phu NH, Mai NT, Chau TT, Loc PP, et al. The pathophysiologic and prognostic significance of acidosis in severe adult malaria. *Crit Care Med.* 2000;28(6):1833-40.
279. Krishna S, Waller DW, ter Kuile F, Kwiatkowski D, Crawley J, et al. Lactic acidosis and hypoglycaemia in children with severe malaria: pathophysiological and prognostic significance. *Trans R Soc Trop Med Hyg.* 1994;88(1):67-73.
280. Dondorp AM, Desakorn V, Pongtavornpinyo W, Sahassananda D, Silamut K, et al. Estimation of the total parasite biomass in acute *falciparum* malaria from plasma PfHRP2. *PLOS Med.* 2005;2(8):e204.
281. von Seidlein L, Olaosebikan R, Hendriksen ICE, Lee SJ, Adedoyin OT, et al. Predicting the clinical outcome of severe *falciparum* malaria in African children: findings from a large randomized trial. *Clin Infect Dis.* 2012;54(8):1080-1090.
282. Dondorp AM, Chau TT, Phu NH, Mai NT, Loc PP, et al. Unidentified acids of strong prognostic significance in severe malaria. *Crit Care Med.* 2004;32(8):1683-8.
283. Brand NR, Opoka RO, Hamre KES and John CC. Differing causes of lactic acidosis and deep breathing in cerebral malaria and severe malarial anemia may explain differences in acidosis-related mortality. *PLOS ONE.* 2016;11(9):e0163728.

284. Maitland K and Newton CR. Acidosis of severe *falciparum* malaria: heading for a shock? Trends Parasitol. 2005;21(1):11-6.
285. Davis TM, Krishna S, Looareesuwan S, Supanaranond W, Pukrittayakamee S, et al. Erythrocyte sequestration and anemia in severe *falciparum* malaria. Analysis of acute changes in venous hematocrit using a simple mathematical model. J Clin Invest. 1990;86(3):793-800.
286. Hanson J, Lam SWK, Mahanta KC, Pattnaik R, Alam S, et al. Relative contributions of macrovascular and microvascular dysfunction to disease severity in *falciparum* malaria. J Infect Dis. 2012;206(4):571-579.
287. Maitland K, Pamba A, Newton CR and Levin M. Response to volume resuscitation in children with severe malaria. Pediatr Crit Care Med. 2003;4(4):426-31.
288. Jarvis JN, Planche T, Bicanic T, Dzeing-Ella A, Kombila M, et al. Lactic acidosis in Gabonese children with severe malaria is unrelated to dehydration. Clin Infect Dis. 2006;42(12):1719-25.
289. Planche T, Onanga M, Schwenk A, Dzeing A, Borrmann S, et al. Assessment of volume depletion in children with malaria. PLOS Med. 2004;1(1):e18.
290. Maitland K, Kiguli S, Opoka RO, Engoru C, Olupot-Olupot P, et al. Mortality after fluid bolus in African children with severe infection. N Engl J Med. 2011;364(26):2483-2495.
291. Seydel KB, Kampondeni SD, Valim C, Potchen MJ, Milner DA, et al. Brain swelling and death in children with cerebral malaria. N Engl J Med. 2015;372(12):1126-37.
292. Newton CR, Kirkham FJ, Winstanley PA, Pasvol G, Peshu N, et al. Intracranial pressure in African children with cerebral malaria. Lancet. 1991;337(8741):573-6.
293. Potchen MJ, Kampondeni SD, Seydel KB, Birbeck GL, Hammond CA, et al. Acute brain MRI findings in 120 Malawian children with cerebral malaria: new insights into an ancient disease. AJNR Am J Neuroradiol. 2012;33(9):1740-1746.
294. Mohanty S, Mishra SK, Patnaik R, Dutt AK, Pradhan S, et al. Brain swelling and mannitol therapy in adult cerebral malaria: a randomized trial. Clin Infect Dis. 2011;53(4):349-355.
295. Maude RJ, Barkhof F, Hassan MU, Ghose A, Hossain A, et al. Magnetic resonance imaging of the brain in adults with severe *falciparum* malaria. Malar J. 2014;13:177-177.

296. Newton CR, Crawley J, Sowumni A, Waruiru C, Mwangi I, et al. Intracranial hypertension in Africans with cerebral malaria. *Arch Dis Child*. 1997;76(3):219-26.
297. Brown HC, Chau TT, Mai NT, Day NP, Sinh DX, et al. Blood-brain barrier function in cerebral malaria and CNS infections in Vietnam. *Neurology*. 2000;55(1):104-11.
298. Medana IM, Day NP, Sachanonta N, Mai NT, Dondorp AM, et al. Coma in fatal adult human malaria is not caused by cerebral oedema. *Malar J*. 2011;10:267.
299. Brown H, Rogerson S, Taylor T, Tembo M, Mwenechanya J, et al. Blood-brain barrier function in cerebral malaria in Malawian children. *Am J Trop Med Hyg*. 2001;64(3-4):207-13.
300. Dorovini-Zis K, Schmidt K, Huynh H, Fu W, Whitten RO, et al. The neuropathology of fatal cerebral malaria in Malawian children. *Am J Pathol*. 2011;178(5):2146-2158.
301. Medana IM, Day NP, Hien TT, Mai NTH, Bethell D, et al. Axonal injury in cerebral malaria. *Am J Pathol*. 2002;160(2):655-666.
302. Brown H, Hien TT, Day N, Mai NT, Chuong LV, et al. Evidence of blood-brain barrier dysfunction in human cerebral malaria. *Neuropathol Appl Neurobiol*. 1999;25(4):331-40.
303. Susomboon P, Maneerat Y, Dekumyoy P, Kalambaheti T, Iwagami M, et al. Down-regulation of tight junction mRNAs in human endothelial cells co-cultured with *Plasmodium falciparum*-infected erythrocytes. *Parasitol Int*. 2006;55(2):107-112.
304. Pino P, Vouldoukis I, Kolb JP, Mahmoudi N, Desportes-Livage I, et al. *Plasmodium falciparum*-infected erythrocyte adhesion induces caspase activation and apoptosis in human endothelial cells. *J Infect Dis*. 2003;187(8):1283-1290.
305. Wilson NO, Huang M-B, Anderson W, Bond V, Powell M, et al. Soluble factors from *Plasmodium falciparum*-infected erythrocytes induce apoptosis in human brain vascular endothelial and neuroglia cells. *Mol Biochem Parasitol*. 2008;162(2):172-176.
306. Tripathi AK, Sullivan DJ and Stins MF. *Plasmodium falciparum*-infected erythrocytes decrease the integrity of human blood-brain barrier endothelial cell monolayers. *J Infect Dis*. 2007;195(7):942-50.
307. Idro R, Karamagi C and Tumwine J. Immediate outcome and prognostic factors for cerebral malaria among children admitted to Mulago Hospital, Uganda. *Ann Trop Paediatr*. 2004;24(1):17-24.

308. Idro R, Carter JA, Fegan G, Neville BGR and Newton CRJC. Risk factors for persisting neurological and cognitive impairments following cerebral malaria. *Arch Dis Child*. 2006;91(2):142-148.
309. van Hensbroek MB, Palmer A, Jaffar S, Schneider G and Kwiatkowski D. Residual neurologic sequelae after childhood cerebral malaria. *J Pediatr*. 1997;131(1 Pt 1):125-9.
310. Boivin MJ, Bangirana P, Byarugaba J, Opoka RO, Idro R, et al. Cognitive impairment after cerebral malaria in children: a prospective study. *Pediatrics*. 2007;119(2):e360-e366.
311. Casals-Pascual C, Idro R, Gicheru N, Gwer S, Kitsao B, et al. High levels of erythropoietin are associated with protection against neurological sequelae in African children with cerebral malaria. *Proc Natl Acad Sci USA*. 2008;105(7):2634-2639.
312. White NJ and Ho M. The pathophysiology of malaria. *Adv Parasitol*. 1992;31:83-173.
313. Hughes KR, Biagini GA and Craig AG. Continued cytoadherence of *Plasmodium falciparum* infected red blood cells after antimalarial treatment. *Mol Biochem Parasitol*. 2010;169(2):71-78.
314. Ch'ng J-H, Moll K, Quintana MdP, Chan SCL, Masters E, et al. Rosette-disrupting effect of an anti-plasmodial compound for the potential treatment of *Plasmodium falciparum* malaria complications. *Sci Rep*. 2016;6:29317.
315. Yipp BG, Robbins SM, Resek ME, Baruch DI, Looareesuwan S, et al. Src-family kinase signaling modulates the adhesion of *Plasmodium falciparum* on human microvascular endothelium under flow. *Blood*. 2003;101(7):2850-7.
316. Dondorp AM, Silamut K, Charunwatthana P, Chuasuwanchai S, Ruangveerayut R, et al. Levamisole inhibits sequestration of infected red blood cells in patients with *falciparum* malaria. *J Infect Dis*. 2007;196(3):460-466.
317. Maude RJ, Silamut K, Plewes K, Charunwatthana P, Ho M, et al. Randomized controlled trial of levamisole hydrochloride as adjunctive therapy in severe *falciparum* malaria With high parasitemia. *J Infect Dis*. 2014;209(1):120-129.
318. Carlson J, Ekre HP, Helmby H, Gysin J, Greenwood BM, et al. Disruption of *Plasmodium falciparum* erythrocyte rosettes by standard heparin and heparin devoid of anticoagulant activity. *Am J Trop Med Hyg*. 1992;46(5):595-602.

319. Kyriacou HM, Steen KE, Raza A, Arman M, Warimwe G, et al. *In vitro* inhibition of *Plasmodium falciparum* rosette formation by curdlan sulfate. *Antimicrob Agents Chemother.* 2007;51(4):1321-1326.
320. Bastos MF, Albrecht L, Kozlowski EO, Lopes SCP, Blanco YC, et al. Fucosylated chondroitin sulfate inhibits *Plasmodium falciparum* cytoadhesion and merozoite invasion. *Antimicrob Agents Chemother.* 2014;58(4):1862-1871.
321. Vogt AM, Pettersson F, Moll K, Jonsson C, Normark J, et al. Release of sequestered malaria parasites upon injection of a glycosaminoglycan. *PLOS Pathog.* 2006;2(9):e100.
322. Leitgeb AM, Blomqvist K, Cho-Ngwa F, Samje M, Nde P, et al. Low anticoagulant heparin disrupts *Plasmodium falciparum* rosettes in fresh clinical isolates. *Am J Trop Med Hyg.* 2011;84(3):390-396.
323. Dilaforette 2014. Dilaforette presents results from exploratory Phase I/II clinical trial in uncomplicated malaria. Stockholm, Sweden: Karolinska Development.
324. Evans SG, Morrison D, Kaneko Y and Havlik I. The effect of curdlan sulphate on development *in vitro* of *Plasmodium falciparum*. *Trans R Soc Trop Med Hyg.* 1998;92(1):87-9.
325. Havlik I, Looareesuwan S, Vannaphan S, Wilairatana P, Krudsood S, et al. Curdlan sulphate in human severe/cerebral *Plasmodium falciparum* malaria. *Trans R Soc Trop Med Hyg.* 2005;99(5):333-340.
326. Riddle MS, Jackson JL, Sanders JW and Blazes DL. Exchange transfusion as an adjunct therapy in severe *Plasmodium falciparum* malaria: A meta-analysis. *Clin Infect Dis.* 2002;34(9):1192-1198.
327. Tan KR, Wiegand RE and Arquin PM. Exchange transfusion for severe malaria: evidence base and literature review. *Clin Infect Dis.* 2013;57(7):923-928.
328. Kwiatkowski D, Molyneux ME, Stephens S, Curtis N, Klein N, et al. Anti-TNF therapy inhibits fever in cerebral malaria. *Q J Med.* 1993;86(2):91-8.
329. van Hensbroek MB, Palmer A, Onyiorah E, Schneider G, Jaffar S, et al. The effect of a monoclonal antibody to tumor necrosis factor on survival from childhood cerebral malaria. *J Infect Dis.* 1996;174(5):1091-7.
330. Ward A and Clissold SP. Pentoxifylline. A review of its pharmacodynamic and pharmacokinetic properties, and its therapeutic efficacy. *Drugs.* 1987;34(1):50-97.

331. Di Perri G, Di Perri IG, Monteiro GB, Bonora S, Hennig C, et al. Pentoxifylline as a supportive agent in the treatment of cerebral malaria in children. *J Infect Dis.* 1995;171(5):1317-22.
332. Lell B, Köhler C, Wamola B, Olola CHO, Kivaya E, et al. Pentoxifylline as an adjunct therapy in children with cerebral malaria. *Malar J.* 2010;9:368-368.
333. Das BK, Mishra S, Padhi PK, Manish R, Tripathy R, et al. Pentoxifylline adjunct improves prognosis of human cerebral malaria in adults. *Trop Med Int Health.* 2003;8(8):680-684.
334. Looareesuwan S, Wilairatana P, Vannaphan S, Wanaratana V, Wenisch C, et al. Pentoxifylline as an ancillary treatment for severe *falciparum* malaria in Thailand. *Am J Trop Med Hyg.* 1998;58(3):348-53.
335. Hemmer CJ, Hort G, Chiwakata CB, Seitz R, Egbring R, et al. Supportive pentoxifylline in *falciparum* malaria: no effect on tumor necrosis factor alpha levels or clinical outcome: a prospective, randomized, placebo-controlled study. *Am J Trop Med Hyg.* 1997;56(4):397-403.
336. Jiang C, Ting AT and Seed B. PPAR-gamma agonists inhibit production of monocyte inflammatory cytokines. *Nature.* 1998;391(6662):82-6.
337. Ricote M, Li AC, Willson TM, Kelly CJ and Glass CK. The peroxisome proliferator-activated receptor-gamma is a negative regulator of macrophage activation. *Nature.* 1998;391(6662):79-82.
338. Luo Y, Yin W, Signore AP, Zhang F, Hong Z, et al. Neuroprotection against focal ischemic brain injury by the peroxisome proliferator-activated receptor-gamma agonist rosiglitazone. *J Neurochem.* 2006;97(2):435-48.
339. Serghides L, Patel SN, Ayi K, Lu Z, Gowda DC, et al. Rosiglitazone modulates innate immune responses to *Plasmodium falciparum* and improves outcome in experimental cerebral malaria. *J Infect Dis.* 2009;199(10):1536-1545.
340. Serghides L, McDonald CR, Lu Z, Friedel M, Cui C, et al. PPAR γ agonists improve survival and neurocognitive outcomes in experimental cerebral malaria and induce neuroprotective pathways in human malaria. *PLOS Pathog.* 2014;10(3):e1003980.
341. Boggild AK, Krudsood S, Patel SN, Serghides L, Tangpukdee N, et al. Use of peroxisome proliferator-activated receptor γ agonists as adjunctive treatment for *Plasmodium*

- falciparum* malaria: a randomized, double-blind, placebo-controlled trial. Clin Infect Dis. 2009;49(6):841-849.
342. Stevenson MM and Riley EM. Innate immunity to malaria. Nat Rev Immunol. 2004;4(3):169-180.
343. Clark IA and Cowden WB. The pathophysiology of *falciparum* malaria. Pharmacol Ther. 2003;99(2):221-260.
344. Gramaglia I, Sobolewski P, Meays D, Contreras R, Nolan JP, et al. Low nitric oxide bioavailability contributes to the genesis of experimental cerebral malaria. Nat Med. 2006;12(12):1417-1422.
345. Serghides L, Kim H, Lu Z, Kain DC, Miller C, et al. Inhaled nitric oxide reduces endothelial activation and parasite accumulation in the brain, and enhances survival in experimental cerebral malaria. PLOS ONE. 2011;6(11):e27714.
346. Bloch KD, Ichinose F, Roberts JD and Zapol WM. Inhaled NO as a therapeutic agent. Cardiovas Res. 2007;75(2):339-348.
347. Mwangi-Amumpaire J, Carroll RW, Baudin E, Kemigisha E, Nampijja D, et al. Inhaled nitric oxide as an adjunctive treatment for cerebral malaria in children: a phase II randomized open-label clinical trial. Open Forum Infect Dis. 2015;2(3).
348. Hawkes MT, Conroy AL, Opoka RO, Hermann L, Thorpe KE, et al. Inhaled nitric oxide as adjunctive therapy for severe malaria: a randomized controlled trial. Malar J. 2015;14(1):421.
349. Yeo TW, Lampah DA, Gitawati R, Tjitra E, Kenangalem E, et al. Recovery of endothelial function in severe *falciparum* malaria: relationship with improvement in plasma L-arginine and blood lactate concentrations. J Infect Dis. 2008;198(4):602-608.
350. Yeo TW, Lampah DA, Rooslamia I, Gitawati R, Tjitra E, et al. A randomized pilot study of L-arginine infusion in severe *falciparum* malaria: preliminary safety, efficacy and pharmacokinetics. PLOS ONE. 2013;8(7):e69587.
351. Bertinaria M, Orjuela-Sanchez P, Marini E, Guglielmo S, Hofer A, et al. NO-donor dihydroartemisinin derivatives as multitarget agents for the treatment of cerebral malaria. J Med Chem. 2015;58(19):7895-9.

352. Higgins SJ, Purcell LA, Silver KL, Tran V, Crowley V, et al. Dysregulation of angiopoietin-1 plays a mechanistic role in the pathogenesis of cerebral malaria. *Sci Transl Med.* 2016;8(358):358ra128.
353. Stacpoole PW. The pharmacology of dichloroacetate. *Metabolism.* 1989;38(11):1124-44.
354. Stacpoole PW, Henderson GN, Yan Z, Cornett R and James MO. Pharmacokinetics, metabolism and toxicology of dichloroacetate. *Drug Metab Rev.* 1998;30(3):499-539.
355. Holloway PA, Krishna S and White NJ. *Plasmodium berghei*: lactic acidosis and hypoglycaemia in a rodent model of severe malaria; effects of glucose, quinine, and dichloroacetate. *Exp Parasitol.* 1991;72(2):123-33.
356. Holloway PA, Knox K, Bajaj N, Chapman D, White NJ, et al. *Plasmodium berghei* infection: dichloroacetate improves survival in rats with lactic acidosis. *Exp Parasitol.* 1995;80(4):624-32.
357. Krishna S, Supanaranond W, Pukrittayakamee S, Karter D, Supputamongkol Y, et al. Dichloroacetate for lactic acidosis in severe malaria: a pharmacokinetic and pharmacodynamic assessment. *Metabolism.* 1994;43(8):974-81.
358. Krishna S, Supanaranond W, Pukrittayakamee S, Kuile FT, Ruprah M, et al. The disposition and effects of two doses of dichloroacetate in adults with severe *falciparum* malaria. *Br J Clin Pharmacol.* 1996;41(1):29-34.
359. Krishna S, Agbenyega T, Angus BJ, Bedu-Addo G, Ofori-Amanfo G, et al. Pharmacokinetics and pharmacodynamics of dichloroacetate in children with lactic acidosis due to severe malaria. *QJM.* 1995;88(5):341-9.
360. Agbenyega T, Planche T, Bedu-Addo G, Ansong D, Owusu-Ofori A, et al. Population kinetics, efficacy, and safety of dichloroacetate for lactic acidosis due to severe malaria in children. *J Clin Pharmacol.* 2003;43(4):386-96.
361. Maitland K, Levin M, English M, Mithwani S, Peshu N, et al. Severe *P. falciparum* malaria in Kenyan children: evidence for hypovolaemia. *QJM.* 2003;96(6):427-34.
362. Maitland K, Pamba A, English M, Peshu N, Marsh K, et al. Randomized trial of volume expansion with albumin or saline in children with severe malaria: preliminary evidence of albumin benefit. *Clin Infect Dis.* 2005;40(4):538-45.

363. Akech S, Gwer S, Idro R, Fegan G, Eziefula AC, et al. Volume expansion with albumin compared to gelofusine in children with severe malaria: results of a controlled trial. *PLOS Clin Trials*. 2006;1(5):e21.
364. Phu NH, Hanson J, Bethell D, Mai NTH, Chau TTH, et al. A retrospective analysis of the haemodynamic and metabolic effects of fluid resuscitation in Vietnamese adults with severe *falciparum* malaria. *PLOS ONE*. 2011;6(10):e25523.
365. Hanson JP, Lam SW, Mohanty S, Alam S, Pattnaik R, et al. Fluid resuscitation of adults with severe *falciparum* malaria: effects on acid-base status, renal function, and extravascular lung water. *Crit Care Med*. 2013;41(4):972-81.
366. English M, Muambi B, Mithwani S and Marsh K. Lactic acidosis and oxygen debt in African children with severe anaemia. *QJM*. 1997;90(9):563-9.
367. English M, Waruiru C and Marsh K. Transfusion for respiratory distress in life-threatening childhood malaria. *Am J Trop Med Hyg*. 1996;55(5):525-30.
368. Woodruff AW and Dickinson CJ. Use of dexamethasone in cerebral malaria. *Br Med J*. 1968;3(5609):31-32.
369. Oriscello RG. Cerebral malaria. *Br Med J*. 1968;3(5618):617-618.
370. Smitskamp H and Wolthuis FH. New concepts in treatment of malaria with malignant tertian cerebral involvement. *Br Med J*. 1971;1(5751):714-716.
371. Daroff RB, Deller JJ, Jr, Kastl AJ, Jr, et al. Cerebral malaria. *JAMA*. 1967;202(8):679-682.
372. Warrell DA, Looareesuwan S, Warrell MJ, Kasemsarn P, Intaraprasert R, et al. Dexamethasone proves deleterious in cerebral malaria. *N Engl J Med*. 1982;306(6):313-319.
373. Hoffman SL, Rustama D, Punjabi NH, Surampaet B, Sanjaya B, et al. High-dose dexamethasone in quinine-treated patients with cerebral malaria: a double-blind, placebo-controlled trial. *J Infect Dis*. 1988;158(2):325-31.
374. Okoromah CA, Afolabi BB and Wall EC. Mannitol and other osmotic diuretics as adjuncts for treating cerebral malaria. *Cochrane Database Syst Rev*. 2011(4):Cd004615.
375. Namutangula B, Ndeezi G, Byarugaba JS and Tumwine JK. Mannitol as adjunct therapy for childhood cerebral malaria in Uganda: a randomized clinical trial. *Malar J*. 2007;6:138.

376. Carter JA, Mung'ala-Odera V, Neville BG, Murira G, Mturi N, et al. Persistent neurocognitive impairments associated with severe *falciparum* malaria in Kenyan children. *J Neurol Neurosurg Psychiatry*. 2005;76(4):476-81.
377. White NJ, Looareesuwan S, Phillips RE, Chanthavanich P and Warrell DA. Single dose phenobarbitone prevents convulsions in cerebral malaria. *Lancet*. 1988;2(8602):64-6.
378. Crawley J, Waruiru C, Mithwani S, Mwangi I, Watkins W, et al. Effect of phenobarbital on seizure frequency and mortality in childhood cerebral malaria: a randomised, controlled intervention study. *Lancet*. 2000;355(9205):701-6.
379. Abubakar A, Van De Vijver FJR, Mithwani S, Obiero E, Lewa N, et al. Assessing developmental outcomes in children from Kilifi, Kenya, following prophylaxis for seizures in cerebral malaria. *J Health Psychol*. 2007;12(3):417-430.
380. Sakanaka M, Wen T-C, Matsuda S, Masuda S, Morishita E, et al. *In vivo* evidence that erythropoietin protects neurons from ischemic damage. *Proc Natl Acad Sci USA*. 1998;95(8):4635-4640.
381. Brines ML, Ghezzi P, Keenan S, Agnello D, de Lanerolle NC, et al. Erythropoietin crosses the blood–brain barrier to protect against experimental brain injury. *Proc Natl Acad Sci USA*. 2000;97(19):10526-10531.
382. Kaiser K, Texier A, Ferrandiz J, Buguet A, Meiller A, et al. Recombinant human erythropoietin prevents the death of mice during cerebral malaria. *J Infect Dis*. 2006;193(7):987-95.
383. Wiese L, Hempel C, Penkowa M, Kirkby N and Kurtzhals JA. Recombinant human erythropoietin increases survival and reduces neuronal apoptosis in a murine model of cerebral malaria. *Malar J*. 2008;7:3.
384. Bienvenu A-L, Ferrandiz J, Kaiser K, Latour C and Picot S. Artesunate–erythropoietin combination for murine cerebral malaria treatment. *Acta Tropica*. 2008;106(2):104-108.
385. Picot S, Bienvenu A-L, Konate S, Sissoko S, Barry A, et al. Safety of epoietin beta-quinine drug combination in children with cerebral malaria in Mali. *Malar J*. 2009;8(1):169.
386. Shabani E, Opoka RO, Idro R, Schmidt R, Park GS, et al. High plasma erythropoietin levels are associated with prolonged coma duration and increased mortality in children With cerebral malaria. *Clin Infect Dis*. 2015;60(1):27-35.

387. Dalko E, Tchitchek N, Pays L, Herbert F, Cazenave P-A, et al. Erythropoietin levels increase during cerebral malaria and correlate with heme, interleukin-10 and tumor necrosis factor- α in India. *PLOS ONE*. 2016;11(7):e0158420.
388. Lamb TJ, Brown DE, Potocnik AJ and Langhorne J. Insights into the immunopathogenesis of malaria using mouse models. *Expert Rev Mol Med*. 2006;8(6):1-22.
389. Adachi K, Tsutsui H, Kashiwamura S-I, Seki E, Nakano H, et al. *Plasmodium berghei* infection in mice induces liver injury by an IL-12- and toll-like receptor/myeloid differentiation factor 88-dependent mechanism. *J Immunol* 2001;167(10):5928-5934.
390. Belnoue E, Kayibanda M, Vigario AM, Deschemin J-C, van Rooijen N, et al. On the pathogenic role of brain-sequestered $\alpha\beta$ CD8⁺ T cells in experimental cerebral malaria. *J Immunol*. 2002;169(11):6369-6375.
391. White NJ, Turner GD, Medana IM, Dondorp AM and Day NP. The murine cerebral malaria phenomenon. *Trends Parasitol*. 2010;26(1):11-5.
392. McQuillan JA, Mitchell AJ, Ho YF, Combes V, Ball HJ, et al. Coincident parasite and CD8 T cell sequestration is required for development of experimental cerebral malaria. *Int J Parasitol*. 2011;41(2):155-163.
393. Baptista FG, Pamplona A, Pena AC, Mota MM, Pied S, et al. Accumulation of *Plasmodium berghei*-infected red blood cells in the brain is crucial for the development of cerebral malaria in mice. *Infect Immun*. 2010;78(9):4033-4039.
394. Amante FH, Haque A, Stanley AC, Rivera FdL, Randall LM, et al. Immune-mediated mechanisms of parasite tissue sequestration during experimental cerebral malaria. *J Immunol*. 2010;185(6):3632-3642.
395. Claser C, Malleret B, Gun SY, Wong AYW, Chang ZW, et al. CD8⁺ T cells and IFN- γ mediate the time-dependent accumulation of infected red blood cells in deep organs during experimental cerebral malaria. *PLOS ONE*. 2011;6(4):e18720.
396. Shaw TN, Stewart-Hutchinson PJ, Strangward P, Dandamudi DB, Coles JA, et al. Perivascular arrest of CD8⁺ T cells is a signature of experimental cerebral malaria. *PLOS Pathog*. 2015;11(11):e1005210.

397. Howland SW, Poh CM, Gun SY, Claser C, Malleret B, et al. Brain microvessel cross-presentation is a hallmark of experimental cerebral malaria. *EMBO Mol Med.* 2013;5(7):916-931.
398. El-Assaad F, Wheway J, Mitchell AJ, Lou J, Hunt NH, et al. Cytoadherence of *Plasmodium berghei*-infected red blood cells to murine brain and lung microvascular endothelial cells *in vitro*. *Infect Immun.* 2013;81(11):3984-3991.
399. Hall N, Karras M, Raine JD, Carlton JM, Kooij TWA, et al. A comprehensive survey of the *Plasmodium* life cycle by genomic, transcriptomic, and proteomic analyses. *Science.* 2005;307(5706):82.
400. Penet MF, Viola A, Confort-Gouny S, Le Fur Y, Duhamel G, et al. Imaging experimental cerebral malaria *in vivo*: significant role of ischemic brain edema. *J Neurosci.* 2005;25(32):7352-8.
401. Sanni LA, Rae C, Maitland A, Stocker R and Hunt NH. Is ischemia involved in the pathogenesis of murine cerebral malaria? *Am J Pathol.* 2001;159(3):1105-12.
402. Swanson PA, II, Hart GT, Russo MV, Nayak D, Yazew T, et al. CD8+ T cells induce fatal brainstem pathology during cerebral malaria via luminal antigen-specific engagement of brain vasculature. *PLOS Pathog.* 2016;12(12):e1006022.
403. Hill AVS, Allsopp CEM, Kwiatkowski D, Anstey NM, Twumasi P, et al. Common West African HLA antigens are associated with protection from severe malaria. *Nature.* 1991;352(6336):595-600.
404. Finley RW, Mackey LJ and Lambert PH. Virulent *P. berghei* malaria: prolonged survival and decreased cerebral pathology in cell-dependent nude mice. *J Immunol.* 1982;129(5):2213-8.
405. Yañez DM, Manning DD, Cooley AJ, Weidanz WP and van der Heyde HC. Participation of lymphocyte subpopulations in the pathogenesis of experimental murine cerebral malaria. *J Immunol.* 1996;157(4):1620-4.
406. Nitcheu J, Bonduelle O, Combadiere C, Tefit M, Seilhean D, et al. Perforin-dependent brain-infiltrating cytotoxic CD8+ T lymphocytes mediate experimental cerebral malaria pathogenesis. *J Immunol.* 2003;170(4):2221-2228.

407. Grau GE, Piguet PF, Engers HD, Louis JA, Vassalli P, et al. L3T4+ T lymphocytes play a major role in the pathogenesis of murine cerebral malaria. *J Immunol.* 1986;137(7):2348-54.
408. Hermesen C, van de Wiel T, Mommers E, Sauerwein R and Eling W. Depletion of CD4+ or CD8+ T-cells prevents *Plasmodium berghei* induced cerebral malaria in end-stage disease. *Parasitology.* 1997;114 7-12.
409. Boubou MI, Collette A, Voegtlé D, Mazier D, Cazenave P-A, et al. T cell response in malaria pathogenesis: selective increase in T cells carrying the TCR V β 8 during experimental cerebral malaria. *Int Immunol.* 1999;11(9):1553-1562.
410. Hearn J, Rayment N, Landon DN, Katz DR and de Souza JB. Immunopathology of cerebral malaria: morphological evidence of parasite sequestration in murine brain microvasculature. *Infect Immun.* 2000;68(9):5364-5376.
411. Jung S, Unutmaz D, Wong P, Sano G-I, De los Santos K, et al. *In vivo* depletion of CD11c(+) dendritic cells abrogates priming of CD8(+) T cells by exogenous cell-associated antigens. *Immunity.* 2002;17(2):211-220.
412. Merad M, Sathe P, Helft J, Miller J and Mortha A. The dendritic cell lineage: ontogeny and function of dendritic cells and their subsets in the steady state and the inflamed setting. *Annu Rev Immunol.* 2013;31.
413. deWalick S, Amante FH, McSweeney KA, Randall LM, Stanley AC, et al. Cutting edge: conventional dendritic cells are the critical APC required for the induction of experimental cerebral malaria. *J Immunol.* 2007;178(10):6033-6037.
414. Lundie RJ, de Koning-Ward TF, Davey GM, Nie CQ, Hansen DS, et al. Blood-stage *Plasmodium* infection induces CD8+ T lymphocytes to parasite-expressed antigens, largely regulated by CD8 α + dendritic cells. *Proc Natl Acad Sci USA.* 2008;105(38):14509-14514.
415. den Haan JM, Lehar SM and Bevan MJ. CD8(+) but not CD8(-) dendritic cells cross-prime cytotoxic T cells *in vivo*. *J Exp Med.* 2000;192(12):1685-96.
416. Piva L, Tetlak P, Claser C, Karjalainen K, Renia L, et al. Cutting edge: Clec9A+ dendritic cells mediate the development of experimental cerebral malaria. *J Immunol.* 2012;189(3):1128-1132.

417. Krishnegowda G, Hajjar AM, Zhu J, Douglass EJ, Uematsu S, et al. Induction of proinflammatory responses in macrophages by the glycosylphosphatidylinositols of *Plasmodium falciparum*: cell signaling receptors, glycosylphosphatidylinositol (GPI) structural requirement, and regulation of GPI activity. *J Biol Chem.* 2005;280(9):8606-8616.
418. Parroche P, Lauw FN, Goutagny N, Latz E, Monks BG, et al. Malaria hemozoin is immunologically inert but radically enhances innate responses by presenting malaria DNA to Toll-like receptor 9. *Proc Natl Acad Sci USA.* 2007;104(6):1919-1924.
419. Mockenhaupt FP, Cramer JP, Hamann L, Stegemann MS, Eckert J, et al. Toll-like receptor (TLR) polymorphisms in African children: Common TLR-4 variants predispose to severe malaria. *Proc Natl Acad Sci USA.* 2006;103(1):177-182.
420. Omar AH, Yasunami M, Yamazaki A, Shibata H, Ofori MF, et al. Toll-like receptor 9 (TLR9) polymorphism associated with symptomatic malaria: a cohort study. *Malar J.* 2012;11:168-168.
421. Griffith JW, O'Connor C, Bernard K, Town T, Goldstein DR, et al. Toll-like receptor modulation of murine cerebral malaria is dependent on the genetic background of the host. *J Infect Dis.* 2007;196(10):1553-1564.
422. Coban C, Ishii KJ, Uematsu S, Arisue N, Sato S, et al. Pathological role of Toll-like receptor signaling in cerebral malaria. *Int Immunol.* 2007;19(1):67-79.
423. Baccarella A, Huang BW, Fontana MF and Kim CC. Loss of Toll-like receptor 7 alters cytokine production and protects against experimental cerebral malaria. *Malar J.* 2014;13:354.
424. Kordes M, Matuschewski K and Hafalla JCR. Caspase-1 activation of interleukin-1 β (IL-1 β) and IL-18 is dispensable for induction of experimental cerebral malaria. *Infect Immun.* 2011;79(9):3633-3641.
425. Togbe D, Schofield L, Grau GE, Schnyder B, Boissay V, et al. Murine cerebral malaria development is independent of toll-like receptor signaling. *Am J Pathol.* 2007;170(5):1640-1648.
426. Lepenies B, Cramer JP, Burchard GD, Wagner H, Kirschning CJ, et al. Induction of experimental cerebral malaria is independent of TLR2/4/9. *Med Microbiol Immun.* 2008;197(1):39-44.

427. Franklin BS, Ishizaka ST, Lamphier M, Gusovsky F, Hansen H, et al. Therapeutic targeting of nucleic acid-sensing Toll-like receptors prevents experimental cerebral malaria. *Proc Natl Acad Sci USA*. 2011;108(9):3689-3694.
428. Finney CAM, Lu Z, LeBourhis L, Philpott DJ and Kain KC. Disruption of Nod-like receptors alters inflammatory response to infection but does not confer protection in experimental cerebral malaria. *Am J Trop Med Hyg*. 2009;80(5):718-722.
429. Shio MT, Eisenbarth SC, Savaria M, Vinet AF, Bellemare M-J, et al. Malarial hemozoin activates the NLRP3 inflammasome through Lyn and Syk kinases. *PLOS Pathog*. 2009;5(8):e1000559.
430. Dostert C, Guarda G, Romero JF, Menu P, Gross O, et al. Malarial hemozoin is a Nalp3 inflammasome activating danger signal. *PLOS ONE*. 2009;4(8):e6510.
431. Reimer T, Shaw MH, Franchi L, Coban C, Ishii KJ, et al. Experimental cerebral malaria progresses independently of the Nlrp3 inflammasome. *Eur J Immunol*. 2010;40(3):764-769.
432. Hafalla JCR, Burgold J, Dorhoi A, Gross O, Ruland J, et al. Experimental cerebral malaria develops independently of caspase recruitment domain-containing protein 9 signaling. *Infect Immun*. 2012;80(3):1274-1279.
433. Maglinao M, Klopffleisch R, Seeberger PH and Lepenies B. The C-type lectin receptor DCIR is crucial for the development of experimental cerebral malaria. *J Immunol*. 2013;191(5):2551-2559.
434. Liehl P, Zuzarte-Luis V, Chan J, Zillinger T, Baptista F, et al. Host-cell sensors for *Plasmodium* activate innate immunity against liver-stage infection. *Nat Med*. 2014;20(1):47-53.
435. Rénia L, Potter SM, Mauduit M, Rosa DS, Kayibanda M, et al. Pathogenic T cells in cerebral malaria. *Int J Parasitol*. 2006;36(5):547-554.
436. Bagot S, Nogueira F, Collette A, do Rosario V, Lemonnier F, et al. Comparative study of brain CD8+ T cells induced by sporozoites and those induced by blood-stage *Plasmodium berghei* ANKA involved in the development of cerebral malaria. *Infect Immun*. 2004;72(5):2817-2826.
437. Lau LS, Fernandez Ruiz D, Davey GM, de Koning-Ward TF, Papenfuss AT, et al. Blood-stage *Plasmodium berghei* infection generates a potent, specific CD8+ T-cell response

- despite residence largely in cells lacking MHC I processing machinery. *J Infect Dis.* 2011;204(12):1989-1996.
438. Howland SW, Claser C, Poh CM, Gun SY and Rénia L. Pathogenic CD8⁺ T cells in experimental cerebral malaria. *Semin Immunopath.* 2015;37(3):221-231.
439. Poh CM, Howland SW, Grotenbreg GM and Rénia L. Damage to the blood-brain barrier during experimental cerebral malaria results from synergistic effects of CD8⁺ T cells with different specificities. *Infect Immun.* 2014;82(11):4854-4864.
440. Belnoue E, Costa FTM, Vigário AM, Voza T, Gonnet F, et al. Chemokine receptor CCR2 is not essential for the development of experimental cerebral malaria. *Infect Immun.* 2003;71(6):3648-3651.
441. Belnoue E, Kayibanda M, Deschemin JC, Viguier M, Mack M, et al. CCR5 deficiency decreases susceptibility to experimental cerebral malaria. *Blood.* 2003;101(11):4253-9.
442. Miu J, Mitchell AJ, Muller M, Carter SL, Manders PM, et al. Chemokine gene expression during fatal murine cerebral malaria and protection due to CXCR3 deficiency. *J Immunol.* 2008;180(2):1217-30.
443. Campanella GS, Tager AM, El Khoury JK, Thomas SY, Abrazinski TA, et al. Chemokine receptor CXCR3 and its ligands CXCL9 and CXCL10 are required for the development of murine cerebral malaria. *Proc Natl Acad Sci USA.* 2008;105(12):4814-9.
444. Hansen DS, Bernard NJ, Nie CQ and Schofield L. NK cells stimulate recruitment of CXCR3⁺ T cells to the brain during *Plasmodium berghei*-mediated cerebral malaria. *J Immunol.* 2007;178(9):5779-88.
445. Nie CQ, Bernard NJ, Norman MU, Amante FH, Lundie RJ, et al. IP-10-mediated T cell homing promotes cerebral inflammation over splenic immunity to malaria infection. *PLOS Pathog.* 2009;5(4):e1000369.
446. Van den Steen PE, Deroost K, Van Aelst I, Geurts N, Martens E, et al. CXCR3 determines strain susceptibility to murine cerebral malaria by mediating T lymphocyte migration toward IFN-gamma-induced chemokines. *Eur J Immunol.* 2008;38(4):1082-95.
447. Farber JM. A macrophage mRNA selectively induced by gamma-interferon encodes a member of the platelet factor 4 family of cytokines. *Proc Natl Acad Sci USA.* 1990;87(14):5238-5242.

448. Luster AD and Ravetch JV. Biochemical characterization of a gamma interferon-inducible cytokine (IP-10). *J Exp Med.* 1987;166(4):1084-97.
449. Van Raemdonck K, Van den Steen PE, Liekens S, Van Damme J and Struyf S. CXCR3 ligands in disease and therapy. *Cytokine Growth Factor Rev.* 2015;26(3):311-327.
450. Belnoue E, Potter SM, Rosa DS, Mauduit M, Gruner AC, et al. Control of pathogenic CD8⁺ T cell migration to the brain by IFN-gamma during experimental cerebral malaria. *Parasite Immunol.* 2008;30(10):544-53.
451. Amani V, Vigário AM, Belnoue E, Marussig M, Fonseca L, et al. Involvement of IFN- γ receptor-mediated signaling in pathology and anti-malarial immunity induced by *Plasmodium berghei* infection. *Eur J Immunol.* 2000;30(6):1646-1655.
452. Grau GE, Heremans H, Piguet PF, Pointaire P, Lambert PH, et al. Monoclonal antibody against interferon gamma can prevent experimental cerebral malaria and its associated overproduction of tumor necrosis factor. *Proc Natl Acad Sci USA.* 1989;86(14):5572-4.
453. Horowitz A, Newman KC, Evans JH, Korbel DS, Davis DM, et al. Cross-talk between T cells and NK cells generates rapid effector responses to *Plasmodium falciparum*-infected erythrocytes. *J Immunol.* 2010;184(11):6043-6052.
454. Villegas-Mendez A, Greig R, Shaw TN, de Souza JB, Gwyer Findlay E, et al. IFN-gamma-producing CD4⁺ T cells promote experimental cerebral malaria by modulating CD8⁺ T cell accumulation within the brain. *J Immunol.* 2012;189(2):968-79.
455. Miyakoda M, Kimura D, Yuda M, Chinzei Y, Shibata Y, et al. Malaria-specific and nonspecific activation of CD8⁺ T cells during blood stage of *Plasmodium berghei* infection. *J Immunol.* 2008;181(2):1420-1428.
456. Haque A, Best SE, Unosson K, Amante FH, de Labastida F, et al. Granzyme B expression by CD8⁺ T cells is required for the development of experimental cerebral malaria. *J Immunol.* 2011;186(11):6148-56.
457. Howland SW, Poh CM and Rénia L. Activated brain endothelial cells cross-present malaria antigen. *PLOS Pathog.* 2015;11(6):e1004963.
458. Lau LS, Fernandez-Ruiz D, Mollard V, Sturm A, Neller MA, et al. CD8⁺ T cells from a novel T cell receptor transgenic mouse induce liver-stage immunity that can be boosted by blood-stage infection in rodent malaria. *PLOS Pathog.* 2014;10(5):e1004135.

459. Joffre OP, Segura E, Savina A and Amigorena S. Cross-presentation by dendritic cells. *Nat Rev Immunol*. 2012;12(8):557-569.
460. Lackner P, Burger C, Pfaller K, Heussler V, Helbok R, et al. Apoptosis in experimental cerebral malaria: spatial profile of cleaved caspase-3 and ultrastructural alterations in different disease stages. *Neuropathol Appl Neurobiol*. 2007;33(5):560-571.
461. Nacer A, Movila A, Baer K, Mikolajczak SA, Kappe SHI, et al. Neuroimmunological blood brain barrier opening in experimental cerebral malaria. *PLOS Pathog*. 2012;8(10):e1002982.
462. Suidan GL, McDole JR, Chen Y, Pirko I and Johnson AJ. Induction of blood brain barrier tight junction protein alterations by CD8 T cells. *PLOS ONE*. 2008;3(8):e3037.
463. Galea I, Bernardes-Silva M, Forse PA, van Rooijen N, Liblau RS, et al. An antigen-specific pathway for CD8 T cells across the blood-brain barrier. *J Exp Med*. 2007;204(9):2023-30.
464. Prakash MD, Munoz MA, Jain R, Tong PL, Koskinen A, et al. Granzyme B promotes cytotoxic lymphocyte transmigration via basement membrane remodeling. *Immunity*. 2014;41(6):960-72.
465. Potter SM, Chan-Ling T, Rosinova E, Ball HJ, Mitchell AJ, et al. A role for Fas-Fas ligand interactions during the late-stage neuropathological processes of experimental cerebral malaria. *J Neuroimmunol*. 2006;173(1):96-107.
466. Nacer A, Movila A, Sohet F, Girgis NM, Gundra UM, et al. Experimental cerebral malaria pathogenesis—hemodynamics at the blood brain barrier. *PLOS Pathog*. 2014;10(12):e1004528.
467. Owens T, Bechmann I and Engelhardt B. Perivascular spaces and the two steps to neuroinflammation. *J Neuropathol Exp Neurol*. 2008;67(12):1113-21.
468. Potter S, Chaudhri G, Hansen A and Hunt NH. Fas and perforin contribute to the pathogenesis of murine cerebral malaria. *Redox Rep*. 1999;4(6):333-5.
469. Muller M, Carter S, Hofer MJ and Campbell IL. Review: The chemokine receptor CXCR3 and its ligands CXCL9, CXCL10 and CXCL11 in neuroimmunity--a tale of conflict and conundrum. *Neuropathol Appl Neurobiol*. 2010;36(5):368-87.
470. Nakajima C, Mukai T, Yamaguchi N, Morimoto Y, Park WR, et al. Induction of the chemokine receptor CXCR3 on TCR-stimulated T cells: dependence on the release from

- persistent TCR-triggering and requirement for IFN-gamma stimulation. *Eur J Immunol.* 2002;32(6):1792-801.
471. Iwasaki M, Mukai T, Gao P, Park WR, Nakajima C, et al. A critical role for IL-12 in CCR5 induction on T cell receptor-triggered mouse CD4(+) and CD8(+) T cells. *Eur J Immunol.* 2001;31(8):2411-20.
472. Iwasaki M, Mukai T, Nakajima C, Yang YF, Gao P, et al. A mandatory role for STAT4 in IL-12 induction of mouse T cell CCR5. *J Immunol.* 2001;167(12):6877-83.
473. Lighvani AA, Frucht DM, Jankovic D, Yamane H, Aliberti J, et al. T-bet is rapidly induced by interferon-gamma in lymphoid and myeloid cells. *Proc Natl Acad Sci USA.* 2001;98(26):15137-42.
474. Szabo SJ, Kim ST, Costa GL, Zhang X, Fathman CG, et al. A novel transcription factor, T-bet, directs Th1 lineage commitment. *Cell.* 2000;100(6):655-69.
475. Szabo SJ, Sullivan BM, Stemmann C, Satoskar AR, Sleckman BP, et al. Distinct effects of T-bet in TH1 lineage commitment and IFN-gamma production in CD4 and CD8 T cells. *Science.* 2002;295(5553):338-42.
476. Barbi J, Oghumu S, Lezama-Davila CM and Satoskar AR. IFN- γ and STAT1 are required for efficient induction of CXC chemokine receptor 3 (CXCR3) on CD4(+) but not CD8(+) T cells. *Blood.* 2007;110(6):2215-2216.
477. Lord GM, Rao RM, Choe H, Sullivan BM, Lichtman AH, et al. T-bet is required for optimal proinflammatory CD4(+) T-cell trafficking. *Blood.* 2005;106(10):3432-3439.
478. Pearce EL, Mullen AC, Martins GA, Krawczyk CM, Hutchins AS, et al. Control of effector CD8+ T cell function by the transcription factor Eomesodermin. *Science.* 2003;302(5647):1041-3.
479. Zhu Y, Ju S, Chen E, Dai S, Li C, et al. T-bet and eomesodermin are required for T cell-mediated antitumor immune responses. *J Immunol.* 2010;185(6):3174-83.
480. Saraiva M and O'Garra A. The regulation of IL-10 production by immune cells. *Nat Rev Immunol.* 2010;10(3):170-81.
481. Couper KN, Blount DG, Wilson MS, Hafalla JC, Belkaid Y, et al. IL-10 from CD4+CD25-Foxp3-CD127- adaptive regulatory T cells modulates parasite clearance and pathology during malaria infection. *PLOS Pathog.* 2008;4(2):e1000004.

482. Kossodo S, Monso C, Juillard P, Velu T, Goldman M, et al. Interleukin-10 modulates susceptibility in experimental cerebral malaria. *Immunology*. 1997;91(4):536-40.
483. Claser C, De Souza JB, Thorburn SG, Grau GE, Riley EM, et al. Host resistance to *Plasmodium*-induced acute immune pathology is regulated by interleukin-10 receptor signaling. *Infect Immun*. 2017;85(6).
484. Amante FH, Stanley AC, Randall LM, Zhou Y, Haque A, et al. A role for natural regulatory T cells in the pathogenesis of experimental cerebral malaria. *Am J Pathol*. 2007;171(2):548-559.
485. Freitas do Rosário AP, Lamb T, Spence P, Stephens R, Lang A, et al. IL-27 promotes IL-10 production by effector Th1 CD4⁺ T cells: a critical mechanism for protection from severe immunopathology during malaria infection. *J Immunol*. 2012;188(3):1178-1190.
486. Wu JJ, Chen G, Liu J, Wang T, Zheng W, et al. Natural regulatory T cells mediate the development of cerebral malaria by modifying the pro-inflammatory response. *Parasitol Int*. 2010;59(2):232-41.
487. Vigario AM, Gorgette O, Dujardin HC, Cruz T, Cazenave PA, et al. Regulatory CD4⁺ CD25⁺ Foxp3⁺ T cells expand during experimental *Plasmodium* infection but do not prevent cerebral malaria. *Int J Parasitol*. 2007;37(8-9):963-73.
488. Steeg C, Adler G, Sparwasser T, Fleischer B and Jacobs T. Limited role of CD4⁺Foxp3⁺ regulatory T cells in the control of experimental cerebral malaria. *J Immunol*. 2009;183(11):7014-7022.
489. Couper KN, Blount DG, de Souza JB, Suffia I, Belkaid Y, et al. Incomplete depletion and rapid regeneration of Foxp3⁺ regulatory T cells following anti-CD25 treatment in malaria-infected mice. *J Immunol*. 2007;178(7):4136-4146.
490. Haque A, Best SE, Amante FH, Mustafah S, Desbarrieres L, et al. CD4⁺ natural regulatory T cells prevent experimental cerebral malaria via CTLA-4 when expanded *in vivo*. *PLOS Pathog*. 2010;6(12):e1001221.
491. Gupta P, Lai SM, Sheng J, Tetlak P, Balachander A, et al. Tissue-resident CD169(+) macrophages form a crucial front line against *Plasmodium* infection. *Cell Rep*. 2016;16(6):1749-61.

492. Findlay EG, Greig R, Stumhofer JS, Hafalla JCR, de Souza JB, et al. Essential role for IL-27 receptor signaling in prevention of Th1-mediated immunopathology during malaria infection. *J Immunol*. 2010;185(4):2482-2492.
493. Haque A, Best SE, Amante FH, Ammerdorffer A, de Labastida F, et al. High parasite burdens cause liver damage in mice following *Plasmodium berghei* ANKA infection independently of CD8+ T cell-mediated immune pathology. *Infect Immun*. 2011;79(5):1882-1888.
494. Jacobs T, Plate T, Gaworski I and Fleischer B. CTLA-4-dependent mechanisms prevent T cell induced-liver pathology during the erythrocyte stage of *Plasmodium berghei* malaria. *Eur J Immunol*. 2004;34(4):972-80.
495. Kassebaum NJ, Jasrasaria R, Naghavi M, Wulf SK, Johns N, et al. A systematic analysis of global anemia burden from 1990 to 2010. *Blood*. 2014;123(5):615-24.
496. WHO 2016. WHO guideline: daily iron supplementation in infants and children. Geneva, Switzerland: World Health Organization.
497. de Mast Q, Syafruddin D, Keijmel S, Riekerink TO, Deky O, et al. Increased serum hepcidin and alterations in blood iron parameters associated with asymptomatic *P. falciparum* and *P. vivax* malaria. *Haematologica*. 2010;95(7):1068-74.
498. Grantham-McGregor S and Ani C. A review of studies on the effect of iron deficiency on cognitive development in children. *J Nutr*. 2001;131(2s-2):649S-668S.
499. WHO 2001. Iron deficiency anaemia : assessment, prevention and control : a guide for programme managers. Geneva, Switzerland: World Health Organization.
500. WHO 2013. Essential nutrition actions: improving maternal, newborn, infant and young child health and nutrition. Geneva, Switzerland: World Health Organization.
501. Gwamaka M, Kurtis JD, Sorensen BE, Holte S, Morrison R, et al. Iron deficiency protects against severe *Plasmodium falciparum* malaria and death in young children. *Clin Infect Dis*. 2012;54(8):1137-44.
502. Nyakeriga AM, Troye-Blomberg M, Dorfman JR, Alexander ND, Back R, et al. Iron deficiency and malaria among children living on the coast of Kenya. *J Infect Dis*. 2004;190(3):439-47.
503. Sazawal S, Black RE, Ramsan M, Chwaya HM, Stoltzfus RJ, et al. Effects of routine prophylactic supplementation with iron and folic acid on admission to hospital and

- mortality in preschool children in a high malaria transmission setting: community-based, randomised, placebo-controlled trial. *Lancet*. 2006;367(9505):133-43.
504. Ganz T. Systemic iron homeostasis. *Physiol Rev*. 2013;93(4):1721-41.
505. Nemeth E, Tuttle MS, Powelson J, Vaughn MB, Donovan A, et al. Hepcidin regulates cellular iron efflux by binding to ferroportin and inducing its internalization. *Science*. 2004;306(5704):2090-3.
506. McKie AT, Barrow D, Latunde-Dada GO, Rolfs A, Sager G, et al. An iron-regulated ferric reductase associated with the absorption of dietary iron. *Science*. 2001;291(5509):1755-9.
507. Choi J, Masaratana P, Latunde-Dada GO, Arno M, Simpson RJ, et al. Duodenal reductase activity and spleen iron stores are reduced and erythropoiesis is abnormal in Dcytb knockout mice exposed to hypoxic conditions. *J Nutr*. 2012;142(11):1929-34.
508. Gunshin H, Starr CN, Drenth C, Fleming MD, Jin J, et al. Cybrd1 (duodenal cytochrome b) is not necessary for dietary iron absorption in mice. *Blood*. 2005;106(8):2879-83.
509. Gunshin H, Fujiwara Y, Custodio AO, Drenth C, Robine S, et al. Slc11a2 is required for intestinal iron absorption and erythropoiesis but dispensable in placenta and liver. *J Clin Invest*. 2005;115(5):1258-66.
510. Shayeghi M, Latunde-Dada GO, Oakhill JS, Laftah AH, Takeuchi K, et al. Identification of an intestinal heme transporter. *Cell*. 2005;122(5):789-801.
511. Rajagopal A, Rao AU, Amigo J, Tian M, Upadhyay SK, et al. Haem homeostasis is regulated by the conserved and concerted functions of HRG-1 proteins. *Nature*. 2008;453(7198):1127-31.
512. Soe-Lin S, Apte SS, Mikhael MR, Kayembe LK, Nie G, et al. Both Nramp1 and DMT1 are necessary for efficient macrophage iron recycling. *Exp Hematol*. 2010;38(8):609-17.
513. Soe-Lin S, Apte SS, Andriopoulos B, Jr., Andrews MC, Schranzhofer M, et al. Nramp1 promotes efficient macrophage recycling of iron following erythrophagocytosis *in vivo*. *Proc Natl Acad Sci USA*. 2009;106(14):5960-5.
514. Delaby C, Rondeau C, Pouzet C, Willemetz A, Pilard N, et al. Subcellular localization of iron and heme metabolism related proteins at early stages of erythrophagocytosis. *PLOS ONE*. 2012;7(7):e42199.

515. Donovan A, Lima CA, Pinkus JL, Pinkus GS, Zon LI, et al. The iron exporter ferroportin/Slc40a1 is essential for iron homeostasis. *Cell Metab.* 2005;1(3):191-200.
516. Vulpe CD, Kuo YM, Murphy TL, Cowley L, Askwith C, et al. Hephaestin, a ceruloplasmin homologue implicated in intestinal iron transport, is defective in the sla mouse. *Nat Genet.* 1999;21(2):195-9.
517. Harris ZL, Durley AP, Man TK and Gitlin JD. Targeted gene disruption reveals an essential role for ceruloplasmin in cellular iron efflux. *Proc Natl Acad Sci USA.* 1999;96(19):10812-10817.
518. Creamer B. The turnover of the epithelium of the small intestine *Br Med Bull.* 1967;23(3):226-230.
519. Hentze MW, Muckenthaler MU, Galy B and Camaschella C. Two to tango: regulation of Mammalian iron metabolism. *Cell.* 2010;142(1):24-38.
520. Dautry-Varsat A, Ciechanover A and Lodish HF. pH and the recycling of transferrin during receptor-mediated endocytosis. *Proc Natl Acad Sci USA.* 1983;80(8):2258-2262.
521. Gkouvatsos K, Papanikolaou G and Pantopoulos K. Regulation of iron transport and the role of transferrin. *Biochim Biophys Acta.* 2012;1820(3):188-202.
522. Ganz T and Nemeth E. Iron metabolism: interactions with normal and disordered erythropoiesis. *Cold Spring Harb Perspect Med.* 2012;2(5):a011668.
523. Nicolas G, Chauvet C, Viatte L, Danan JL, Bigard X, et al. The gene encoding the iron regulatory peptide hepcidin is regulated by anemia, hypoxia, and inflammation. *J Clin Invest.* 2002;110(7):1037-44.
524. Pinto JP, Ribeiro S, Pontes H, Thowfeequ S, Tosh D, et al. Erythropoietin mediates hepcidin expression in hepatocytes through EPOR signaling and regulation of C/EBPalpha. *Blood.* 2008;111(12):5727-33.
525. Pak M, Lopez MA, Gabayan V, Ganz T and Rivera S. Suppression of hepcidin during anemia requires erythropoietic activity. *Blood.* 2006;108(12):3730-5.
526. Vokurka M, Krijt J, Sulc K and Necas E. Hepcidin mRNA levels in mouse liver respond to inhibition of erythropoiesis. *Physiol Res.* 2006;55(6):667-74.
527. Tanno T, Bhanu NV, Oneal PA, Goh SH, Staker P, et al. High levels of GDF15 in thalassemia suppress expression of the iron regulatory protein hepcidin. *Nat Med.* 2007;13(9):1096-101.

528. Tanno T, Porayette P, Sripichai O, Noh SJ, Byrnes C, et al. Identification of TWSG1 as a second novel erythroid regulator of hepcidin expression in murine and human cells. *Blood*. 2009;114(1):181-6.
529. Casanovas G, Spasić MV, Casu C, Rivella S, Strelau J, et al. The murine growth differentiation factor 15 is not essential for systemic iron homeostasis in phlebotomized mice. *Haematologica*. 2013;98(3):444-447.
530. Kautz L, Jung G, Valore EV, Rivella S, Nemeth E, et al. Identification of erythroferrone as an erythroid regulator of iron metabolism. *Nat Genet*. 2014;46(7):678-684.
531. Ramos E, Kautz L, Rodriguez R, Hansen M, Gabayan V, et al. Evidence for distinct pathways of hepcidin regulation by acute and chronic iron loading in mice. *Hepatology*. 2011;53(4):1333-41.
532. Feng Q, Migas MC, Waheed A, Britton RS and Fleming RE. Ferritin upregulates hepatic expression of bone morphogenetic protein 6 and hepcidin in mice. *Am J Physiol Gastrointest Liver Physiol*. 2012;302(12):G1397-404.
533. Ganz T and Nemeth E. Iron homeostasis in host defence and inflammation. *Nat Rev Immunol*. 2015;15(8):500-510.
534. Babitt JL, Huang FW, Wrighting DM, Xia Y, Sidis Y, et al. Bone morphogenetic protein signaling by hemojuvelin regulates hepcidin expression. *Nat Genet*. 2006;38(5):531-9.
535. Meynard D, Kautz L, Darnaud V, Canonne-Hergaux F, Coppin H, et al. Lack of the bone morphogenetic protein BMP6 induces massive iron overload. *Nat Genet*. 2009;41(4):478-81.
536. Kautz L, Meynard D, Monnier A, Darnaud V, Bouvet R, et al. Iron regulates phosphorylation of Smad1/5/8 and gene expression of Bmp6, Smad7, Id1, and Atoh8 in the mouse liver. *Blood*. 2008;112(4):1503-9.
537. Silvestri L, Pagani A, Nai A, De Domenico I, Kaplan J, et al. The serine protease matriptase-2 (TMPRSS6) inhibits hepcidin activation by cleaving membrane hemojuvelin. *Cell Metab*. 2008;8(6):502-11.
538. Mleczo-Sanecka K, Casanovas G, Ragab A, Breitkopf K, Muller A, et al. SMAD7 controls iron metabolism as a potent inhibitor of hepcidin expression. *Blood*. 2010;115(13):2657-65.

539. Korchynskiy O and ten Dijke P. Identification and functional characterization of distinct critically important bone morphogenetic protein-specific response elements in the Id1 promoter. *J Biol Chem.* 2002;277(7):4883-91.
540. Goswami T and Andrews NC. Hereditary hemochromatosis protein, HFE, interaction with transferrin receptor 2 suggests a molecular mechanism for mammalian iron sensing. *J Biol Chem.* 2006;281(39):28494-8.
541. Corradini E, Meynard D, Wu Q, Chen S, Ventura P, et al. Serum and liver iron differently regulate the bone morphogenetic protein 6 (BMP6)-SMAD signaling pathway in mice. *Hepatology.* 2011;54(1):273-84.
542. Nemeth E, Rivera S, Gabayan V, Keller C, Taudorf S, et al. IL-6 mediates hypoferremia of inflammation by inducing the synthesis of the iron regulatory hormone hepcidin. *J Clin Invest.* 2004;113(9):1271-6.
543. Wrighting DM and Andrews NC. Interleukin-6 induces hepcidin expression through STAT3. *Blood.* 2006;108(9):3204-9.
544. Ryan JD, Altamura S, Devitt E, Mullins S, Lawless MW, et al. Pegylated interferon-alpha induced hypoferremia is associated with the immediate response to treatment in hepatitis C. *Hepatology.* 2012;56(2):492-500.
545. Goodnough LT, Nemeth E and Ganz T. Detection, evaluation, and management of iron-restricted erythropoiesis. *Blood.* 2010;116(23):4754-61.
546. Clark MA, Goheen MM, Fulford A, Prentice AM, Elnagheeb MA, et al. Host iron status and iron supplementation mediate susceptibility to erythrocytic stage *Plasmodium falciparum*. *Nat Commun.* 2014;5:4446.
547. Portugal S, Carret C, Recker M, Armitage AE, Gonçalves LA, et al. Host mediated regulation of superinfection in malaria. *Nat Med.* 2011;17(6):732-737.
548. Burte F, Brown BJ, Orimadegun AE, Ajetunmobi WA, Afolabi NK, et al. Circulatory hepcidin is associated with the anti-inflammatory response but not with iron or anemic status in childhood malaria. *Blood.* 2013;121(15):3016-22.
549. Casals-Pascual C, Huang H, Lakhali-Littleton S, Thezenas ML, Kai O, et al. Hepcidin demonstrates a biphasic association with anemia in acute *Plasmodium falciparum* malaria. *Haematologica.* 2012;97(11):1695-1698.

550. Odunukwe NN, Salako LA, Okany C and Ibrahim MM. Serum ferritin and other haematological measurements in apparently healthy adults with malaria parasitaemia in Lagos, Nigeria. *Trop Med Int Health*. 2000;5(8):582-6.
551. Menendez C, Kahigwa E, Hirt R, Vounatsou P, Aponte JJ, et al. Randomised placebo-controlled trial of iron supplementation and malaria chemoprophylaxis for prevention of severe anaemia and malaria in Tanzanian infants. *Lancet*. 1997;350(9081):844-50.
552. van Hensbroek MB, Morris-Jones S, Meisner S, Jaffar S, Bayo L, et al. Iron, but not folic acid, combined with effective antimalarial therapy promotes haematological recovery in African children after acute *falciparum* malaria. *Trans R Soc Trop Med Hyg*. 1995;89(6):672-6.
553. Thurnham DI, McCabe LD, Haldar S, Wieringa FT, Northrop-Clewes CA, et al. Adjusting plasma ferritin concentrations to remove the effects of subclinical inflammation in the assessment of iron deficiency: a meta-analysis. *Am J Clin Nutr*. 2010;92(3):546-55.
554. Zlotkin S, Newton S, Aimone AM, Azindow I, Amenga-Etego S, et al. Effect of iron fortification on malaria incidence in infants and young children in Ghana: a randomized trial. *JAMA*. 2013;310(9):938-47.
555. Neuberger A, Okebe J, Yahav D and Paul M. Oral iron supplements for children in malaria-endemic areas. *Cochrane Database Syst Rev*. 2016;2:Cd006589.
556. Gera T, Sachdev HP, Nestel P and Sachdev SS. Effect of iron supplementation on haemoglobin response in children: systematic review of randomised controlled trials. *J Pediatr Gastroenterol Nutr*. 2007;44(4):468-86.
557. de Mast Q, Nadjm B, Reyburn H, Kemna EH, Amos B, et al. Assessment of urinary concentrations of hepcidin provides novel insight into disturbances in iron homeostasis during malarial infection. *J Infect Dis*. 2009;199(2):253-62.
558. Prentice AM, Doherty CP, Abrams SA, Cox SE, Atkinson SH, et al. Hepcidin is the major predictor of erythrocyte iron incorporation in anemic African children. *Blood*. 2012;119(8):1922-8.
559. Doherty CP, Cox SE, Fulford AJ, Austin S, Hilmers DC, et al. Iron incorporation and post-malaria anaemia. *PLOS ONE*. 2008;3(5):e2133.

560. Cercamondi CI, Egli IM, Ahouandjinou E, Dossa R, Zeder C, et al. Afebrile *Plasmodium falciparum* parasitemia decreases absorption of fortification iron but does not affect systemic iron utilization: a double stable-isotope study in young Beninese women. *Am J Clin Nutr.* 2010;92(6):1385-1392.
561. Glinz D, Hurrell RF, Righetti AA, Zeder C, Adiossan LG, et al. In Ivorian school-age children, infection with hookworm does not reduce dietary iron absorption or systemic iron utilization, whereas afebrile *Plasmodium falciparum* infection reduces iron absorption by half. *Am J Clin Nutr.* 2015;101(3):462-70.
562. Cusick SE, Opoka RO, Abrams SA, John CC, Georgieff MK, et al. Delaying iron therapy until 28 days after antimalarial treatment is associated with greater iron incorporation and equivalent hematologic recovery after 56 days in children: a randomized controlled trial. *J Nutr.* 2016;146(9):1769-74.
563. Glinz D, Kamiyango M, Phiri KS, Munthali F, Zeder C, et al. The effect of timing of iron supplementation on iron absorption and haemoglobin in post-malaria anaemia: a longitudinal stable isotope study in Malawian toddlers. *Malar J.* 2014;13(1):397.
564. Atkinson SH, Armitage AE, Khandwala S, Mwangi TW, Uyoga S, et al. Combinatorial effects of malaria season, iron deficiency, and inflammation determine plasma hepcidin concentration in African children. *Blood.* 2014;123(21):3221-9.
565. Regis G, Bosticardo M, Conti L, De Angelis S, Boselli D, et al. Iron regulates T-lymphocyte sensitivity to the IFN-gamma/STAT1 signaling pathway *in vitro* and *in vivo*. *Blood.* 2005;105(8):3214-21.
566. Tonks NK. Protein tyrosine phosphatases: from genes, to function, to disease. *Nat Rev Mol Cell Biol.* 2006;7(11):833-46.
567. Mustelin T, Vang T and Bottini N. Protein tyrosine phosphatases and the immune response. *Nat Rev Immunol.* 2005;5(1):43-57.
568. Mustelin T, Coggeshall KM, Isakov N and Altman A. T cell antigen receptor-mediated activation of phospholipase C requires tyrosine phosphorylation. *Science.* 1990;247(4950):1584-7.
569. Alonso A, Sasin J, Bottini N, Friedberg I, Friedberg I, et al. Protein tyrosine phosphatases in the human genome. *Cell.* 2004;117(6):699-711.

570. Stuckey JA, Schubert HL, Fauman EB, Zhang ZY, Dixon JE, et al. Crystal structure of Yersinia protein tyrosine phosphatase at 2.5 Å and the complex with tungstate. *Nature*. 1994;370(6490):571-5.
571. Zhang ZY, Wang Y and Dixon JE. Dissecting the catalytic mechanism of protein-tyrosine phosphatases. *Proc Natl Acad Sci USA*. 1994;91(5):1624-1627.
572. Denu JM, Stuckey JA, Saper MA and Dixon JE. Form and function in protein dephosphorylation. *Cell*. 1996;87(3):361-4.
573. Denu JM, Lohse DL, Vijayalakshmi J, Saper MA and Dixon JE. Visualization of intermediate and transition-state structures in protein-tyrosine phosphatase catalysis. *Proc Natl Acad Sci USA*. 1996;93(6):2493-8.
574. Hengge AC, Denu JM and Dixon JE. Transition-state structures for the native dual-specific phosphatase VHR and D92N and S131A mutants. Contributions to the driving force for catalysis. *Biochemistry*. 1996;35(22):7084-92.
575. Zhang ZY. Kinetic and mechanistic characterization of a mammalian protein-tyrosine phosphatase, PTP1. *J Biol Chem*. 1995;270(19):11199-204.
576. Jia Z, Barford D, Flint AJ and Tonks NK. Structural basis for phosphotyrosine peptide recognition by protein tyrosine phosphatase 1B. *Science*. 1995;268(5218):1754-8.
577. Zhang ZY. Protein tyrosine phosphatases: structure and function, substrate specificity, and inhibitor development. *Annu Rev Pharmacol Toxicol*. 2002;42:209-34.
578. Zhang ZY, Maclean D, McNamara DJ, Sawyer TK and Dixon JE. Protein tyrosine phosphatase substrate specificity: size and phosphotyrosine positioning requirements in peptide substrates. *Biochemistry*. 1994;33(8):2285-90.
579. Wiesmann C, Barr KJ, Kung J, Zhu J, Erlanson DA, et al. Allosteric inhibition of protein tyrosine phosphatase 1B. *Nat Struct Mol Biol*. 2004;11(8):730-7.
580. Sarmiento M, Zhao Y, Gordon SJ and Zhang Z-Y. Molecular basis for substrate specificity of protein-tyrosine phosphatase 1B. *J Biol Chem*. 1998;273(41):26368-26374.
581. Huang Z, Zhou B and Zhang ZY. Molecular determinants of substrate recognition in hematopoietic protein-tyrosine phosphatase. *J Biol Chem*. 2004;279(50):52150-9.
582. Wiland AM, Denu JM, Mourey RJ and Dixon JE. Purification and kinetic characterization of the mitogen-activated protein kinase phosphatase rVH6. *J Biol Chem*. 1996;271(52):33486-92.

583. Zhao Y and Zhang ZY. The mechanism of dephosphorylation of extracellular signal-regulated kinase 2 by mitogen-activated protein kinase phosphatase 3. *J Biol Chem.* 2001;276(34):32382-91.
584. Gomez MA, Alisaraie L, Shio MT, Berghuis AM, Lebrun C, et al. Protein tyrosine phosphatases are regulated by mononuclear iron dicitrate. *J Biol Chem.* 2010;285(32):24620-24628.
585. Lorenz U, Ravichandran KS, Pei D, Walsh CT, Burakoff SJ, et al. Lck-dependent tyrosyl phosphorylation of the phosphotyrosine phosphatase SH-PTP1 in murine T cells. *Mol Cell Biol.* 1994;14(3):1824-34.
586. Dadke S, Kusari A and Kusari J. Phosphorylation and activation of protein tyrosine phosphatase (PTP) 1B by insulin receptor. *Mol Cell Biochem.* 2001;221(1):147-154.
587. Bilwes AM, den Hertog J, Hunter T and Noel JP. Structural basis for inhibition of receptor protein-tyrosine phosphatase-alpha by dimerization. *Nature.* 1996;382(6591):555-9.
588. Tonks NK. Redox redux: revisiting PTPs and the control of cell signaling. *Cell.* 2005;121(5):667-70.
589. Lee SR, Yang KS, Kwon J, Lee C, Jeong W, et al. Reversible inactivation of the tumor suppressor PTEN by H₂O₂. *J Biol Chem.* 2002;277(23):20336-42.
590. Posner BI, Faure R, Burgess JW, Bevan AP, Lachance D, et al. Peroxovanadium compounds. A new class of potent phosphotyrosine phosphatase inhibitors which are insulin mimetics. *J Biol Chem.* 1994;269(6):4596-604.
591. Huyer G, Liu S, Kelly J, Moffat J, Payette P, et al. Mechanism of inhibition of protein-tyrosine phosphatases by vanadate and pervanadate. *J Biol Chem.* 1997;272(2):843-51.
592. Barr AJ, Ugochukwu E, Lee WH, King ON, Filippakopoulos P, et al. Large-scale structural analysis of the classical human protein tyrosine phosphatome. *Cell.* 2009;136(2):352-63.
593. Olivier M, Romero-Gallo B-J, Matte C, Blanchette J, Posner BI, et al. Modulation of interferon- γ -induced macrophage activation by phosphotyrosine phosphatases inhibition: effect on murine leishmaniasis progression. *J Biol Chem.* 1998;273(22):13944-13949.

594. Matte C, Marquis JF, Blanchette J, Gros P, Faure R, et al. Peroxovanadium-mediated protection against murine leishmaniasis: role of the modulation of nitric oxide. *Eur J Immunol.* 2000;30(9):2555-64.
595. Bisti S, Konidou G, Papageorgiou F, Milon G, Boelaert JR, et al. The outcome of *Leishmania major* experimental infection in BALB/c mice can be modulated by exogenously delivered iron. *Eur J Immunol.* 2000;30(12):3732-40.
596. Straus DB and Weiss A. Genetic evidence for the involvement of the lck tyrosine kinase in signal transduction through the T cell antigen receptor. *Cell.* 1992;70(4):585-93.
597. Isakov N, Wange RL, Burgess WH, Watts JD, Aebersold R, et al. ZAP-70 binding specificity to T cell receptor tyrosine-based activation motifs: the tandem SH2 domains of ZAP-70 bind distinct tyrosine-based activation motifs with varying affinity. *J Exp Med.* 1995;181(1):375-80.
598. Chan AC, Dalton M, Johnson R, Kong GH, Wang T, et al. Activation of ZAP-70 kinase activity by phosphorylation of tyrosine 493 is required for lymphocyte antigen receptor function. *EMBO J.* 1995;14(11):2499-2508.
599. Zhang W, Sloan-Lancaster J, Kitchen J, Tribble RP and Samelson LE. LAT: the ZAP-70 tyrosine kinase substrate that links T cell receptor to cellular activation. *Cell.* 1998;92(1):83-92.
600. Bubeck Wardenburg J, Fu C, Jackman JK, Flotow H, Wilkinson SE, et al. Phosphorylation of SLP-76 by the ZAP-70 protein-tyrosine kinase is required for T-cell receptor function. *J Biol Chem.* 1996;271(33):19641-4.
601. Bergman M, Mustelin T, Oetken C, Partanen J, Flint NA, et al. The human p50csk tyrosine kinase phosphorylates p56lck at Tyr-505 and down regulates its catalytic activity. *EMBO J.* 1992;11(8):2919-24.
602. Sicheri F and Kuriyan J. Structures of Src-family tyrosine kinases. *Curr Opin Struct Biol.* 1997;7(6):777-85.
603. Salmond RJ, Filby A, Qureshi I, Caserta S and Zamoyska R. T-cell receptor proximal signaling via the Src-family kinases, Lck and Fyn, influences T-cell activation, differentiation, and tolerance. *Immunol Rev.* 2009;228(1):9-22.

604. Ostergaard HL, Shackelford DA, Hurley TR, Johnson P, Hyman R, et al. Expression of CD45 alters phosphorylation of the lck-encoded tyrosine protein kinase in murine lymphoma T-cell lines. *Proc Natl Acad Sci USA*. 1989;86(22):8959-8963.
605. Veillette A and Fournel M. The CD4 associated tyrosine protein kinase p56lck is positively regulated through its site of autophosphorylation. *Oncogene*. 1990;5(10):1455-62.
606. McNeill L, Salmond RJ, Cooper JC, Carret CK, Cassady-Cain RL, et al. The differential regulation of Lck kinase phosphorylation sites by CD45 is critical for T cell receptor signaling responses. *Immunity*. 2007;27(3):425-37.
607. Chiang GG and Sefton BM. Specific dephosphorylation of the Lck tyrosine protein kinase at Tyr-394 by the SHP-1 protein-tyrosine phosphatase. *J Biol Chem*. 2001;276(25):23173-8.
608. Hasegawa K, Martin F, Huang G, Tumas D, Diehl L, et al. PEST domain-enriched tyrosine phosphatase (PEP) regulation of effector/memory T cells. *Science*. 2004;303(5658):685-9.
609. Secrist JP, Burns LA, Karnitz L, Koretzky GA and Abraham RT. Stimulatory effects of the protein tyrosine phosphatase inhibitor, pervanadate, on T-cell activation events. *J Biol Chem*. 1993;268(8):5886-93.
610. O'Shea JJ, McVicar DW, Bailey TL, Burns C and Smyth MJ. Activation of human peripheral blood T lymphocytes by pharmacological induction of protein-tyrosine phosphorylation. *Proc Natl Acad Sci USA*. 1992;89(21):10306-10310.
611. Grau GE, Fajardo LF, Piguet PF, Allet B, Lambert PH, et al. Tumor necrosis factor (cachectin) as an essential mediator in murine cerebral malaria. *Science*. 1987;237(4819):1210-2.
612. Grau GE, Bieler G, Pointaire P, De Kossodo S, Tacchini-Cotier F, et al. Significance of cytokine production and adhesion molecules in malarial immunopathology. *Immunol Lett*. 1990;25(1-3):189-94.
613. Grau GE, Piguet PF, Vassalli P and Lambert PH. Tumor-necrosis factor and other cytokines in cerebral malaria: experimental and clinical data. *Immunol Rev*. 1989;112:49-70.

614. Chang-Ling T, Neill AL and Hunt NH. Early microvascular changes in murine cerebral malaria detected in retinal whole mounts. *Am J Pathol.* 1992;140(5):1121-30.
615. Hunt NH, Golenser J, Chan-Ling T, Parekh S, Rae C, et al. Immunopathogenesis of cerebral malaria. *Int J Parasitol.* 2006;36(5):569-82.
616. Hermsen CC, Mommers E, van de Wiel T, Sauerwein RW and Eling WM. Convulsions due to increased permeability of the blood-brain barrier in experimental cerebral malaria can be prevented by splenectomy or anti-T cell treatment. *J Infect Dis.* 1998;178(4):1225-7.
617. Sarween N, Chodos A, Raykundalia C, Khan M, Abbas AK, et al. CD4+CD25+ cells controlling a pathogenic CD4 response inhibit cytokine differentiation, CXCR-3 expression, and tissue invasion. *J Immunol.* 2004;173(5):2942-51.
618. Good MF, Chapman DE, Powell LW and Halliday JW. The effect of experimental iron-overload on splenic T cell function: analysis using cloning techniques. *Clin Exp Immunol.* 1987;68(2):375-83.
619. Angelini G, Gardella S, Ardy M, Ciriolo MR, Filomeni G, et al. Antigen-presenting dendritic cells provide the reducing extracellular microenvironment required for T lymphocyte activation. *Proc Natl Acad Sci U S A.* 2002;99(3):1491-6.
620. Burkitt MJ and Mason RP. Direct evidence for in vivo hydroxyl-radical generation in experimental iron overload: an ESR spin-trapping investigation. *Proc Natl Acad Sci U S A.* 1991;88(19):8440-4.
621. Yan Z, Garg SK, Kipnis J and Banerjee R. Extracellular redox modulation by regulatory T cells. *Nat Chem Biol.* 2009;5(10):721-3.
622. de Souza JB and Riley EM. Cerebral malaria: the contribution of studies in animal models to our understanding of immunopathogenesis. *Microbes Infect.* 2002;4(3):291-300.
623. Hansen DS, Siomos MA, Buckingham L, Scalzo AA and Schofield L. Regulation of murine cerebral malaria pathogenesis by CD1d-restricted NKT cells and the natural killer complex. *Immunity.* 2003;18(3):391-402.
624. Franke-Fayard B, Janse CJ, Cunha-Rodrigues M, Ramesar J, Buscher P, et al. Murine malaria parasite sequestration: CD36 is the major receptor, but cerebral pathology is unlinked to sequestration. *Proc Natl Acad Sci USA.* 2005;102(32):11468-73.

625. Grau GE, Frei K, Piguet PF, Fontana A, Heremans H, et al. Interleukin 6 production in experimental cerebral malaria: modulation by anticytokine antibodies and possible role in hypergammaglobulinemia. *J Exp Med.* 1990;172(5):1505-8.
626. Potter S, Chan-Ling T, Ball HJ, Mansour H, Mitchell A, et al. Perforin mediated apoptosis of cerebral microvascular endothelial cells during experimental cerebral malaria. *Int J Parasitol.* 2006;36(4):485-496.
627. Lazarevic V, Glimcher LH and Lord GM. T-bet: a bridge between innate and adaptive immunity. *Nat Rev Immunol.* 2013;13(11):777-89.
628. Bach EA, Szabo SJ, Dighe AS, Ashkenazi A, Aguet M, et al. Ligand-induced autoregulation of IFN-gamma receptor beta chain expression in T helper cell subsets. *Science.* 1995;270(5239):1215-8.
629. Wessling-Resnick M. Iron homeostasis and the inflammatory response. *Annu Rev Nutr.* 2010;30:105-22.
630. Spottiswoode N, Duffy PE and Drakesmith H. Iron, anemia and hepcidin in malaria. *Front Pharmacol.* 2014;5:125.
631. Manning L, Laman M, Rosanas-Urgell A, Michon P, Aipit S, et al. Severe anemia in Papua New Guinean children from a malaria-endemic area: a case-control etiologic study. *PLOS Negl Trop Dis.* 2012;6(12):e1972.
632. Matsuzaki-Moriya C, Tu L, Ishida H, Imai T, Suzue K, et al. A critical role for phagocytosis in resistance to malaria in iron-deficient mice. *Eur J Immunol.* 2011;41(5):1365-75.
633. Hershko C and Peto TE. Deferoxamine inhibition of malaria is independent of host iron status. *J Exp Med.* 1988;168(1):375-87.
634. Scott MD, Ranz A, Kuypers FA, Lubin BH and Meshnick SR. Parasite uptake of desferroxamine: a prerequisite for antimalarial activity. *Br J Haematol.* 1990;75(4):598-602.
635. Mabeza GF, Loyevsky M, Gordeuk VR and Weiss G. Iron chelation therapy for malaria: a review. *Pharmacol Ther.* 1999;81(1):53-75.
636. Smith HJ and Meremikwu M. Iron chelating agents for treating malaria. *Cochrane Database Syst Rev.* 2003(2):Cd001474.

637. Van Wyck D, Anderson J and Johnson K. Labile iron in parenteral iron formulations: a quantitative and comparative study. *Nephrol Dial Transplant*. 2004;19(3):561-5.
638. Van Den Ham KM, Shio MT, Rainone A, Fournier S, Krawczyk CM, et al. Iron prevents the development of experimental cerebral malaria by attenuating CXCR3-mediated T cell chemotaxis. *PLOS One*. 2015;10(3):e0118451.
639. Roncarolo MG, Gregori S, Battaglia M, Bacchetta R, Fleischhauer K, et al. Interleukin-10-secreting type 1 regulatory T cells in rodents and humans. *Immunol Rev*. 2006;212:28-50.
640. Gagliani N, Magnani CF, Huber S, Gianolini ME, Pala M, et al. Coexpression of CD49b and LAG-3 identifies human and mouse T regulatory type 1 cells. *Nat Med*. 2013;19(6):739-746.
641. Pouliot P, Bergeron S, Marette A and Olivier M. The role of protein tyrosine phosphatases in the regulation of allergic asthma: implication of TC-PTP and PTP-1B in the modulation of disease development. *Immunology*. 2009;128(4):534-542.
642. Caron D, Savard PE, Doillon CJ, Olivier M, Shink E, et al. Protein tyrosine phosphatase inhibition induces anti-tumor activity: evidence of Cdk2/p27 kip1 and Cdk2/SHP-1 complex formation in human ovarian cancer cells. *Cancer Lett*. 2008;262(2):265-75.
643. Liu Y, Chen Y, Li Z, Han Y, Sun Y, et al. Role of IL-10-producing regulatory B cells in control of cerebral malaria in *Plasmodium berghei* infected mice. *Eur J Immunol*. 2013;43(11):2907-2918.
644. Rai D, Pham N-LL, Harty JT and Badovinac VP. Tracking the total CD8 T cell response to infection reveals substantial discordance in magnitude and kinetics between inbred and outbred hosts. *J. Immunol*. 2009;183(12):7672-7681.
645. Duffner U, Lu B, Hildebrandt GC, Teshima T, Williams DL, et al. Role of CXCR3-induced donor T-cell migration in acute GVHD. *Exp Hematol*. 2003;31(10):897-902.
646. Piper KP, Horlock C, Curnow SJ, Arrazi J, Nicholls S, et al. CXCL10-CXCR3 interactions play an important role in the pathogenesis of acute graft-versus-host disease in the skin following allogeneic stem-cell transplantation. *Blood*. 2007;110(12):3827-32.
647. Tsubaki T, Takegawa S, Hanamoto H, Arita N, Kamogawa J, et al. Accumulation of plasma cells expressing CXCR3 in the synovial sublining regions of early rheumatoid

- arthritis in association with production of Mig/CXCL9 by synovial fibroblasts. *Clin Exp Immunol.* 2005;141(2):363-371.
648. O'Boyle G, Fox CRJ, Walden HR, Willet JDP, Mavin ER, et al. Chemokine receptor CXCR3 agonist prevents human T-cell migration in a humanized model of arthritic inflammation. *Proc Natl Acad Sci USA.* 2012;109(12):4598-4603.
649. Sorensen TL, Tani M, Jensen J, Pierce V, Lucchinetti C, et al. Expression of specific chemokines and chemokine receptors in the central nervous system of multiple sclerosis patients. *J Clin Invest.* 1999;103(6):807-15.
650. Jenh CH, Cox MA, Cui L, Reich EP, Sullivan L, et al. A selective and potent CXCR3 antagonist SCH 546738 attenuates the development of autoimmune diseases and delays graft rejection. *BMC Immunol.* 2012;13(2).
651. Colvin RA, Campanella GS, Sun J and Luster AD. Intracellular domains of CXCR3 that mediate CXCL9, CXCL10, and CXCL11 function. *J Biol Chem.* 2004;279(29):30219-27.
652. Dagan-Berger M, Feniger-Barish R, Avniel S, Wald H, Galun E, et al. Role of CXCR3 carboxyl terminus and third intracellular loop in receptor-mediated migration, adhesion and internalization in response to CXCL11. *Blood.* 2006;107(10):3821-31.
653. Lovegrove FE, Gharib SA, Pena-Castillo L, Patel SN, Ruzinski JT, et al. Parasite burden and CD36-mediated sequestration are determinants of acute lung injury in an experimental malaria model. *PLoS Pathog.* 2008;4(5).